Role of DDR2 in Synovial Cell Invasion: Implications for Rheumatoid Arthritis

---

Iwona Majkowska

A thesis submitted to Imperial College London

for the degree of Doctor of Philosophy

Kennedy Institute of Rheumatology

Department of Medicine, Imperial College London

June 2014

Abstract

A hallmark of rheumatoid arthritis (RA) is cartilage erosion by pannus — an inflamed, hyperplastic and highly invasive synovial tissue. Cartilage degradation is primarily mediated by invading synovial fibroblasts. At the cartilage invasion front of the pannus, these cells destroy the tissue, leading to the permanent loss of joint structure and function. It has been shown that membrane type 1 metalloproteinase (MT1-MMP) plays a key role in promoting RA synovial fibroblast invasion into the cartilage. However little is known about regulatory mechanisms of MT1-MMP in RA synovial fibroblasts.

MT1-MMP is highly upregulated in RA synovium, but mechanisms regulating its expression are not well understood. Interestingly, several reports show high MT1-MMP levels in fibroblasts at the pannus-cartilage junction. In addition, MT1-MMP expression and activity in cultured cells can be induced by collagen. We hypothesised that cartilage, more specifically cartilage collagen, induces MT1-MMP activity in the pannus. In this study, I have confirmed that both collagen and cartilage induce MT1-MMP activity and expression in RA synovial fibroblasts. To understand mechanisms of collagen signalling I have also investigated the role of collagen receptors, namely integrins and discoidin domain receptor 2 (DDR2), in MT1-MMP activation. Knockdown of DDR2, but not collagen-binding integrins, resulted in decreased MT1-MMP activity and expression upon collagen stimulation. DDR2 knockdown also inhibited MT1-MMP-dependent collagen degradation and invasion by RA synovial fibroblasts.

Analysis of DDR2 binding to intact or telopeptide-devoid collagens indicates that collagen structure might influence cell signalling. Furthermore, activation of MT1-MMP by cartilage, which is also mediated by DDR2, is enhanced by removal of proteoglycans. In summary, I have demonstrated that cartilage signalling through collagen receptor DDR2 induces MT1-MMP activity in RA synovial fibroblasts.

DECLARATION

I hereby confirm that this thesis is an original work, representing my own academic effort and that all sources have been fully acknowledged.

4th June 2014 Iwona Majkowska

Acknowledgements

First and foremost, I would like to thank my supervisor Dr. Yoshifumi Itoh for his support, guidance and encouragement throughout my PhD. I would also like to thank Professor Hideaki Nagase for his expert advice.

I am also grateful to Dr. Linda Troeberg for her kind words of encouragement and careful proofreading of my thesis.

Huge thanks go to all members of Dr. Itoh's group, past and present, especially to Noriko Ito; Kazuyo Kaneko; Ania Woskowicz and Michał Rysz for their help with confocal microscopy; Yasu Shitomi for helping me with protein purification and for answering all my questions. This project would not be possible without their support and guidance.

To Grace Chu, Chris Doherty and Lorena Zuliani Alvarez — thank you for all the chats, discussions and laughs we shared in the lab, and your kind help that made my London-Oxford journeys more bearable.

Special thanks go to Wing To and The Biscuiteer Team for all the climbing sessions during writing of this thesis, they really uplifted my spirits!

I would also like to thank my family, especially Mum and Dad, for their endless support and faith in me.

Finally, special thanks to my husband, Marek, for your great patience and that you were always there for me. Thank you.

To Szymon and Cysia, like always

Table of Contents

List of Figures

List of Tables

List of Abbreviations

2D	Two-dimensional
3D	Three-dimensional
β-Me	β-mercaptoethanol
A.U.	Arbitrary units
ACPA	Anti-citrullinated protein antibody
ACR	American College of Rheumatology
ADAMTS	A disintegrin and metalloproteinase with thrombospondin motifs
ADAM	A disintegrin and metalloproteinase
ANOVA	Analysis of variance
AP-2	Adaptor protein 2
APC	Antigen presenting cell
AP	Alkaline phosphatase
bp	Base pair
BSA	Bovine serum albumin
Cat	Catalytic domain
cDNA	Complementary deoxyribonucleic acid
CD	Cluster of differentiation
ConA	Concanavalin A
Ct	Threshold cycle
DAPI	4',6-diamidino-2-phenylindole
DDR	Discoidin domain receptor
dH_2O	Deionised water
DMARD	Disease-modifying anti-rheumatic drug
DMEM	Dulbecco's Modified Eagle Medium
DMSO	Dimethyl sulphoxide
DNA	Deoxyribonucleic acid
dNTP	Deoxyribonucleotide triphosphate
DPBS	Dulbecco's phosphate buffered saline
ECD	Extracellular domain
ECM	Extracellular matrix
EDTA	Ethylenediaminetetraacetic acid
EGF	Epidermal growth factor
ERM	Erzin/radixin/moesin
EULAR	European League Against Rheumatism
F-actin	Actin filaments
FBS	Fetal bovine serum

FDA	Food and Drug Administration
GM6001	Ilomastat
GPI	Glycosylphosphatidylinositol
HEK	Human embryonic kidney cells
HEPES	4-(2-hydroxyethyl)-1-piperazineethanesulfonic acid
HLA	Human leukocyte antigen
Hpx	Hemopexin domain
HRP	Horseradish peroxidase
IC50	Half maximal inhibitory concentration
Ig	Immunoglobulin
IL	Interleukin
INF-γ	Interferon γ
ITGB1	Integrin β1
kb	Kilo base
kDa	Kilo Dalton
LB	Luria-Bertani
MAP	Mitogen-activated protein
MMP	Matrix metalloproteinases
mRNA	Messenger RNA
MT-MMP	Membrane-type matrix metalloproteinase
N-WASP	Neuronal Wiskott-Aldrich Syndrome protein
NF-κB	Nuclear factor kappa-B
OA	Osteoarthritis
OMIM	Online Mendelian Inheritance in Man
PAGE	Polyacrylamide gel electrophoresis
PBS	Phosphate buffered saline
PCR	Polymerase chain reaction
PET	Polyethylene terephthalate
PFA	Paraformaldehyde
pFc1	pFUSE–rIgG–Fc1 DNA plasmid vector
PKC	Protein kinase C
PVDF	Polyvinylidene difluoride
pY	Phosphotyrosine
qPCR	Quantitative polymerase chain reaction
RANKL	Receptor activator of nuclear factor kappa-B ligand
RASF	Rheumatoid arthritis synovial fibroblasts
RA	Rheumatoid arthritis
RF	Rheumatoid factor
RNA	Ribonucleic acid
rpm	Revolutions per minute
RTK	Receptor tyrosine kinase
SCIT	Single cell invasion tunnel
SDS	Sodium dodecyl sulfate
SD	Standard deviation
SEM	Standard error of the mean
siNT	Non-targeting siRNA transfected cells
siRNA	Small interfering RNA
SPARC	Secreted protein acidic and rich in cysteine

T_H cell	T helper cell
TAE	Tris-acetate-EDTA
TCA	Trichloroacetic acid
TEMED	N,N,N',N'-Tetramethylethylenediamine
TE	Tris-EDTA
TGF-β	Transforming growth factor β
THP	Triple helical peptide
TIMP	Tissue inhibitor of metalloproteinases
TMB	3,3',5,5'-tetramethylbenzidine
Tm	Melting temperature
TNF-α	Tumour necrosis factor α
UV	Ultraviolet
v/v	Volume per volume
VAMP7	Vesicle associated membrane protein 7
VEGF	Vascular endothelial growth factor
vWF	Von Willebrand factor
w/v	Weight per volume
WB	Western blot

Chapter 1

Introduction

1.1 Rheumatoid arthritis

Rheumatoid arthritis (RA) is one of the most common causes of joint disease. It is an autoimmune disorder, characterised by chronic inflammation of multiple diarthrodial joints. Affected joints become stiff, swollen, tender and painful. Chronic inflammation leads to a progressive and irreversible damage of the joint (Lee and Weinblatt, 2001).

In Europe and the United States, around 0.5–1% of the population is affected by RA (Kvien, 2004). In 2010, the committee of American College of Rheumatology and European League Against Rheumatism (ACR/EULAR) published updated classification criteria for RA, which take into account the number of involved joints, duration of symptoms, levels of autoantibodies and acute-phase reactants (Table 1.1) (Aletaha et al., 2010).

Identification of rheumatoid factor (RF), an autoantibody against the Fc portion of an IgG, resulted in classification of RA as an autoimmune disease (Firestein, 2003). However, RF expression is not limited to RA patients. Another autoantibody known as anti-citrullinated protein antibody (ACPA) is more specific for RA and is detected in 70% of patients, who usually show more severe symptoms (Nishimura et al., 2007).

Table 1.1: The 2010 ACR/EULAR classification criteria for RA. Patients with a score of 6 or more are classified as having RA (Aletaha et al., 2010).

Classification criteria	Score
A. Joint involvement	
1 large joint	0
2–10 large joints	1
1–3 small joints (with or without involvement of large joints)	2
4–10 small joints (with or without involvement of large joints)	3
>10 joints (at least 1 small joint)	5
B. Serology	
Negative RF and negative ACPA	0
Low–positive RF or low–positive ACPA	2
High–positive RF or high–positive ACPA	3
C. Acute-phase reactants	
Normal C-reactive protein and normal erythrocyte sedimentation rate	0
Abnormal C-reactive protein or abnormal erythrocyte sedimentation rate	1
D. Duration of symptoms	
less than 6 weeks	0
$\geq$ 6 weeks	1

Despite extensive research, the initial cause of the disease is still unknown. Women are affected 3 times more frequently than men and the average age of onset is around the fifth decade of life (Humphreys et al., 2013). MacGregor et al. (2000) estimated that the heritability of RA is around 60%, which indicates that both genetic and environmental factors play a role in RA pathogenesis. Bronchial stress, such as tobacco smoking, is one of the major environmental risk factors (Padyukov et al., 2004; Silman et al., 1996). The human leukocyte antigen (HLA) locus contributes 30 to 50% of genetic susceptibility to RA (MacGregor et al., 2000). The strongest genetic association was found among alleles of the *HLA-DRB1* gene, which encodes a β-chain of the class II HLA-DR molecules (Raychaudhuri et al., 2012). Risk conferring *HLA-DRB1* alleles have a 'shared epitope': a specific amino acid sequence at positions 70–74 within the antigen binding groove of the HLA-DR β-chain (du Montcel et al., 2005; Gregersen et al., 1987). Recent genome-wide association studies identified many non-HLA loci associated with RA, such as *PTPN22*, *PADI4* or *STAT4*. However, their overall contribution to genetic susceptibility to RA is relatively modest (Ruyssen-Witrand et al., 2012).

Furthermore, RA is a systemic disease and is associated with increased mortality (Gabriel and Michaud, 2009). Systemic manifestations include acute-phase protein production, anaemia, cardiovascular disease and osteoporosis (Choy, 2012). Patients suffer from persistent pain, fatigue, depression and as the disease progresses, they have to face increasing physical disability due to joint damage (Bombardier et al., 2012; Choy, 2012).

At present, RA cannot be effectively cured (Scott, 2012). The goal of therapy is stable remission, which is a prerequisite to stop the joint damage (Lukas et al., 2010). Recently developed therapies which block pro-inflammatory pathways have remarkably improved outcomes of the disease. Nevertheless, it has been reported that in clinical practice less than half of RA patients achieve sustained remission (Prince et al., 2012).

1.1.1 Clinical features

The main sites of disease activity in RA are diarthrodial (synovial) joints, most often those of hands, feet and knees. In a healthy diarthrodial joint, a layer of hyaline cartilage covers the surfaces of articulating bones (Figure 1.1). The cartilage provides a smooth gliding surface, ensures friction-less joint movement and even load distribution onto the subchondral bone (Goldring and Goldring, 2012). A fibrous capsule encloses joint components and forms a joint cavity. The intra-articular part of the capsule is lined with the synovial membrane (synovium), consisting of a cellular lining layer (intima) and collagenous sublining tissue (subintima). The lining layer faces the joint cavity and is one to three cells thick. It predominantly contains fibroblast-like cells, also known as type B synoviocytes, and some macrophage-like cells or type A synoviocytes (Smith, 2011). Sublining tissue contains blood and lymphatic vessels and interspersed sublining fibroblasts. Synovial fibroblasts secrete a hyaluronan-rich, viscous fluid into the joint cavity. They also produce lubricin, a glycoprotein which helps to lubricate the cartilage (Jay et al., 2000).

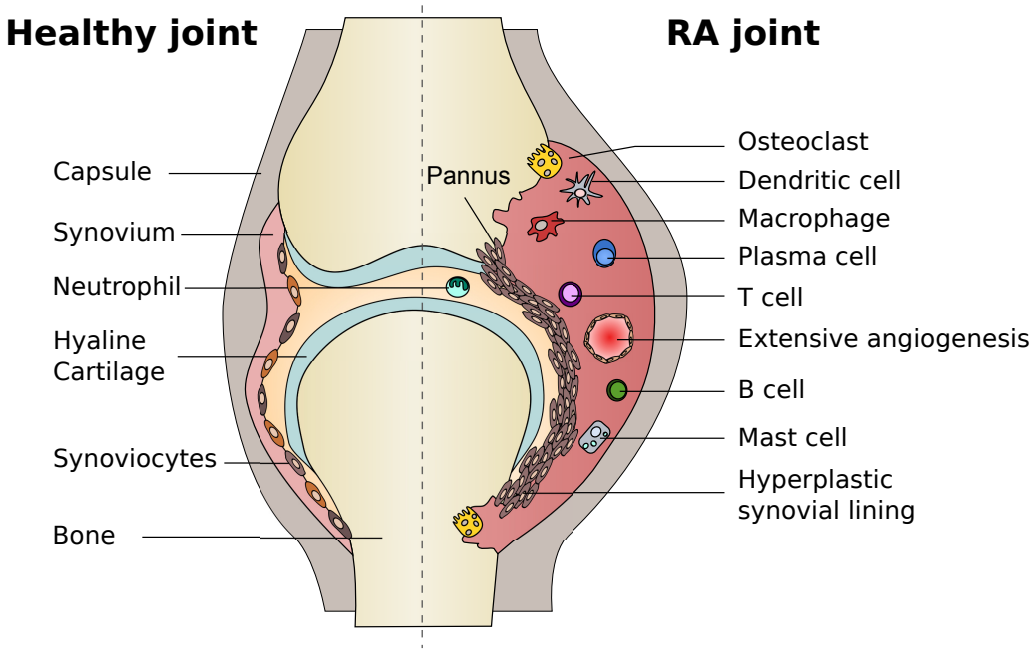

Figure 1.1: Schematic representation of healthy and RA diarthrodial joints. In a healthy joint, the lining layer of the synovial membrane is one to three cells thick. During RA many inflammatory cells infiltrate the synovial membrane including T and B cells. The synovial lining becomes hyperplastic and can be up to 20 cells thick. Membrane overgrowth is supported by angiogenesis. The hyperplastic synovium forms an invasive pannus tissue, rich in synovial fibroblasts and macrophages and also containing activated osteoclasts. The pannus attaches to and degrades cartilage and bone and subsequently invades into those tissues. Figure adapted from Choy (2012).

The hallmark of RA is chronic inflammation and hyperplasia of the synovial membrane. In RA large numbers of immune cells infiltrate the synovial membrane, including T and B cells, plasma cells, macrophages, dendritic cells and mast cells (Figure 1.1) (Hitchon and El-Gabalawy, 2003, 2011). Although not present in the synovium, neutrophils can be found in the synovial fluid. Infiltrated cells become activated and produce a variety of cytokines and growth factors which contribute to the joint inflammation by paracrine and autocrine signalling pathways. There is an overall increase in synoviocyte numbers, due to increased local proliferation or loss of apoptosis, and an additional influx of bone-marrow derived macrophages (Ceponis et al., 1999, 1998; Tohyama et al., 2006). Increased numbers of both types of synoviocytes lead to pronounced hyperplasia of the synovial lining. With

the outgrowth of synovial membrane and chronic inflammation, the joint becomes swollen and painful.

As a result of an influx of immune cells and synovial hyperplasia, the joint environment also becomes hypoxic (Ng et al., 2010). Hypoxia leads to expression of angiogenesis promoting cytokines and growth factors such as vascular endothelial growth factor (VEGF) (Hitchon et al., 2002). Extensive angiogenesis supports further growth of the synovial membrane. At the cartilage and bone junction, where the synovium membrane is attached, the synovial lining expands and forms a characteristic tissue called the pannus (Allard et al., 1990; Kobayashi and Ziff, 1975). The pannus is a highly invasive, tumour-like tissue, which gradually overlays the cartilage and invades deep into the cartilage and bone (Allard et al., 1991; Bromley et al., 1985; Kobayashi and Ziff, 1975; Shiozawa et al., 1983). Synovial fibroblasts and macrophages are predominant cells at the pannus invasion front, but activated osteoclasts can also be found at the sites of bone resorption (Allard et al., 1991; Kobayashi and Ziff, 1975; Miller et al., 2009; Schett, 2007; Shiozawa et al., 1983). These cells gradually invade and degrade the underlaying structures, leading to progressive joint damage and deformity (Allard et al., 1991).

1.1.2 Pathogenesis of RA and available therapies

The exact mode of RA pathogenesis is not completely understood. The proposed mechanism involves activation of both innate and adaptive immunological responses in genetically susceptible individuals (Smolen and Steiner, 2003). One of the initial events is activation of T cells by antigen presenting cells (APCs), such as dendritic cells, macrophages or B cells present in the synovium (Figure 1.2) (Aarvak and Natvig, 2001). APCs present antigens to T-cell receptors in the context of HLA class II molecules. However, the exact antigen or autoantigen has not yet been elucidated (Imboden, 2009; Lundy et al., 2007). The process of T cell activation is augmented by the presence of cytokines and requires co-stimulatory signals mediated

by interaction of T-cell specific surface molecule CD28 with CD80 or CD86 present on APCs (Kotani et al., 2006).

Activated T cells undergo polarisation towards pro-inflammatory T helper type 1 (T_H1) and T_H17 cells, characterised by expression of interferon (IFN)-γ and interleukin (IL)-17 respectively. Few anti-inflammatory T_H2 cells are found in the RA synovium and the imbalance towards T_H1 and T_H17 cell subsets promotes chronic inflammation. B cells and plasma cells produce cytokines, antibodies and autoantibodies, and become additionally activated by T-cell-dependent mechanisms (Mauri and Ehrenstein, 2007). Immune complexes formed of autoantibodies are able to activate complement or cell surface Fc receptors, leading to further release of pro-inflammatory cytokines.

T_H1 and T_H17 cells are able to activate synovial macrophages and fibroblasts via direct cell-to-cell contact and release of INF-γ, tumour necrosis factor (TNF)-α and IL-17. Activated macrophages are the principal source of pro-inflammatory cytokines: TNF-α, IL-1 and IL-6, which play a central role in initiating signalling pathways and perpetuating inflammation (Feldmann et al., 1996; McInnes and Schett, 2011). High levels of these cytokines are present in synovial fluid and serum of RA patients. They activate leukocytes, induce cytokine cascades, increase expression of chemokines, adhesion molecules and matrix degrading enzymes, such as matrix metalloproteinases (MMPs) and a disintegrin and metalloproteinases with thrombospondin motifs (ADAMTSs) in synovial cells and chondrocytes. They also promote differentiation of bone-degrading osteoclasts, thereby directly orchestrating joint damage (Figure 1.2).

Activated synovial fibroblasts secrete cytokines, chemokines and growth factors (such as VEGF) and are the main source of cartilage matrix-degrading enzymes in the joint milieu. They show invasive properties, as they attach to and invade into articular cartilage (Miller et al., 2009; Shiozawa et al., 1983). In addition, they show several signs of tumour-like transformation. They remain activated and highly invasive even in the absence of inflammatory signals. Isolated RA synovial fibroblasts,

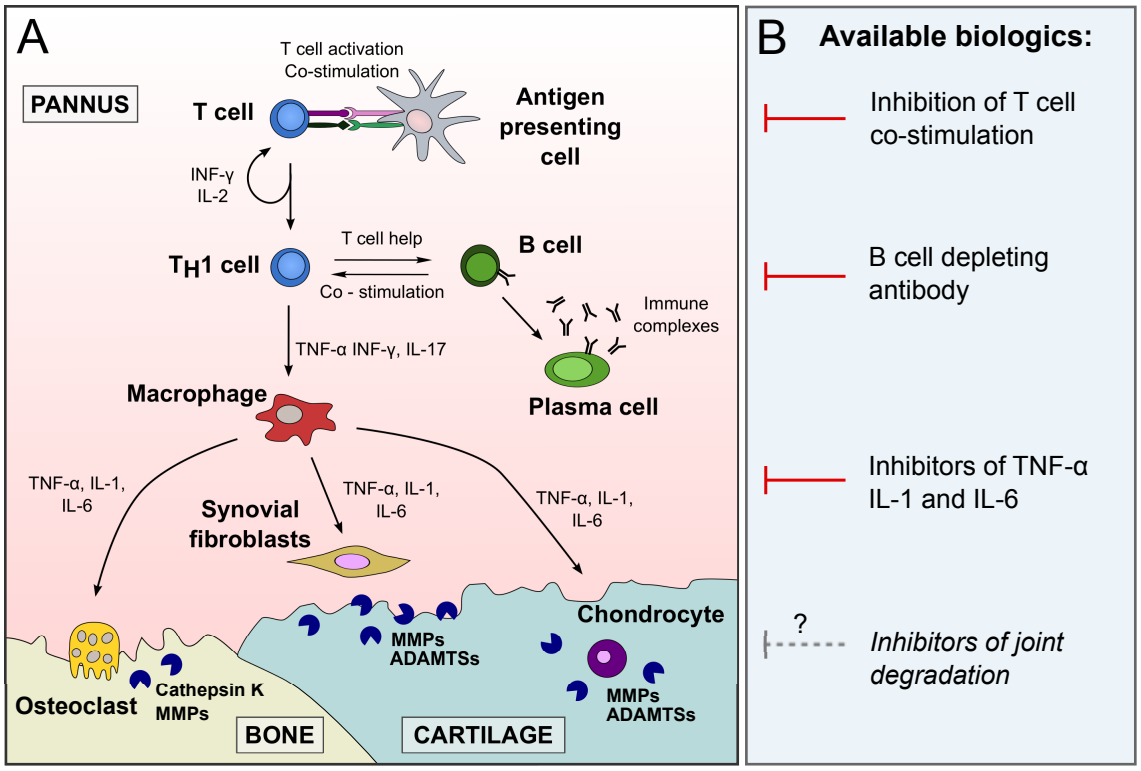

Figure 1.2: Pathogenesis of rheumatoid arthritis. (A) APCs activate T cells, which differentiate mainly to T_H1 cells in a process supported by INF-γ and IL-2. T_H1 cells further activate B cells and macrophages. B cells and plasma cells express antibodies as well as RF and ACPA, which can form immune complexes. TNF-α, IL-1 and IL-6 overexpressed by macrophages activate fibroblasts, chondrocytes and osteoclasts. These cells produce enzymes responsible for cartilage and bone degradation (ADAMTSs, MMPs, cathepsin K). **(B)** Biologics suppress major inflammatory pathways involved in RA pathogenesis, but do not directly inhibit proteolytic enzymes damaging the joint. Figure adapted from Smolen and Steiner (2003).

but not normal or osteoarthritis (OA) synovial fibroblasts, deeply invaded cartilage explants when engrafted into mice with severe-combined immunodeficiency (Ceponis et al., 1998; Müller-Ladner et al., 1996). Somatic mutations in the tumour suppressing gene *TP53* were identified in pannus-derived fibroblasts and lower expression of the tumour suppressive protein PTEN was found in lining layer fibroblasts (Firestein et al., 1997; Pap et al., 2000a; Yamanishi et al., 2005). *In vitro* cultured isolated RA synovial fibroblasts grow in an anchorage independent manner and escape contact inhibition (Lafyatis et al., 1989).

Available therapeutics

The main treatments for RA include disease-modifying anti-rheumatic drugs (DMARDs), which reduce inflammation, joint swelling and slow or halt joint damage. DMARDs can be divided into synthetic small molecule DMARDs and biologics, which are large molecules engineered to target and block inflammatory pathways (Burmester, 2012; Feldmann and Maini, 2008). The first approved biologic was the anti-TNF-α neutralising antibody, infliximab, confirming the central role of TNF-α in RA (Elliott et al., 1994). Since then several types of biologics have been developed, including four additional inhibitors of TNF-α signalling (adalimumab, golimumab, certolizumab and etanercept); an inhibitor of T cell co-stimulation (abatacept); an anti-CD20 B cell depleting antibody (rituximab); an antibody against IL-6 receptor (tocilizumab) and an IL-1 receptor antagonist — anakinra (Figure 1.2B) (Choy et al., 2013). Biologics are most often used in combination therapy with conventional DMARDs. In addition, non-steroidal anti-inflammatory drugs and glucocorticoids are often used to alleviate pain and inflammation.

1.1.3 Characterisation of joint damage in RA

Besides hyperplasia of the synovial membrane, another key feature of RA is erosive degradation of bone and cartilage mediated by cells present in the pannus. Bone and cartilage are two structurally distinct tissues and different mechanisms contribute to their breakdown. Typically, degradation is progressive and irreversible. Clinical data show that the majority of patients develop joint injury within two years of initial symptoms and current therapies are only partially effective in preventing joint damage (Machold et al., 2007).

Bone erosions

Bone is a complex tissue, rich in blood and nerve supply. 70% of the tissue consists of a mineralised inorganic material called hydroxyapatite, 25% of organic material

(mostly collagen type I) and 5% of water. The three major types of cells responsible for tissue homeostasis are bone-producing osteoblasts, bone-degrading osteoclasts and osteocytes residing inside the bone tissue (Schett, 2012).

Localised bone loss initially appears at the bone-pannus junction and is visible as bony erosions on radiographs (Goldring, 2003; Karmakar et al., 2010; Schett and Gravallese, 2012). Resorption of mineralised bone is mediated by activated osteoclasts derived from the pannus tissue (Gravallese et al., 1998). Osteoclasts are multinucleated cells which differentiate from monocyte/macrophage precursors upon activation by receptor activator of nuclear factor kappa-B ligand (RANKL) (Komano et al., 2006; Schett, 2007). Additionally, macrophage colony stimulating factor induces proliferation of osteoclast precursor cells and is required for osteoclast differentiation (Danks et al., 2002). In the RA synovium, RANKL is produced by synovial fibroblasts and T cells (Gravallese et al., 2000; Kotake et al., 2005; Tunyogi-Csapo et al., 2008). TNF-α, IL-1, IL-6 and IL-17 induce expression of RANKL and promote RANKL-mediated osteoclastogenesis (Karmakar et al., 2010). To solubilise the bone matrix, osteoclasts maintain an acidic environment at the cell-matrix junction. In addition, they secrete enzymes such as cathepsin K and MMPs to degrade collagen type I (Delaissé et al., 2003). Infrequent bone repair was observed in some patients receiving combinational DMARD therapy, especially in those without joint swelling (Lukas et al., 2010).

Cartilage degradation

Cartilage is an avascular and an anervous tissue, mainly composed of water (70%) and extracellular matrix (ECM) proteins: collagen type II and aggrecan, which account for 15–25% and 10% of wet weight respectively (Figure 1.3A). Other matrix molecules are collagens type VI, IX, X and XI, link protein, hyaluronan, fibronectin, cartilage oligomeric matrix protein and small leucine-rich proteoglycans (Goldring, 2012). The only cells present in cartilage are chondrocytes, and they account for

1–2% of the tissue volume. Chondrocytes are responsible for cartilage homeostasis as they synthesise, maintain and remodel the ECM (Goldring, 2012).

Collagen type II has a triple helical structure and is assembled into long fibrils, which act as a scaffold for the tissue and provide it with tensile strength. The structure of collagen is described in detail in Section 1.3.2. Aggrecan is the main proteoglycan in the cartilage and it forms large aggregates by non-covalent binding to hyaluronan chains and link protein. Its core protein contains attachment sites for sulfated glycosaminoglycan chains: keratan sulfate and chondroitin sulfate (Figure 1.3B). Their negative charge draws water into the cartilage, creating osmotic pressure and enabling cartilage to withstand compression.

In RA, cartilage is degraded by the invasive synovial pannus tissue which is the source of the majority of proteolytic enzymes. Cytokine-activated macrophages and fibroblasts in the pannus as well as neutrophils in the synovial fluid secrete soluble proteases. Accumulation of these proteases in the synovial fluid surrounding the cartilage results in a degradation of the cartilage matrix. In addition, chondrocytes within cartilage also produce proteases and contribute to tissue destruction. It is believed that aggrecan degradation is one of the initial events in cartilage damage during the development of RA (Nagase and Kashiwagi, 2003; van Meurs et al., 1999). As aggrecan endows cartilage with resistance to compression, loss of this proteoglycan causes major functional defects of the tissue. In addition, aggrecan has been shown to protect cartilage from collagen degradation in experiments *in vitro* (Pratta et al., 2003) and in *in vivo* models of RA (Little et al., 2007).

Aggrecan is cleaved at several sites by ADAMTSs and MMPs. Cleavage within the interglobular domain of aggrecan at $\text{NITEGE}^{373}\downarrow\text{A}^{374}$ by ADAMTSs or at $\text{VDIPEN}^{341}\downarrow\text{F}^{342}$ by MMPs results in release of the glycosaminoglycan-bearing fragment from the cartilage and loss of protein function (Nagase and Kashiwagi, 2003) (Figure 1.3B). Although both neoepitopes (NITEGE and VDIPEN) can be detected in RA cartilage and synovial fluid, ADAMTSs are regarded as the primary

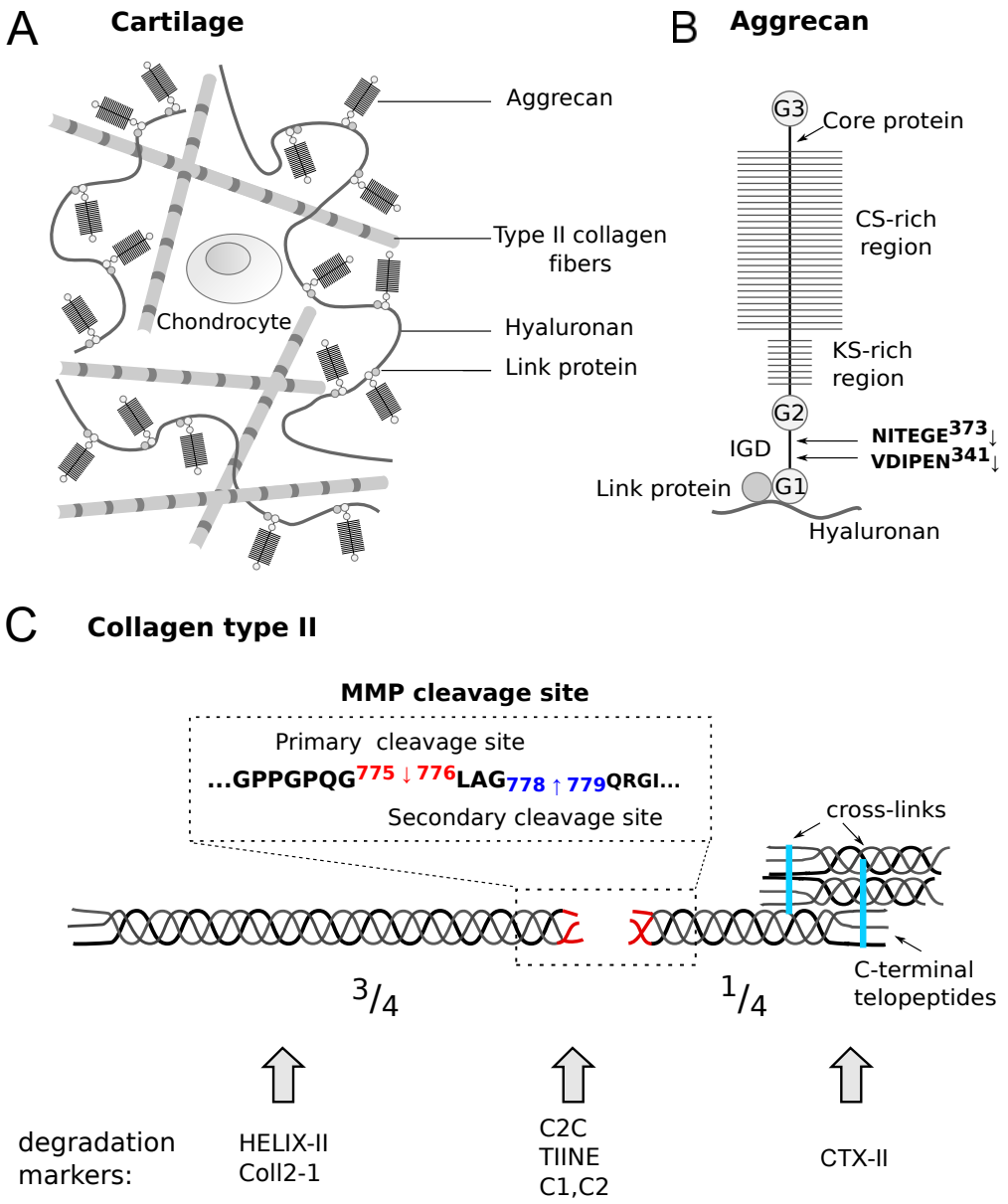

Figure 1.3: Main components of articular cartilage. **(A)** Collagen type II fibrils and large aggregates of aggrecan bound to hyaluronan and link protein are the main components of cartilage. Chondrocytes are the only cell type present in cartilage. **(B)** Aggrecan core protein has three globular domains and it associates with hyaluronan and link protein through its N-terminal globular domain (G1). Negatively charged keratan sulfate and chondroitin sulfate glycosaminoglycan chains are attached to the core protein. Neoepitopes created by MMP (VDIPEN) or ADAMTS (NITEGE) cleavage are indicated. **(C)** Collagen type II is cleaved by MMP collagenases into $^{3}/_{4}$ and $^{1}/_{4}$ fragments. Collagen degradation can be detected by immunoassays recognising $^{3}/_{4}$ fragments (C2C; TIINE; C1,C2), cross-linked C-terminal telopeptides (CTX-II) or fragments of triple helix released by degradation (HELIX-II; Coll2-1). Figure adapted from Nagase and Kashiwagi (2003) and Heinegård (2009). *CS - chondroitin sulfate; G1,G2,G3 - globular domains; IGD - interglobular domain; KS - keratan sulfate.*

aggrecan degrading enzymes (Durigova et al., 2010; Lark et al., 1997; van Meurs et al., 1999).

Initial reports using light and electron microscopy showed marked invasion of the pannus into the cartilage, indicating that this process is primarily responsible for conspicuous tissue loss. Immunohistochemical analysis of cartilage from the patients with advanced RA showed collagen degradation throughout the cartilage tissue, whereas little or no degradation was detected in the normal cartilage (Dodge and Poole, 1989). Electron microscopy confirmed extensive damage to collagen fibrils in the cartilage of RA patients (Dodge et al., 1991). Collagenases from the MMP family are the main collagen-degrading enzymes. They cleave fibrillar collagens (such as collagen type II) into $^{3}/_{4}$ and $^{1}/_{4}$ fragments. Primary MMP cleavage in collagen type II occurs at the $G^{775}{\downarrow}L^{776}$ site and is followed by cleavage at the nearby $G^{778}{\downarrow}Q^{779}$ site, leading to collagen denaturation (Figure 1.3C) (Billinghurst et al., 1997). Numerous immunoassays were developed to detect neoepitopes generated by collagen degradation (Karsdal et al., 2011). Markers used to detect the collagen type II breakdown include C-terminal cross-linked telopeptides (CTX-II), triple helical fragments (HELIX-II, Coll2-1) and MMP-generated neoepitopes in $^{3}/_{4}$ fragments (C2C; C1,C2 and TIINE assays)(Figure 1.3C). The presence of these markers in biological fluids often correlates with RA progression (Garnero et al., 2002; Karsdal et al., 2011; Verstappen et al., 2006).

Cleavage of both aggrecan and collagen severely reduce tissue capability to withstand compressive and mechanical forces. Furthermore, cartilage, unlike bone, has a limited healing potential. Recent clinical data indicate that joint space narrowing, an indicator of cartilage loss, is more strongly correlated with irreversible physical disability than bone damage (Aletaha et al., 2011). Early stages of RA are characterised by reduced synthesis of collagen type II, and additionally IL-1 suppresses proteoglycan production in chondrocytes (Fraser et al., 2003). Aggrecan loss is reversible only in the absence of the collagen damage (Karsdal et al., 2008). The presence of IL-1, IL-17A and reactive nitrogen intermediates induce chondrocyte

apoptosis, which markedly compromises the ability of the cartilage to regenerate (Allard et al., 1991; Goldring and Marcu, 2009; Kobayashi and Ziff, 1975). At present, no specific inhibitors of cartilage damage are available to prevent future disability (Figure 1.2B).

1.1.4 Cartilage degradation in RA is mediated by metalloproteinases

Destruction of the cartilage matrix is mediated by enzymes from two proteinase families: ADAMTSs and MMPs (Rengel et al., 2007). They belong to the metzincin subgroup within the metalloproteinase superfamily (Gomis-Rüth, 2003; Stöcker et al., 1995). The catalytic domains of these enzymes have a conserved HExxHxxGxxH zinc binding motif in their active site (where 'x' is any amino acid). The three histidines coordinate a zinc ion required for hydrolysis. Near the active site, they also have a conserved methionine forming a β-turn.

Many of these metalloproteinases are overexpressed in the RA synovium in response to inflammatory cytokines and upregulated growth factors. TIMPs (tissue inhibitors of metalloproteinases) are endogenous inhibitors of MMPs and some members of ADAM (a disintegrin and metalloproteinase) and ADAMTS families. TIMPs are soluble proteins which inhibit enzymes by forming complexes at a 1:1 ratio. TIMPs have two domains, N-terminal and C-terminal. The N-terminal inhibitory domain binds to the active site of metalloproteinases and inhibits their activity. There are four TIMPs in mammals, namely TIMP-1, -2, -3 and -4 (Brew and Nagase, 2010; Murphy, 2011). Although TIMP expression is also upregulated in RA, it is thought that an imbalance towards matrix-degrading enzymes leads to the degradation of cartilage components (Tchetverikov et al., 2004; Yoshihara et al., 2000). As DMARDs do not directly prevent joint damage, considerable research is focused on proteases responsible for cartilage degradation and on mechanisms regulating their expression.

ADAMTSs

The ADAMTS family consists of 19 members of soluble enzymes expressed in connective tissues and responsible for their homeostasis and remodelling (Fosang et al., 2008; Stanton et al., 2011). ADAMTSs are the major enzymes that degrade proteoglycans including aggrecan, versican, neurocan, brevican and small leucine-rich proteoglycans (Nagase and Kashiwagi, 2003; Stanton et al., 2011). The domain structure of ADAMTSs comprises a signal peptide, a pro-domain, a catalytic domain, a disintegrin-like domain, a central thrombospondin type I repeat, a cysteine-rich region and a spacer domain (Figure 1.4) (Porter et al., 2005). Additional C-terminal thrombospondin type I repeats are also present, with the exception of ADAMTS-4 (Figure 1.4). Enzymes are synthesised as inactive zymogens (pro-enzymes) and are activated during secretion by proprotein convertases such as furin.

Although aggrecan can be cleaved by both ADAMTSs and MMPs, some members of the ADAMTS family appear to be primarily responsible for aggrecan loss in RA (Durigova et al., 2010; Lark et al., 1997). ADAMTS-4 and ADAMTS-5 expressed by synovial fibroblasts and chondrocytes are believed be the major aggrecanases in human cartilage pathology (Fosang et al., 2008; Song et al., 2007; Yamanishi et al., 2002). Aggrecan neoepitopes characteristic for ADAMTS cleavage were identified in patients with RA (Lark et al., 1997). ADAMTSs expression in the cartilage was reported to be induced by cytokines such as IL-1, TNF-α and oncostatin M (Fosang et al., 2008). ADAMTS-5–deficient mice (but not ADAMTS-4–deficient) are protected from cartilage degradation in inflammatory arthritis (Stanton et al., 2005) or OA models (Glasson et al., 2005). It is still not clear whether ADAMTS-5 is the main enzyme responsible for the aggrecan degradation in human RA, as aggrecan loss is induced by both enzymes in human cartilage explants (Song et al., 2007). Activity of these enzymes is inhibited by TIMP-3 and α_2-macroglobulin (Kashiwagi et al., 2001; Tortorella et al., 2004).

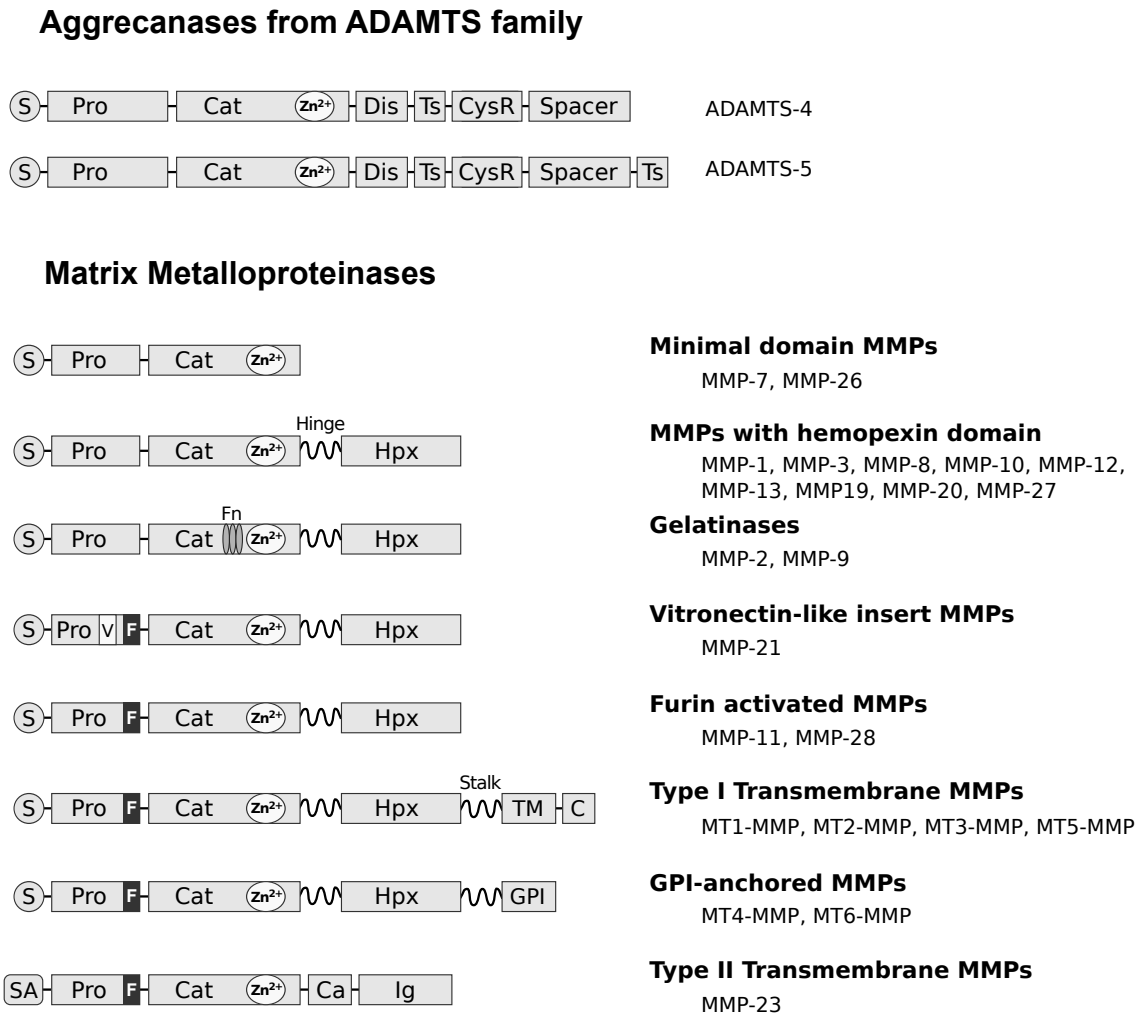

Figure 1.4: ADAMTS and MMP domain structure. Members of ADAMTS and MMP families have similar domain structure: a signal peptide, pro-domain and catalytic domain with conserved Zn^{2+} binding site. ADAMTS-4 and ADAMTS-5 are the major aggrecanases within the ADAMTS family and have an additional disintegrin-like domain, thrombospondin type I repeats, cysteine-rich region and spacer domain. Most MMPs have additional hinge regions and hemopexin domains, with the exception of MMP-7, MMP-23 and MMP-26. Six membrane-bound MMPs (MT-MMPs) are tethered to the plasma membrane via a transmembrane domain or GPI anchor. MMP-23 has a cysteine array region and Ig-like domain. (Troeberg and Nagase, 2012).

MMPs

There are 23 MMPs in humans: 17 soluble-type and 6 membrane-type enzymes (Brinckerhoff and Matrisian, 2002; Murphy and Nagase, 2011). Under physiological conditions MMPs are involved in tissue remodelling as they are able to degrade the complete ECM repertoire, including collagens, proteoglycans, laminins and fibronectin. However, they are often upregulated in pathological conditions such as cancer, OA, RA, and atherosclerosis (Egeblad and Werb, 2002; Page-McCaw et al., 2007).

MMPs share a similar domain structure consisting of a signal peptide, a pro-domain, a catalytic domain, a hinge region (a linker) and a hemopexin domain (Figure 1.4). Six membrane-bound MMPs (membrane type MMPs or MT-MMPs) are tethered to the plasma membrane via a transmembrane domain or a glycophosphatidylinositol (GPI) anchor. Many soluble-type MMPs are synthesised as zymogens and activated extracellularly by enzymatic cleavage of their pro-domain by other MMPs or serine proteases. Some soluble MMPs and all MT-MMPs that harbour a basic amino acid motif at the end of the pro-domain are activated during the secretary pathway by proprotein converting enzymes. While soluble MMPs can be inhibited by all four TIMPs, transmembrane-type MT-MMPs are inhibited by TIMP-2, -3 and -4 but not by TIMP-1.

Fibrillar collagens are resistant to cleavage by many proteinases because of their triple helical structure. The only mammalian enzymes able to efficiently degrade collagen at neutral pH are collagenases belonging to the MMP family. MMP-1, MMP-2, MMP-8, MMP-13 and membrane type I MMP (MT1-MMP or MMP-14) are able to cleave collagen into $^3/_4$ and $^1/_4$ fragments (Page-McCaw et al., 2007).

Many MMPs are highly upregulated in RA synovium, both at the mRNA and protein level. Synovial fibroblasts are the main source of MMPs in the RA joint and produce MMP-1, -2, -3, -9, -13, MT1-MMP and MT3-MMP (Murphy and Nagase, 2008). Cytokines such as IL-1, TNF-α, IL-17 and oncostatin M upregulate

expression of many MMPs (Murphy and Nagase, 2008). High levels of MMP-1, MMP-3, MMP-8, MMP-9 and MMP-13 are often found in synovial fluid of RA patients (Tchetverikov et al., 2004; Yoshihara et al., 2000). MMP-1 and MMP-3 are among the most upregulated and are also found in serum (Andereya et al., 2006; Garnero et al., 2002; Tchetverikov et al., 2004). In a study by Soto et al. (2008), analysis of a gene expression array from human RA synovial membranes showed over 250-fold upregulation of MMP-1 mRNA. However, the precise role of these MMPs in RA progression is not well understood.

Recently, MT1-MMP has been reported as a pivotal collagenase during cartilage invasion by the synovial pannus in RA joints (Miller et al., 2009; Sabeh et al., 2010). Its expression is upregulated in RA synovium (Konttinen et al., 1999a; Miller et al., 2009; Pap et al., 2000b; Soto et al., 2008; Yamanaka et al., 2000). Synovial fibroblasts in the RA pannus tissue express high levels of MT1-MMP, which promotes collagen degradation and cartilage invasion (Miller et al., 2009; Rutkauskaite et al., 2005; Sabeh et al., 2010). It has been shown that knockdown of MT1-MMP, but not other MMP collagenases, resulted in decreased invasion of RA synovial fibroblasts into cartilage explants (Sabeh et al., 2010). These data suggest that MT1-MMP is a crucial collagenolytic enzyme that promotes cartilage invasion by synovial fibroblasts.

1.2 Membrane type 1 matrix metalloproteinase

1.2.1 Domain structure of MT1-MMP

MT1-MMP shares similar domain structure with other MMPs and consists of a pro-domain with a signal peptide (M^{1}–R^{111}), a catalytic domain (Y^{112}–G^{285}), a hinge region (linker 1) (E^{286}–I^{318}), a hemopexin domain (C^{319}–C^{508}), a stalk region (linker 2) (P^{509}–S^{538}), a transmembrane domain (A^{539}–F^{562}) and a cytoplasmic tail (R^{563}–V^{582}) (Figure 1.5) (Itoh and Seiki, 2006).

MT1-MMP is synthesised as a pre-proenzyme to allow secretion. The signal peptide is cleaved within the endoplasmic reticulum, resulting in a latent pro-enzyme (Nagase et al., 2006). The remaining pro-domain of MT1-MMP contains a conserved amino acid motif PR$\underline{C}^{93}$GVPD - the 'cysteine switch' (Wart and Birkedal-Hansen, 1990). The cysteine (underlined) in this motif interacts with the active-site zinc, keeping the enzyme inactive. Proteolytic activation of MT1-MMP occurs within the trans-Golgi network by furin and related proprotein convertases, which cleave the inhibitory pro-domain. Furin recognises and cleaves the $RRKR^{111}{\downarrow}Y^{112}$ sequence located at the junction of the pro-peptide and catalytic domain (Figure 1.5) (Sato et al., 1996; Yana and Weiss, 2000). Active MT1-MMP is then secreted to the cell

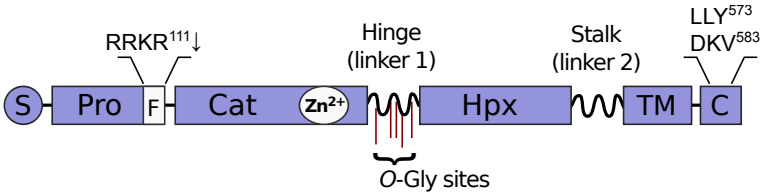

Figure 1.5: Domain organisation of MT1-MMP. MT1-MMP domain structure includes a signal peptide (***S***), a pro-domain (***Pro***), a catalytic domain with Zn^{2+} binding site (***Cat***), a hinge region (linker 1), a hemopexin domain (***Hpx***), a stalk (linker 2), a transmembrane domain (***TM***) and a short cytoplasmic tail (***C***). Furin (***F***) cleavage site at $RRKR^{111}$ sequence is located at the pro-domain–catalytic domain junction. In the hinge region five *O*-glycosylation (***O*-Gly**) sites were identified. LLY^{573} is a binding motif for the µ2 subunit of AP-2 and the DKV^{583} sequence is required for MT1-MMP recycling to the cell surface. Figure adapted from Itoh (2006).

surface, where it forms a homodimer with another MT1-MMP by non-covalent association between their hemopexin domains (Itoh et al., 2001; Lehti et al., 2002) and transmembrane domains (Itoh et al., 2008). The crystal structure and mutagenesis of MT1-MMP hemopexin domain revealed symmetrical interaction of those domains (Tochowicz et al., 2011). Dimerisation was found to be an important regulatory mechanism of MT1-MMP function (See Section 1.2.10).

1.2.2 MT1-MMP function

MT1-MMP is broadly expressed in different tissues including heart, lung, liver, placenta, muscle, kidney and pancreas (Takino et al., 1995). Its expression is induced during tissue remodelling: in endothelial cells during angiogenesis (Yana et al., 2007), in fibroblasts and keratinocytes during skin wound healing (Okada et al., 1997; Zigrino et al., 2012). MT1-MMP is the major activator of proMMP-2 *in vivo* (See Section 1.2.6) and both enzymes are often co-expressed (Nuttall et al., 2004). Mutations in human *MMP-2* (Martignetti et al., 2001) or *MT1-MMP* genes (Evans et al., 2012) cause the rare Winchester or 'vanishing bone' syndrome, characterised by multicentric osteolysis, short stature and arthritis (OMIM: 259600).

The essential role of MT1-MMP in bone development and tissue remodelling is reflected by the profound phenotype of MT1-MMP deficient mice. *Mt1-mmp* $^{-/-}$ mice are viable; however, soon after birth they develop severe abnormalities due to impaired collagen turnover: soft tissues fibrosis, systemic arthritis, osteopenia, skeletal defects, dwarfism and they die within a few weeks (Holmbeck et al., 1999, 2005, 2004; Zhou et al., 2000). The finding that knock-out of no other *Mmp* results in such severe defects emphasises the indispensable role of MT1-MMP during postnatal development (Holmbeck et al., 1999; Page-McCaw et al., 2007).

MT1-MMP was also shown to play an important role in angiogenesis. Zhou et al. (2000) reported defective vascularisation of chondroepiphyses in *Mt1-mmp* $^{-/-}$ mice and lack of neovascularisation in a cornea angiogenesis assay. During angio-

genesis MT1-MMP is expressed in endothelial tip cells and it mediates collagen degradation at the sites of developing neovessels (Yana et al., 2007). MT1-MMP is also involved in many other processes, including kidney development (Riggins et al., 2010), generation of white adipose tissue (Chun et al., 2006) and differentiation of B cells in the bone marrow (Jin et al., 2011).

The role of MT1-MMP in cancer has been extensively investigated. High expression of MT1-MMP was detected in many cancers including ovarian (Adley et al., 2009), breast (Jiang et al., 2006; Okada et al., 1995; Perentes et al., 2011), pancreatic (Määttä et al., 2000), cervical (Gilles et al., 1996), head and neck (Okada et al., 1995), prostate (Cardillo et al., 2006), neuroblastoma (Zhang et al., 2012) and colon (Kanazawa et al., 2010; Okada et al., 1995). MT1-MMP was also detected in cancer-associated stromal cells: fibroblasts, macrophages and endothelial cells (Afzal et al., 1998; Bisson et al., 2003; Ohtani et al., 1996; Okada et al., 1995; Polette et al., 1997, 1996). Upregulation of MT1-MMP correlates with the presence of invasive, more aggressive tumours, increased tumour growth, lymph node metastasis and poorer outcome (Hotary et al., 2003; Jiang et al., 2006; Kamat et al., 2006; Sato et al., 1994; Zhang et al., 2012).

1.2.3 Transcriptional regulation

Tissue remodelling requires stringent transcriptional regulation of proteolytic enzymes such as MT1-MMP. Although several research groups investigated transcriptional regulation of MT1-MMP, mechanisms regulating its expression are not yet established, especially *in vivo*. Analysis of the promoter region of *MT1-MMP* gene by Lohi et al. (2000) showed a lack of a conserved TATA sequence and AP-1 binding site, which are present in many MMP promoters. As no TATA box is present, MT1-MMP transcription starts at multiple sites (Lohi et al., 2000). In contrast to other MMPs, MT1-MMP gene expression is not induced by inflammatory cytokines or growth factors (Yan and Boyd, 2007).

A proximal GC box at −92bp relative to the putative transcription start site maintains binding of Sp-1 transcription factor which is required for basal promoter activity (Lohi et al., 2000; Petrella et al., 2005; Sroka et al., 2007). A binding site for Egr-1 transcription factor, which partially overlaps with the Sp-1 site, was also identified as an important inducer of MT1-MMP expression in several cell types including ovarian carcinoma cells (Barbolina et al., 2007), *v-src* transformed Madin–Darby canine kidney cells (Cha et al., 2000) and endothelial cells (Haas et al., 1999; Yun et al., 2002). In a study conducted by Petrella et al. (2005) in von Hippel-Lindau renal cell carcinoma, cooperative binding of Sp-1 and HIF-2α is required for maximal induction of MT1-MMP expression under hypoxic conditions. β-catenin/Tcf-4 binding to the *MT1-MMP* promoter was reported in the human SW480 colorectal cancer cell line (Takahashi et al., 2002). A putative binding site for nuclear factor kappa B (NF-κB) was also found in the 5' flanking region and NF-κB signalling was implicated in induction of MT1-MMP expression in skin fibroblasts stimulated with TNF-α and collagen type I (Han et al., 2001). However, the effect of TNF-α on MT1-MMP expression is not consistent between different cells and investigators, and thus it is yet to be proven if this NF-κB binding site is truly functional.

1.2.4 Post-translational modifications

Several modifications of amino acid residues within MT1-MMP have been reported. Five *O*-glycosylation sites at T^{291}, T^{299}, T^{300}, S^{301} and S^{304} were identified within the hinge region of MT1-MMP (Figure 1.5) (Remacle et al., 2006; Shuo et al., 2012; Wu et al., 2004). *O*-glycosylation was suggested to protect MT1-MMP from auto-catalytic degradation and to be required for proMMP-2 activation, at least in some cell types (Remacle et al., 2006; Wu et al., 2004). Another modification was found in the cytoplasmic domain. It was reported that cysteine (C^{574}) in the cytoplasmic tail was palmitoylated and this lipid modification was shown to be essential for

its clathrin-dependent endocytosis and cell migration promoting activity (Anilkumar et al., 2005). Ubiquitination of another cytoplasmic residue – L^{581}, regulates MT1-MMP trafficking and promotes invasion in three-dimensional (3D) collagen matrices (Eisenach et al., 2012). Several reports show that cytoplasmic tyrosine Y^{573} becomes phosphorylated by Src kinase and that phosphorylation is required for cell motility, collagen gel invasion, MT1-MMP-induced VEGF-A expression and tumour growth (Eisenach et al., 2012; Nyalendo et al., 2008, 2007; Wang and McNiven, 2012; Williams and Coppolino, 2011).

1.2.5 Substrate specificity

Major MT1-MMP substrates include fibril-forming collagens type I, II and III. Like other MMP collagenases, MT1-MMP cleaves fibrillar collagens into characteristic $^3/_4$ and $^1/_4$ fragments (Ohuchi et al., 1997). ECM substrates of MT1-MMP are listed in Table 1.2.

Table 1.2: Summary of ECM substrates of MT1-MMP.

Extracellular matrix proteins	**Reference**
fibril-forming collagens (type I, II, III)	Ohuchi et al. (1997)
gelatin	Ohuchi et al. (1997)
fibronectin	d'Ortho et al. (1997); Ohuchi et al. (1997)
vitronectin	Ohuchi et al. (1997)
laminin 1	Ohuchi et al. (1997)
laminin 2/4	Ohtake et al. (2006)
laminin 5 γ2 chain	Koshikawa et al. (2000, 2004)
laminin 10	Bair et al. (2005)
aggrecan	d'Ortho et al. (1997)
fibrin and fibrinogen	Bini et al. (1999); Hotary et al. (2002)
perlecan	d'Ortho et al. (1997)
lumican	Li et al. (2004)
tenascin	d'Ortho et al. (1997)
nidogen	d'Ortho et al. (1997)

Apart from ECM degradation, MT1-MMP was shown to shed several ECM receptors, such as CD44, the major hyaluronan receptor on the cell surface. CD44 shedding by MT1-MMP was demonstrated to stimulate cell migration (Kajita et al., 2001). Furthermore, shed forms of CD44 and MT1-MMP were co-localised in tissue specimens of oral, gastric and hepatic tumours, suggesting that CD44 shedding by MT1-MMP contributes to progression of these cancers (Nakamura et al., 2004). MT1-MMP was also reported to shed syndecan 1 (Endo et al., 2003) and cell surface tissue transglutaminase (Belkin et al., 2001). It also processes α_v integrin (Deryugina et al., 2002; Ratnikov et al., 2002). MT1-MMP also cleaves the cell-cell adhesion receptors N- and E-cadherins and low-density lipoprotein receptor-related protein-1, a plasma membrane endocytic and signalling receptor (Covington et al., 2006; Rozanov et al., 2004; Selvais et al., 2011). MT1-MMP can also degrade other membrane proteins such as RANKL (Hikita et al., 2006), pro-angiogenic semaphorin 4D (Basile et al., 2007), transmembrane mucin glycoprotein MUC1 (Thathiah and Carson, 2004) or protein tyrosine kinase-7 (Golubkov et al., 2010).

MT1-MMP was also shown to proteolytically modify cytokines, chemokines and growth factors, resulting in either pro- or anti-inflammatory responses. It was shown that MT1-MMP activates as well as degrades proTNF-α (d'Ortho et al., 1997; Tam et al., 2004). It cleaves chemokines such as stromal cell-derived factor-1 (McQuibban et al., 2001), monocyte chemoattractant protein-3 (McQuibban et al., 2002) and processes latent transforming growth factor β (Karsdal et al., 2002; Mu et al., 2002). However, the significance of these events *in vivo* is yet to be elucidated.

The sequence specificity of MT1-MMP was investigated using peptide phage display libraries. MT1-MMP recognises the consensus sequence PXX'$\downarrow X_{Hy}$ at substrate's P_3–P_1' sites, which is present in collagens (Jabaiah and Daugherty, 2011; Kridel et al., 2002; Ohkubo et al., 1999). Hydrophobic residues (X_{Hy}) like leucine or isoleucine are often present at P_1'. This consensus sequence is not-specific for MT1-MMP as it is recognised by many other MMPs, including MMP-2 and MMP-9. Highly selective substrates were subsequently identified (Kridel et al., 2002).

Although no clear consensus sequence has been found, cleaved peptides often contained arginine at the P_4 position, a hydrophobic residue at P_1' and lacked proline at P_3 (Kridel et al., 2002). This indicates that MT1-MMP has two substrate binding modes, one unique and one common with other MMPs (Kridel et al., 2002).

1.2.6 ProMMP-2 activation by MT1-MMP

One of the major functionalities of MT1-MMP is activation of proMMP-2 on the cell surface. MT1-MMP was originally identified as a cellular activator of proMMP-2 (Sato et al., 1994; Strongin et al., 1995). Since then, the mechanism of MT1-MMP-dependent proMMP-2 activation have been extensively investigated and it has been revealed that proMMP-2 activation by MT1-MMP is not a simple enzyme-substrate interaction, but involves several protein-protein interactions and requires the presence of TIMP-2 (Figure 1.6).

First, the N-terminal domain of TIMP-2 binds to the active site of MT1-MMP and forms an enzyme-inhibitor complex. The exposed C-terminal domain of the TIMP-2 has an affinity for the hemopexin domain of proMMP-2. Therefore, the MT1-MMP–TIMP-2 complex can act as a receptor for proMMP-2, resulting in formation of an MT1-MMP–TIMP-2–proMMP-2 tri-molecular complex on the cell surface. Because the catalytic site of the MT1-MMP is inhibited by TIMP-2, another MT1-MMP molecule needs to be present in close proximity to this complex to proteolytically activate proMMP-2. This is achieved by homodimerisation of MT1-MMP and formation of proMMP-2–TIMP-2–$(\text{MT1-MMP})_2$ complex (Itoh et al., 2001). Active (TIMP-2 'free') MT1-MMP in this complex cleaves within the pro-domain of MMP-2 between N^{37} and L^{38}. This results in a partially activated intermediate form of MMP-2, which is then released. Subsequent intermolecular auto-processing generates fully active MMP-2. ProMMP-2 activation is thought to be particularly important for cancer cell invasion into basement membranes as MT1-MMP does not degrade its major component, type IV collagen, but activated

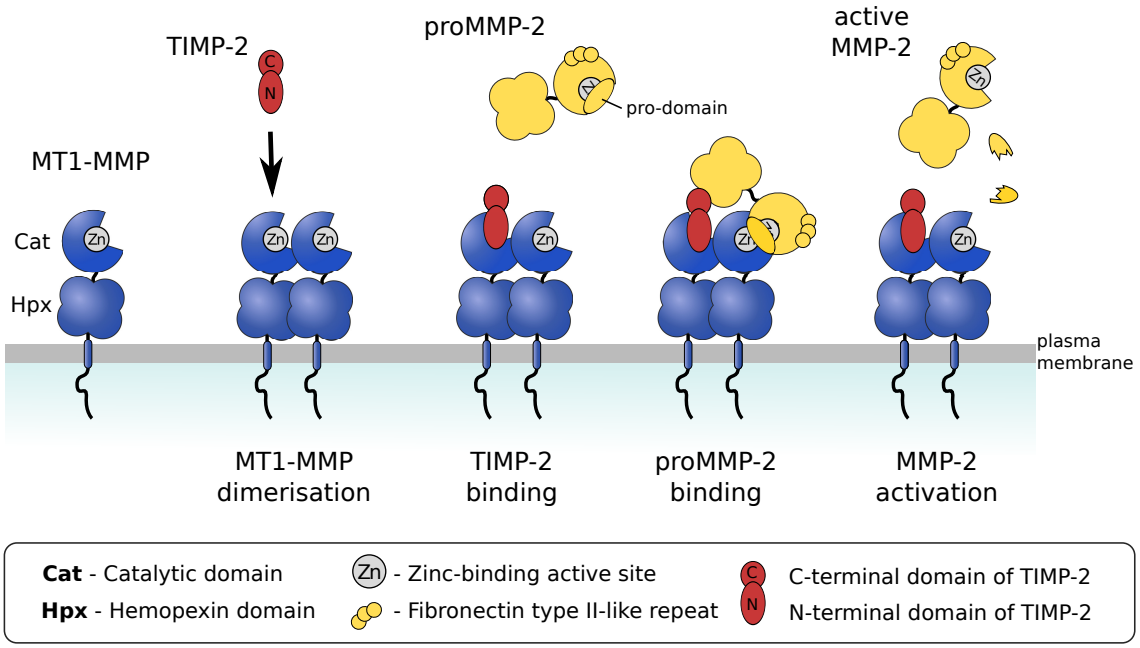

Figure 1.6: Mechanism of proMMP-2 activation by MT1-MMP. MT1-MMP is present on the cell surface as an active enzyme and forms a dimer with other MT1-MMP molecules through the hemopexin domain. Catalytic domain of MT1-MMP binds N-terminal domain of TIMP-2. TIMP-2 in this complex binds hemopexin domain of proMMP-2, and another, active MT1-MMP in the complex cleaves the pro-domain of MMP-2 and the active enzyme is released.

MMP-2 does (Taniwaki et al., 2007). In addition to proMMP-2, MT1-MMP was also shown to activate proMMP-13 (Knäuper et al., 2002). The mechanism of proMMP-13 activation is not fully understood, but Knäuper et al. (2002) showed that it is a TIMP-2-independent process.

1.2.7 Autocatalytic processing

The presence of an active MT1-MMP on the cell surface results in its auto-degradation and formation of 18 kDa soluble and 44 kDa inactive, membrane-bound MT1-MMP species (Lehti et al., 1998; Stanton et al., 1998). The cleavage occurs at $G^{284}{\downarrow}G^{285}$ in the hinge region, resulting in a loss of the catalytic domain from the cell surface (Hernandez-Barrantes et al., 2000; Toth et al., 2002). Processed forms of MT1-MMP are correlated with high activity of MT1-MMP on the cell surface and with proMMP-2 activation (Stanton et al., 1998). Membrane-bound 44 kDa MT1-MMP

species were detected in cells expressing either endogenous (Ellerbroek et al., 1999; Stanton et al., 1998) or recombinant MT1-MMP (Cho et al., 2008; Hernandez-Barrantes et al., 2000; Lehti et al., 1998). These were also found in rheumatoid arthritis synovial tissue extracts (Konttinen et al., 1998), platelets (Kazes et al., 2000) and in cancer cell lines (Ellerbroek et al., 1999; Stanton et al., 1998).

1.2.8 MT1-MMP inhibitors

MT1-MMP activity can be inhibited by endogenous tissue inhibitors of metalloproteinases including TIMP-2, TIMP-3 and TIMP-4, whereas TIMP-1 is a poor inhibitor for MT1-MMP (Seiki, 2003). Other endogenous inhibitors include GPI-anchored reversion-inducing cysteine-rich protein with Kazal motifs (Oh et al., 2001) and testican family proteoglycans (Nakada et al., 2001).

As MMPs are considered responsible for tissue destructive processes in diseases such as cancer and arthritis, pharmaceutical companies developed several broad-spectrum, synthetic MMP inhibitors including ilomastat (GM6001) or marimastat (BB2516). These are small molecule, peptide-based MMP inhibitors, containing a hydroxamate group which chelates the zinc ion in the active site of the enzymes. Unfortunately, during clinical trials they showed low efficacy and significant side effects including musculoskeletal pain and joint stiffness (Fingleton, 2008). It is now considered that the side effects are due to the non-selective nature of these inhibitors. There are more than 60 metalloproteinases that share similar topology of their active site and most of them could be inhibited by these compounds. Thus it is important to identify the target enzyme and inhibit it in a highly selective manner.

The biopharmaceutical company Dyax Corp created a humanised anti–MT1-MMP inhibitory antibody named DX-2400 (Devy et al., 2009). DX-2400 is highly selective and does not block activity of other MMPs. It was shown that DX-2400 in-

hibited the biological functions of MT1-MMP and inhibited cancer invasion, metastasis, growth and angiogenesis using *in vitro* and *in vivo* models (Devy et al., 2009).

1.2.9 Trafficking and cell surface localisation of MT1-MMP

MT1-MMP on the cell surface is readily internalised by clathrin- and caveolae-dependent processes (Figure 1.7) (Gálvez et al., 2004; Jiang et al., 2001; Remacle et al., 2003; Uekita et al., 2001). The main route of MT1-MMP uptake is via clathrin-coated membrane pits and is dependent on interaction of the LLY^{573} motif in the cytoplasmic tail of MT1-MMP with the µ2 subunit of adaptor protein (AP)-2 (Figure 1.5). AP-2 binding initiates clathrin attachment and formation of endocytic vesicles (Uekita et al., 2001). Clathrin-mediated endocytosis is very rapid and the half-life of MT1-MMP on the cell surface is reportedly less than 30 minutes (Anilkumar et al., 2005; Uekita et al., 2001). A second route of MT1-MMP internalisation is via caveolae, which are flask-shaped, cholesterol-rich membrane domains associated with caveolin 1 protein (Annabi et al., 2001; Gálvez et al., 2004; Remacle et al., 2003). Caveolae-dependent endocytosis is much slower and it has been shown that the half-life of mutant MT1-MMP with defects in clathrin-mediated endocytosis is around one hour (Anilkumar et al., 2005).

Once internalised, MT1-MMP-containing vesicles are fused to early endosome and late endosomal/lysosomal compartments (Figure 1.7) (Eisenach et al., 2012; Jiang et al., 2001; Remacle et al., 2003, 2005; Steffen et al., 2008; Takino et al., 2003; Wang et al., 2004b; Williams and Coppolino, 2011). MT1-MMP can be then recycled back to the cell surface or degraded within lysosomes (Remacle et al., 2003; Steffen et al., 2008; Takino et al., 2003; Wang et al., 2004b; Williams and Coppolino, 2011). It has been shown that recycling of MT1-MMP is dependent on the DKV^{582} motif at the end of the cytoplasmic tail (Wang et al., 2004c) Recently it was also reported that K^{581} within this motif is mono-ubiquitinated, and lack of this modification decreased cell surface levels of MT1-MMP (Figure 1.5) (Eisenach et al., 2012). Whether these

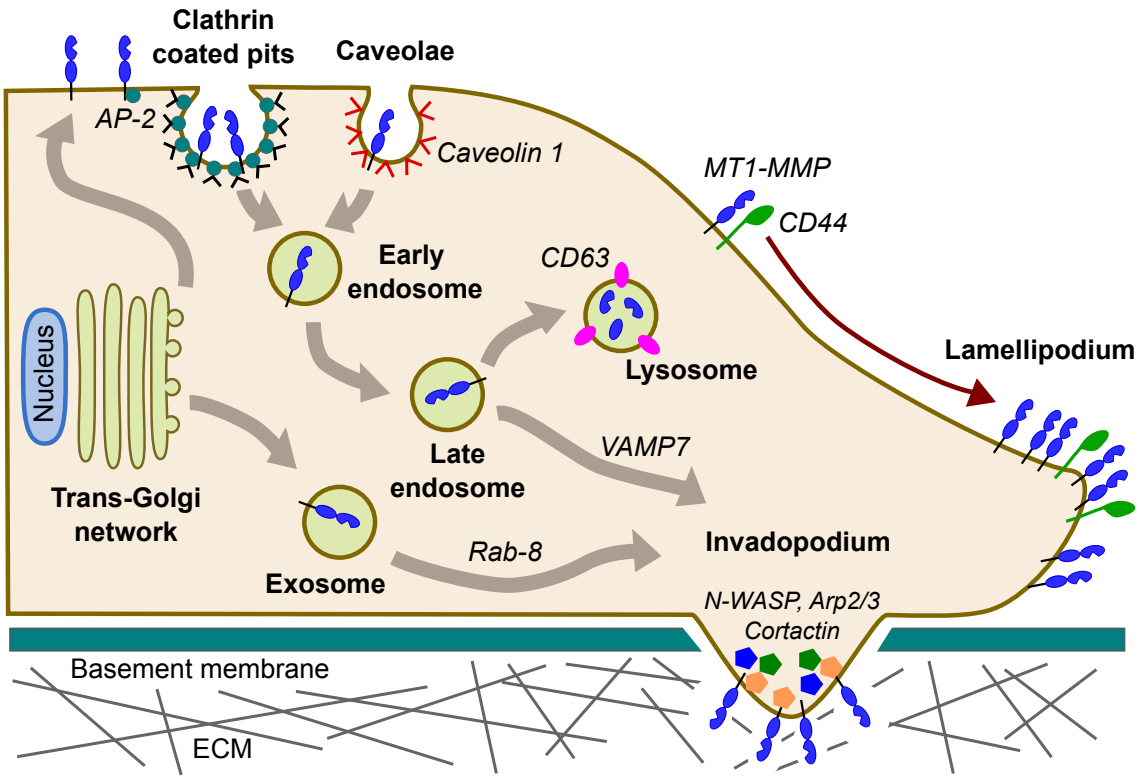

Figure 1.7: Endocytosis and intracellular trafficking of MT1-MMP. The main routes of MT1-MMP endocytosis are through clathrin- or caveolae-dependent mechanisms. Internalised MT1-MMP can be then degraded in CD63-positive lysosomes or recycled back to the cell surface. The enzyme is targeted to lamellipodia and invadopodia, where ECM degradation occurs. Figure adapted from Frittoli et al. (2011); Itoh and Seiki (2006) and Poincloux et al. (2009).

two findings are related or not is still to be confirmed. Association of MT1-MMP with tetraspanin transmembrane protein CD63 induces trafficking of MT1-MMP-containing vesicles into lysosomes and promotes its degradation (Takino et al., 2003). On the other hand, it has been reported that a significant portion of MT1-MMP is stored in intracellular compartments (Li et al., 2008; Remacle et al., 2003; Williams and Coppolino, 2011). It is possible that this intracellular pool of MT1-MMP is for rapid delivery to the cell surface when its activity is required.

MT1-MMP has been shown to localise at motility-associated membrane structures. Invadopodia are one such structure and are characterised as actin-rich membrane protrusions where focal degradation of ECM occurs (Murphy and Courtneidge, 2011). MT1-MMP is considered a marker of invadopodia formation, as

it accumulates at these structures and mediates ECM degradation (Artym et al., 2006; Steffen et al., 2008). MT1-MMP co-localises with cortactin which, together with N-WASP (neuronal Wiskott–Aldrich Syndrome protein) and Arp2/3 complex, promotes actin polymerisation and formation of mature invadopodia (Figure 1.7) (Artym et al., 2006; Ridley, 2011). Trafficking of MT1-MMP to invadopodia is thought to be mediated by transport of MT1-MMP-containing secretory vesicles on microtubules (Ridley, 2011). In late endosome/lysosomal compartments, MT1-MMP co-localises with VAMP7 (vesicle associated membrane protein 7), a membrane protein required for delivery and fusion of vesicles to their target membranes (Steffen et al., 2008; Williams and Coppolino, 2011). VAMP7 was reported to regulate exocytosis of MT1-MMP and deliver it to invadopodia (Steffen et al., 2008; Williams and Coppolino, 2011). MT1-MMP accumulation at plasma membrane areas attached to collagen substrate was also reported (Bravo-Cordero et al., 2007). Enrichment of MT1-MMP at these sites is though to be through Rab8-mediated exocytosis of MT1-MMP-containing vesicles from the endosome (Bravo-Cordero et al., 2007).

Another motility-associated membrane structure where MT1-MMP is localised is the lamellipodium, a migration front of the cell cultured on a two-dimensional (2D) substrate (Mori et al., 2002). It has been reported that targeted localisation to lamellipodia is mediated by interaction of MT1-MMP with CD44, through the hemopexin domain of the enzyme and the stalk region of CD44. This interaction results in indirect association of MT1-MMP with the actin cytoskeleton, as CD44 binds F-actin-associated ezrin/radixin/moesin (ERM) proteins (Mori et al., 2002).

1.2.10 Dimerisation as a regulatory mechanism

Another mechanism regulating MT1-MMP activity is homo-dimerisation. On the cell surface MT1-MMP forms dimers and oligomers, which are required for its two fundamental functions: proMMP-2 activation and collagen degradation (Itoh et al.,

2006, 2001; Lehti et al., 2002). It was reported that MT1-MMP dimerisation at lamellipodia and filopodia (thin, actin-rich membrane protrusions) was controlled by the small GTPases Rac1 and Cdc42. In cells migrating in collagen gels, dimerisation was always detected at the cells' migration front (Itoh et al., 2011).

MT1-MMP forms a dimer through both its hemopexin domain and transmembrane domain, but the primary dimer interface is thought to be through hemopexin domains (Itoh et al., 2008, 2001). The recent crystal structure of MT1-MMP hemopexin domain shows that it has a β-propeller structure with four blades, with an overall disc-like shape similar to other MMPs (Tochowicz et al., 2011). In this report, the dimer interface between the hemopexin domains was also identified. Two hemopexin domains form a symmetrical interaction through blades II and III, which is facilitated by residues $D^{385,}$ K^{386}, T^{412} and Y^{436}. Hemopexin domain-mediated dimerisation was reported to be crucial for cell surface collagen film degradation, collagen invasion and *in vivo* tumour growth (Itoh et al., 2006, 2008; Remacle et al., 2012; Wang et al., 2004a). ProMMP-2 activation, however, is not dependent on hemopexin-mediated dimer formation (Itoh et al., 2008; Remacle et al., 2012; Wang et al., 2004a), but on transmembrane domain-mediated dimerisation (Itoh et al., 2008).

1.2.11 Role of MT1-MMP in cellular invasion

MT1-MMP emerged as a central pericellular collagenase. Although overexpression of MT1-MMP as well as MT2-MMP and MT3-MMP (but not soluble MMPs) results in acquisition of the ability to invade basement membranes or fibrin gels, only MT1-MMP expression supports collagen type I degradation and invasion (Hotary et al., 2006, 2002). Cells derived from *Mt1-mmp*$^{-/-}$ mice are unable to degrade collagen and that defect cannot be rescued by other collagenases (Holmbeck et al., 1999). Degradation of collagen matrix has been reported to depend solely on MT1-MMP in a variety of cells, including skin fibroblasts (Holmbeck et al., 1999; Madsen et al.,

2007; Sabeh et al., 2009a, 2004; Zhang et al., 2006b), pulmonary fibroblasts (Rowe et al., 2011), cardiac fibroblasts (Koenig et al., 2012), endothelial cells (Chun et al., 2004), vascular smooth muscle cells (Filippov et al., 2005), human mesenchymal stem cells (Lu et al., 2010) and rheumatoid synovial fibroblasts (Miller et al., 2009; Sabeh et al., 2010).

For MT1-MMP to promote collagen invasion, anchoring to the membrane appears to be a crucial feature (Hotary et al., 2000; Sabeh et al., 2009a, 2004). However, simply anchoring a collagenase to the membrane does not make this enzyme a promotor of invasion. When soluble MMP-13 was fused with the transmembrane and cytoplasmic domains of MT1-MMP, cells expressing this chimera were not able to degrade collagen. (Itoh et al., 2006). Addition of MT1-MMP-derived hemopexin domain to this chimera was necessary to induce enzyme dimerisation and enable collagen degradation (Itoh et al., 2006).

In addition to cell invasion, MT1-MMP was also shown to promote tumour growth within a 3D collagen environment where it creates space for cells to grow (Hotary et al., 2000). A crucial role for MT1-MMP in cancer metastasis has been demonstrated in *Mt1-mmp*$^{-/-}$ mice, which show reduced tumour dissemination (Szabova et al., 2008). Additionally, mice treated with the anti-MT1-MMP antibody DX-2400 show reduced tumour growth and metastasis in xenograft models (Devy et al., 2009).

1.2.12 Functional activation of MT1-MMP by collagen

Expression of MT1-MMP in healthy tissue is usually low and increases when cells need to remodel the surrounding ECM in physiological or pathological situations. As described in the previous sections, MT1-MMP function is regulated by many different processes, including endocytosis and dimerisation. However, the presence of the active form of MT1-MMP on the cell surface does not necessarily indicate that the enzyme is 'functionally active'. For example, although primary fibrob-

lasts constitutively express MT1-MMP, MMP-2 and TIMP-2 when in culture — all molecules required for proMMP-2 activation — no active MMP-2 was detected during normal cell culture conditions (Zigrino et al., 2001). These results indicate that although MT1-MMP is expressed, activated and targeted to cell surface, it is unable to activate MMP-2 and is therefore considered functionally inactive. Cells require an 'activator' to induce MT1-MMP activity. The mechanisms underlying the functional activation of MT1-MMP are not completely understood, but it is believed that they include both transcriptional and non-transcriptional processes. Concanavalin A and phorbol 12-myristate 13-acetate are examples of such activators, and they can induce proMMP-2 activation and a significant increase in MT1-MMP expression in a variety of cells (Lohi and Keski-Oja, 1995; Lohi et al., 1996; Overall and Sodek, 1990). It has been proposed that concanavalin A-induced proMMP-2 activation is due to reduced endocytosis of MT1-MMP and increased levels and activity of the enzyme on the cell surface (Jiang et al., 2001; Remacle et al., 2003).

Among physiological stimuli, collagen type I is known to induce proMMP-2 activation in a number of cells including fibroblasts and cancer cells. ProMMP-2 activation was observed in cells cultured in the presence of type I collagen, but not in cells cultured on plastic or other commonly used ECM molecules including gelatin (denatured collagen), laminin, fibronectin, collagen type IV or Matrigel, and this activation is often accompanied by an increase in MT1-MMP expression (Azzam and Thompson, 1992; Guo and Piacentini, 2003; Nguyen et al., 2000; Ruangpanit et al., 2001; Zigrino et al., 2001). Collagen-induced activation of proMMP-2 was observed in primary fibroblasts from human skin (Azzam and Thompson, 1992; Han et al., 2001; Lee et al., 1997; Ruangpanit et al., 2001, 2002; Zigrino et al., 2001), breast (Lafleur et al., 2006) and lung (Tomasek et al., 1997), as well as in endothelial cells (Haas et al., 1998; Nguyen et al., 2000). In skin fibroblasts, proMMP-2 activation was observed also in the presence of collagen type II and III (Ruangpanit et al., 2001). Similarly to fibroblasts, hepatic stellate cells express proMMP-2, MT1-MMP and TIMP-2 in culture, but no active MMP-2 is detected. ProMMP-2 activation

occurs only when they are co-cultured with hepatocytes, characterised by extensive ECM production (including collagens) (Théret et al., 1999). Tumour cells, such as ovarian cancer (Ellerbroek et al., 2001), HT1080 (Takino et al., 2004) and malignant mesothelioma cells (Sakai et al., 2011), also show proMMP-2 activation in response to collagen. Therefore collagen appears to be a functional activator of MT1-MMP and may play an important role in upregulating MT1-MMP in tissues.

1.3 Collagen as a signalling molecule

In the human body, collagens are the most abundant proteins. They are major components of the extracellular matrix in general and account for approximately 30% of total protein mass (Myllyharju and Kivirikko, 2004). Collagens support tissue structure, assemble into cellular barriers such as basement membranes and provide signals for cell growth, differentiation and migration.

1.3.1 Collagen structure

Collagens are formed from three polypeptide chains, known as α chains. Within one collagen molecule, individual α chains can be identical or different, resulting in the formation of homo- or heterotrimers. So far, 46 α chains have been identified, which assemble into 28 distinct collagen types (Ricard-Blum, 2011). Collagen type I is a heterotrimer of two α1(I) and one α2(I) chains, whereas three identical α1(II) or α1(III) chains form collagen type II or III respectively (collagen type in parentheses). A characteristic feature of collagens is the presence of one or multiple triple helical domains, and their lengths and numbers vary greatly between collagens. Several collagen types have additional domains, e.g. membrane-associated collagens with interrupted triple helices have transmembrane domains.

In a single collagen molecule three α chains are interwoven around each other and form a right-handed triple helix. Polypeptide chains contain a repeated Gly-X-Y amino acid sequence, where X is often proline and Y is often 4-hydroxyproline

(Shoulders and Raines, 2009). The presence of a small and flexible glycine at every third amino acid is required for formation of a tight helical structure. Proline and 4-hydroxyproline stabilise the α chains before triple helix assembly, and 4-hydroxyproline at position Y increases thermal stability of collagen (Shoulders and Raines, 2009).

Collagens interact with each other and form supramolecular assemblies such as fibrils (e.g. type I, II, III), networks (type IV) or hexagonal networks (type VIII and X), beaded filaments (type VI) or anchoring fibrils (type VII). Fibril-associated collagens with interrupted triple helices, such as type IX, bind to collagen fibrils (Myllyharju and Kivirikko, 2004). Some collagens are widely distributed within the human body, while expression of other collagen types is restricted to specific tissues. The most prevalent is type I collagen. It is found in the majority of tissues including skin, bones, vessel walls, tendons and ligaments. On the contrary, collagen type II is mostly found in cartilage and vitreous, type IV is only present in basement membranes and collagen type X is found exclusively in hypertrophic cartilage (Myllyharju and Kivirikko, 2004).

1.3.2 Assembly of collagen fibrils

The subfamily of fibril-forming collagens include collagen type I, II, III, V, XI, XXIV and XXVII (Myllyharju and Kivirikko, 2004; Ricard-Blum, 2011). Their α chains are more than 1000 amino acid long polypeptides. Prior to triple helix assembly, they are posttranslationally modified in the endoplasmic reticulum. Proline and lysine are hydroxylated to 3- and 4-hydroxyproline and hydroxylysine respectively. Additionally, asparagine and hydroxylysine are glycosylated and inter- and intrachain disulfide bonds are formed. Three α chains are assembled intracellularly into procollagen molecules with a one residue stagger between them. Procollagen of fibrillar collagens consists of a central, uninterrupted triple helical domain with N- and C-terminal pro-peptides, separated by short non-helical sequences known as telopep-

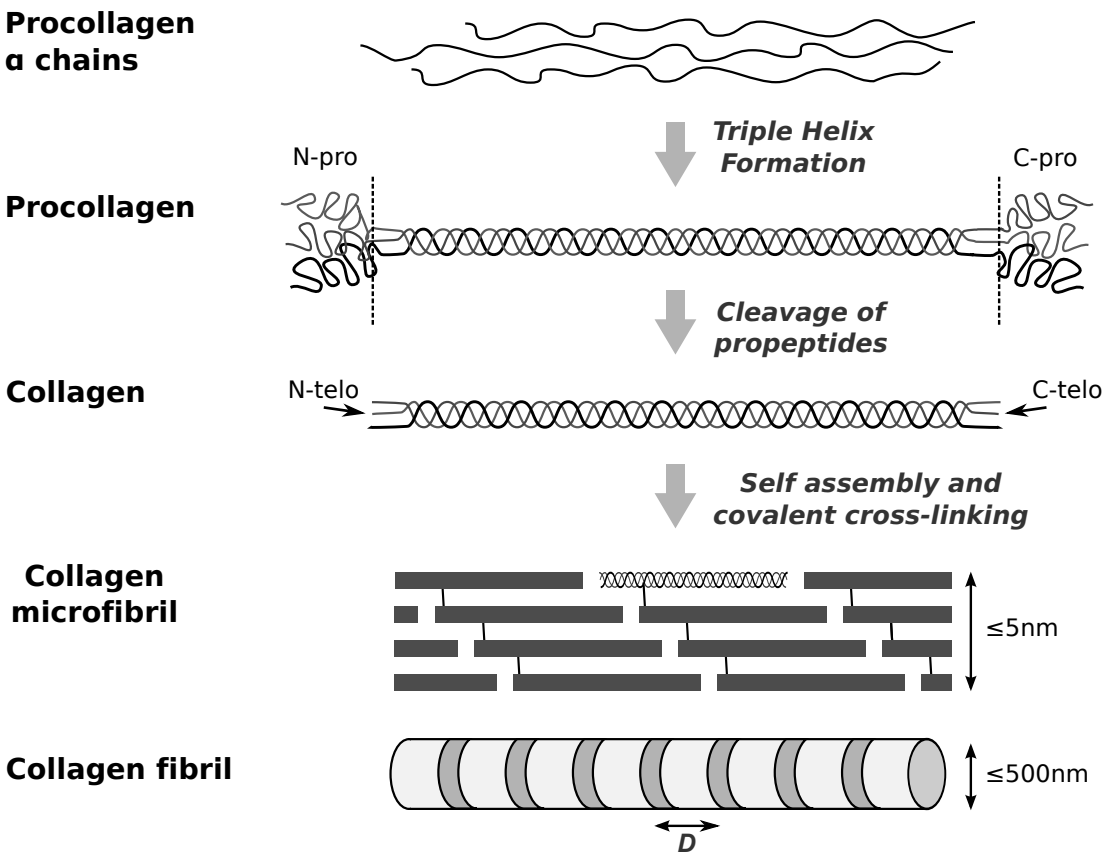

Figure 1.8: Formation of collagen fibrils. Synthesis of procollagen α chains of fibril-forming collagens and their assembly into triple helical structure takes place in the endoplasmic reticulum. After secretion, pro-peptidases cleave N- and C-terminal pro-peptides (***pro***), exposing non-helical telopeptides (***telo***). Matured collagen molecules self-assemble into collagen microfibrils and then into larger fibrils, which show banding pattern (with D periodicity). Covalent cross-linking in the telopeptides is facilitated by lysyl oxidase. Figure adapted from Myllyharju and Kivirikko (2004) and Shoulders and Raines (2009).

tides (Figure 1.8). After secretion, pro-domains are removed by pro-peptidases: the N-terminal pro-peptide is cleaved by ADAMTS-2 and the C-terminal one by bone morphogenetic protein-1. After removal of pro-peptides, the N- and C-terminal telopeptides become exposed and individual collagen molecules self-assemble into intermediate fibrils (microfibrils) with a diameter up to 5 nm (Figure 1.8). Merging of microfibrils results in the formation of mature collagen fibrils with a diameter varying from 15 nm to 500 nm (Ricard-Blum, 2011). Because of a staggered arrangement of collagen monomers within a fibril, electron microscopy images of collagens show

a characteristic banding pattern with a D periodicity of 64–67 nm. Telopeptides are essential for proper fibril assembly and cross-linking. After assembly, lysines, hydroxylysines and histidines in telopeptides from the same or adjacent collagen molecules become cross-linked by lysyl oxidase. Cross-linking increases strength and stability of collagen fibrils (Shoulders and Raines, 2009).

1.3.3 Collagen function

One of the main functions of collagen is to support tissue architecture as well as to provide a scaffold for cell attachment and migration. Due to their high stability and exceptional tensile strength, collagens facilitate mechanical properties of connective tissues such as skin, tendons, cartilage and bone. Collagens such as network-forming collagen type IV also constitute barriers for cell migration including basement membranes. Mutations in collagen genes often perturb collagen triple helical structure and are associated with many disorders. Mutations in the most common type I collagen cause osteogenesis imperfecta, characterised by fragile bones (Ricard-Blum, 2011). An increasing body of evidence shows that collagen also acts as a signalling molecule and induces cell growth, motility, survival, differentiation and morphogenesis. Altered collagen expression characterises pathologies such as atherosclerosis, cancer and tissue fibrosis. Basal membranes maintain the polarity of endothelial and epithelial cells that reside on top of them. Presence of some minor collagen types is often needed for tissue homeostasis. For example, expression of collagen type X is required for endochondral ossification and collagen VII is essential for integrity of dermal tissues. Collagen signalling is linked to acquisition of mesenchymal phenotype by epithelial cells, in a process known as endothelial-to-mesenchymal transition (Medici and Nawshad, 2010). Moreover, stiffness of the collagenous matrix appears to regulate differentiation of mesenchymal stem cells into bone, neurones or muscle cells (Engler et al., 2006).

Cell-matrix interactions are mediated by plasma membrane receptors, whose functions extend beyond substrate attachment, as they are able to transduce signals and initiate signalling pathways. Integrins and discoidin domain receptors (DDRs) are two major families of collagen receptors that mediate collagen signalling.

1.3.4 Integrins

Integrins are a large family of ubiquitous cell adhesion receptors (Hynes, 2002). On the cell surface they form non-covalently bound heterodimers, composed of α and β subunits. In humans and higher vertebrates, 18 α and 8 β subunits associate into 24 distinct integrin receptors (Figure 1.9A). Those can be divided into four groups based on their primary ligand specificity: RGD-recognising integrins, collagen integrins, laminin integrins and leukocyte-associated integrins (Barczyk et al., 2010; Hynes, 2002). However, the list of integrin ligands is far longer and includes fibronectin, vitronectin, osteopontin, tenascin, fibrinogen, thrombospondin, E-cadherin and more (Humphries et al., 2006).

The overall structure of integrins can be described as a ligand binding headpiece, a 'leg', transmembrane domain and short cytoplasmic tail (Figure 1.9B). The extracellular structure of the α subunit consists of a seven-bladed β-propeller, a 'thigh' and two 'calf' regions: calf-1 and calf-2 . Among 18 α subunits, nine of them have an additional αI domain inserted between blades 2 and 3 of the β-propeller domain (Figure 1.9). In these integrins, the αI domain is responsible for ligand binding. The extracellular part of the β subunit contains: βI domain, hybrid domain, a plexin-semaphorin-integrin domain, tandem of four epidermal growth factor (EGF)-like domains and β-tail domain. In integrins without an αI domain, ligand binding is facilitated by both the β-propeller of the α subunit and the βI domain of the β subunit (Hynes, 2002; Luo et al., 2007).

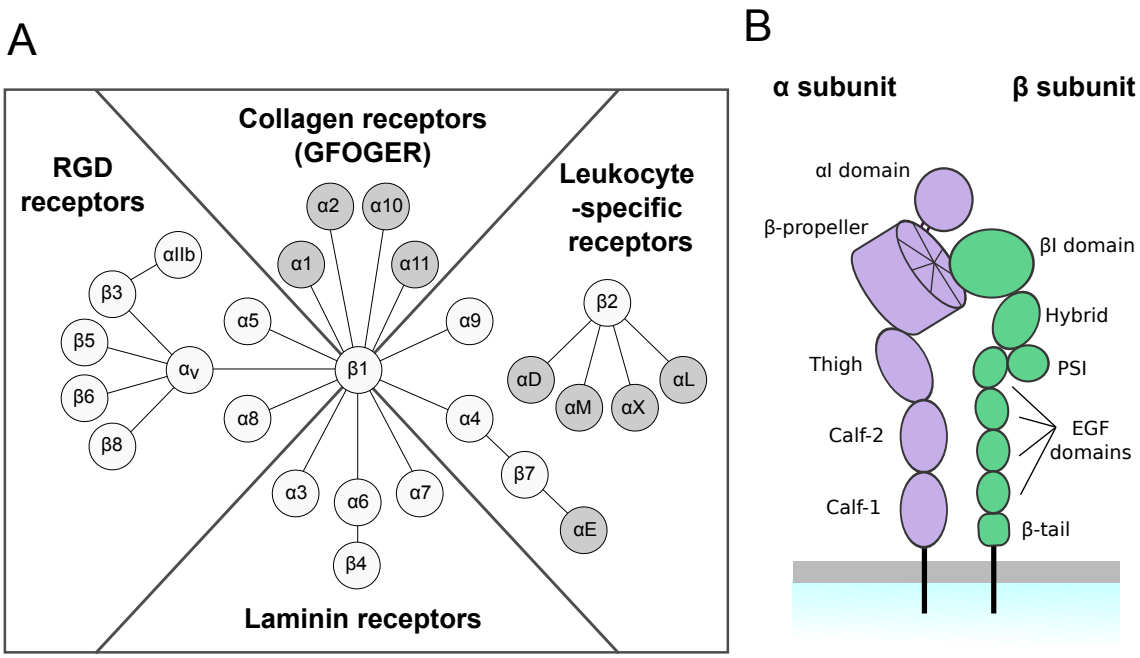

Figure 1.9: Family of integrin receptors. (A) The family of integrins consists of 24 receptor heterodimers formed from 18 α and 8 β subunits. Integrins are divided into four major groups based on their specificity of ligand binding. Collagen-binding integrins recognise the GFOGER motif present in fibrillar collagens. The nine α subunits containing an additional ligand-binding αI domain are highlighted in dark grey. **(B)** Schematic structure of an integrin dimer on the cell surface, with α subunit containing αI domain. Figure adapted from Barczyk et al. (2010). *EGF - epidermal growth factor-like; PSI - plexin-semaphorin-integrin.*

Collagen binding receptors include integrins α1β1, α2β1, α10β1 and α11β1 (Leitinger, 2011). Collagen binding integrins are involved in inflammatory signalling, tissue fibrosis, wound healing, and tumour progression. Integrins α1β1 are widely expressed in many cell types, especially in mesenchymal cells; α2β1 integrins are expressed in epithelial cells and platelets; expression of α10β1 integrins is restricted to chondrocytes and α11β1 integrins are expressed in mesenchymal non-muscle cells at the sites where interstitial collagen is highly organised (Barczyk et al., 2010; Popova et al., 2007). Mice deficient in α1, α2, α10 or α11 subunit are viable and show only mild defects, which indicates redundancy in function of α subunits (Leitinger, 2011), while deficiency of the β1 subunit is lethal at the embryo stage (Stephens et al., 1995). Integrins α1β1 and α10β1 preferentially bind network-forming collagen type IV to fibril-forming collagen type I, whereas integrins α2β1

and $\alpha 11\beta 1$ bind more to collagen type I than IV (Barczyk et al., 2010; Popova et al., 2007). Binding motifs in fibrillar collagens are well characterised and GFOGER was the first identified high-affinity sequence found in collagens type I and II (Knight et al., 1998, 2000). Since then, several binding motifs have been characterised, leading to identification of the minimal consensus binding sequence Gxx'GEx" in fibrillar collagens (Raynal et al., 2006; Xu et al., 2000; Zhang et al., 2003).

At the ECM attachment sites, integrins cluster and form focal adhesions. Several adaptor molecules are recruited to the integrin cytoplasmic domains, including focal adhesion kinase, paxillin, talin, tensin, vinculin and α-actinin, forming the focal adhesion complex. Through these adaptor molecules, integrins link the ECM to the actin cytoskeleton, which also allows generation of traction force required for cell migration. In addition to their cell adhesion property, integrins can mediate inside-out and outside-in signalling in a bidirectional manner (Harburger and Calderwood, 2009). On the cell surface they exist in one of two conformations: bent (with headpiece pointing towards the cell membrane) or open (headpiece facing away from the cell membrane), corresponding to low- and high-affinity states respectively (Luo et al., 2007). Binding of adaptor proteins e.g. talin to the cytoplasmic tails can induce conformational changes to the high-affinity state (inside-out signalling) (Harburger and Calderwood, 2009). Ligand binding promotes the open conformation, formation of integrin clusters and initiation of signalling pathways required for cell spreading, migration, growth and proliferation (outside-in signalling). Ligand-mediated integrin clusters are stabilised by binding of talin and paxillin to the integrin cytoplasmic tail. In turn, talin and paxillin recruit focal adhesion kinase and actin-binding proteins, leading to the formation of mature focal adhesions. Focal adhesion kinase is a non-receptor tyrosine kinase, which becomes phosphorylated and forms a complex with Src kinase upon integrin activation. This complex further phosphorylates proteins present at focal adhesions and propagates signal transduction (Berrier and Yamada, 2007; Mitra et al., 2005; Nagano et al., 2012).

1.3.5 Discoidin domain receptors

Discoidin domain receptors (DDRs) are widely expressed cell surface collagen receptors and they belong to the family of receptor tyrosine kinases (RTKs) (Johnson et al., 1993; Leitinger, 2011; Shrivastava et al., 1997; Vogel et al., 1997). Unlike other RTKs, ligands of DDRs are not soluble molecules but collagens (Shrivastava et al., 1997; Vogel et al., 2000, 1997). There are only two members of this family: DDR1 and DDR2, with approximately 78% sequence homology. DDRs appear to be well conserved among species (Leitinger, 2011; Vogel et al., 2000). Their extracellular domains share sequence homology to discoidin-I, a protein involved in cell aggregation in the slime mold *Dictyostelium discoideum*, therefore the name of this receptor family (Johnson et al., 1993). The structure of DDRs comprises extracellular, globular discoidin domain and discoidin-like domains, followed by a transmembrane domain, a large intracellular juxtamembrane region and a kinase domain at the C-terminus (Figure 1.10) (Carafoli et al., 2012; Playford et al., 1996; Vogel, 1999).

DDRs are expressed during embryogenesis and in adult tissues, with distinct expression patterns (Marco et al., 1993; Vogel et al., 2006). DDR1 is found in lung, colon, kidney, brain, placenta as well as in keratinocytes, hepatocytes and smooth muscle cells. DDR2 is expressed in heart, skeletal muscles, lung, brain, kidney and connective tissue (Vogel et al., 2006). DDR1 is mainly expressed in epithelial cells, while DDR2 is found in mesenchymal cells. In humans, DDR1 is present in 5 isoforms (transcript variants 1–5) due to alternative splicing and variants 4 and 5 are deficient in kinase activity. DDR2 has only 1 identified isoform (Alves et al., 2001; Song et al., 2011).

DDRs are implicated in cell growth, motility, MMP expression, cancer and metastasis (Leitinger and Hohenester, 2007; Vogel et al., 2006). Mutations in human DDR2 lead to a rare, autosomal recessive spondylo-meta-epiphyseal dysplasia short limb-abnormal calcification type syndrome (OMIM:271665), which is charac-

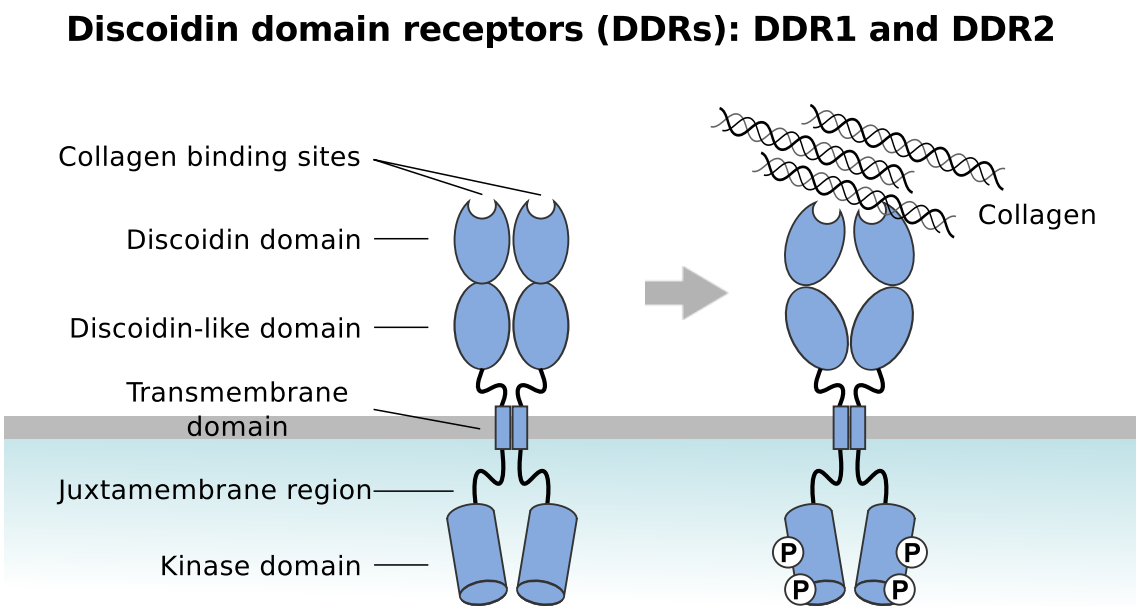

Figure 1.10: Structure of discoidin domain receptors. DDR1 and DDR2, the only members of the DDR family, belong to the receptor tyrosine kinase superfamily. DDR structure comprises discoidin domain, discoidin-like domain, transmembrane domain and kinase domain. They form constitutive dimers on the cell surface through their transmembrane domains. DDRs bind collagens in their native triple helical form and do not bind denatured collagens. Each molecule has a collagen binding site in the discoidin domain. However, the specific binding mode has not been defined.

terised by short stature and shortening of upper and lower limbs (Ali et al., 2010; Bargal et al., 2009). Correspondingly, *Ddr2*$^{-/-}$ mice show dwarfism, craniofacial deformities, decreased chondrocyte proliferation and shortening of long bones (Kano et al., 2008; Labrador et al., 2001). *Ddr1*$^{-/-}$ mice are also smaller than their littermates and show defects in mammary gland development (Vogel et al., 2001). Both DDRs are implicated in cancer (Johnson et al., 1993; Valiathan et al., 2012; Zhang et al., 2012), atherosclerosis (Ferri et al., 2004; Franco et al., 2008) and liver fibrosis. Expression levels of DDR2 are elevated in RA in the synovial intimal lining and are correlated with increased expression of MMP-13 (Su et al., 2009). Activation of DDR2 is also linked to the induction of MMP-13 in mouse models of OA (Xu et al., 2005, 2011).

DDRs bind collagens through their discoidin domain and binding induces phosphorylation of tyrosines in the cytoplasmic kinase domain independently of integrins (Carafoli et al., 2009; Vogel et al., 2000). As opposed to other RTKs, phosphorylation is slow and sustained and reaches a maximum after hours instead of minutes (Shrivastava et al., 1997; Vogel et al., 2000, 1997). On the cell surface, DDRs form stable homodimers prior to ligand binding as a result of tight interactions of their transmembrane domains (Noordeen et al., 2006).

Both DDR receptors are activated by fibrillar collagens type I, II, III and V (Shrivastava et al., 1997; Vogel et al., 1997). Other ECM molecules such as fibronectin or laminin do not induce autophosphorylation (Leitinger, 2003; Vogel et al., 1997). DDR1 is also activated by collagen type IV and VIII (Hou et al., 2001; Leitinger, 2003; Shrivastava et al., 1997; Vogel et al., 1997). DDR2 does not bind to collagen IV, but instead binds collagen type X and preferentially binds collagen type II, both found in cartilage (Leitinger and Kwan, 2006; Leitinger et al., 2004). Denatured collagens do not induce activation of DDRs, indicating that native triple helical structure is required for recognition and binding (Leitinger, 2003; Vogel, 1999). Recently, the minimal binding motif in collagens I-III was identified as GVMGFO. Triple helical peptides containing the GVMGFO sequence where found to induce DDR autophosphorylation with kinetics similar to native collagen (Konitsiotis et al., 2008; Xu et al., 2011). Purified DDR2 discoidin domain binds triple helical peptides with 1:1 stoichiometry and the crystal structure of this complex identified residues required for ligand binding. However, the exact model of collagen binding by the DDR dimer on the cell surface is not known (Carafoli et al., 2009; Konitsiotis et al., 2008).

1.4 Cartilage signalling in synovial cell invasion

In RA synovium, MT1-MMP shows a characteristic pattern of expression (Figure 1.11). Analysis of several samples of human RA cartilage showed consistently higher MT1-MMP expression in cells invading the cartilage and in direct contact with the cartilage matrix (Konttinen et al., 1998; Miller et al., 2009; Petrow et al., 2002). In normal synovium, little or no expression of MT1-MMP, MMP-2 and TIMP-2 is detected and no activation of MMP-2 is observed (Goldbach-Mansky et al., 2000; Petrow et al., 2002; Yamanaka et al., 2000). The expression of all three proteins is elevated in RA and MT1-MMP often co-localises with MMP-2 and TIMP-2 in synovial membrane, particularly in lining layer fibroblasts (Konttinen et al., 1999a, 1998; Pap et al., 2000b; Petrow et al., 2002; Yamanaka et al., 2000). Secreted MMP-2 accumulates in the synovial fluid and its levels have been found to correlate with cartilage erosions (Goldbach-Mansky et al., 2000; Tchetverikov et al., 2004). Active MMP-2 was detected in synovial fluid and synovial membranes of RA patients as well as in the conditioned medium from RA synovial fibroblasts (Smolian et al., 2001; Tchetverikov et al., 2004; Yamanaka et al., 2000). These findings indicate that MT1-MMP, which is a cellular activator of proMMP-2, is functionally active in RA synovial cells.

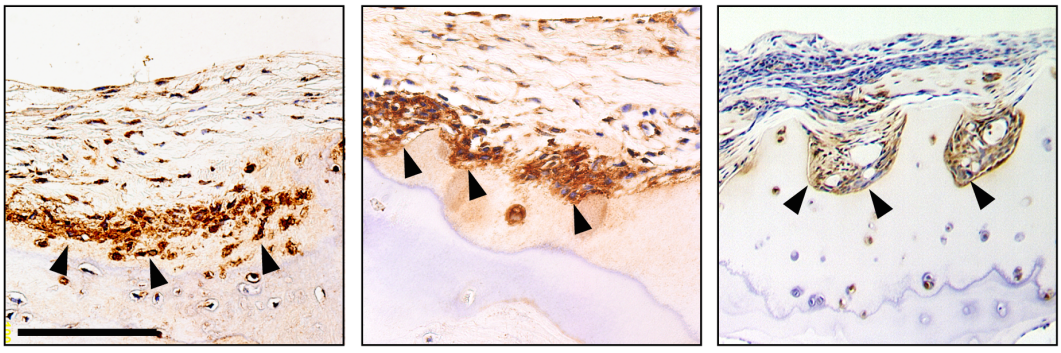

Figure 1.11: MT1-MMP is expressed at pannus-cartilage junctions in RA joint. Sections of RA joints were stained against MT1-MMP. Arrowheads indicate cartilage-pannus junction and high expression of MT1-MMP. Figures courtesy of Dr. Yoshifumi Itoh, Kennedy Institute of Rheumatology, University of Oxford. Scale bar: 100 µm.

As described above, fibrillar collagens were shown to activate MT1-MMP and induce proMMP-2 activation in a variety of cells. Several research groups investigated the role of collagen receptors in this process, predominantly integrins. However, their role in this process is not fully understood. It has been reported that aggregation of integrins using bead-immobilised anti-β1 integrin antibodies increases MT1-MMP expression and induces proMMP-2 activation in ovarian cancer cell lines (Ellerbroek et al., 1999, 2001). In skin fibroblasts cultured in the presence of collagen, MT1-MMP expression was also reported to be at least partially mediated by integrins (Zigrino et al., 2001). Antibodies against α2 integrin subunit reduced proMMP-2 activation in human umbilical vein endothelial cells cultures within collagen gels. On the contrary, a study by Sakai et al. (2011) shows that knockdown of β1 integrin expression does not affect MT1-MMP synthesis or proMMP-2 activation in human malignant mesothelioma cells cultured in 3D collagen. Another study showed that function inhibiting anti-β1 integrin antibodies alone, or in combination with anti-α2 integrin antibodies, did not block collagen-induced proMMP-2 activation in hepatic stellate cells (Théret et al., 1999). In addition, β1 integrin often co-localises with MT1-MMP at the cell invasion front, both on 2D substrates and within 3D matrices (Ellerbroek et al., 2001; Gálvez et al., 2002; Wolf et al., 2007; Woskowicz et al., 2013). This led to the conclusion that β1 integrin and MT1-MMP cooperate in ECM cleavage. Although both can be found in the same invasive structures, there is inconclusive evidence that MT1-MMP is in direct contact with β1 integrin and some studies were unable to efficiently co-immunoprecipitate MT1-MMP and β1 integrin (Gálvez et al., 2002; Woskowicz et al., 2013). The role of DDRs in collagen-induced MMP-2 activation has not been studied in detail. Overexpression of DDR2, but not of DDR1, promoted collagen-induced proMMP-2 activation in smooth muscle cells (Ferri et al., 2004). In isolated RA synovial fibroblasts stimulated with collagen type II, DDR2 was implicated in mediating increase of MMP-1 and MMP-2 expression (Zhang et al., 2006a). Additionally, *Ddr2*$^{-/-}$ mice show impaired wound healing and lower levels of proMMP-2 (Olaso et al., 2011).

1.5 Hypothesis and aims of the thesis

In RA, cartilage destruction by pannus invasion is an irreversible process, in which synovial fibroblasts are actively involved. These cells show several signs of transformation and, when isolated, deeply invade into the cartilage even without the inflammatory environment of the RA joint (Miller et al., 2009; Rutkauskaite et al., 2005; Sabeh et al., 2010). During progression of the disease, synovial fibroblasts express a variety of proteolytic enzymes which degrade the cartilage components. Among these, MT1-MMP - a membrane-bound collagenase - appears to be crucial for promoting synovial cell invasion. Recent studies demonstrated that MT1-MMP is required for collagen degradation and cartilage invasion by RA synovial fibroblasts (Miller et al., 2009; Sabeh et al., 2010).

Interestingly, MT1-MMP is highly expressed in synovial fibroblasts invading the cartilage and in close contact with cartilage's major ECM component: fibrillar collagen type II (Miller et al., 2009). It has been demonstrated that one of the activators of MT1-MMP in many cell types, by yet unknown mechanisms, is fibrillar collagen (Ellerbroek et al., 2001; Haas et al., 1998; Ruangpanit et al., 2001; Takino et al., 2004; Zigrino et al., 2001).

Therefore, we hypothesise that collagen is a likely functional activator of MT1-MMP in RA synovial fibroblasts. Indeed, RA synovial fibroblasts invade deeper into aggrecan-depleted cartilage, where collagen fibrils are more exposed (Miller et al., 2009).

Although considerable research has been carried out to identify collagens receptors involved in induction of MT1-MMP activation by fibrillar collagens, no conclusive agreement has been found. Thus the objective of this study is to determine collagen receptors involved in collagen-induced MT1-MMP activation in RA synovial fibroblasts.

Aims of this thesis:

- confirm that collagen induces MT1-MMP expression and activity in RA synovial fibroblasts.
- investigate mechanisms of collagen-induced expression and activity of MT1-MMP in RA synovial fibroblasts.
- identify collagen receptor(s) involved in collagen-induced MT1-MMP activation.
- examine role of collagen receptors in MT1-MMP-dependent degradation of collagen and gelatin as well as in MT1-MMP-dependent collagen invasion.
- determine ability of cartilage tissue to activate MT1-MMP and investigate role of collagen receptors in this process.

Chapter 2

Materials and Methods

2.1 Reagents

2.1.1 Antibodies

Primary antibodies

Mouse anti-(human MT1-MMP hemopexin domain) monoclonal antibody (222-1D8) was a gift from Professor Motoharu Seiki (University of Tokyo, Japan); rabbit anti-(human MT1-MMP catalytic domain) monoclonal antibody (clone EP1264Y) was from Epitomics, Abcam (Cambridge, UK); humanised anti-(human MT1-MMP catalytic domain) monoclonal antibody DX-2400 was a gift from Dyax Corp. (Burlington, USA); goat anti-(human G-actin) polyclonal antibody (I-19) was from Santa Cruz Biotechnology Inc. (Santa Cruz, USA); goat anti-(human DDR1 extracellular domain) polyclonal antibody (AF2396) and goat anti-(human DDR2 extracellular domain) polyclonal antibody (AF2538) were from R&D Systems (Abingdon, UK); mouse anti-phosphotyrosine antibody (clone 4G10); rabbit anti-(human β1 integrin) polyclonal antibody (AB1952); mouse anti-(human β1 integrin) monoclonal antibody, azide-free (clone 6S6) and mouse anti-(human β1 integrin) monoclonal antibody, azide-free (clone P4G11) were from Millipore (Watford, UK). Antibodies supplied in azide-free solution were suitable for the cell culture.

Secondary antibodies

The following alkaline phosphatase (AP)-conjugated antibodies were from Sigma-Aldrich (Dorset, UK): rabbit anti-(goat IgG), goat anti-(mouse IgG Fc specific) and goat anti-(mouse IgG Fab specific). AP-conjugated goat anti-(rabbit IgG) antibody was from Promega (Southampton, UK). Horseradish peroxidase (HRP)-conjugated swine anti-(rabbit IgG) antibody was from Dako UK Ltd. (Ely, UK).

2.1.2 Cell culture reagents

Human synovial fibroblasts were isolated from samples obtained from rheumatoid arthritis patients undergoing joint replacement surgery. Human dermal fibroblasts were isolated from skin samples obtained from healthy donors. HT1080 fibrosarcoma cell line and human embryonic kidney 293 (HEK293) cells were purchased from LGC Promochem and HEK293-EBNA cells were purchased from Life Technologies (Paisley, UK). HEK293-EBNA stably expressing DDR2 (in pCEP4 vector) were a kind gift from Dr. Yasuyuki Shitomi (Kennedy Institute of Rheumatology, University of Oxford, UK).

Dulbecco's Modified Eagle's Medium (DMEM) was from Lonza (Verviers, Belgium). Dulbecco's phosphate buffered saline (DPBS), fetal bovine serum (FBS) and OptiMEM reduced serum medium were from Life Technologies (Paisley, UK). 1 M HEPES buffer, hygromycin B (50 mg/ml in PBS), penicillin (10,000 units/ml), streptomycin (10 mg/ml), trypsin/EDTA in DPBS were from PAA Laboratories (Pasching, Austria). Concanavalin A type VI, Cytodex 3 microcarrier beads, sterile dimethyl sulfoxide (DMSO), type A gelatin from porcine skin and $10 \times$ RPMI-1640 were from Sigma-Aldrich (Dorset, UK). Interferin transfection reagent and 12-well 8 µm polyethylene terephthalate (PET) track-etched membrane culture inserts (transwells) were from VWR International Ltd. (Lutterworth, UK). Corning CellBIND 12-well plates were from Costar (Amsterdam, The Netherlands). SMARTpool ON-TARGETplus siRNAs for MT1-MMP, DDR2 and integrin β1 (ITGB1)

as well as non-targeting siRNA were purchased from Dharmacon, ThermoScientific (Northumberland, UK). Recombinant human TNF-α and IL-1β were from Peprotech (London, UK). TransIT-2020 Transfection Reagent was from Mirus (Madison, USA). GM6001 (Ilomastat) was purchased from Elastin Products Company (Missouri, USA). PureCol collagen type I from bovine hide was from Advanced BioMatrix (Leimuiden, The Netherlands); CellMatrix Type I-A collagen type I from porcine tendon was from Nitta-Gelatin Inc. (Osaka, Japan). Guinea pig acid- and pepsin-extracted collagens were provided by Dr. Rob Visse (Kennedy Institute of Rheumatology, University of Oxford, UK). Human and bovine collagen type II from articular cartilage were from Chondrex Inc. (Redmond, WA, USA). Purified recombinant human TIMP-1 and TIMP-2 were provided by Dr. Yoshifumi Itoh (Kennedy Institute of Rheumatology, University of Oxford, UK). Activated recombinant MMP-1 was provided by Dr. Mohammad Nickdel (Kennedy Institute of Rheumatology, University of Oxford, UK). Triple helical peptides were a kind gift from Dr. Birgit Leitinger (Imperial College London, UK).

2.1.3 Molecular biology reagents

2-amino-2-methyl-1,3-propanediol (ammediol), ammonium chloride (NH_4Cl), bovine serum albumin (BSA), bromophenol blue, calcium chloride ($CaCl_2$), glutaraldehyde, glycine, magnesium chloride ($MgCl_2$), β-mercaptoethanol (β-Me) and Trizma base were purchased from Sigma-Aldrich (Dorset, UK). Acetic acid, ammonium persulfate, butanol, Coomassie Brilliant Blue R-250, formic acid, glycerol, hydrochloric acid (HCl), methanol, $10\times$ phosphate buffered saline (PBS), sodium azide (NaN_3), sodium chloride (NaCl), sodium dodecyl sulfate (SDS), sodium hydroxide (NaOH), sodium bicarbonate ($NaHCO_3$), sucrose, sulfuric acid (H_2SO_4), N, N, N', N'-tetramethylethylenediamine (TEMED), toluene, Triton X-100, Tween 20 and zinc chloride ($ZnCl_2$) were from VWR International Ltd. (Lutterworth, UK). Trans-Blot Turbo 0.2 µm polyvinylidene difluoride (PVDF) Membrane Transfer Packs were

from Bio-Rad Laboratories (Hemel Hempstead, UK). Marvel dry skimmed milk was from Premier Foods, UK. Western Blue stabilised substrate for AP was purchased from Promega (Southampton, UK). Novex 4–16% casein zymogram Tris-glycine gels were from Life Technologies (Paisley, UK). BCA Protein Assay Kit, Maxima Probe/ROX quantitative polymerase chain reaction (qPCR) Master Mix (2×) and Page Ruler Plus Pre-stain Protein Ladder were purchased from ThermoScientific (Northumberland, UK). Micro RNeasy RNA extraction kit and 0.1 ml PCR tubes with lids were from Qiagen (Crawley, UK). Gene expression TaqMan assay for human MT1-MMP (ID: Hs00237119-m1; FAM probe), Ribosomal RNA Control Reagents (VIC probe) and High-Capacity cDNA Reverse Transcription Kit were from Applied Biosystems, Life Technologies (Paisley, UK). 30% (w/v) acrylamide/bis-acrylamide (37.5 : 1) was from Severn Biotech Ltd. 3,3',5,5'-tetramethylbenzidine (TMB) Microwell Peroxidase Substrate System was from KPL (Gaithersburg, MD, USA). Corning 96-well EIA/RIA High Binding flat bottomed plates were from Costar (Amsterdam, The Netherlands).

2.1.4 Molecular cloning reagents

Agarose (electrophoresis grade), 100 mM dNTP Set, DH5α and TOP10 *Escherichia coli* electrocompetent cells, LB medium, LB agar, pCEP4 DNA plasmid vector and zeocin (100 mg/ml) were from Life Technologies (Paisley, UK). pFUSE–rIgG–Fc1 DNA plasmid vector (with zeocin resistance gene) was from InvivoGen, Source BioScience (Nottingham, UK). Chloroform, ethanol, sodium acetate ($C_2H_3NaO_2$) and SYBR Green I nucleic acid stain (10,000×) were from Sigma-Aldrich (Dorset, UK). CloneJET PCR Cloning Kit (with pJET1.2 DNA plasmid vector), FastAP Thermosensitive Alkaline Phosphatase, FastDigest restriction enzymes, FastDigest universal buffer, GeneJET Gel Extraction Kit, Gene Ruler 1 kb Plus DNA Ladder, Phusion Hot Start II High Fidelity polymerase (F-549), 5 × Phusion High Fidelity reaction buffer (F-518), Rapid DNA Ligation Kit, T4 DNA Ligase and ZipRuler

Express DNA Ladder Set were from ThermoScientific (Northumberland, UK). *Pfu* polymerase and $10 \times$ *Pfu* reaction buffer were from Agilent Technologies (Wokingham, UK). *Taq* polymerase and $10 \times$ *Taq* reaction buffer were from New England Biolabs Ltd (Hitchin, UK). PureYield plasmid Midiprep system with endotoxin removal was from Promega (Southampton, UK). Ethidium bromide, ethylenediaminetetraacetic acid (EDTA), electroporation cuvettes (2 mm gap) and potassium acetate (CH_3CO_2K) were from VWR International Ltd. (Lutterworth, UK). Carbenicillin was purchased from Millipore (Watford, UK). RNase A from bovine pancreas (DNase-free) was from Qiagen (Crawley, UK).

2.1.5 Immunocytochemistry reagents

Alexa Fluor 488- and Alexa Fluor 568-conjugated phalloidin, Alexa Fluor 488 sulfodichlorophenol ester, 4',6-diamidino-2-phenylindole (DAPI), goat serum and ProLong Gold mounting solution were purchased from Life Technologies (Paisley, UK); glass cover slips ($\varnothing$ 18 mm) and Menzel-Gläser microscope slides were obtained from VWR International Ltd. (Lutterworth, UK); paraformaldehyde (PFA) was from Sigma-Aldrich (Dorset, UK).

2.1.6 Plasmid DNA constructs

DDR1 (transcript variant 1; accession number NM001954.4) and DDR2 (transcript variant 2; accession number NM006182.2) full length cDNA clones in pSG5 vector (DDR1/pSG5 and DDR2/pSG5) were provided by Dr. Yoshifumi Itoh (Kennedy Institute of Rheumatology, University of Oxford, UK). The following plasmids were also provided by Dr. Itoh: DDR1-W53A/pSG5 – DDR1 with introduced W^{53} to Ala mutation and DDR1-NHA-R105A-CF/pSG5 – DDR1 with introduced R^{105} to Ala mutation, N-terminal HA tag (NHA) and C-terminal FLAG tag (CF).

2.2 Culture of mammalian cells

2.2.1 Cell culture conditions

Mammalian cells were cultured in DMEM supplemented with 10% (v/v) FBS, 100 U/ml penicillin and 100 µg/ml streptomycin and maintained in sterile conditions at 37°C in 5% (v/v) CO_2 atmosphere in the humidified incubator. Cells were routinely sub-cultured when they reached confluency. To detach cells from culture dishes, they were washed twice in DPBS and incubated with trypsin/EDTA for 5 minutes at 37°C. Cells were harvested with serum-containing DMEM and centrifuged at $510 \times g$ for 5 minutes in a bench top centrifuge. Cell pellets were resuspended in fresh growth medium and seeded onto new dishes. RA synovial fibroblasts and dermal fibroblasts were split at ratios 1:3 or 1:5, respectively. HT1080 and HEK cells were split at 1:5 ratio. Medium was changed every 2–3 days.

2.2.2 Cryopreservation of cells

Cells where cryopreserved in growth medium containing DMSO as a protective agent. Cells were harvested by trypsinization and resuspended in a mixture of DMEM (40% v/v), DMSO (10% v/v) and FBS (50% v/v). Aliquots of cell suspensions were frozen overnight at −80°C in freezing containers with a cooling rate of 1°C per minute. Cell stocks were thereafter stored in liquid nitrogen (−196°C). To recover cells from the frozen stock, cryovials were quickly thawed in the 37°C water bath, the cell suspension mixed with 9 ml of pre-warmed DMEM and centrifuged for 5 minutes at $510 \times g$. Cell pellets were resuspended in fresh growth medium and seeded onto culture dishes.

2.2.3 Transfection of cells with siRNAs

SMARTpool ON-TARGETplus siRNA sets containing 4 different siRNA duplexes were used to knockdown expression of individual genes. Non-targeting siRNA (siNT) was used as a negative control. 2.5×10^4 cells were transfected with 5 nM siRNAs in a 24-well plate with 2 µl of Interferin as a transfection reagent. Alternatively, 2×10^5 cells were transfected with 5 nM siRNAs in a 60 mm culture dish with 15 µl of Interferin. Conditions for transfection are summarised in Table 2.1. Duplexes of siRNAs were first diluted in OptiMEM, then mixed with Interferin, dispensed onto the dishes and incubated at room temperature for 20 minutes to allow formation of siRNA-Interferin transfection complexes.

Cells in growth medium were then added into the dishes and cultured for 24–48 h before proceeding with further experiments. Efficiency of gene knockdown was confirmed on a protein level by SDS-PAGE and Western Blotting, usually 48 h after transfection. Densitometry analysis of Western blot bands intensities was performed using Phoretix 1D Gel Analysis Software.

Table 2.1: Transfection of mammalian cells with 5 nM siRNA.

Culture Dish	siRNA Duplexes	OptiMEM Volume	Interferin Volume	Cell Number in Medium	Total Volume
24-well	3 pmol	100 µl	2 µl	2.5×10^4 in 500 µl	600 µl
60 mm	22 pmol	400 µl	15 µl	2×10^5 in 4 ml	4.4 ml

Optimisation of siRNA transfections

Three siRNA concentrations were tested (5 nM, 10 nM and 20 nM) to determine the lowest effective siRNA concentration for transfection of fibroblasts. All concentrations showed high efficiency of gene expression knockdown in both RA synovial (Figure 2.1A) and dermal fibroblasts (Figure 2.1B). Densitometry analysis of Western blots of DDR2 and integrin β1 showed more than 80% reduction of expression at the protein level 48 h after transfection. Transfection with 5 nM siRNA provides

more that 80% expression knockdown for up to 5 days, therefore this concentration was used throughout the study (Figure 2.1C).

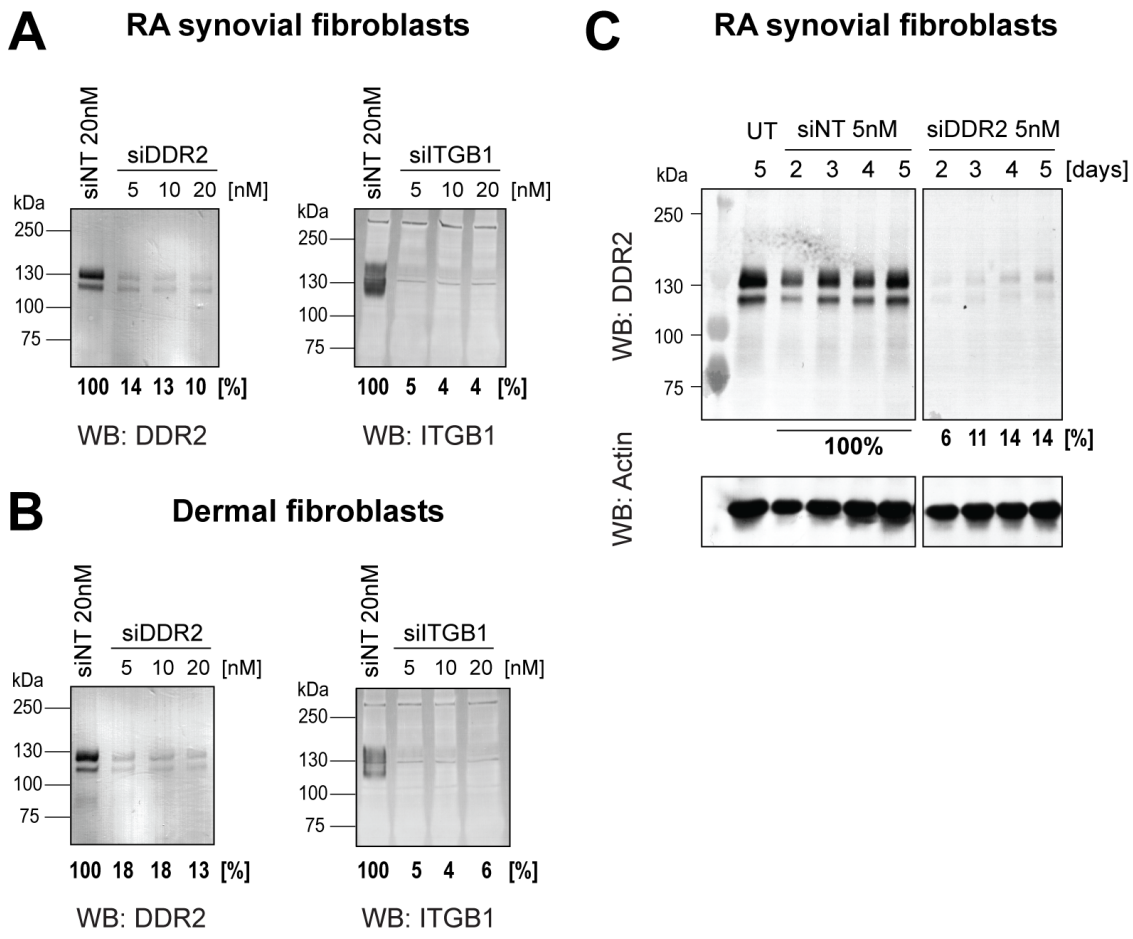

Figure 2.1: Optimisation of fibroblast transfection with siRNAs. RA synovial fibroblasts **(A)** or dermal fibroblasts **(B)** were transfected with 20 nM non-targeting siRNA and 5, 10 or 20 nM of siRNAs for DDR2 and ITGB1 in 24-well plates. Cells were lysed after 48 h and protein levels evaluated by Western Blotting. **(C)** RA synovial fibroblasts were transfected with 5 nM siNT and siDDR2 in 24-well plates and gene knockdown analysed at 2, 3, 4 and 5 days after transfection. Untreated (UT) cells at 5 days were also analysed. Percent of remaining gene expression was calculated by comparison with same day siNT transfected cells.

2.2.4 Transfection of mammalian cells with plasmid DNA

2×10^5 cells were seeded in 6-well plates 24 h before transfection, in growth medium without antibiotics. The next day, cells were usually 60–70% confluent and medium was changed to 2 ml of fresh growth medium also without antibiotics. For transfection, 1 µg of DNA was mixed with 3 µl of TransIT transfection reagent in 100 µl of OptiMEM, vortexed and incubated for 20 minutes at room temperature and then drop-wise added to cells. The medium was changed the following day to full growth medium. Cells were used for further experiments 24–48 h after transfection. Protein expression was evaluated by SDS-PAGE and Western Blotting, usually 48 h after transfection.

2.2.5 Establishment of stable cell lines

HEK293-EBNA cells were transfected with DNA constructs cloned into pCEP4 vector. pCEP4 vectors carry an Epstein-Barr Virus replication origin (oriP) and nuclear antigen (encoded by the EBNA-1 gene) enabling its episomal replication in HEK293-EBNA. Cells were transfected in a 6-well plate format, with 1 µg DNA and TransIT transfection reagent as described above (Section 2.2.4). 48 h after transfection, the medium was changed to complete growth medium supplemented with 400 µg/ml of hygromycin B. The medium was changed every 2–3 days to remove dead cells and to replenish the antibiotic. Cells were split in 1:3 ratio when they reached confluence. Stable cell lines were established by continuous culture in the presence of hygromycin B for approximately 2–3 weeks, until the majority of non-transfected cells died. Frozen cell stocks were prepared from early established cultures.

2.3 Molecular cloning techniques

2.3.1 Solutions used for molecular cloning

Alkaline lysis solution I

25 mM Tris-HCl (pH 8.0), 10 mM EDTA (pH 8.0).

Alkaline lysis solution II

0.2 M NaOH, 1% (w/v) SDS.

Alkaline lysis solution III

3 M potassium acetate, 11.5% (v/v) acetic acid.

Carbenicillin stock solution (1000 ×)

Carbenicillin (ampicillin analogue) dissolved at 100 mg/ml in water, 0.22 µm filter sterilised and stored in aliquots at −20°C.

DNA loading buffer (6 ×)

30% (v/v) glycerol, 0.25% (w/v) bromophenol blue.

Tris-Acetate-EDTA (TAE) electrophoresis buffer (0.5 ×)

20 mM Tris, 10 mM acetate, 0.5 mM EDTA (pH 8.0).

Tris-EDTA (TE) buffer (pH 8.0) with RNase A

10 mM Tris-HCl (pH 8.0), 1 mM EDTA (pH 8.0), 100 µg/ml RNase A.

2.3.2 Conditions for bacterial culture

LB medium and LB agar were prepared according to manufacturer's instructions and sterilised by autoclaving at 121°C. Prior to use, they were supplemented with appropriate antibiotics (100 µg/ml of carbenicillin or 25 µg/ml of zeocin). Usually 50–100 µl of liquid bacteria culture were spread on agar plates or bacteria were streaked using a sterile loop. Plates were incubated at 37°C in an incubator for 16–18 h to allow growth of single colonies. Thereafter plates were stored at 4°C. For liquid cultures, LB medium was inoculated with bacteria from a single colony or a small volume of culture and incubated for 16–18 h at 37°C with 220 rpm shaking.

2.3.3 Preparation of bacteria glycerol stocks

Bacteria from overnight cultures were pelleted down by centrifugation at 16,000 × g for 3 minutes in a 1.5 ml microfuge tube with a screw cap, resuspended in 20% (v/v) sterile glycerol in LB medium, vortexed thoroughly and snap frozen in liquid nitrogen. Glycerol stocks were stored at −80°C.

2.3.4 Alkaline lysis for isolation of plasmid DNA

An alkaline lysis method was used for isolation of plasmid DNA from small volumes (3–4 ml) of bacteria cultures (Sambrook and Russell, 2001). Cells from overnight cultures were pelleted down by centrifugation for 3 minutes and supernatants discarded. All centrifugation steps were performed at 16,000 × g. Cell pellets were thoroughly resuspended in 100 µl of ice cold Alkaline Lysis Solution I and lysed in 200 µl of room temperature Solution II, mixed by inversion and incubated on ice for 5 minutes. 150 µl of Solution III was added to the cell lysate, mixed by inversion and incubated on ice for a further 5 minutes. To help remove proteins, 10 µl of chloroform was added, the lysate briefly vortexed and centrifuged for 10 minutes. The supernatant was transferred to a new 1.5 ml microfuge tube and mixed with 2 volumes of 100% ethanol, incubated at room temperature for 2–3 minutes and centrifuged for 10 minutes. The DNA pellet was washed once with 700 µl of 70% ethanol and air dried. DNA was resuspended in 50 µl of TE buffer with RNase A and incubated at 37°C for 30 minutes to remove RNA.

2.3.5 Medium scale isolation of plasmid DNA with silica-membrane columns

To isolate plasmid DNA from medium size bacteria cultures (50–100 ml) PureYield Plasmid Midiprep System with endotoxin removal was used to obtain high quality DNA for transfection of mammalian cells. Plasmid DNA was isolated with silica-

membrane columns according to manufacturer's instructions. DNA was eluted from the column with 500–800 µl of nuclease-free water.

2.3.6 Measurement of DNA concentration

DNA concentrations were measured by sample absorbance at 260 nm using a NanoDrop 1000 Spectrophotometer. Additionally, purity of the samples was measured as a ratio of absorbance at 260 nm (absorbance peak for DNA) and 280 nm (absorbance peak from protein). Samples with 260/280 ratio higher than 1.8 were considered pure.

Alternatively, DNA fragments were separated by agarose gel electrophoresis (See Section 2.3.8) alongside serial dilutions of DNA ladders with known concentrations of DNA fragments. DNA concentration was estimated by comparison to intensities of DNA ladder fragments of similar size.

2.3.7 Restriction enzyme digestion of DNA

FastDigest restriction enzymes were used to digest plasmid DNA. Their activity is described as such that 1 µl of the Fast Digest enzyme can cleave up to 1 µg of DNA in FastDigest buffer during 5–15 minutes incubation time in 20 µl reaction volume.

Individual enzymes were used at $^1/_{20}$ reaction volume supplemented with universal $10\times$ FastDigest buffer to a final $1\times$ concentration. If not otherwise stated, reaction components were mixed, briefly spun and incubated between 30 minutes to 2 h at 37°C, but no longer than specified to avoid unspecific DNA cleavage (star activity).

2.3.8 Agarose gel electrophoresis

DNA fragments were separated by electrophoresis using 1% (w/v) agarose minigels prepared in $0.5\times$ TAE buffer supplemented with 0.5 µg/ml ethidium bromide. DNA samples were mixed with $6\times$ DNA loading buffer prior to loading. Gels were

run for 15–30 minutes at 135 V in 0.5 × TAE buffer. DNA ladders (0.5 µg per well) were run alongside the DNA samples as weight markers. Gels were scanned using a Molecular Imager Gel Doc XR+ Image System (Bio-Rad Laboratories, Hemel Hempstead, UK) with UV Transilluminator and analysed with Quantity One 1-D Analysis Software (Bio-Rad Laboratories, Hemel Hempstead, UK).

2.3.9 Extraction of DNA fragments from agarose gels

A GeneJET Gel Extraction Kit was used for purification of DNA fragments separated by gel electrophoresis. Prior to loading samples onto the gel, they were mixed with SYBR green I and separated on 1% agarose gels prepared without ethidium bromide. DNA bands were identified under the UV Transilluminator, excised with a clean scalpel and transferred to pre-weighted 1.5 ml microfuge tubes. DNA was extracted from agarose gels according to manufacturer's instructions and eluted from the column in 20 µl of Elution Buffer or nuclease-free water.

2.3.10 Ligation of DNA fragments

To ligate DNA fragments, 2 µg to 4 µg of plasmid DNA were digested using appropriate enzymes in 40 µl total reaction volume and enzymes inactivated according to their specifications. To prevent re-circularisation of the empty vector, 1 µl (1 U) of FastAP Thermosensitive Alkaline Phosphatase was added to the linearised vector and incubated for 30 minutes at 37°C to remove 5'- and 3'-phosphate groups from the DNA ends. DNA fragments were separated by agarose electrophoresis followed by DNA extraction from the gel. To estimate the concentration of extracted DNA, 1 µl of DNA was run on an agarose gel alongside weight markers. Ligation of vector and insert DNA fragments was performed at room temperature for 30 minutes, using 1 µl (5 U) T4 DNA ligase in 20 µl total reaction volume supplemented with 1 × Rapid Ligation Buffer and 1:3 molar excess of insert. Usually 50 to 100 ng of vector were used per reaction, and the amount of insert required for ligation was

calculated from the following equation:

$$\text{ng of insert} = \frac{\text{ng of vector} \times \text{insert size (in kb)}}{\text{vector size (in kb)}} \times \frac{\text{molar amount of insert}}{\text{molar amount of vector}}$$

To remove T4 DNA ligase after ligation, 20 µl of chloroform was added, after which the mixture was briefly vortexed and spun for 10 minutes at $16{,}000 \times$ g to separate the phases. The upper aqueous phase was transferred to a new microfuge tube and used for transformation.

2.3.11 Transformation of bacteria by electroporation

An electroporation protocol was used for transformation of competent cells with plasmid DNA. A vial with 50 µl of electrocompetent bacteria was thawed on ice, mixed with 1 µl of DNA (1–10 ng) and transferred to a disposable electroporation cuvette with a 2 mm electrode gap. Cells were electroporated with a 5 ms pulse and the following parameters: voltage – 2.5 kV, capacitor – 25 µF and resistor – 200 Ohms. Cells were recovered from the cuvette with 1 ml LB medium and incubated at 37°C for 1 h with 220 rpm shaking to allow the expression of the antibiotic resistance gene. 10–200 µl from each transformation was spread on LB agar plates containing an appropriate antibiotic. Plates were incubated at 37°C overnight.

2.4 Molecular biology techniques

2.4.1 RNA extraction

Total RNA from less than 5×10^5 cells was extracted with a RNeasy Micro Kit, according to manufacturer's instructions. RNA was eluted from the column with 16 µl of nuclease-free water. RNA concentration and purity was measured by NanoDrop 1000 Spectrophotometer.

2.4.2 Synthesis of cDNA

Extracted RNA was reverse-transcribed to single stranded cDNA with a High Capacity cDNA Reverse Transcription Kit, according to manufacturer's protocol. Reaction components are listed in Table 2.2. Up to 2 µg of total RNA was used per 20 µl reaction. Reverse transcription was performed in a thermocycler with the following conditions: 10 minutes at 35°C, 120 minutes at 37°C followed by heat inactivation at 85°C for 5 minutes.

2.4.3 Real-time quantitative PCR

Gene expression was analysed by real-time quantitative PCR (qPCR) using TaqMan Gene Expression Assays from Applied Biosystems. These assays consist of gene specific, pre-mixed, unlabelled primers and TaqMan Minor Groove Binding probes (labelled with FAM fluorophore). Ribosomal RNA Control Reagents (with VIC labelled probe) were used for amplification of the 18S gene as an endogenous control.

Real-time qPCR was performed in triplicate in 10 µl, using 1 µl cDNA as a template, 5 µl of 2 × Maxima Probe/ROX qPCR Master Mix, 1 µl of 10 × Primer and Probe TaqMan Mix and 3 µl of nuclease-free water. Separate (singleplex) reactions were set up for each gene. Negative control reactions with no template were performed in each PCR run. Amplification and detection were performed in 0.1 ml tubes with lids in a Corbett Rotor Gene 6000 (Corbett Life Science) equipped with a 72-well Rotor-Disc. Cycling conditions were as follows: initial denaturation for 10 minutes at 94°C followed by 40 three-step cycles: 10 seconds denaturation at 95° C, 10 seconds annealing at 55°C and 20 seconds extension at 72°C. The FAM fluorophore was detected in the Green Channel (excitation 470 nm, detection 510 nm) and the VIC fluorophore was detected in the Yellow Channel (excitation 530 nm, detection 555 nm). Corbett Rotor Gene 6000 Software was used to analyse the results of the real-time quantitative PCR reaction and to set up the threshold cycle (C_T).

Table 2.2: Reverse transcription reaction components.

Components	**Volume**
Reverse Transcription Buffer (10 ×)	2.0 µl
dNTP Mix (25 ×)	0.8 µl
Reverse Transcription Random Primers (10 ×)	2.0 µl
MultiScribe™ Reverse Transcriptase	1.0 µl
Nuclease-free water	3.2 µl
RNA (up to 2 µg)	10.0 µl
Total volume	**20 µl**

Relative quantification of gene expression with $\Delta\Delta C_T$ method

The comparative $\Delta\Delta C_T$ method was used to calculate relative gene expression for MT1-MMP (Livak and Schmittgen, 2001). In this method, levels of target gene expression (MT1-MMP) are first normalised to the endogenous control (18S), by calculation of the ΔC_T value. ΔC_T is defined as the difference between the average C_T values of target and control genes for an individual sample. Finally, expression of the target gene in the treated samples is presented as a fold change over expression in untreated samples. Fold change was calculated from the following formula:

$$\text{Fold change} = 2^{-\Delta\Delta C_T}$$

$$\text{where } \Delta\Delta C_T = \Delta C_{T\ \text{Treated}} - \Delta C_{T\ \text{Untreated}}$$

$$\text{and } \Delta C_T = C_{T\ \text{Target Gene}} - C_{T\ \text{Control Gene}}$$

All calculations were performed in Microsoft Office Excel Software.

2.5 SDS-PAGE

2.5.1 Solutions used for SDS-PAGE

Anode reservoir buffer (pH 8.23; 4 ×)

62.5 mM ammediol, 50 mM HCl.

Cathode reservoir buffer (pH 9.39; 4 ×)

41 mM ammediol, 40 mM glycine, 0.4% (w/v) SDS.

De-staining solution

30% (v/v) methanol, 1% (v/v) formic acid.

Resolving gel buffer (pH 8.96)

110 mM ammediol, 47 mM HCl, 0.02% (w/v) NaN_3.

SDS-PAGE sample buffer (2 ×)

2% (w/v) SDS, 0.1% (w/v) bromophenol blue, 40% (v/v) glycerol, 50% (v/v) stacking gel buffer (4 ×), 0.9% β-mercaptoethanol.

Stacking gel buffer (pH 8.37)

84 mM ammediol, 62 mM HCl, 0.02% (w/v) NaN_3.

Staining solution

0.1% (w/v) Coomassie Brilliant Blue R-250, 50% (v/v) methanol, 20% (v/v) acetic acid.

Sucrose solution 50% (w/v) sucrose, 0.03% (v/v) toluene, 0.02% (w/v) NaN_3.

Proteins were separated by SDS polyacrylamide gel electrophoresis (SDS–PAGE) based on the ammediol buffer system (Bury, 1981). For SDS-PAGE, protein samples were mixed at 1:1 ratio with 2 × sample buffer or cells were directly lysed in 1 × sample buffer. SDS-PAGE sample buffer contains SDS, which binds to proteins proportional to their molecular weight and provides them with a negative charge. During electrophoresis, SDS-coated and therefore negatively charged proteins migrate in the electric field according to their molecular weight. Resolving (7.5%) and stacking (4%) gels were used for SDS-PAGE throughout the study and their components are listed in Table 2.3.

Table 2.3: Composition of SDS-PAGE gels. Components of 7.5% resolving and 4% stacking gels for SDS-PAGE.

Components	**Resolving gel (7.5%)**	**Stacking gel (4%)**
30% (w/v) acrylamide/bis-acrylamide	1500 µl	320 µl
Resolving / stacking gel buffer	1500 µl	642 µl
Sucrose solution	1290 µl	642 µl
dH_2O	1710 µl	963 µl
10% (w/v) ammonium persulfate	42 µl	31 µl
TEMED	4.5 µl	6.75 µl

Polyacrylamide mini-gels were cast between glass slabs with 1.5 mm spacers. First, the resolving gel was poured between the slabs, overlaid with water-saturated butanol and allowed to polymerise. The butanol layer ensured an even interface between resolving and stacking gels by excluding oxygen from a polymerising gel. After polymerisation, butanol was decanted and gels washed with dH_2O. The stacking gel was poured on top of the resolving gel, 1.5 mm thick combs were inserted and the gel was allowed to polymerise. Samples prepared in $1 \times$ SDS-PAGE sample buffer were boiled for 15 minutes prior to loading, unless otherwise stated. Usually 15 µl of sample was loaded onto the gel with 6 µl of pre-stained protein marker. Gels were run at 150 V (constant voltage) for approximately 60 minutes until the bromophenol blue dye reached the bottom of the gel.

2.6 Western Blotting

2.6.1 Solutions used for Western Blotting

Antibody dilution buffer

1% (w/v) BSA, 50 mM Tris-HCl (pH 7.5), 150 mM NaCl, 0.05% (v/v) Tween 20, 0.02% (w/v) NaN_3.

Non-fat dry milk, 5%

5% (w/v) dry skimmed milk, 10 mM Tris-HCl (pH 7.5), 150 mM NaCl, 0.02% (w/v) NaN_3.

PBS-T

0.05% (v/v) Tween 20, 0.02% (w/v) NaN_3 in PBS.

After SDS-PAGE, proteins were transferred from gels onto 0.2 µm PVDF membranes using a Trans-Blot Turbo Transfer System (Bio-Rad Laboratories, Hemel Hempstead, UK). The blotting sandwich was assembled according to manufacturer's instructions and proteins (30–150 kDa) were transferred for 7–10 minutes at a constant current of 1.3 A and a voltage of up to 25 V. Membranes were blocked in 5% non-fat dry milk for 20 minutes and washed 3 times for 5 minutes in PBS-T. Primary antibodies were diluted as indicated (usually 1:500–1:1000, see Table 2.4) in antibody dilution solution and incubated with membranes overnight at 4°C. Afterwards, membranes were washed 3 times for 5 minutes each in PBS-T and incubated for 1h at room temperature with secondary AP-conjugated antibodies diluted at 1:10,000 in antibody dilution solution. After washing twice with PBS-T, membranes were incubated with 6–8 ml of AP substrate for 30–60 minutes until bands appeared.

Table 2.4: Primary antibodies used for Western Blotting.

Antibodies	**Dilution**	**Concentration**
anti-actin	1:500	0.4 µg/ml
anti-β1 integrin	1:1000	n / a
anti-DDR1	1:1000	0.2 µg/ml
anti-DDR2	1:1000	0.2 µg/ml
anti-MT1-MMP hemopexin domain (222-1D8)	1:1000	0.5 µg/ml
anti-MT1-MMP catalytic domain	1:2000	n / a
anti-phosphotyrosine	1:1000	1ug/ml

n / a - data non available

2.7 Zymography of metalloproteinases

2.7.1 General solutions

SDS-PAGE sample buffer (2 ×)

2% (w/v) SDS, 0.1% (w/v) bromophenol blue, 40% (v/v) glycerol, 50% (v/v) stacking gel buffer (pH 8.37; 4 ×).

Washing buffer for zymography

2.5% (v/v) Triton X-100, 50 mM Tris-HCl (pH 7.5), 5 mM $CaCl_2$, 5 µM $ZnCl_2$, 0.02% NaN_3.

Tris-glycine SDS-PAGE running buffer (1 ×)

25 mM Tris, 192 mM glycine, 0.1% SDS.

Staining solution

0.1% (w/v) Coomassie Brilliant Blue R-250, 50% (v/v) methanol, 20% (v/v) acetic acid.

De-staining solution

30% (v/v) methanol, 1% (v/v) formic acid.

Zymography is a simple and sensitive technique that allows for detection of enzyme activity e.g. in conditioned medium. (Troeberg and Nagase, 2004). It is based on a modified SDS-PAGE method, where an enzyme substrate such as gelatin or casein is incorporated into the gel. Protein samples are prepared under denaturing (SDS) and non-reducing conditions. After electrophoresis, SDS is replaced with Triton X-100 to allow refolding of the protein, and during incubation enzymes digest the incorporated substrate. Afterwards gels are stained with Coomassie Brilliant Blue R-250, and digested areas can be visualised as white bands against a dark background. Gelatin zymography is most commonly used to detect the gelatinases MMP-2 and MMP-9. SDS in sample buffer disrupts interaction of the pro-domain cysteine with the active site zinc, leading to enzyme activation without proteolytic cleavage, therefore both latent and active MMPs can be detected (Troeberg and

Nagase, 2004). Size difference allows to distinguish between the two forms and to asses levels of protein activation.

2.7.2 Gelatin zymography

Gelatin zymography was used to detect gelatinase activity in the conditioned medium collected from cultured cells. Gelatin was incorporated into 7.5% resolving polyacrylamide gels at a concentration of 0.8 mg/ml. Culture medium was mixed with 2 × SDS-PAGE sample buffer without β-Me at a 2:1 ratio and 15 µl of the mix used for loading the gel (without boiling). Gels were run at 150 V for 60–70 minutes. After electrophoresis, gels were equilibrated in zymography washing buffer for 1 h, with changes of buffer every 15 minutes to replace SDS with Triton X-100. After washing, gels were incubated in washing buffer for 16–18 h at room temperature or at 37°C. Gels were stained with staining solution for 30 minutes–1 h and incubated with de-staining solution until thoroughly destained.

2.7.3 Casein zymography

Pre-cast 4–16% gradient Tris-glycine casein zymograms were used to detect casein activity in the conditioned culture medium. Culture medium was mixed with 2 × SDS-PAGE sample buffer without β-Me and up to 32 µl of the mix used for loading (without boiling). Gels were run at 125 V for 90 minutes using Tris-glycine SDS-PAGE running buffers. After electrophoresis gels were equilibrated in zymography washing buffer for 1 h, with changes of buffer every 15 minutes to replace SDS with Triton X-100. Gels were incubated for 24 h at 37°C. Staining was not necessary, as gels had a proprietary dye already incorporated into the gel.

2.8 Gelatin film degradation assay

2.8.1 Preparation of Alexa Fluor 488-labelled gelatin

To label gelatin with Alexa Fluor 488 fluorescent dye, 100 µg of Alexa Fluor 488 sulfodichlorophenol ester was dissolved in 250 µl of 20 mg/ml gelatin in 0.1 M sodium bicarbonate. The mixture was stirred for 1 h at room temperature and the reaction stopped by addition of 50 µl of 1 M ammonium chloride. Next, 50 µl of $10 \times$ PBS was added and the concentration of gelatin adjusted to 10 mg/ml with dH_2O. Labelled gelatin solution was dialysed against 1 L of autoclaved PBS for 18 h at 4° C. Finally, the concentration of Alexa Fluor 488-labelled gelatin (Alexa488-gelatin) was adjusted to 1 mg/ml using 50% (v/v) glycerol in PBS and the solution stored in aliquots at −20°C.

2.8.2 Coating glass coverslips with Alexa488-gelatin

To coat glass coverslips with fluorescently labelled gelatin, Alexa488-gelatin was diluted in dH_2O to 50 µg/ml and incubated at 60°C for 20 minutes to completely dissolve the gelatin. Coverslips were incubated on top of 150 µl of Alexa488-gelatin drops for 20 minutes, followed by 15 minutes cross-linking with 1% (v/v) glutaraldehyde and 15 minutes incubation with 1 M ammonium chloride. Coverslips were transferred gelatin side up into a 12-well plate containing 70% (v/v) ethanol and incubated from 2 h to overnight at 4°C for sterilisation.

2.8.3 Gelatin film degradation assay setup

Before seeding cells, coverslips were washed at least three times in DPBS or serum-free DMEM in sterile conditions under a tissue culture hood. 2.5×10^4 cells were seeded per coverslip and cultured for 48 h in 2% FBS DMEM. After the culture period, cells were fixed in 3% (w/v) PFA in PBS for 15 minutes and washed in PBS. To stain nuclei and F-actin, coverslips were incubated for 1 h with 0.2% (v/v) Triton X-

100 solution containing DAPI (1:400 dilution) and Alexa Fluor 568-conjugated phalloidin (1:100 dilution). Coverslips were washed once in PBS and mounted on glass slides with ProLong Gold and secured with nail polish. Images were acquired with a Nikon Eclipse TE2000-E inverted fluorescence microscope with a CCD-camera using $4\times$ objective lenses and analysed in Volocity 3D Image Analysis Software (PerkinElmer, Cambridge, UK).

2.9 Collagen film degradation assay

PureCol type I collagen (9 volumes) was mixed on ice with 1 volume of ice-cold $10\times$ RPMI-1640 and neutralised by drop-wise addition of 1 M NaOH until the pH reached 7.5–8 as checked by pH papers. The final concentration of neutralised collagen was 2.7 mg/ml. Costar CellBIND 12-well plates were chilled on ice and the bottom of the wells was evenly coated with 100 µl of neutralised collagen, by addition of 800 µl of collagen and removal of 700 µl. Plates were thereafter incubated for 1 h at 37°C to allow collagen fibril formation. 0.5×10^5 cells were seeded on top of the collagen layer in 0.5 ml serum-free DMEM and cultured for 3 days. Afterwards cells were gently washed twice with DPBS and lifted from collagen by incubation with trypsin/EDTA. The collagen layer was fixed with 3% PFA in PBS for 15 minutes and incubated with staining solution [(0.1% (w/v) Coomassie Brilliant Blue R-250, 50% (v/v) methanol, 20% (v/v) acetic acid)] for 30 minutes. Plates were then washed in de-staining solution [(30% (v/v) methanol, 1% (v/v) formic acid)], followed by washing with dH_2O and allowed to air dry. Images were captured with a light microscope with a CCD-camera using $4\times$ objective lenses and analysed in Volocity Software. Degraded regions appeared as white areas against darkly stained intact collagen.

2.10 Alexa488-collagen degradation (Collagen488)

Collagen solution was neutralised on ice, using 9 volumes of collagen and 1 volume of 10 × PBS and drop-wise addition of 1 M NaOH until the pH reached 7.5-8. The concentration of neutralised collagen was 2.7 mg/ml. 500 µl of neutralised collagen was added per well in a 12-well plate and 250 µl per well in a 24-well plate. Collagen was polymerised for 1 h at 37°C, and then incubated for 30 minutes at room temperature with 500 µl of sterile 0.1 M $NaHCO_3$ applied per well. Alexa Fluor 488 sulfodichlorophenol ester was dissolved in 0.1 M $NaHCO_3$ at 2–20 µg/ml. Collagens were incubated with Alexa Fluor 488 sulfodichlorophenol ester solution for 2 h at room temperature, washed three times with 1 × PBS and DMEM. Afterwards, 2.5×10^4 dermal fibroblasts were seeded in 300 µl serum-free and phenol red-free DMEM and incubated between 2–5 days, as indicated. Culture medium was collected, spun down at 16,000 × g and 200 µl used to detect Alexa Fluor 488 fluorophore released into the medium. Bacterial collagenase (100 µg/ml) was used to digest the remaining collagen, for 1 h at 37°C. Solution fluorescence was measured using a spectrophotometer, using an excitation wavelength 485 nm and emission wavelength of 538 nm.

2.11 Analysis of cell invasion in 3D collagen

Microcarrier beads invasion assay and transwell invasion assay were carried out as described by Palmisano and Itoh (2010).

2.11.1 Microcarrier beads invasion assay

Attachment of cells to beads

Gelatin-coated Cytodex 3 microcarrier beads were prepared, autoclaved and suspended in sterile PBS according to Palmisano and Itoh (2010). Before experiments, an aliquot of bead suspension was diluted to 250 beads per 1 ml of serum-free DMEM

with antibiotics. A suspension of 5×10^4 cells was prepared in 1 ml of serum-free DMEM and mixed with 1 ml of 250 beads in 2 ml microfuge tubes. The medium was supplemented with HEPES buffer (pH 7.5) at 100 mM final concentration to avoid changes in the pH. Tubes were incubated at 37°C with gentle agitation for 4–6 h until cells attached to the beads, as inspected under the light microscope. Afterwards beads were allowed to settle at the bottom of the tube and were washed twice with DMEM to remove unattached cells. All but approximately 50 µl of medium was removed and remaining cell-beads suspension cooled on ice.

Mixing collagen with cell-beads suspension

9 volumes of type I collagen were mixed with 1 volume of $10 \times$ RPMI-1640 and neutralised by drop-wise addition of 1 M NaOH until the pH reached 7.5–8. For this purpose CellMatrix Type I-A collagen or a mixture of CellMatrix Type I-A and PureCol collagens was used. 650 µl of neutralised collagen solution was mixed with the cell-beads suspension and transferred into 12-well plates. The final collagen concentration was approximately 2.5 mg/ml. Plates were incubated at 37°C for 1 h to allow collagen fibril formation. 1 ml of 10% serum DMEM was added on top of the polymerised collagen and cells incubated at 37°C. During the incubation time, cells migrated away from the bead surface into the surrounding collagen gel. After 72 h, medium was removed and cells were fixed in 3% (w/v) PFA in PBS for 1 h at room temperature. Images were captured with a light microscope with a CCD-camera using $10 \times$ objective lenses. Distances between cells (cell nucleus) and the bead surface were measured in pixels in ImageJ software (National Institutes of Health) and then converted to µm (1.25 µm/pixel) (Figure 2.2).

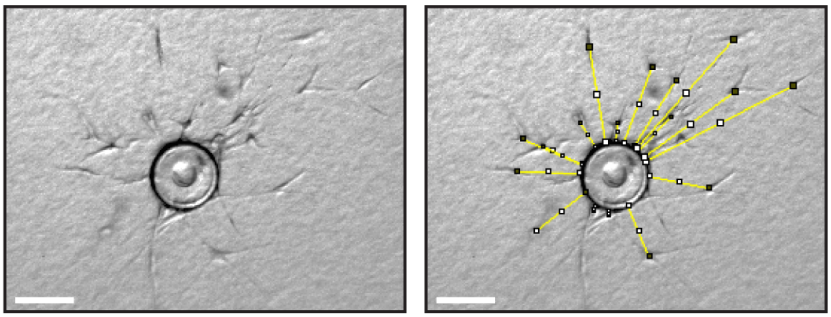

Figure 2.2: Example of measurement of cell migration distance in microcarrier beads invasion assay. ImageJ was used to measure distances between cell nucleus and bead surface (right panel). Distances were measured in pixels and converted to µm (1.25 µm/pixel). Scale bar: 110 µm.

2.11.2 Transwell invasion assay

For the transwell invasion assay, 12-well transwell chambers were used, which were fitted with PET removable membranes with 8 µm diameter pores through which cells can migrate (Figure 2.3). PET membranes at the bottom of transwells were coated with 50 µl of neutralised collagen by addition of 200 µl of collagen and removal of 150 µl. For this purpose CellMatrix Type I-A collagen was used at final concentration of 2.7 mg/ml. Collagen-coated transwells were incubated at 37°C for 60 minutes to allow fibril formation. 5×10^4 cells in 1 ml of serum-free medium were added to the top chamber and 1.5 ml of 10% FBS DMEM was added to the bottom chamber and incubated at 37°C for 3 days. After incubation, media were removed from both chambers and cells fixed with 3% (w/v) PFA in PBS for 20 minutes at room temperature. Collagen and cells that did not migrate were removed from the upper chamber by swabbing with a cotton bud (Figure 2.3). Cells that migrated through the membrane remained at the bottom side of the chamber and were stained with DAPI (1:400) and Alexa Fluor 488-conjugated phalloidin (1:100) dissolved in 0.2% (v/v) Triton X-100 for 1 h to visualise the nuclei and F-actin respectively. Membranes were removed with a sharp scalpel and mounted with ProLong Gold solution on microscope slides, covered with glass coverslips and secured with nail polish. Thirty images covering the whole membrane area were taken with a Nikon Eclipse

TE2000-E inverted fluorescence microscope with a CCD-camera with 4 × objective lenses. Cells were automatically counted in Volocity Software based on detection of DAPI-stained nuclei.

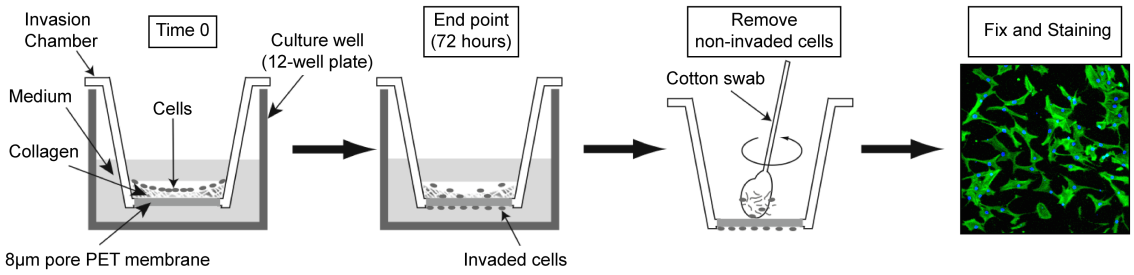

Figure 2.3: Protocol of transwell invasion assay. In the transwell invasion assay, cells are seeded on top of collagen type I-coated transwells in serum-free medium. Transwells are placed into 12-well plates filled with 10% FBS medium, and FBS acts as a chemoattractant. During 72 h of culture, cells invade into collagen and migrate through pores to the bottom side of the membrane. Cells that did not invade are removed with a cotton bud together with the collagen layer. Remaining cells are fixed with 3% PFA, stained with DAPI (blue) and Alexa Fluor 488-conjugated phalloidin (green) and counted. Figure and protocol adapted from Palmisano and Itoh (2010).

2.12 Cloning, expression and purification of DDR-Fc tagged proteins

Dimeric soluble extracellular domains (ECD) of DDR1 and DDR2 were used to examine their binding properties (described in Results Chapter 5). First, DNA fragments encoding ECD of DDRs were amplified by PCR, sequenced and cloned into pFUSE–rIgG–Fc1 (pFc1) DNA vector to introduce a Fc tag at the C-terminus to allow for dimerisation of the protein. Next, DDR-ECD-Fc fragments were cloned into pCEP4 vector and transfected into HEK293-EBNA to generate stable cell lines. Proteins were then purified from conditioned media using Protein A Sepharose. Detailed methodology is described in Sections 2.12.1 and 2.12.2. Along with wild type DDR-Fc/pCEP4 constructs (DDR1-Fc and DDR2-Fc), the following constructs with in-

troduced mutations were created as negative controls:

– DDR1-W53A-Fc/pCEP4

– DDR1-R105A-Fc/pCEP4

– DDR2-W52A-Fc/pCEP4

2.12.1 PCR amplification of ECDs

PCR amplification of DDR1-ECD, DDR2-ECD and DDR1-W53A-ECD

Primers for amplification of ECDs of DDR1 and DDR2 were designed in DNA Dynamo software, based on analysis of cDNA sequence and information about domain structure available from the UniProt website (www.uniprot.org; DDR1 ID Q08345-1; DDR2 ID Q16832, January 2011). Primers were designed so that they amplified the endogenous Kozak consensus sequences and the first 416 amino acids for DDR1 (M^1–T^{416}) and the first 398 amino acids for DDR2 (M^1–R^{399}). Additional restriction enzyme sites in the primers introduce *Xho*I sites at both 5' and 3' ends of the amplified sequence. Primers were synthesised by Eurofins MWG Operon (Ebersberg, Germany) and their sequences are presented below, with underlined *Xho*I sites:

DDR1-ECD Forward (*Xho*I): 5'-GTGCTCGAGCAGGAGCTATGGGACCAG-3'

DDR1-ECD Reverse (*Xho*I): 5'-GTCTCGAGGTCGGGCTCCCCTCGG-3'

DDR2-ECD Forward (*Xho*I): 5'-GAGCTCGAGCACCATCTTCTGAGATGATCC-3'

DDR2-ECD Reverse (*Xho*I): 5'-GTCTCGAGCGAGTGTTGCTGTCATCAAC-3'

DNA fragments coding DDR ECDs were amplified by PCR. Reaction components are listed in Table 2.5. DDR1/pSG5, DDR2/pSG5 and DDR1-W53A/pSG5 were used as a DNA templates to amplify DDR1-ECD, DDR2-ECD and DDR1-W53A-ECD. Negative PCR controls were also prepared, where DNA template was replaced by dH_2O. PCR cycling conditions were as follows: initial denaturation for 2 minutes at 94°C, followed by 30 three-step cycles: 30 sec denaturation at 94°C,

30 sec annealing at 55°C and 1 min 15 sec extension at 72°C and final extension for 10 min at 72°C. PCR products (1 µl) were analysed by agarose gel electrophoresis (Figure 2.4).

Table 2.5: Components of PCR to amplify ECDs of DDRs.

Components	**Volume**	**Final concentration**
DNA template (10 ng/µl)	1.0 µl	0.2 ng/µl
Pfu reaction buffer (10 ×)	5.0 µl	1 ×
Forward primer (10 mM)	1.5 µl	0.3 µM
Reverse primer (10 mM)	1.5 µl	0.3 µM
dNTPs (10 mM each)	1.0 µl	0.2 µM
dH_2O	39.0 µl	–
Pfu Polymerase (2.5 U/µl)	1.0 µl	0.05 U/µl
Total volume	**50 µl**	

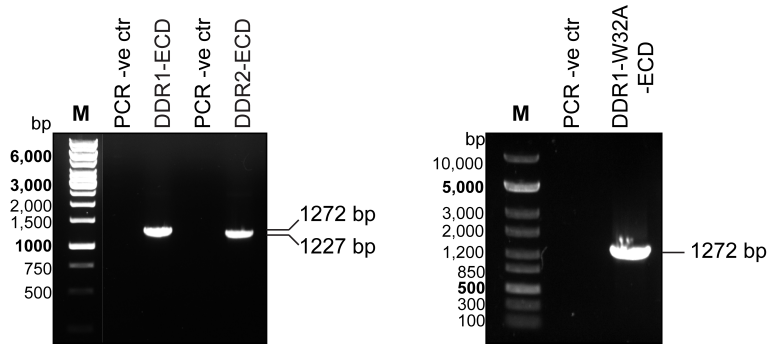

Figure 2.4: Results of PCR amplification of DDR ECDs. PCR products (1 µl) were separated by agarose electrophoresis. Expected sizes of the DNA fragments are indicated (DDR1-ECD: 1272 bp and DDR2-ECD: 1227 bp). PCR negative controls (PCR -ve ctr) generated no bands, as expected. *M - DNA marker*

Strand overlap extension PCR to create DDR2-ECD-W52A

The W52→A mutation was introduced in DDR2 cDNA by strand overlap extension PCR, where two rounds of PCR reactions are performed using 4 different primers (Figure 2.5). DDR2-ECD-Forward and DDR2-ECD-Reverse primers were used, as well as two additional primers DDR2-W52A-Forward and DDR2-W52A-Reverse, which were designed in DNA Dynamo Software and synthesised as previously described. These primers are partially complementary and contain a modified sequence (GCG instead of TGG) to introduce the W52A mutation. They are shown below, the mutation is indicated in red and the overlapping sequence is underlined:

DDR2-W52A Forward: 5'-CCAGTCAGGCGTCAGAGTCCACAGCTGC-3'

DDR2-W52A Reverse: 5'-GACTCTGACGCCTGACTGGAAGCTGTGATGT-3'

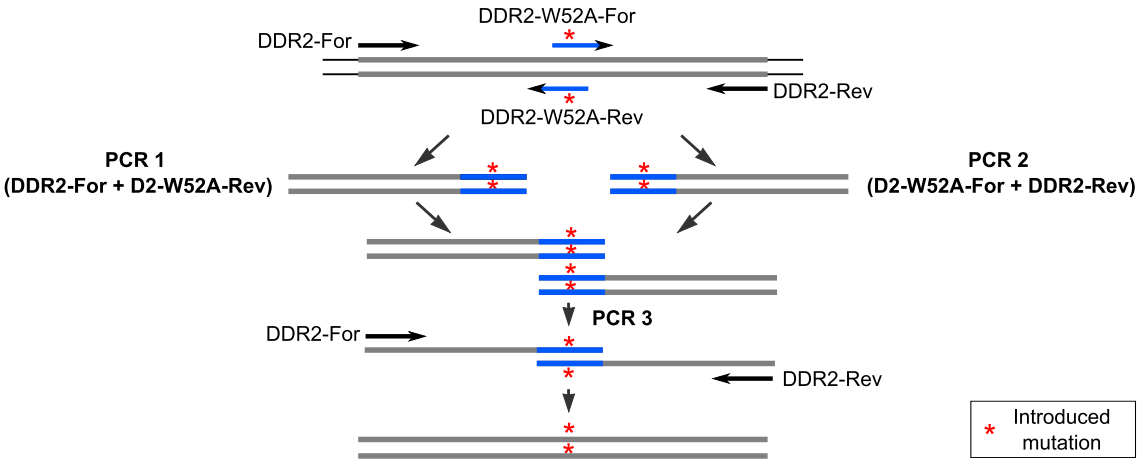

Figure 2.5: Schematic representation of PCR mutagenesis by strand overlap extension. Mutation W52→A (marked by asterisk) is introduced in DDR2-W52A Forward and Reverse primers which are partially overlapping. These primers and DDR-ECD Forward and Reverse are used in the first round of two separate PCR reactions – PCR1 (DDR2-ECD-For and DDR2-W52A-Rev) and PCR2 (DDR2-W52A-For and DDR2-ECD-Rev). Two partially overlapping and shorter DNA products are created. In the third PCR reaction (PCR3), products of PCR1 and PCR2 are purified, combined and amplified with DDR2-ECD Forward and Reverse primers, resulting in full length product DDR2-ECD with introduced W52A mutation.

Tm for primers were calculated according to guidelines for Phusion Hot Start II polymerase and the annealing temperature was 3°C higher than the lower primer Tm. PCR components used in all reactions are listed in Table 2.6. During the first round of PCR, two DNA fragments with short overlapping sequence are amplified in two separate reactions (PCR1 and PCR2, Figure 2.5), and the mutation is introduced in the overlap. In the second round of PCR, overlapping DNA products are combined and extended, resulting in the full length product with the introduced mutation.

Table 2.6: Components of the strand overlap PCR.

Components	**Volume**	**Final concentration**
DNA template (1 ng/µl)	2.0 µl	0.02 ng/µl
Phusion HF reaction buffer (5 ×)	10.0 µl	1 ×
Forward primer (10 mM)	2.5 µl	0.5 µM
Reverse primer (10 mM)	2.5 µl	0.5 µM
dNTPs (10 mM each)	1.0 µl	0.2 µM
dH_2O	31.5 µl	–
Phusion Hot Start II (2 U/µl) Polymerase	0.5 µl	0.02 U/µl
Total volume	**50 µl**	

DDR2/pSG5 was used as a template in the first round of PCRs. PCR1 uses primers DDR2-ECD Forward and DDR2-W52A Reverse and PCR2 uses primers DDR-W52A Forward and DDR-ECD Reverse. Cycling conditions were as follows: initial denaturation for 30 sec at 98°C followed by 30 three-step cycles: 10 sec denaturation at 98°C, 15 sec annealing at 63°C and 25 sec extension at 72°C, finished by final extension for 10 minutes at 72°C. PCR products were confirmed by agarose gel electrophoresis (Figure 2.6A).

PCR-generated fragments were then extracted from the gel and 1 µl of each product used as a template in PCR3. Primers used in PCR3 were DDR2-ECD Forward and Reverse resulting in same length product as DDR2-ECD. The following

cycling conditions were used: initial denaturation for 30 sec at 98°C followed by 30 three-step cycles: 10 sec denaturation at 98°C, 15 sec annealing at 67°C and 30 sec extension at 72°C and final extension for 10 minutes at 72°C. The expected full length DDR2-W52A-ECD fragment of 1227 bp was confirmed by agarose gel electrophoresis (Figure 2.6B). Negative PCR controls with DNA templates substituted by dH_2O were used in all PCR reactions.

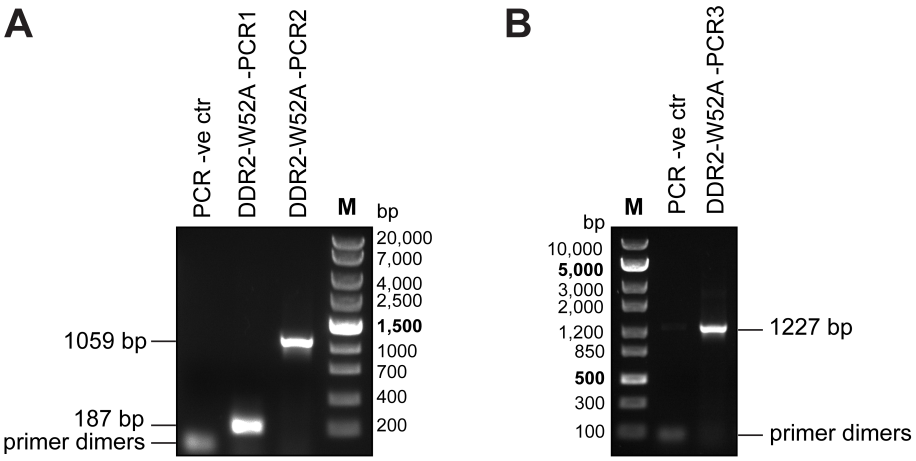

Figure 2.6: Results of the strand overlap extension PCR. PCR products (1 µl) from first **(A)** and second **(B)** round of PCR reactions were separated by agarose electrophoresis. Expected sizes of the DNA fragments are indicated (PCR1: 1059 bp, PCR2: 187 bp, PCR3 DDR2-W53A-ECD: 1227 bp). PCR negative controls (PCR -ve ctr) generated no bands, as expected. *M - DNA marker*

Cloning into pJET1.2 and pFUSE-rIgG-Fc1

PCR products of DDR1-ECD, DDR1-W53A-ECD, DDR2-ECD and DDR2-W52A-ECD were purified from agarose gels, blunt-end ligated into pJET1.2 cloning vector and electroporated into *E. coli* DH5α. DNA from several single colonies was purified by the alkaline lysis method and samples positive for an insert were identified by digest with *Xho*I. Positive DNA samples were sequenced at Eurofins MWG Operon to confirm they did not carry additional mutations. Introduced mutations were also confirmed (Figure 2.7). DDR-ECD fragments were excised from pJET1.2 vector via

*Xho*I sites and subcloned into the reading frame of pFc1 vector, and electroporated into *E. coli* TOP10 cells. DNA was isolated from several single colonies and the presence and orientation of the insert checked by restriction digest with *Pst*I.

Generation of DDR1-R105A-ECD by domain swapping

To generate the DDR1-R105A-ECD construct, an 895 bp fragment containing the R105A mutation was cut from DDR1-NHA-R105A-CF/pSG5 vector with *Sca*I and *Bst*XI restriction enzymes and ligated in place of the identical fragment (without mutation) in DDR1-ECD/pFc1. *E. coli* TOP10 was electroporated with the ligation product and confirmation of insert presence were carried out as described above. The introduced mutation was confirmed by sequencing (Figure 2.7).

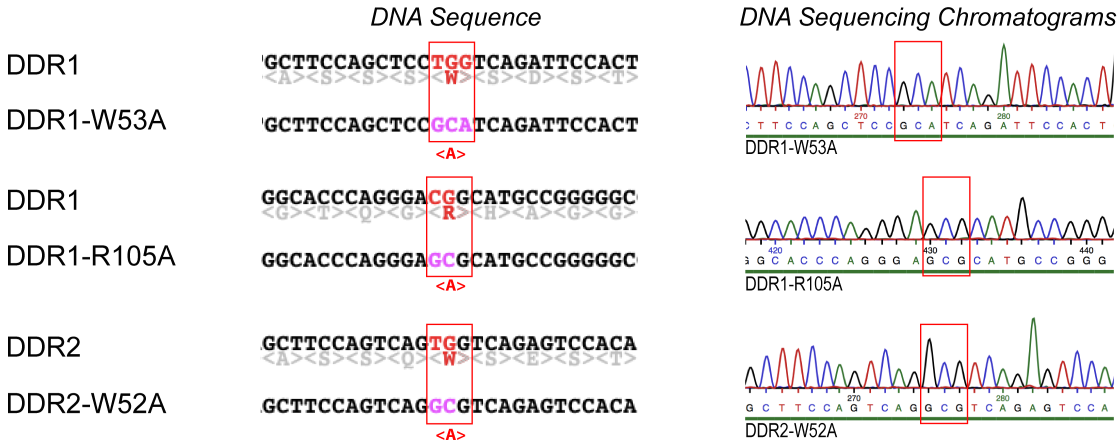

Figure 2.7: Results of DNA sequencing. DNA from positive clones were sequenced by Eurofins MWG Operon. Sequence alignment of obtained sequencing results was made in DNA Dynamo software. Comparison of DDR1-W53A, DDR1-R105A and DDR2-W52A ECDs to wild type DDRs show the presence of introduced mutations. DNA sequencing chromatograms of DDR1-W53A, DDR1-R105A and DDR2-W52A are also presented.

Cloning into pCEP4 vector and confirmation of expression

DDR-ECD-Fc fragments were excised with *Eco*RV and *Nhe*I restriction enzymes, cloned into pCEP4 via *Pvu*II and *Nhe*I sites and electroporated into *E. coli* DH5α. Positive colonies were identified by digestion with *Nru*I and *Sal*I restriction enzymes (Figure 2.8). Endotoxin-free DNA from positive clones was purified and used to transfect HEK293-EBNA cells. Five stable 293-EBNA cell lines expressing each DDR-ECD-Fc protein were established in the presence of hygromycin B (See Section 2.2.5).

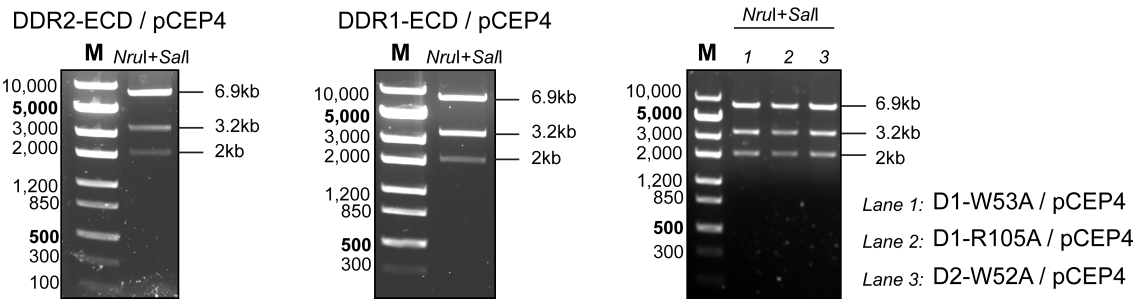

Figure 2.8: Restriction enzyme digestion of DDR-Fc/pCEP4 constructs. DNA from five DDR-Fc/pCEP4 construct was digested with *Nru*I and *Sal*I restriction enzymes and separated by agarose gel electrophoresis. All constructs are positive for insert. *M - DNA marker*

2.12.2 Protein purification

HEK293-EBNA cells expressing DDR-ECD-Fc constructs were cultured in several 150 cm^2 dishes in the presence of hygromycin B until confluent. Then, medium was changed to 35 ml serum-free DMEM and collected three times at 48 h intervals. Collected media were spun down at 3000 rpm for 10 minutes to remove cell debris and frozen at -20°C until purification. Thawed medium was filtered using a 0.22 µm filter and the concentration of phosphates adjusted to 20 mM with 10 $\times$ PBS. Protein A Sepharose Fast Flow (0.5 ml) was packed in a chromatography column and equilibrated with 10 volumes of sterile PBS. Medium (up to 200 ml) was applied to the column using a peristaltic pump at a rate of 1 ml/minute. Afterwards, the column

was washed with 20–30 ml of PBS. Bound proteins were eluted from the column with sterile 100 mM Glycine buffer (pH 3.0) in 6 × 1ml fractions and immediately neutralised with 30 µl of sterile 1 M Tris-HCl pH 9.0. To identify protein fractions, 15 µl of protein samples were mixed 1:1 with 2 × SDS sample buffer (with β-Me), boiled for 5 minutes and 20 µl analysed by SDS-PAGE. Fractions with high protein concentrations were pooled and dialysed against PBS. After dialysis, samples were centrifuged at 4000 rpm for 20 minutes at 4°C. Supernatants were transferred to new tubes and protein concentration was measured by NanoDrop absorbance at 280 nm as well as by BCA Protein Assay Kit using BSA dilutions as a standard (microplate procedure, working range 20–2000 µg/ml). 25 µl sample or its two–fold dilutions were used in triplicates and samples incubated for 30 minutes at 37°C. Absorbance was measured at 560 nm using a FLUOstar Omega microplate reader (BMG Labtech) and a standard curve plotted using using 4-parameter fit in MARS Data Analysis Software (BMG Labtech). Unknown protein concentrations were calculated from the standard curve. Protein concentration was adjusted to 1 µM in PBS, aliquoted and stored −20°C.

2.13 Solid phase binding assay

The solid phase binding assay was modified from Leitinger (2003); Leitinger and Kwan (2006); Xu et al. (2010). 96-well EIA/RIA flat bottom plates were used in the assay. Plates were coated overnight at 4°C with 50 µl of 100 µg/ml collagen type I (either PureCol or CellMatrix), neutralised with 1 M NaOH and diluted in PBS. Cell Matrix collagen type I was neutralised with 1M NaOH and diluted with PBS to 0.75 mg/ml, 10 µl was placed in the centre of the well and incubated at 37° C for 1 h to allow fibril formation. Plates were washed three times with PBS-T [0.05% (v/v) Tween 20 in 1 × PBS] and blocked with 150 µl of 0.05 mg of κ-casein in PBS-T for 1 h at room temperature on an orbital shaker. DDR-Fc proteins were diluted in blocking solution prior to assay and 50 µl of protein was applied per well

and incubated for 3 h, at room temperature on a shaker, and washed three times with PBS-T. Wells were incubated with 50 µl of swine anti-rabbit-HRP antibody diluted 1:3000 in blocking solution for 1 h. Afterwards plates were washed $6\times$ in PBS-T for a total time of 1 h, due to non-specific binding of antibodies to high concentration collagen. Long washing did not affect detection of protein bound to diluted collagen. Proteins were detected with TMB substrate, and reaction stopped with 2 M H_2SO_4. Plates were read at 450 nm using a FLUOstar Omega microplate reader (BMG Labtech). Background readings (no protein samples) were subtracted from sample readings.

2.14 Statistical analysis

All statistical analyses were performed in GraphPad Prism statistics software (GraphPad Software, Inc.). One-way analysis of variance (ANOVA) with Bonferroni Multiple Comparison Test (for comparison of more than two groups) was used. P-values ≤ 0.05 were considered significant and thus: $p > 0.05$ is non-significant (ns), * $p \leq 0.05$, ** $p \leq 0.01$ and *** $p \leq 0.001$.

Chapter 3

Dissection of collagen signalling in proMMP-2 activation

3.1 Introduction

In the RA joint, synovial cells degrade the cartilage by the action of several proteolytic enzymes (Allard et al., 1991; Bromley et al., 1985; Kobayashi and Ziff, 1975; Shiozawa et al., 1983). Aggrecan and other proteoglycans are cleaved by metalloproteinases including ADAMTSs and MMPs, and the remaining collagen type II is then degraded by collagenolytic MMPs. Although soluble MMP collagenases such as MMP-1, MMP-2, MMP-8 and MMP-13 are often upregulated and present in high levels in the synovial fluid, they do not appear to directly support the synovial cell invasion (Sabeh et al., 2010). MT1-MMP, a membrane associated collagenase, is thought to be the key collagen-degrading enzyme during invasion of RA synovial fibroblasts into the cartilage (Miller et al., 2009; Sabeh et al., 2010). MT1-MMP was shown to play a major role in collagen turnover *in vivo* (Holmbeck et al., 1999) as well as in cell migration (Itoh et al., 2001), and is often highly upregulated in invasive cancers (Sato et al., 1994).

Expression of MT1-MMP in a normal synovium is usually low. A number of studies have detected MT1-MMP mRNA in synovial tissues by PCR (Davidson

et al., 2006; Konttinen et al., 1999a; Pap et al., 2000b; Petrow et al., 2002; Yamanaka et al., 2000) or by *in situ* hybridisation (Pap et al., 2000b; Petrow et al., 2002). Although these reports show the presence of mRNA, only a few studies have detected MT1-MMP protein in normal synovial tissues by immunohistochemistry (Goldbach-Mansky et al., 2000; Konttinen et al., 1998). Konttinen et al. (1998) found that MT1-MMP was present in only a few stromal cells in the synovial membrane, accompanied by expression in the vascular endothelium. It has been also reported that MT1-MMP protein was absent in synovial tissue lysates (Jain et al., 2009; Yamanaka et al., 2000).

In contrast to non-arthritic synovium, the majority of examined RA tissue samples show markedly increased MT1-MMP expression at both protein and mRNA levels (Jain et al., 2009; Konttinen et al., 1999a, 1998; Miller et al., 2009; Mitsui et al., 2001; Pap et al., 2000b; Petrow et al., 2002; Soto et al., 2008; van Lent et al., 2005; Yamanaka et al., 2000). Several immunohistochemistry analyses demonstrated that MT1-MMP is mainly expressed in synovial lining cells, with some expression in the sublining layer and in endothelial cells (Konttinen et al., 1998; Pap et al., 2000b; Petrow et al., 2002; van Lent et al., 2005; Yamanaka et al., 2000). The majority of MT1-MMP-expressing cells are CD68-negative synovial fibroblasts and some CD68-positive macrophage-like cells (Konttinen et al., 1998; Miller et al., 2009; Pap et al., 2000b; Petrow et al., 2002). In samples which analyse the cartilage-pannus junction, where cells are in a direct contact with the cartilage, MT1-MMP levels are particularly high (Konttinen et al., 1998; Miller et al., 2009; Petrow et al., 2002) (Figure 1.11).

Although isolated RA synovial fibroblasts express MT1-MMP, proMMP-2 and TIMP-2, proMMP-2 activation is not readily detected, indicating that MT1-MMP is functionally inactive under these conditions. Initial data from our lab showed that addition of collagen to these cells induced proMMP-2 activation (Yoshifumi Itoh, unpublished results). As RA synovial cells at the cartilage-pannus junction express

high levels of MT1-MMP, we hypothesised that cartilage collagen is an activator of MT1-MMP expression as well as function.

The aim of this chapter is thus to identify mechanisms of collagen-induced MT1-MMP activation in RA synovial fibroblasts.

3.2 Results

3.2.1 Collagen induces proMMP-2 activation in RA synovial fibroblasts

Collagen was reported to induce proMMP-2 activation in both fibroblasts and cancer cell lines; however, this process has not been thoroughly investigated in RA synovial fibroblasts (RASF). Here, I addressed the question of whether collagen can induce proMMP-2 activation in RASF in comparison with HT1080 cells and human dermal fibroblasts. HT1080 is a human fibrosarcoma-derived cell line characterised by invasive properties and high MT1-MMP expression. It has been shown that HT1080 cells activate proMMP-2 when cultured on top or within collagen type I (Takino et al., 2004) or on fibronectin (Stanton et al., 1998). Collagen type I, II and III, but not other ECM proteins, were reported to induce proMMP-2 activation in dermal fibroblasts (Ruangpanit et al., 2001).

12-well culture plates were coated with a thin layer of neutralised collagen type I (PureCol, 2.7 mg/ml) and incubated for 1 h at 37°C to induce formation of collagen fibrils. HT1080 (0.75×10^5), RASF (1×10^5) and dermal fibroblasts (1×10^5) were plated onto the collagen layer in 0.5 ml of serum-free DMEM and cultured for 48 h. Where indicated, medium was supplemented with the MMP inhibitor GM6001 at 10 µM. Conditioned media were collected at the end of the experiment and then cells were lysed in 1 × SDS loading buffer with β-mercaptoethanol. Media were analysed for MMP-2 by gelatin zymography and cell lysates were subjected to Western Blotting and analysed for expression of MT1-MMP and actin (Figure 3.1).

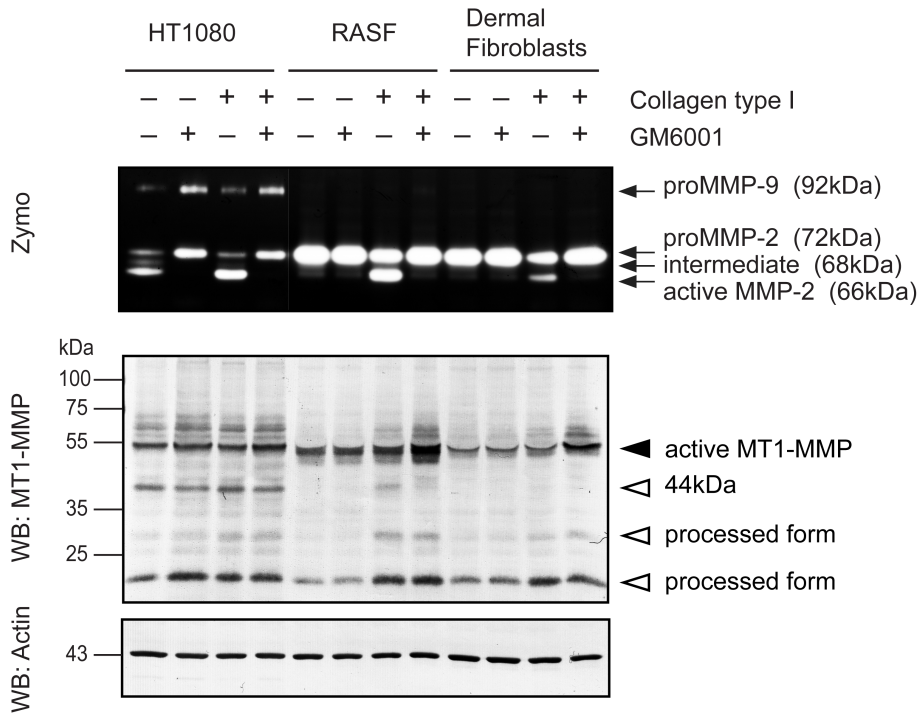

Figure 3.1: Analysis of collagen-induced proMMP-2 activation in different cell types. HT1080, RASF and dermal fibroblasts were cultured atop of plastic (–) or collagen film (+)(PureCol, 2.7mg/ml) in 0.5 ml of serum-free DMEM for 48 h. Cells were cultured in the absence (–) or presence (+) of a MMP inhibitor GM6001 at 10 µM. Conditioned media were analysed by gelatin zymography (Zymo; top panel). Areas degraded by gelatinases (MMP-2 and MMP-9) appear as clear bands against a dark background and both pro- and active species can be detected. MT1-MMP and actin expression were analysed by Western Blotting using anti-(MT1-MMP hemopexin domain) 222-1D8 antibody and anti-actin antibody (WB; middle and bottom panel respectively). Active full length MT1-MMP and its processed forms (including 44 kDa) are indicated by arrowheads. The data show the representative of two independent experiments.

As shown in Figure 3.1, HT1080 cells activated proMMP-2 in the absence of collagen and show an intermediate MMP-2 form of 68 kDa and fully active 66 kDa form. Activation was further enhanced by collagen and cells predominantly show fully active form of MMP-2. In RASF and dermal fibroblasts, activation of MMP-2 was not detected in cells cultured on plastic, but was induced by collagen. GM6001 completely inhibited proMMP-2 activation. As discussed above, no activation of MMP-2 is observed in the absence of collagen, despite high levels of MT1-MMP expression in cells cultured on plastic.

MT1-MMP is detected as a 57 kDa active form. An additional 44 kDa band was also detected in HT1080 cells regardless of collagen or GM6001 addition. In RASF, the 44 kDa MT1-MMP band was only observed in cells cultured on collagen and its generation was effectively inhibited by GM6001. In dermal fibroblasts, 44 kDa was not detected. Further processed forms of MT1-MMP (15–30 kDa) were also observed in all cells. These forms were more pronounced in HT1080 samples and in collagen-treated RASF and dermal fibroblasts. RASF and dermal fibroblasts cultured on collagen in the presence of GM6001 showed a slightly increased level of 57 kDa MT1-MMP. This is likely due to prevention of autocatalytic processing as reported previously (Hernandez-Barrantes et al., 2000; Toth et al., 2002).

It has been demonstrated that the presence of the 44 kDa form is correlated with MT1-MMP-dependent proMMP-2 activation (Stanton et al., 1998), and my data are in agreement with these studies. MT1-MMP 44 kDa processed forms are only present in fibroblasts cultured on collagen and displaying proMMP-2 activation. These data have confirmed that in RASF, collagen induces activation of MT1-MMP function as well as increases MT1-MMP expression.

A time course analysis was performed to analyse further proMMP-2 activation in RASF. Cells were plated at 1×10^5 in 12-well plates and the following day media were replaced with serum-free DMEM. Concanavalin A (ConA; 50 µg/ml) was added to one sample as a positive control for proMMP-2 activation. ConA is a known inducer of proMMP-2 activation and MT1-MMP expression in a variety of cells, including RASF and normal human fibroblasts (Azzam and Thompson, 1992; Smolian et al., 2001). Type I collagen (PureCol, 100 µg/ml) was added to the medium and cells were cultured for the indicated times over a period of 26 h, without replacing the culture medium. As shown in Figure 3.2A, RASF showed no activation of proMMP-2 without collagen treatment (0 h) and with collagen incubation times for up to 5 h. After 18 h, active MMP-2 began to be detected and was highest at 26 h. The ConA treatment induced an efficient activation of proMMP-2 and levels of active MMP-2 were significantly higher than those induced by collagen.

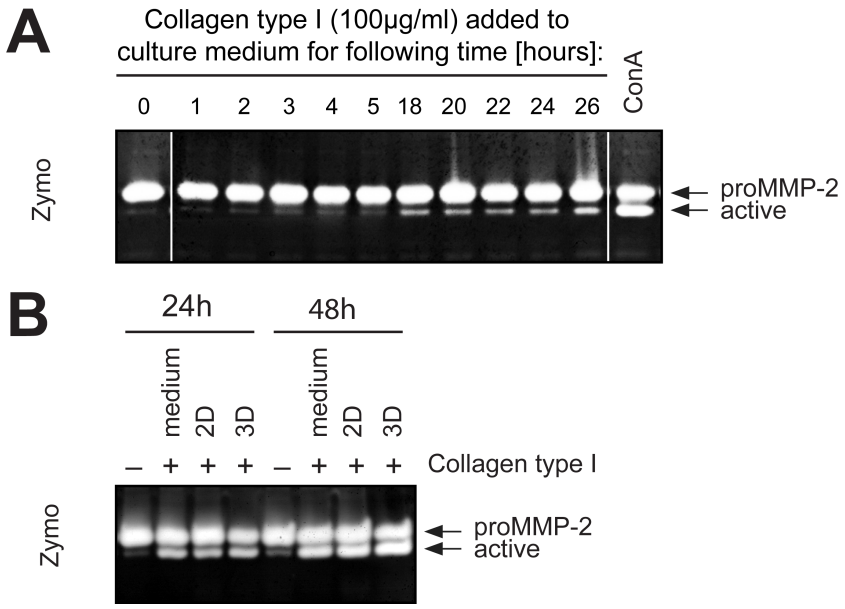

Figure 3.2: Time course analysis of proMMP-2 activation in RASF. (A) RASF were cultured in serum-free medium and PureCol collagen was added to the medium at 100 µg/ml for the indicated times. All samples were seeded at the same time, collagen added for indicated periods of time and all samples were collected at the same time (26 h after addition of collagen to the first sample). ConA was added at 50 µg/ml and cells cultured for 26 h as well. **(B)** RASF were cultured in the absence (–) or presence (+) of collagen. Collagen was either added to the medium at 100 µg/ml (**'medium'**); cells were plated on top of collagen-coated wells (**'2D'**) or mixed with 100 µl of 2.7 mg/ml collagen, incubated for 1 h at 37°C and overlaid with medium (**'3D'**). Cells were cultured in serum-free DMEM for 24 h or 48 h as indicated.

Next, I compared three different approaches to using collagen to induce proMMP-2 activation in cells. For this experiment a pepsin-extracted porcine type I collagen, PureCol, was used. The same numbers of RASF were either: cultured in serum-free medium supplemented with 100 µg/ml collagen; seeded on top of collagen-coated wells (2.7 mg/ml) or mixed with 100 µl of 2.7 mg/ml collagen. Cells mixed with collagen were incubated for 1 h at 37°C to form a collagen gel and were overlaid with serum-free medium. Cells were cultured for 24 h or 48 h. All collagen treatments induced proMMP-2 activation when compared to untreated cells (Figure 3.2B). There was no significant difference between collagen treatments. More proMMP-2 activation was observed after 48 h than 24 h. The data indicate that

proMMP-2 activation by collagen is time-dependent and all collagen treatments are efficient in inducing this activation and therefore can be used in further experiments.

3.2.2 ProMMP-2 activation in RASF is MT1-MMP dependent

Activation of proMMP-2 in RASF appears to be MMP-dependent, as it was inhibited by GM6001. MMP-2 processing has been shown to be mediated by MT1-MMP in HT1080 cells and dermal fibroblasts (Cho et al., 2008; Ruangpanit et al., 2001). However, mRNA of MT2-MMP and MT3-MMP, which were reported to activate proMMP-2, were also detected in RASF in previous studies (Hotary et al., 2000; Pap et al., 2000b; Pei, 1999; Seiki, 1999; Takino et al., 1995).

To confirm that collagen-induced proMMP-2 processing in RASF is dependent on MT1-MMP, cells were cultured with several specific inhibitors of MMPs and MT1-MMP. RASF were cultured for 48 h in 12-well plates, in 0.5 ml of serum-free DMEM supplemented with 100 µg/ml of collage type I (PureCol). The following MMP inhibitors were used: GM6001 (10 µM), TIMP-1 (0.5 µM), TIMP-2 (0.5 µM) and anti-MT1-MMP inhibitory antibody DX-2400 (0.5 µM). DX-2400 was used at 0.5 µM, as this concentration almost completely inhibited proMMP-2 activation in dermal fibroblasts (Figure 3.3B).

Zymography data showed that collagen-induced proMMP-2 activation was inhibited by addition of GM6001, TIMP-2 and DX-2400, but not by TIMP-1 (Figure 3.3A). TIMP-1 inhibits all soluble MMPs, but not membrane-type MT-MMPs, including MT1-, MT2-, MT3- and MT5-MMP. Addition of GM6001 and TIMP-2, but not DX-2400 prevented formation of 44 kDa processed MT1-MMP (Figure 3.3A). These samples also showed higher MT1-MMP expression levels. This may be due to incomplete inhibition of MT1-MMP by large IgG molecules.

To further confirm the involvement of MT1-MMP in proMMP-2 activation, MT1-MMP expression was knocked down by siRNA. RASF and dermal fibroblasts

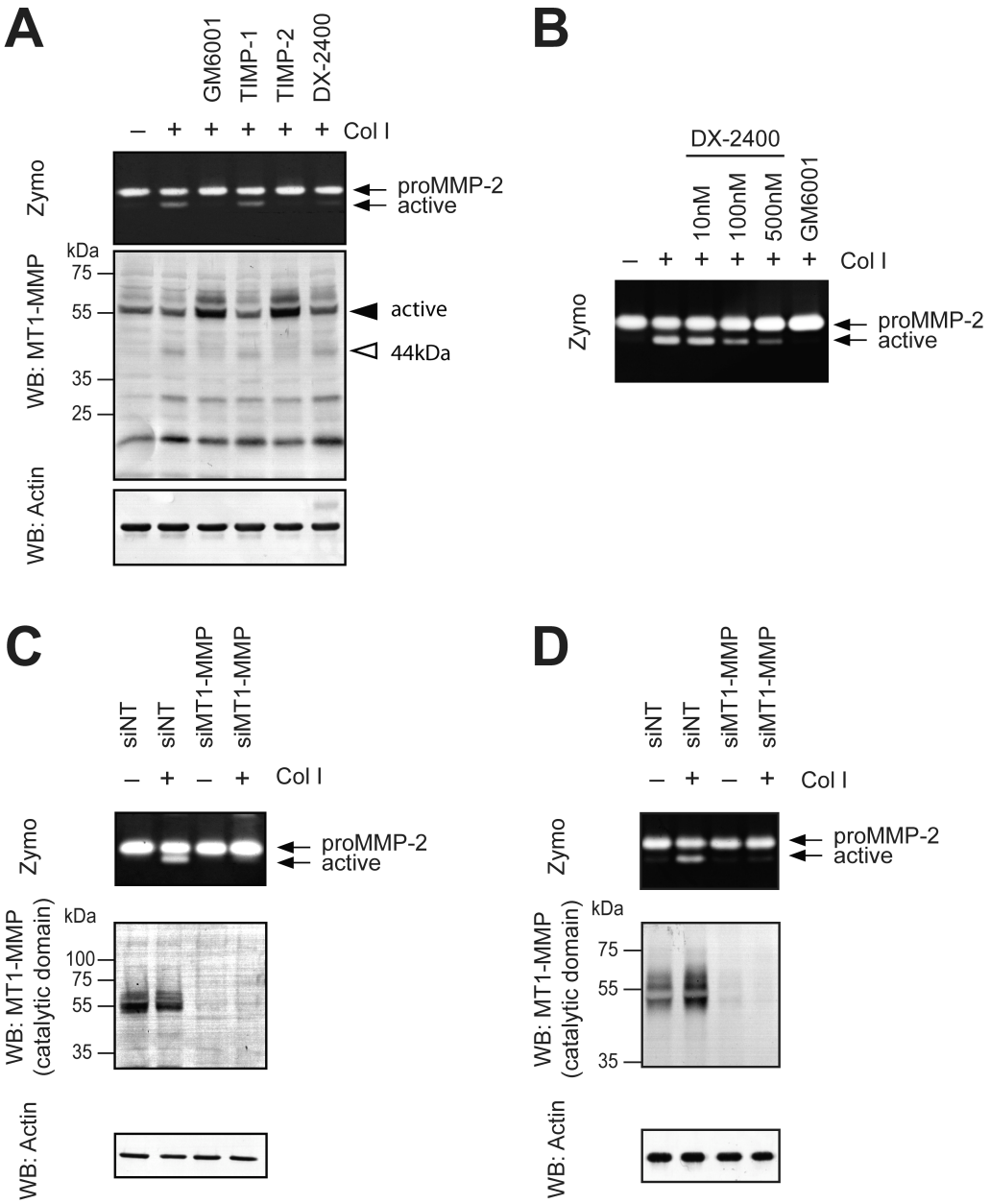

Figure 3.3: Collagen-induced proMMP-2 activation is MT1-MMP-dependent in RA synovial fibroblasts. (A) RA synovial fibroblasts were cultured in the presence of collagen type I for 48 h and culture media were analysed by zymography. MT1-MMP and actin expression were analysed by Western Blotting using anti-(MT1-MMP hemopexin domain) antibodies (222-1D8) and anti-actin antibodies. Concentrations of inhibitors were as follows: 10 µM GM6001, 0.5 µM TIMP-1, 0.5 µM TIMP-2 and 0.5 µM DX-2400. **(B)** Zymography analysis of conditioned medium from dermal fibroblasts cultured on collagen films and treated with increasing concentrations of DX-2400 inhibitory anti-MT1-MMP antibody. GM6001 was supplemented at 10 µM. **(C)** RA synovial fibroblasts and **(D)** dermal fibroblasts were transfected with siNT and siMT1-MMP. After 48 h medium was replaced with serum-free DMEM containing 100 µg/ml collagen type I and cells cultured for further 48 h. MT1-MMP and actin expression were analysed by Western Blotting using anti-(MT1-MMP catalytic domain) antibodies and anti-actin antibodies.

were transfected with 5 nM siRNA for MT1-MMP (siMT1-MMP) or non-targeting siRNA control (siNT) followed by stimulation of cells with 100 µg/ml collagen. As shown in Figure 3.3, MT1-MMP expression was effectively knocked down by siRNA and prevented collagen-induced proMMP-2 activation in RASF (Figure 3.3C) and dermal fibroblasts (Figure 3.3D). Taken together, these results show that MT1-MMP is essential for collagen-induced proMMP-2 activation in RA synovial fibroblasts as well as dermal fibroblasts.

3.2.3 Analysis of collagens inducing proMMP-2 activation

Next, I examined the ability of different collagen preparations to induce proMMP-2 activation in RASF. There are four different collagen type I preparations available in Dr. Itoh's lab, including CellMatrix, PureCol, acid- and pepsin-extracted collagens from guinea pig skin (Table 3.1). Acid-extracted collagens are typically isolated from tissues by solubilising collagens using only acetic acid, thus they retain intact telopeptide regions and cross-links. Pepsin-extracted collagens have intact triple helical domains but telopeptide regions are cleaved by pepsin and as a result they are devoid of cross-links (Sabeh et al., 2009b; Sato et al., 2000).

Cells isolated from three different donors were used (indicated **A**, **B** and **C** on Figure 3.4). RASF were cultured either on top of collagen-coated wells (2 mg/ml) or plated on plastic and collagens were added to the culture medium at 100 µg/ml.

Table 3.1: List of type I collagens used in the study.

Collagen preparation	**Extraction method**	**Tissue type**	**Presence of telopeptides**
CellMatrix *	acid-extracted	porcine tendon	+
PureCol *	pepsin-extracted	bovine hide (skin)	—
Guinea pig †	acid-extracted	skin	+
Guinea pig †	pepsin-extracted	skin	—

* *commercially available*; † *extracted by Dr. Rob Visse, Kennedy Institute of Rheumatology.*

ConA was added at 50 µg/ml. Cells were cultured in 1 ml of serum-free medium for 24 h (Figure 3.4A,B) or 48 h (Figure 3.4C). Conditioned media were analysed by zymography and cell lysates by Western Blotting for MT1-MMP and actin expression.

There were notable differences in proMMP-2 activation between donors as well as between collagens used in the experiment. In general, cells cultured for 48 h showed higher proMMP-2 activation than cells cultured for 24 h. ConA induced substantial proMMP-2 activation in sample **A** and **C**, but did not induce proMMP-2 activation in sample **B**, although increase in MT1-MMP levels and formation of 44 kDa species were observed in this sample (lane 2). In general, cells cultured on top of collagen (lanes 3–6) showed higher MMP-2 activation and greater increase in MT1-MMP expression and processing than cells cultured with collagen in the medium (lanes 7–10).

Among collagen preparations tested, the pepsin-extracted PureCol consistently induced proMMP-2 activation in all samples, although levels of active MMP-2 varied between cell donors. MT1-MMP expression and its processing to the 44 kDa form was also induced in the majority of cells cultured in the presence of PureCol. PureCol elicited a particularly high response in donor **C** (lanes 4 and 8). The pepsin-extracted guinea pig collagen also induced high proMMP-2 activation in cells cultured on top of the collagen matrix (lane 5); however, when this collagen was added to the medium, it induced activation of MMP-2 and increase of MT1-MMP expression only in donor **A** (lane 9). The acid-extracted guinea pig collagen was also able to induce proMMP-2 activation in the majority of samples (lanes 6 and 10); however, it didn't increase MT1-MMP levels and processing as much as e.g. PureCol. In general, the CellMatrix collagen didn't activate proMMP-2 very well, which is particularly notable in donor **C** (lanes 3 and 7). Only a limited increase in the full length and 44 kDa MT1-MMP species was observed in CellMatrix-treated cells.

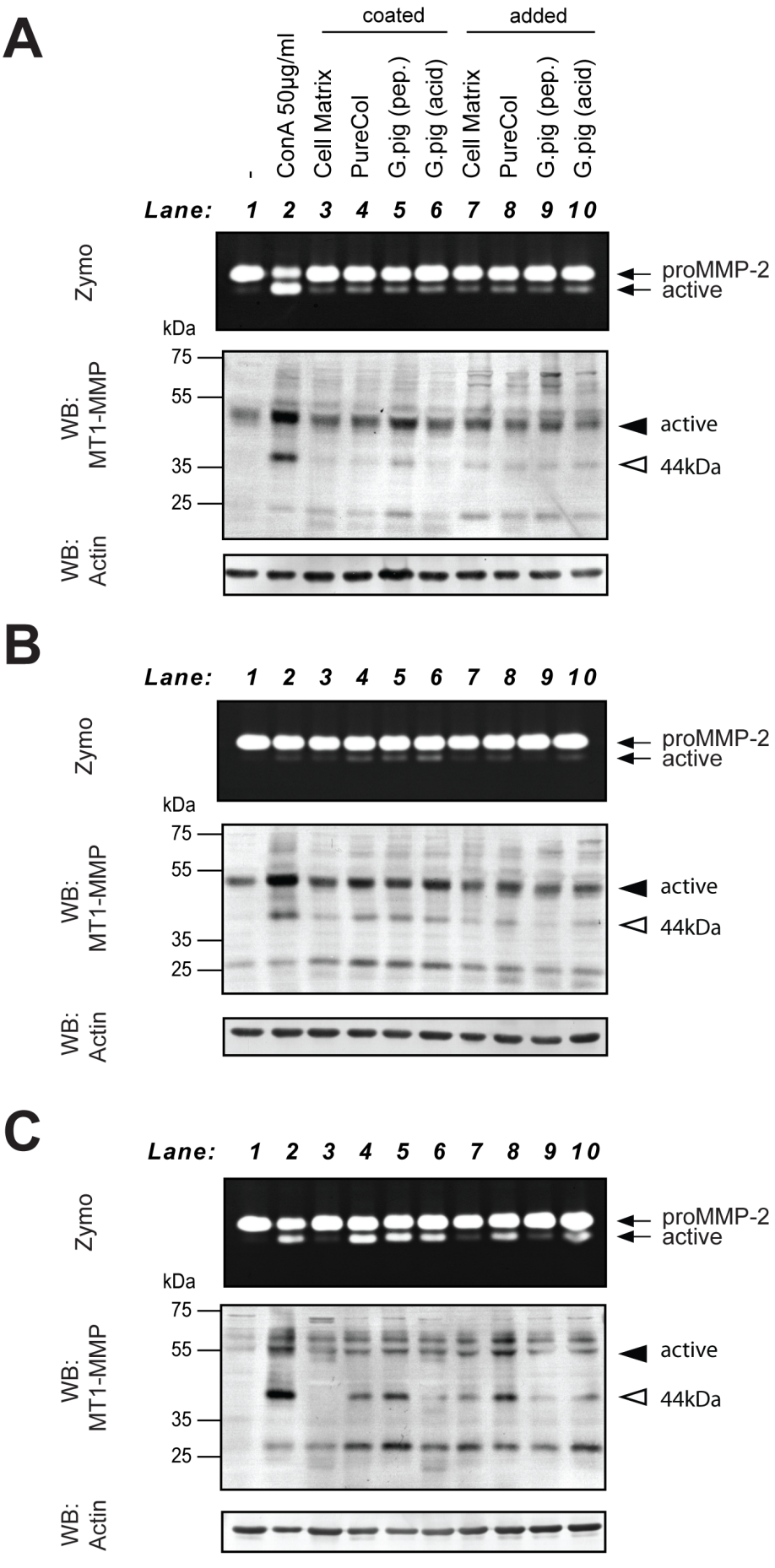
A
coated
added
-
ConA 50µg/ml
Cell Matrix
PureCol
G.pig (pep.)
G.pig (acid)
Cell Matrix
PureCol
G.pig (pep.)
G.pig (acid)
Lane: 1 2 3 4 5 6 7 8 9 10
Zymo
proMMP-2
active
kDa
75
55
35
25
WB: MT1-MMP
active
44kDa
WB: Actin
B
Lane: 1 2 3 4 5 6 7 8 9 10
Zymo
proMMP-2
active
kDa
75
55
35
25
WB: MT1-MMP
active
44kDa
WB: Actin
C
Lane: 1 2 3 4 5 6 7 8 9 10
Zymo
proMMP-2
active
kDa
75
55
35
25
WB: MT1-MMP
active
44kDa
WB: Actin

Figure 3.4: Collagen functionally activates MT1-MMP in RA synovial fibroblasts. RASF (1×10^5) from three donors **(A,B,C)** were cultured in 12-well plates for 24 h **(A,B)** or 48 h **(C)** in the presence of various type I collagen preparations (Table 3.1). Plates were either coated with a thin layer of 2 mg/ml neutralised collagen (**'coated'** – lanes 3-6) or collagen was added to the medium at 100 µg/ml (**'added'** – lanes 7-10). ConA was supplemented at 50 µg/ml (lane 2). *G.pig* - Guinea pig, *pep.* - pepsin-extracted, *acid* - acid-extracted.

Overall, among all collagens tested, treatments with the pepsin-extracted PureCol resulted in the most consistent activation of MMP-2 and MT1-MMP (Figure 3.2B and 3.4). Therefore, I decided to use PureCol in all further experiments, unless otherwise stated.

3.2.4 Collagen increases expression of MT1-MMP gene

Western blot analyses of MT1-MMP protein in RASF have shown processing of the enzyme to the 44 kDa from upon collagen stimulation, as demonstrated in Figures 3.1, 3.3 and 3.4. This is due to the autocatalytic processing by MT1-MMP itself initiated by the collagen, and addition of GM6001 inhibits formation of the 44 kDa MT1-MMP. At the same time, cells simultaneously treated with collagen and GM6001 showed increased levels of full length MT1-MMP protein, likely reflecting increased MT1-MMP expression in these cells. I therefore next examined if this increase in MT1-MMP protein is reflected at the mRNA level.

RASF and dermal fibroblasts were cultured in triplicate on top of collagen-coated wells for 24 h or 48 h. Total RNA was extracted, reverse-transcribed to cDNA and MT1-MMP and 18S expression levels were measured by qPCR using specific TaqMan probes and primers. MT1-MMP expression was normalised to 18S, using the $\Delta\Delta C_T$ method. Relative changes in MT1-MMP expression data are presented as a mean fold difference in MT1-MMP mRNA levels in comparison to untreated cells at 24 h (Figure 3.5). Statistical analysis was performed using one-way ANOVA with Bonferroni Multiple Comparison Test.

MT1-MMP expression in RASF increased 6-fold in collagen-treated cells at 24 h (*** $p \leq 0.001$) and approximately 8-fold at 48 h (*** $p \leq 0.001$)(Figure 3.5A). In comparison, MT1-MMP expression in dermal fibroblasts increased around 2.5-fold (** $p \leq 0.01$) at 24 h and 48 h (Figure 3.5B). Basal MT1-MMP expression levels did not change significantly at 24 and 48 h in both RASF and dermal fibroblasts. These data confirm that collagen indeed upregulates MT1-MMP gene expression.

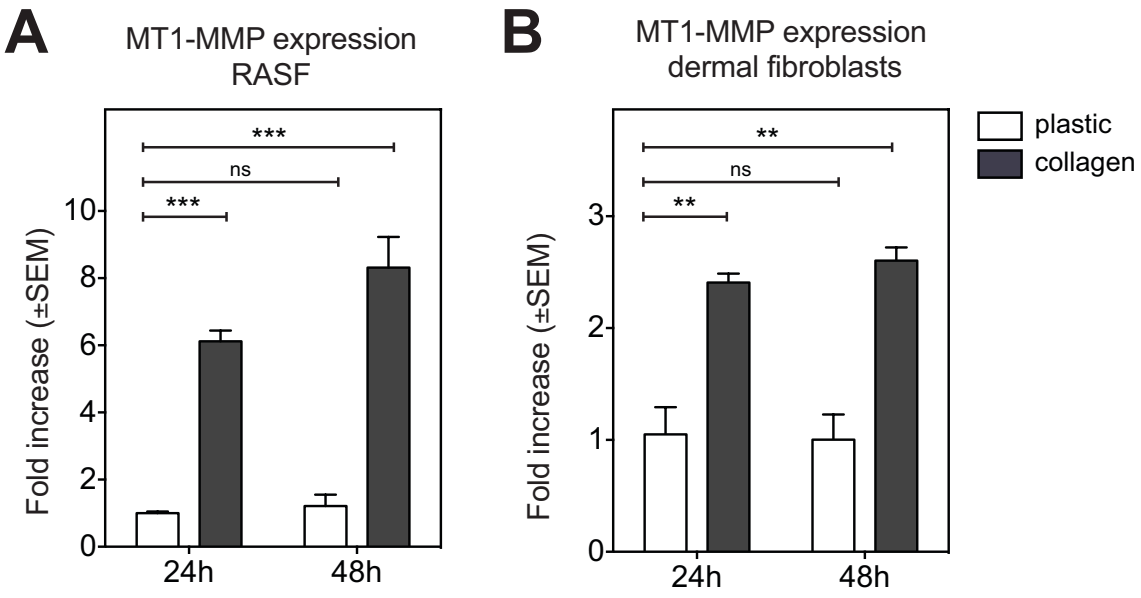

Figure 3.5: Collagen-induced MT1-MMP mRNA expression. RASF (**A**) or dermal fibroblasts (**B**) were cultured on collagen type I-coated plates for 24 h or 48 h. Total RNA was extracted, reverse-transcribed to cDNA and analysed by quantitative PCR. MT1-MMP expression was normalised to 18S expression. MT1-MMP expression across time points was compared to non-treated samples at 24 h and represented as a fold increase. Data are expressed as mean ± standard error of the mean (SEM); n = 3; ** $p \leq 0.01$, *** $p \leq 0.001$.

3.2.5 Detection of active MMP-2 in RASF treated with collagen type II

It has been well-established that type I collagen stimulates the activation of MT1-MMP. In order to examine whether cartilage collagen (type II collagen) can induce proMMP-2 activation as well, RASF were cultured in the presence of human or bovine collagen type II and compared with PureCol-stimulated cells. Concentration of collagens in the medium was adjusted to 100 µg/ml and cells were cultured for 48 h. As shown in Figure 3.6, all three collagens induced MMP-2 activation; however, treatment with human collagen type II generated lower levels of active MMP-2. The 44 kDa processed form of MT1-MMP was also present in all collagen-treated samples and correlated with levels of active MMP-2. These results indicate that cartilage collagen type II induces MT1-MMP activity similarly to type I collagen.

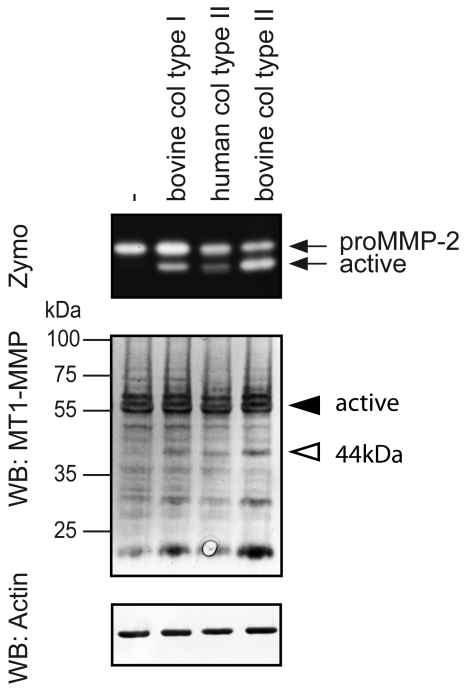

Figure 3.6: Collagen type II induces proMMP-2 activation. RASF were cultured in serum-free DMEM supplemented with 100 µg/ml of the following collagens: PureCol, human and bovine type II collagens. Culture media were analysed by zymography and MT1-MMP and actin expression by Western Blotting.

3.2.6 Effect of signalling molecule inhibitors on collagen-induced proMMP-2 activation

To gain insight into pathways that might mediate the collagen signalling, I examined a panel of inhibitors of several key molecules involved in signal transduction. Their specificity and concentrations used in the experiment are listed in Table 3.2. Dermal fibroblasts were used to investigate the role of these compounds in collagen-induced proMMP-2 activation. Fibroblasts were pre-incubated with inhibitors at indicated concentrations for 1 h, and thereafter cultured in the presence of 100 µg/ml collagen type I and inhibitors in the medium (Figure 3.7A). In a separate experiment fibroblasts were plated on PureCol-coated plates (2.7 mg/ml) and cultured for 3 days with specified inhibitors (Figure 3.7B).

The protein kinase C (PKC) family of protein kinase enzymes consists of several isoenzymes. They are involved in the transduction of extracellular signals and regulate cell proliferation, migration and survival. Several broad and selective PKC inhibitors were used in this study. Bisindolylmaleimide I (1 µM), an inhibitor of several PKC isozymes, prominently increased proMMP-2 activation especially in

Table 3.2: Inhibitors used in the study.

Inhibitor name	**Description**	**Working concentration**
Bisindolylmaleimide I	Protein kinase C (PKC) inhibitor (PKC α, β_I, β_{II}, γ and ε isozymes)	1 µM
Gö6976	PKC α and β_I isozymes inhibitor	1 µM
PKC β inhibitor	Inhibitor of PKC β_I and β_{II} isozymes	500 nM
PKC ζ Inhibitor	PKC ζ pseudosubstrate inhibitor, myristoylated	10 µM
PD98059	Inhibitor of MAP kinase kinase (MEK1/2)	10 µM
SB202190	Inhibitor of p38 MAP kinase	10 µM
Wortmannin	Inhibitor of phosphoinositide 3-kinase	1 µM
PP2	Inhibitor of Src kinase family	5 or 10 µM
Cli-095	Inhibitor of Toll-like receptor 4 signalling	5 µM
SN50	Inhibitor of NF-κB nuclear translocation	100 µg/ml
SN50M	Inactive control for SN50 peptide	100 µg/ml

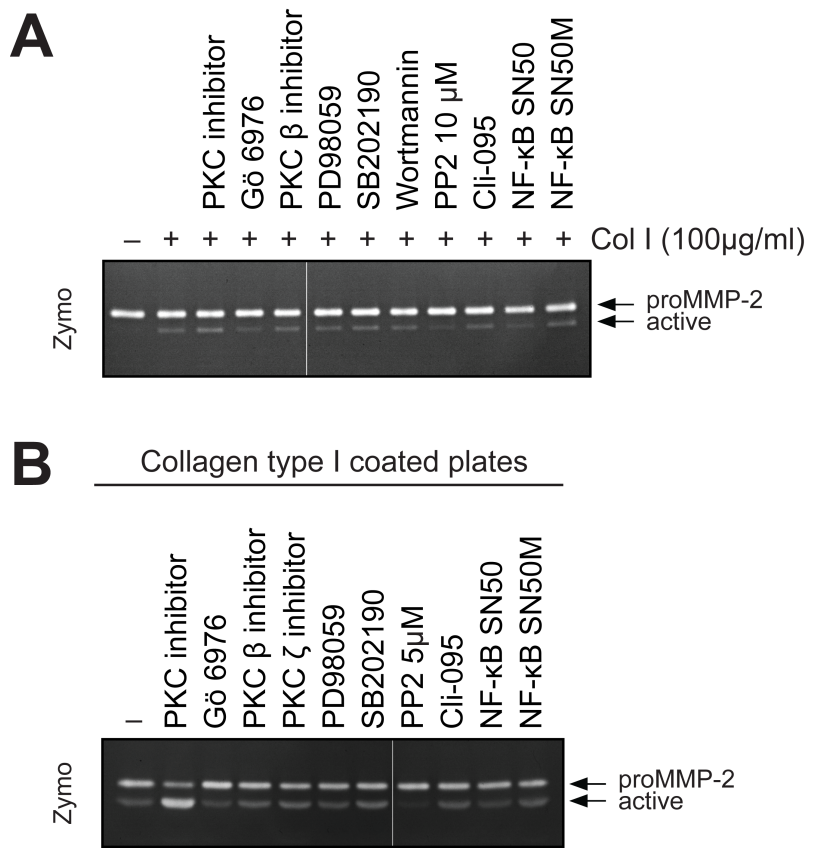

Figure 3.7: Role of inhibitors of various signalling pathways on collagen-induced proMMP-2 activation in dermal fibroblasts. Gelatin zymography analysis of conditioned medium from dermal fibroblasts cultured in the presence of indicated inhibitors. Their concentrations are presented in Table 3.2. **(A)** Dermal fibroblasts were seeded on plastic wells, and cultured in the absence (–) or presence (+) of 100 µg/ml of collagen type I in serum-free medium for 2 days. **(B)** Dermal fibroblasts were cultured on top of collagen type I-coated wells (2.7 mg/ml) for three days, in serum-free medium supplemented with indicated inhibitors.

cells cultured on collagen-coated plates. Bisindolylmaleimide I inhibits PKC α, β_I, β_{II}, γ and ε isoezymes. In contrast, Gö6976 (1 µM), which is an inhibitor of PKC α and β_I isozymes, inhibited proMMP-2 activation. Gö6976 does not inhibit PKC δ, ε or ζ. However, a PKC β-selective inhibitor did not affect proMMP-2 activation at 500 nM. The inhibitor of PKC ζ showed cytotoxicity at 50 µM, therefore it was used at 10 µM at which concentration it did not exert any effect on proMMP-2 activation on cells cultured on collagen-coated plates.

PP2 (Src kinase inhibitor) used at 10 µM reduced proMMP-2 activation notably, but it also showed some cytotoxicity (Figure 3.7A). To eliminate the possibil-

ity of cytotoxic effects on proMMP-2 activation, cells were also treated with 5 µM PP2 and activation was also inhibited (Figure 3.7B), suggesting that Src kinase indeed plays a role in this process. SN50 is an inhibitory peptide preventing translocation of NF-κB into the nucleus, therefore it interferes with NF-κB signalling. At 100 µg/ml SN50 slightly decreased proMMP-2 activation. Inactive control peptide SN50M (100 µg/ml) did not show any effect on MMP-2 levels.

The following inhibitors had no effect on the collagen-induced proMMP-2 activation: PD98059 — a highly selective inhibitor of MEK1/2; SB202190 — a potent inhibitor of p38 mitogen-activated protein (MAP) kinase; Wortmannin — a specific, irreversible inhibitor of phosphoinositide 3-kinase; Toll-like receptor 4 signalling inhibitor Cli-095. These data indicate that PKC α, Src kinases, and potentially NF-κB may be involved in collagen-induced proMMP-2 activation.

3.2.7 Effect of cytokines on MT1-MMP activity

Next, I examined the effect of pro-inflammatory cytokines, TNF-α and IL-1 on proMMP-2 activation in RASF and dermal fibroblasts. These cytokines are known to induce expression of various soluble MMPs, but there is a discrepancy between studies about their effect on regulation of MT1-MMP expression and activity. In a study by Han et al. (2001), collagen-induced proMMP-2 activation in dermal fibroblasts was enhanced by addition of TNF-α, while no effect of these cytokines was detected in Dr. Itoh's lab previously (Miller et al., 2009).

RASF and dermal fibroblasts were cultured for 4 days in serum-free medium with either 10 ng/ml of TNF-α or IL-1β or a combination of the two cytokines supplemented at 10 ng/ml each. PureCol was added to the medium at 100 µg/ml where indicated. After this time medium was collected and analysed by gelatin (Figure 3.8) and casein (Figure 3.9) zymography. Cell lysates were subjected to Western Blotting (Figure 3.8).

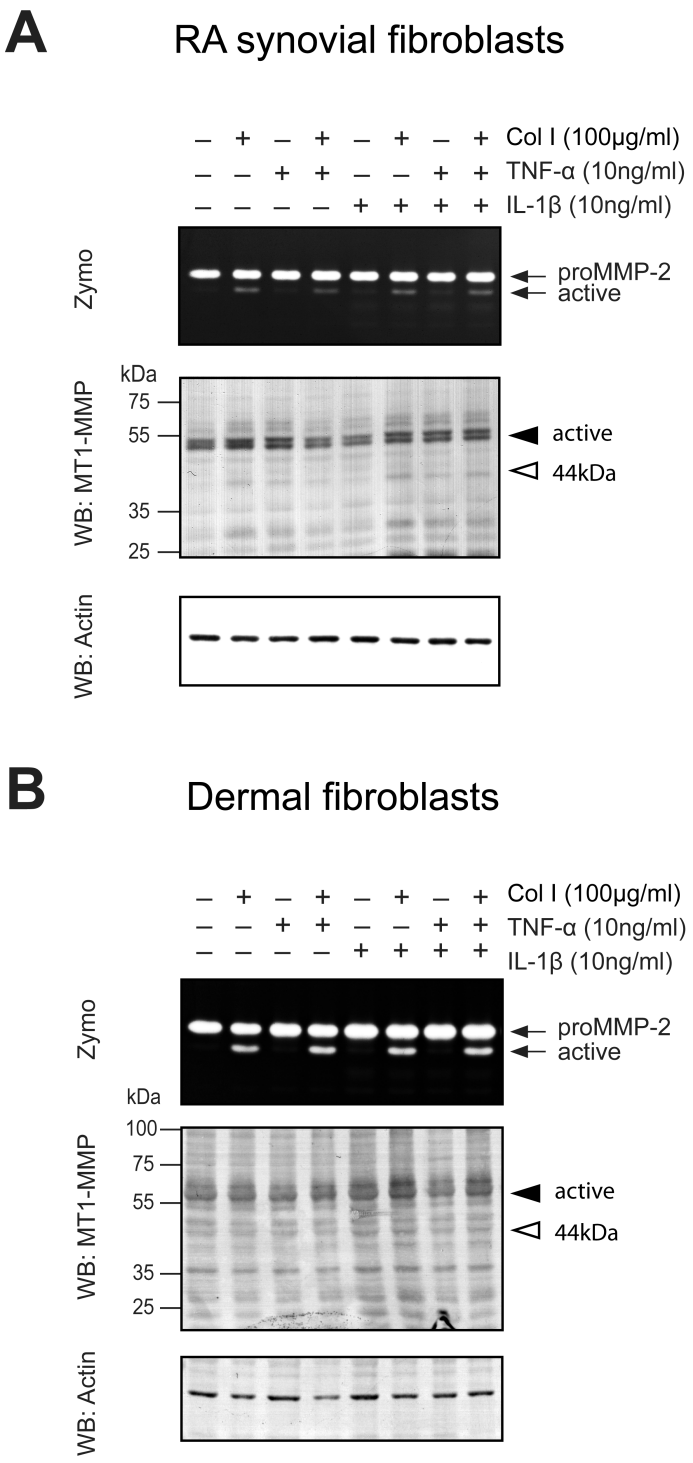

Figure 3.8: Cytokines TNF-α and IL-1β do not induce proMMP activation in RASF and dermal fibroblasts. RASF (**A**) and dermal fibroblasts (**B**) were cultured for 4 days in 0.5 ml of serum-free DMEM. Cell were cultured in absence (–) or presence (+) of collagen type I (100 µg/ml), TNF-α (10 ng/ml) or IL-1β (10 ng/ml) alone or in combination. Conditioned media were analysed by gelatin zymography and cell lysates by Western Blotting and probed for MT1-MMP and actin.

The addition of either TNF-α or IL-1β alone or in combination didn't induce proMMP-2 activation or marked increase in MT1-MMP expression in RASF and dermal fibroblasts (Figure 3.8). The addition of collagen promoted proMMP-2 activation in all samples, however the presence of cytokines (alone or in combination) didn't further increase proMMP-2 activation in these samples (Figure 3.8).

To confirm that TNF-α and IL-1β indeed activated fibroblasts, conditioned medium was also analysed by casein zymography. The above cytokines are known to induce expression of MMP-1 and MMP-3, which are able to digest casein. Analysis of conditioned medium from cytokine- and collagen-induced fibroblasts by casein zymography showed increase in caseinolytic activity in cytokine-treated RASF and dermal fibroblasts (Figure 3.9A,C). Prominent double bands of around 50 kDa in size were detected. Bands were much more prominent in IL-1β-treated cells than with TNF-α treatment. Addition of both cytokines did not further promote casein degradation. In RASF, addition of collagen appeared to minimally increase degradation of casein.

To further verify that the casein degradation is MMP-dependent, a casein zymogram gel was incubated in buffer containing GM6001. Active MMP-1 (40 kDa) was applied as a control. Casein gels were incubated in the absence or presence of GM6001 for 24 hours at 37°C (Figure 3.9B). No caseinolytic bands were observed in the gel incubated with GM6001, and clear degradation areas were observed in the control zymogram. The data suggest that IL-1β and TNF-α were active and cytokine-induced caseinolytic bands were indeed created by MMPs.

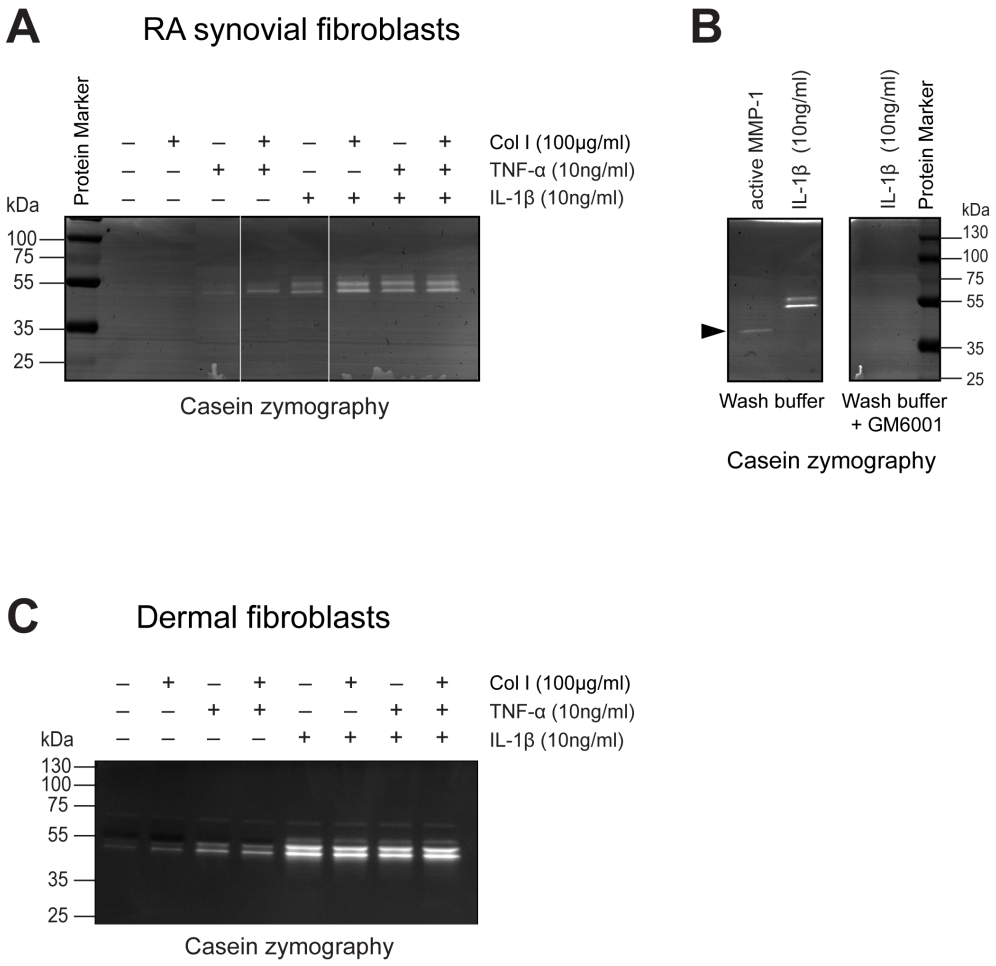

Figure 3.9: Analysis of MMP activities by casein zymography. RASF (**A**) and dermal fibroblasts (**C**) were cultured for 4 days with (+) or without (–) collagen type I (100 µg/ml), TNF-α (10 ng/ml) or IL-1β (10 ng/ml) alone or in combination, as indicated. Conditioned medium was analysed by casein zymography. (**B**) 40 kDa active MMP-1 and conditioned medium from IL-1β-treated RASF were subjected to casein zymography in the presence or absence of GM6001. Both gels were incubated for equal time at 37°C. Note that both the MMP-1 band and the band detected in the conditioned medium disappeared when the gel was incubated with GM6001, suggesting that the enzymes were metalloproteinases.

3.2.8 Anti-integrin β1 antibodies do not affect proMMP-2 activation

Integrins α1β1, α2β1, α10β1 and α11β1 are considered as principal collagen receptors (Leitinger, 2011). An increased expression of integrin subunits of α1, α2, α3, α4, α5, β1 and β4 was detected in RASF, with particularly high levels of α1, α5, αv and β1 (Lowin and Straub, 2011; Rinaldi et al., 1997). Subunits α10 and α11 were not tested in the above studies. Integrins have also been implicated in collagen-induced proMMP-2 activation in ovarian carcinoma (Ellerbroek et al., 1999) and in normal human dermal fibroblasts (Zigrino et al., 2001). However, integrin β1 was found to be non-essential in this process in malignant mesothelioma cells (Sakai et al., 2011).

A common approach to analyse the role of collagen-binding integrins is to target β1 integrin, as all of them contain this subunit. It has been shown that anti-β1 integrin antibodies inhibit attachment of cells to collagen type I (Sarkissian and Lafyatis, 1999; Wilkins et al., 1996). In my experiments I used two types of anti-integrin β1 antibodies to determine its role in proMMP-2 activation: function blocking (clone 6S6) and activating antibodies (clone P4G11). These antibodies were shown to inhibit or promote adhesion of cells to collagen substrate, respectively.

RASF were seeded in 12-well plates. After 2 h, media were replaced with 500 µl of serum-free DMEM with or without anti-integrin antibodies, 20 µg/ml each, and incubated with antibodies for 30 minutes at 37°C. Without replacing the medium, cells were stimulated with collagen by adjusting its concentration in the medium to 100 µg/ml. Cells were further cultured for 24 h.

Gelatin zymography showed that neither of the two antibodies induces activation of proMMP-2 (Figure 3.10). No changes in MT1-MMP expression or processing were observed. Cells cultured in the presence of collagen showed marked increase in proMMP-2 activation, MT1-MMP expression and formation of 44 kDa MT1-MMP species. With antibodies and collagen, a slight increase of both pro- and active

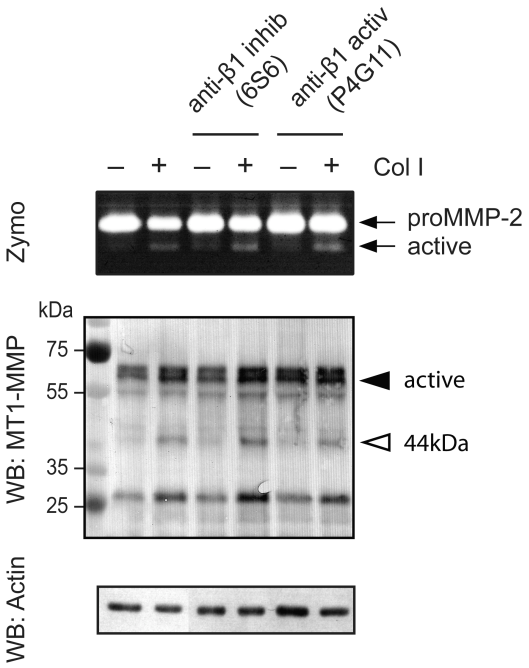

Figure 3.10: β1 integrin antibodies do not affect collagen-induced proMMP-2 activation. RASF were preincubated with 20 µg/ml anti-integrin antibodies, either function inhibiting (6S6 clone) or activating (P4G11 clone), for 30min followed by addition of collagen to medium (adjusting final concentration to 100 µg/ml). Cells were further cultured for 24 h, and medium and cells were analysed by zymography and Western Blotting for MT1-MMP and actin expression.

MMP-2 was observed compared to control cells, however there were no differences between activating and blocking antibodies used. Control collagen-treated cells also appeared to contain somewhat fewer cells than other samples, based on actin levels on Western blot (equal volumes applied for SDS-PAGE), thus it is likely that these differences are due to variation in cell number at the end of experiments.

3.2.9 Activation of proMMP-2 is inhibited by DDR2 knockdown

As antibodies against β1 integrin did not appear to affect proMMP-2 activation, I further examined role of integrins and DDRs by knocking down their expression using siRNAs. First, HT1080, RASF and dermal fibroblasts were analysed for expression of β1 integrin (ITGB1), DDR1 and DDR2 by Western Blotting (Figure

3.11A). All cells expressed β1 integrin, which runs as a broad 130 kDa band of glycosylated protein. DDR2 was detected in all cell types, and fibroblasts show higher expression of DDR2 than HT1080 cells. Two major bands were detected at around 130 kDa and the top one corresponds to the glycosylated protein (Blissett et al., 2009). RASF and dermal fibroblasts do not express DDR1.

To evaluate the role of these receptors in collagen signalling their expression was knocked down with specific siRNAs (5 nM). Non-targeting siRNA was used as a control (siNT). After 2 days media were replaced with serum-free DMEM with 100 µg/ml collagen type I. An efficient knockdown of each gene was confirmed two days after the transfection (Figure 3.11C). After 3 days conditioned media were collected and analysed by zymography. Cell lysates were analysed by Western Blotting (Figure 3.11B). Samples were prepared in triplicate, and densitometric analysis of bands corresponding to active MMP-2 on gelatin zymogram was performed in Phoretix 1D software. Levels of active MMP-2 in siNT cells treated with collagen were arbitrarily set to 100%. All other values are represented in relation to this value (Figure 3.11B). On average DDR2 knockdown reduced MMP-2 activation by 80%, while knockdown of ITGB1 showed minimal changes in activation (decreased by only 4%). Knockdown of both DDR2 and ITGB1 also resulted in significant reduction of proMMP-2 activation by 70%. Western blot analysis showed no increase in MT1-MMP expression and processing upon collagen stimulation of siDDR2 cells (Figure 3.11B). Knockdown of ITGB1 resulted in comparable increase in MT1-MMP expression and processing upon collagen stimulation as control cells, and knockdown of the two collagen receptors resulted in moderate inhibition of processing and expression.

I next examined whether DDR2 knockdown inhibits proMMP-2 activation induced by type II collagen. RASF were transfected with 5 nM siRNAs and cultured for 2 days. Cells were then plated in 12-well plates and cultured for further 2 days in the absence or presence of human or bovine type II collagen (100 µg/ml). Conditioned media were analysed by zymography and cell lysates by Western Blotting

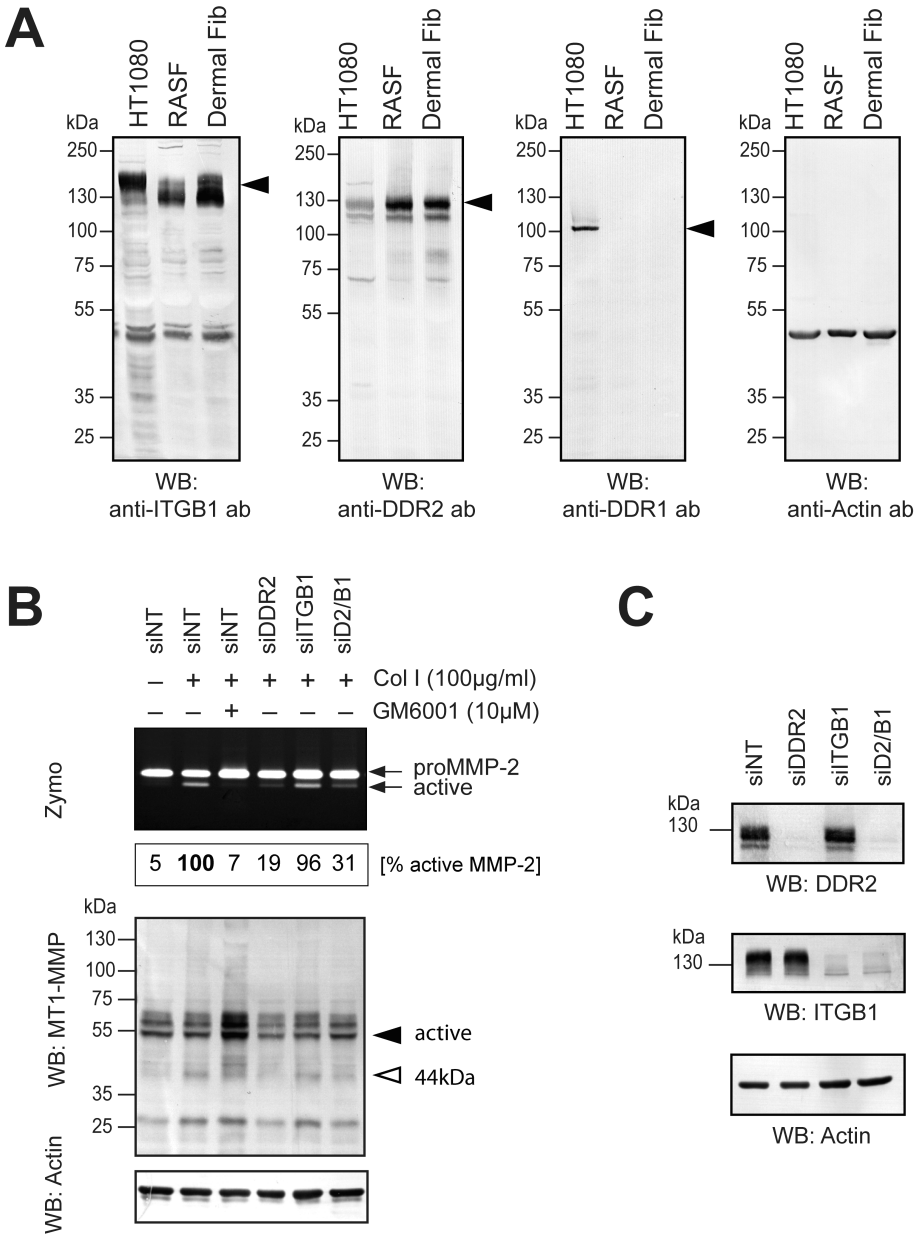

Figure 3.11: Knockdown of DDR2 inhibits proMMP-2 activation. (A) Cell lysates from 1×10^5 HT1080, RASF or dermal fibroblasts were analysed by Western Blotting, and probed against β1 integrin (ITGB1), DDR2, DDR1 and actin. Arrows indicate specific bands of full length proteins. All cells express β1 integrin, HT1080 cells express both DDR1 and DDR2, whereas fibroblasts express only DDR2. **(B)** RASF (0.25×10^5) were siRNA-treated, 3 wells per treatment, after 2 days collagen was added to the cell culture medium (serum-free) and cultured for further 3 days. Media were analysed by zymography and bands intensity was measured. Average % of active proMMP-2 from 3 wells are presented below zymogram. Active MMP-2 band corresponding to collagen-treated control siRNA transfected cells (siNT) was set as 100%. **(C)** Efficiency of protein knockdown two days after siRNA transfection. *siD2/B1* - double siDDR2 and siITGB1 knockdown.

for MT1-MMP and actin (Figure 3.12). No MMP-2 activation was observed in non-treated cells. Addition of bovine or human type II collagen resulted in proMMP-2 activation, but more efficient proMMP-2 activation and MT1-MMP processing (to 44 kDa) were detected in cells treated with the bovine collagen. The knockdown of DDR2 resulted in a decrease in proMMP-2 activation and inhibition of MT1-MMP processing. Treatment with siITGB1 did not inhibit processing of MT1-MMP, however proMMP-2 activation was slightly lower than in control cells.

In conclusion, both type I and II collagens are able to induce proMMP-2 activation and this process is inhibited by knockdown of DDR2 in RA synovial fibroblasts, accompanied by suppression of processing of MT1-MMP to 44 kDa. These data suggest that DDR2 is the major receptor that transmits collagen signals for activation of MT1-MMP function in fibroblasts.

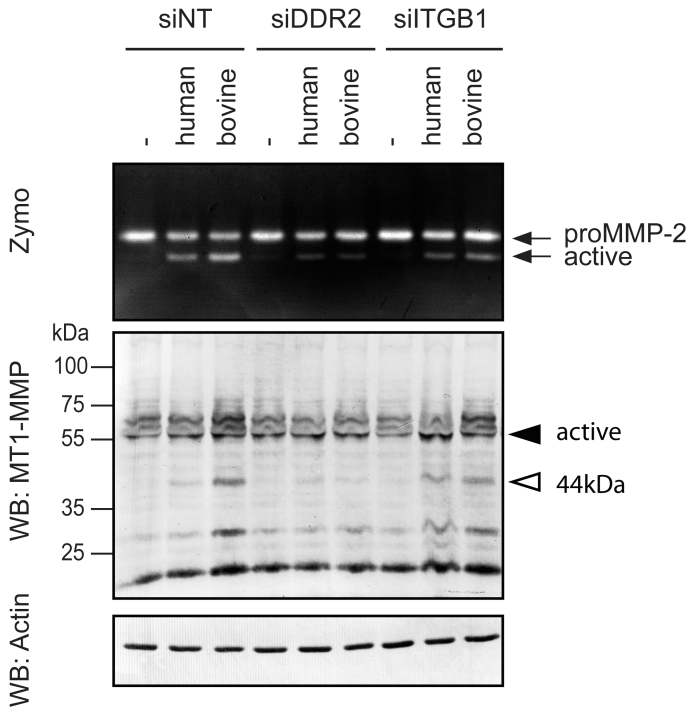

Figure 3.12: DDR2 knockdown inhibits collagen type II induced MT1-MMP activity. RASF were transfected with 5 nM siRNAs and after 2 days seeded in 12-well plates. Collagen type II (human or bovine) was added to serum-free medium at 100 µg/ml. Cells were cultured for a further 2 days.

3.2.10 DDR2 knockdown prevents collagen-induced MT1-MMP expression

I have demonstrated that collagen regulates MT1-MMP mRNA levels in RASF. Next, I examined the effect of knockdown of collagen receptors on MT1-MMP gene expression. RASF were transfected with 5 nM siRNAs and after 2 days they were either seeded on collagen type I-coated wells or plastic wells in serum-free medium. Total RNA was extracted after 24 h, reverse-transcribed to cDNA and expression of MT1-MMP and 18S rRNA measured by qPCR. MT1-MMP expression was normalised to 18S and compared to non-targeting siRNA-transfected cells (siNT) cultured in the absence of collagen ($\Delta\Delta C_T$ method). Cells from four different origins were analysed. Each sample treatment was performed in triplicate (n = 3, per experiment). Data are represented as mean ± SEM and statistical analysis performed using one-way ANOVA with Bonferroni Multiple Comparison Test.

Comparable results were obtained in all four donors tested (Figure 3.13). In every experiment MT1-MMP expression increased approximately 2.5–3.5-fold during 24 h upon plating cells on collagen film. The fold increase was lower than in the previous experiment (Section 3.2.4), but MT1-MMP mRNA was nevertheless significantly upregulated in three donors (#2,#3 and #4). Knockdown of DDR2 expression almost completely inhibited collagen-induced increase in MT1-MMP mRNA in donor 1 and 4, but only partial inhibition by 40-50% was observed in donor 2 and 3.

Although some differences in MT1-MMP levels between collagen-treated siNT and siDDR2 cells were observed, they did not show statistical significance. However, in two samples there was also no significant difference between control cells seeded on plastic and collagen-treated siDDR2 cells (Figure 3.13C,D). For siITGB1-treated cells, expression of MT1-MMP did not differ significantly from control cells, indicating that knockdown of β1 integrin does not inhibit collagen-induced MT1-MMP expression.

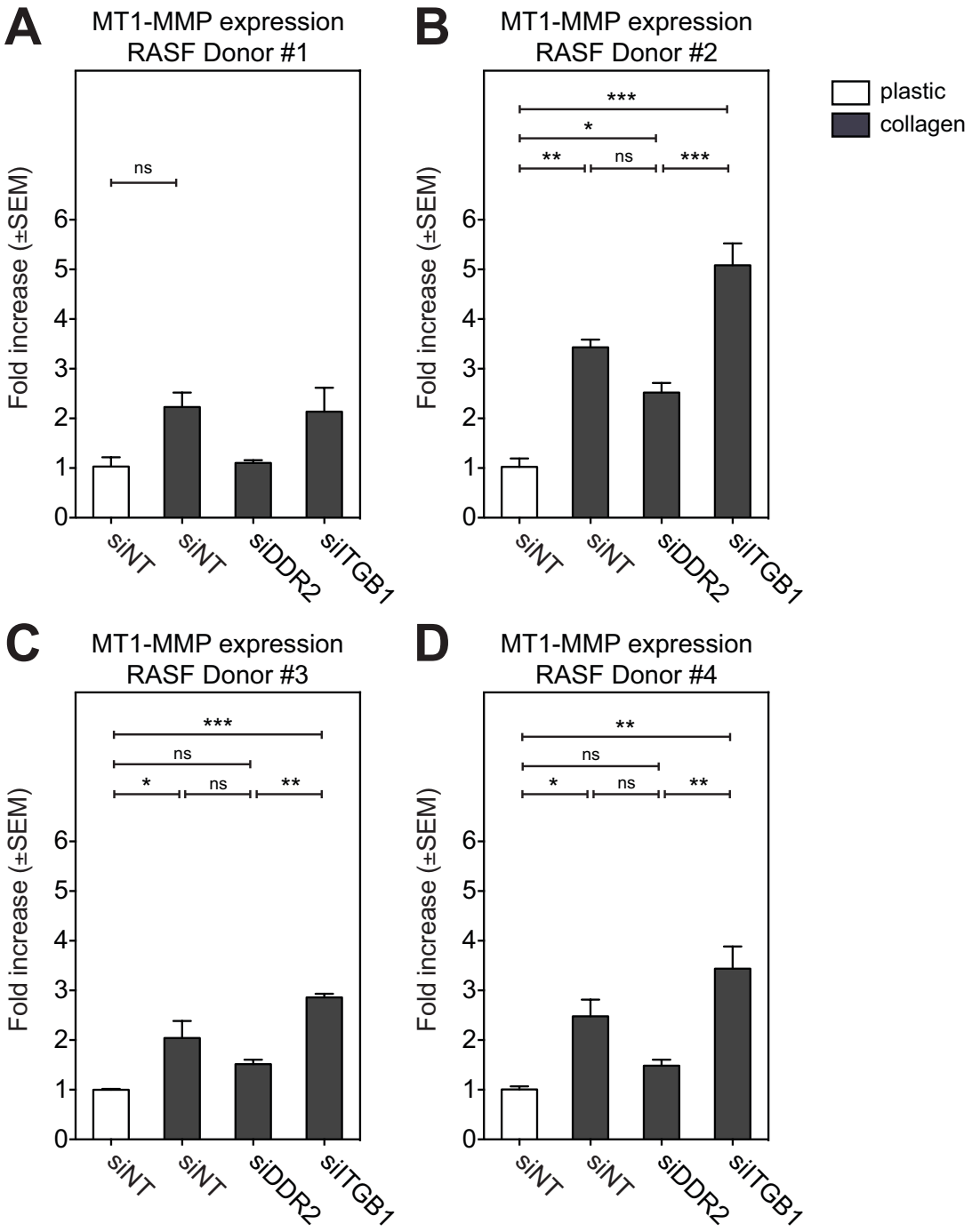

Figure 3.13: Effect of knockdown of β1 integrin and DDR2 on MT1-MMP gene expression. Expression of DDR2 and β1 integrin was knocked down by siRNA transfection of RASF from four different donors **(A–D)**. After 2 days cells were plated either on plastic or collagen type I-coated wells. Total RNA was extracted after 24 h, reverse transcribed to cDNA and MT1-MMP mRNA and 18S rRNA levels analysed by qPCR. MT1-MMP expression was normalised to 18S and results are represented as a fold increase in MT1-MMP expression versus untreated siNT. Data are shown as mean ± SEM; n = 3; * $p \leq 0.05$, ** $p \leq 0.01$, *** $p \leq 0.001$.

For a more comprehensive analysis, results from all four qPCR experiments were pooled together (Figure 3.13; donors #1–4). Pooled data were statistically analysed using one-way ANOVA with Bonferroni correction and data represented on Figure 3.14A ($n = 12$). Significant change in MT1-MMP expression was observed for siNT (2.55-fold, *** $p \leq 0.001$) and siITGB1 (3.38-fold, *** $p \leq 0.001$) cells upon collagen treatment. MT1-MMP expression was not significantly different between collagen-treated siNT and siITGB1 transfected cells. A fold difference of 1.7 was observed in siDDR2 cells. Moreover, there were no significant changes between untreated siNT cells and siDDR2 collagen-treated cells. This indicates that DDR2 knockdown inhibits increase in MT1-MMP expression when cells are cultured in presence of collagen. In these experiments, each treatment has only three samples. It is possible that increasing the number of each sample would lead to statistical significance.

Findings obtained by qPCR were confirmed by Western Blot analysis of MT1-MMP protein expression (Figure 3.14B). Collagen stimulation results in autocatalytic processing of MT1-MMP to the 44 kDa species and further degradation products, which makes comparison of the protein levels difficult. Therefore, to compare MT1-MMP protein levels, GM6001 was added to the medium while cells were treated with collagen to prevent autocatalytic processing and degradation. β1 integrin and DDR2 were knocked down by siRNA transfection. After 2 days cells were seeded on collagen type I-coated wells in the absence or presence of GM6001 (10 µM).

In agreement with previous results, addition of GM6001 to siNT transfected cells that were not stimulated with collagen did not change levels of MT1-MMP (Figure 3.14B). On the other hand, GM6001 treatment notably increased the level of active MT1-MMP in collagen-treated cells while decreasing the level of the 44 kDa form. This increase in MT1-MMP protein is due to inhibition of collagen-induced autocatalytic degradation of MT1-MMP. Thus, GM6001 treatment allows direct comparison of MT1-MMP levels when cells are stimulated with collagen. Knock-

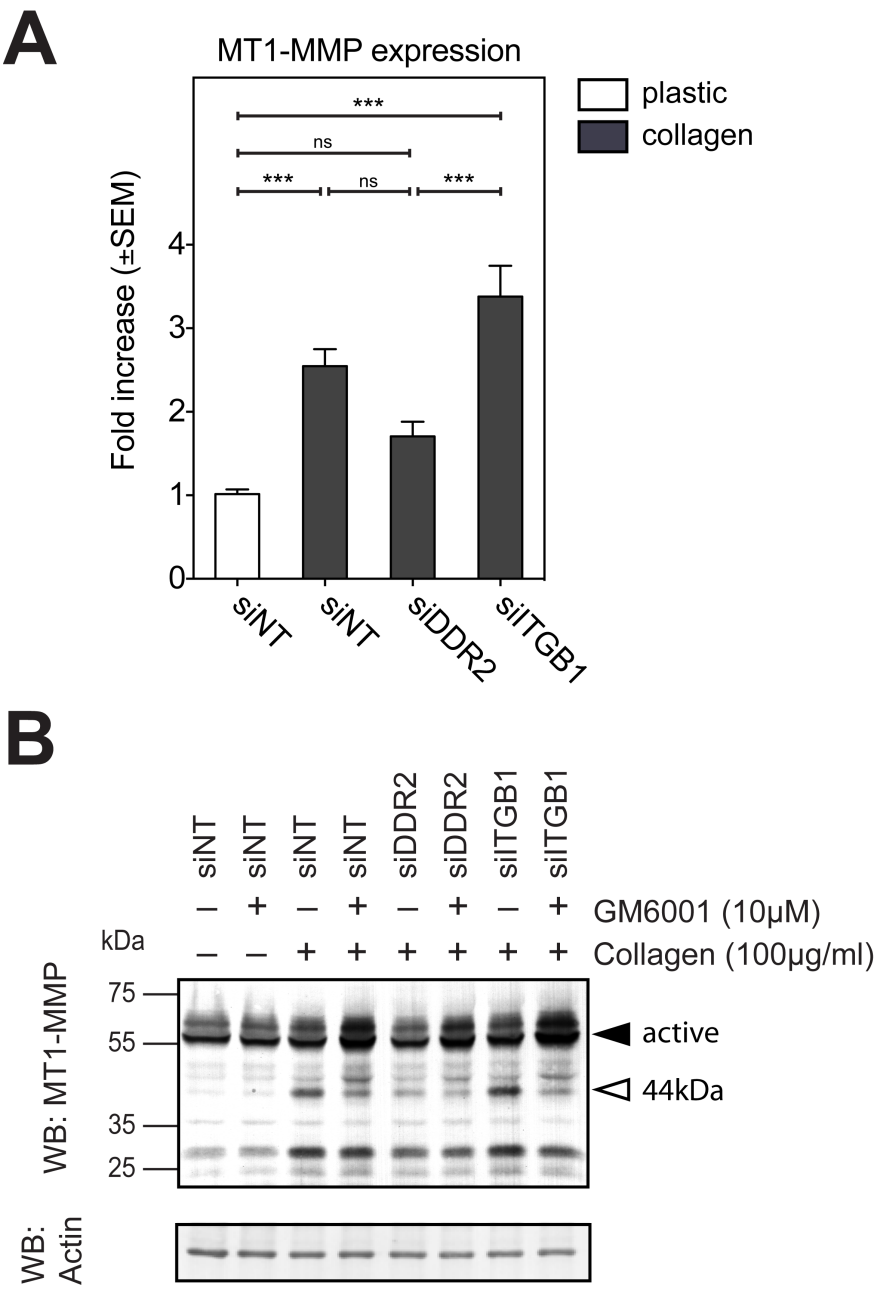

Figure 3.14: DDR2 knockdown in RASF prevents increase in MT1-MMP mRNA and protein expression. (A) Quantitative PCR analysis of MT1-MMP expression. Graph represents data combined from four separate experiments (four donors). Data are expressed as mean ± SEM; n = 12; *** $p \leq 0.001$. **(B)** RASF were cultured in the absence (–) or presence (+) of GM6001 at 10 µM and/or collagen film in serum-free medium. Cells were cultured for 3 days, lysed and analysed by Western Blotting.

down of DDR2 reduced formation of the 44 kDa band upon collagen treatment. Levels of MT1-MMP protein were also lower in siDDR2 cells cultured in the presence of GM6001 than in siNT cells. Knockdown of β1 integrin resulted in a slight increase in generation of the 44 kDa species (without GM6001) as well as in increase in MT1-MMP levels (with GM6001). Taken together, protein levels of MT1-MMP corroborated qPCR data and both experiments show that the collagen-induced increase in MT1-MMP mRNA and protein levels are mediated by DDR2.

3.2.11 Effect of triple helical peptides on fibroblasts

DDRs are activated by collagen independently of integrins and recognise distinct motifs within collagen molecules (Konitsiotis et al., 2008; Vogel et al., 2000). DDR2 binding sites in type II and III collagen were identified by Leitinger and colleagues using triple helical peptide Toolkits (Konitsiotis et al., 2008; Xu et al., 2011). Toolkits are sets of triple helical, 20–30 amino acid long synthetic peptides encompassing sequences from homotrimer collagens II and III (Farndale et al., 2008). GVMGFO is a minimal sequence supporting binding of DDRs and this sequence is present in collagens I–III. However, autophosphorylation of recombinant DDR2 expressed in HEK293 is only induced by peptides containing a longer GPRGQOGVMGFO motif, which also induce full binding of recombinant DDR2 (Konitsiotis et al., 2008). When compared to collagen type I, this peptide induced DDR2 phosphorylation with similar kinetics (Konitsiotis et al., 2008).

As knockdown of DDR2 inhibits collagen-induced MT1-MMP activity, next I investigated whether activation of DDR2 using triple helical peptides would be enough to induce proMMP-2 activation. Triple helical peptides (THPs) used in this study were a kind gift from Dr. Birgit Leitinger (Imperial College London, UK). The following THPs were used: negative control peptide THP-GPP-10, THP-GVMGFO and THP-GV**Nle**GFO, where Nle is norleucine (leucine isomer). The substitution of methionine to norleucine resulted in increased binding affinity of

this peptide to Fc-tagged discoidin domain of DDR2, as reported by Carafoli et al. (2009). THP-GPP-10, which contains ten GPP repeats, does not support DDR2 or integrin binding or activation (Konitsiotis et al., 2008; Raynal et al., 2006). The sequences of THPs are as follows:

THP-GPP-10: GPC-$(GPP)_{10}$-GPC-NH_2

THP-GVMGFO: GPC-$(GPP)_5$-GPRGQOGVMGFO-$(GPP)_5$-GPC-NH_2

THP-GV<u>Nle</u>GFO: GPC-$(GPP)_5$-GPRGQOGV**<u>Nle</u>**GFO-$(GPP)_5$-GPC-NH_2

Due to limited availability of the peptides the experimental set up was scaled down. RASF (1.25×10^4) and dermal fibroblasts (1.25×10^4) were seeded in 48-well plates. After 24 h medium was replaced with 100 µl of serum-free DMEM supplemented with PureCol (100 µg/ml) or with indicated THPs (also at 100 µg/ml) (Figure 3.15). Cells were cultured for a further 3 days. Due to the low number of cells used in these experiments, I could obtain only zymography data.

Zymography showed that PureCol, but not THPs, induced proMMP-2 activation in RASF and dermal fibroblasts (Figure 3.15). THP-GVMGFO and THP-GV**<u>Nle</u>**GFO peptides, but not THP-GPP-10, induced expression of proMMP-9 and a slight shift in the proMMP-2 band. The high affinity GV**<u>Nle</u>**GFO peptide appear to induce more proMMP-9 production. In conclusion, selective activation of DDR2 did not result in proMMP-2 activation in RASF or dermal fibroblasts. These data suggest that activation of only DDR2 may not be enough to induce proMMP-2 activation.

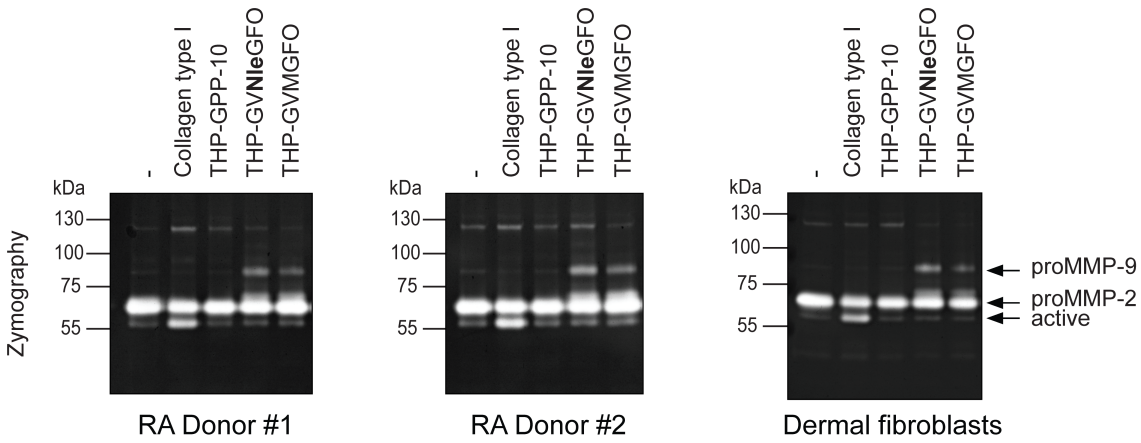

Figure 3.15: Analysis of proMMP-2 activation by triple helical peptides. RA synovial fibroblasts and dermal fibroblasts were cultured for 3 days in the absence (non-treated cells) or presence of collagen type I or THPs at 100 µg/ml in serum-free medium. THP-GPP-10 was used as a negative control peptide and both THP-GV**Nle**GFO and THP-GVMGFO were reported to induce DDR2 autophosphorylation. THP-GV**Nle**GFO has higher DDR2 binding affinity than THP-GVMGFO (Carafoli et al., 2009).

3.3 Discussion

I have shown that type I and II collagens are able to induce proMMP-2 activation in RA synovial fibroblasts and dermal fibroblasts. Activation of MMP-2 was confirmed to be solely due to MT1-MMP. In addition to functional activation of MT1-MMP, resulting in MMP-2 cleavage, collagen also increases MT1-MMP mRNA and protein levels.

Fibrillar collagens, including type II collagen present in articular cartilage, activate RASF and therefore identification of the receptor mediating this activation is important to understand the pathogenesis of RA. Here, I demonstrated that DDR2 mediates collagen-dependent activation of MT1-MMP in both RA synovial fibroblasts and dermal fibroblasts. Knockdown of DDR2 resulted in decreased proMMP-2 activation in collagen-treated cells. DDR2 also mediates an increase in MT1-MMP expression and autolytic processing. Interestingly, although knocking down DDR2 inhibits these processes, selective activation of DDR2 by THPs did not result in proMMP-2 activation. Instead, levels of proMMP-9 were increased by THPs that

were reported to activate DDR2 signalling. Since this MMP-9 upregulation was not observed by collagen stimulation, it seems to be specific to THPs. However, due to limited availability of THPs, further analysis of their effects on fibroblasts was not possible.

I have found that collagen-binding integrins do not play a role in the process of collagen-induced proMMP-2 and MT1-MMP activation in RASF. Knockdown of β1 integrin, which is the common subunit in all collagen-binding integrin receptors, did not have any significant effect on proMMP-2 activation, MT1-MMP expression or activity. Moreover, addition of either function blocking or activating anti-ITGB1 antibodies to RASF also did not change the proMMP-2 activation pattern. The majority of studies on the role of integrins in collagen-induced proMMP-2 activation were conducted using various anti-integrin antibodies, with conflicting results depending on cell types used. A recent study by Sakai et al. (2011) demonstrated that knockdown of ITGB1 subunit by siRNA in malignant mesothelioma cells does not affect proMMP-2 activation in collagen-treated cells. Although the cell types are different, my data confirmed their observation.

TNF-α and IL-1 are among cytokines that are highly upregulated in RA joints and play a central role in perpetuating systemic inflammation in RA. Their expression is also high at the pannus-cartilage junction (Konttinen et al., 1999b). As they are able to induce MMP expression, they are candidates to increase MT1-MMP expression and activity as well. Increase in MMP-2 and MT1-MMP expression in RASF treated with TNF-α were reported (Migita et al., 1996; Pakozdi et al., 2006). Migita et al. (1996) also reported an increase in levels of active MMP-2 in these cells. Moreover, Han et al. (2001) reported that collagen-induced proMMP-2 activation in dermal fibroblasts is enhanced by addition of TNF-α. In contrast, a study by Sabeh et al. (2010) demonstrated that IL-1β does not promote proMMP-2 activation in RASF. In my experiment, proMMP-2 activation was not affected by addition of either TNF-α nor IL-1β. These cytokines were confirmed to activate fibroblasts, as demonstrated by the increase in MMP-dependent caseinolytic

activity detected in conditioned media. I thus conclude that upregulation of MT1-MMP in RASF is neither due to or enhanced by TNF-α or IL-1β. The data using signalling molecule inhibitor showed that Gö6976 (inhibitor of PKC α and β), PP2 (inhibitor of Src) and SN50 (inhibitor of NF-κB signalling) notably suppressed collagen-induced proMMP-2 activation. NF-κB is one of the common transcription factors unregulated by inflammatory cytokines, but NF-κB activation through cytokines was not enough to induce proMMP-2 activation. Therefore, although NF-κB may play a role in collagen-induced proMMP-2 activation, it may not be a direct role and other factors may be required. Further investigation of collagen signalling through DDR2 that leads into activation of the MT1-MMP gene and function would be important to understand the mechanism of MT1-MMP expression in RA joints.

Chapter 4

Role of collagen receptors in collagen degradation and invasion

4.1 Introduction

RASF are highly invasive cells, which mediate pannus invasion and cartilage damage in RA. In contrast to fibroblasts isolated from healthy skin or synovium tissues, RASF deeply invade cartilage explants (Müller-Ladner et al., 1996; Rutkauskaite et al., 2005; Seemayer et al., 2003). Furthermore, *in vitro* cartilage invasion by RASF is facilitated without inflammatory signals provided by immune cells. The above observations led to the conclusion that the aggressive behaviour of RASF is an intrinsic feature of these cells (Seemayer et al., 2003). Damage to the collagen network is a prerequisite for cell invasion into the cartilage. RASF and other types of fibroblasts rely on MT1-MMP to degrade type I and II collagen layers, to invade 3D collagen or the cartilage matrix (Holmbeck et al., 1999; Sabeh et al., 2010, 2004). Increased MT1-MMP expression exacerbates collagen invasion by RASF (Miller et al., 2009). It is therefore important to determine factors that contribute to the increase in MT1-MMP expression and function.

In Chapter 3, I demonstrated that collagen was able to induce MT1-MMP activity and expression, resulting in activation of proMMP-2. The observed MT1-MMP activation was mediated through the collagen receptor DDR2, rather than by integrins or pro-inflammatory cytokines. I hypothesised that in addition to proMMP-2 activation, collagen can also modulate the ability of RASF to invade and degrade collagen-rich tissues such as cartilage by increasing MT1-MMP activity.

The aim of this chapter is to further examine the roles of collagen receptors, DDR2 in particular, in MT1-MMP-dependent degradation of type I collagen and gelatin as well as in MT1-MMP-dependent collagen invasion. I will also investigate the effect of a DDR2 inhibitor, dasatinib, on MT1-MMP activity, including proMMP-2 activation, collagen degradation and invasion using a transwell assay.

4.2 Results

4.2.1 Analysis of gelatin film degradation by fibroblasts

Fluorescently labelled ECM proteins, such as gelatin or fibronectin, are often used to evaluate invasive properties of cells *in vitro*, as they allow detection of localised matrix degradation (Artym et al., 2006; Chen et al., 1985; Martin et al., 2012). Thin layers of such labelled proteins are coated and fixed onto glass coverslips and their degradation can be easily visualised by fluorescence microscopy.

In this study, I employed a gelatin film degradation assay to analyse the effect of collagen on RASF and dermal fibroblasts degradation of the ECM. Gelatin was labelled with Alexa Fluor 488 dye (Alexa488-gelatin). First, I examined the ability of fibroblasts to degrade the Alexa488-gelatin. RASF or dermal fibroblasts were seeded on top of Alexa488-gelatin-coated glass coverslips in 2% FBS DMEM for 48 h. Cells were cultured in the absence or presence of PureCol in the culture medium, at 100 µg/ml. The following inhibitors were also added to media as indicated: GM6001

(10 µM), TIMP-1 (0.5 µM), TIMP-2 (0.5 µM) and DX-2400 (0.5 µM). After 48 h media were removed, then cells were fixed with 3% PFA and stained with DAPI to visualise nuclei (RASF; Figure 4.1A) or Alexa Fluor 568-conjugated phalloidin to visualise F-actin (dermal fibroblasts; Figure 4.1B). Representative images for each treatment showing similar cell numbers are presented on Figure 4.1. Degradation of the gelatin is visible as dark areas against the bright fluorescent background (green).

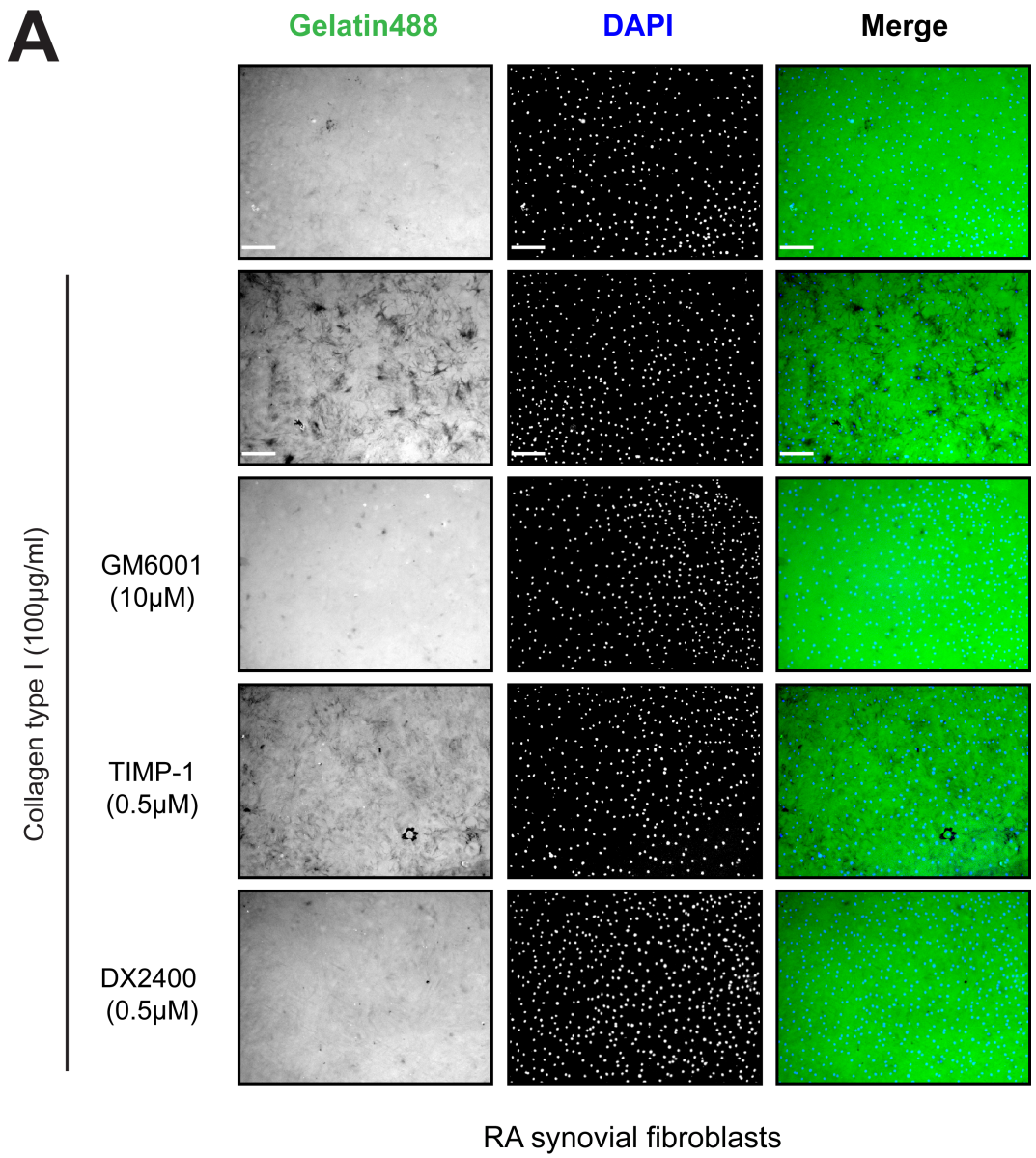

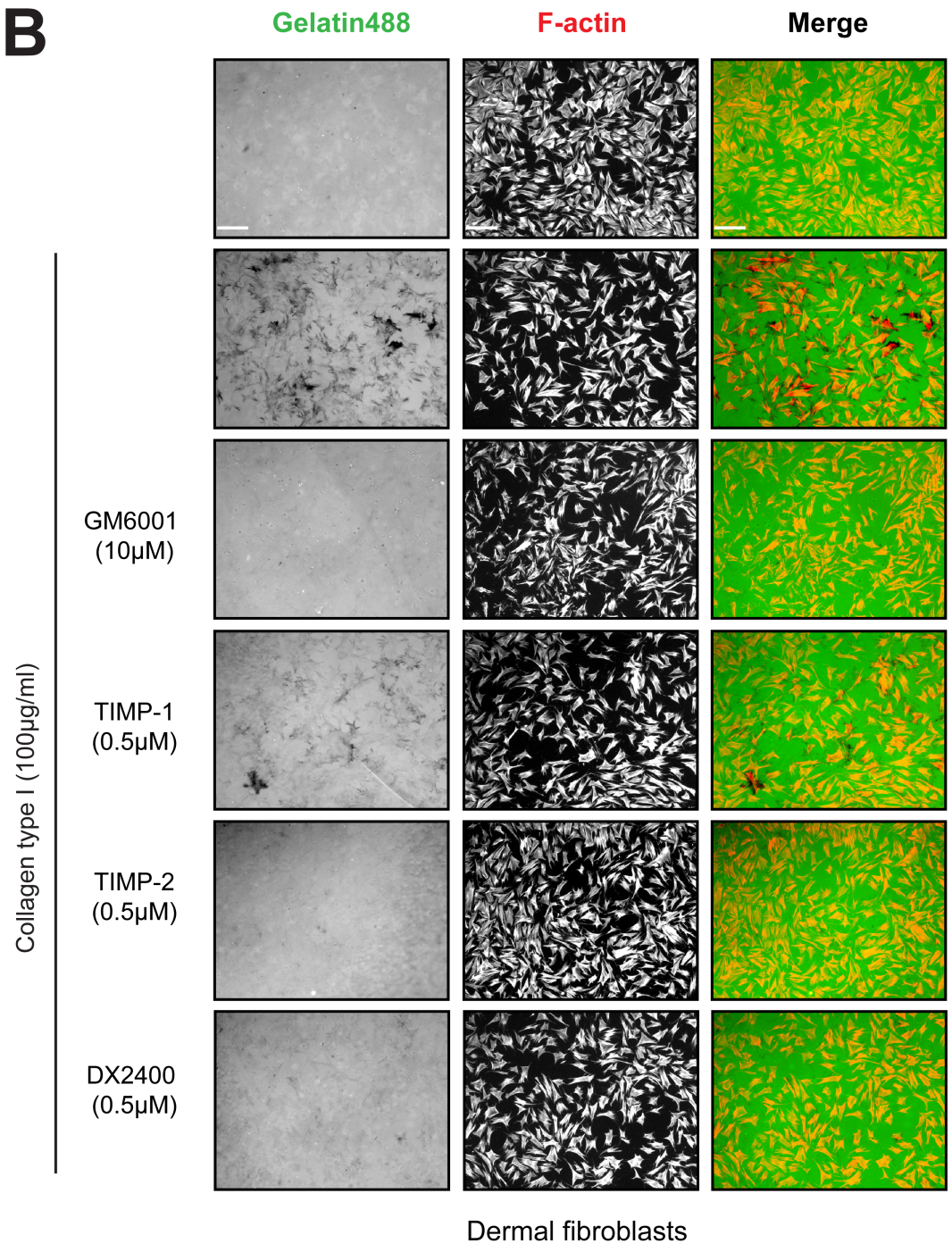

Figure 4.1: MT1-MMP dependent Alexa488-gelatin degradation by fibroblasts is induced by collagen type I. (A) RASF or **(B)** dermal fibroblasts were seeded on top of Alexa488-gelatin-coated glass coverslips. Cells were cultured in 2% FBS DMEM with or without PureCol at 100 µg/ml. Inhibitors were added as indicated: GM6001 (10 µM), TIMP-1 (0.5 µM) or DX-2400 (0.5 µM). After 2 days, cells were fixed and stained with DAPI **(A)** or Alexa Flour 568-conjugated phalloidin **(B)**. Images were taken with fluorescence microscope using 4 × objective lenses. Scale bar: 270 µm.

Cancer cells are usually incubated on fluorescent ECM substrates for 2–24 h to visualise degradation. Surprisingly, fibroblasts cultured in the absence of collagen did not degrade Alexa488-gelatin and remained 'inactive' towards the readily available substrate even during a prolonged culture time (48 h). However, gelatin degradation by fibroblasts was markedly increased when collagen was added to the media. Also, RASF cleaved gelatin to the higher degree than dermal fibroblasts as more degraded (dark) areas were observed in synovial cells. Degradation was inhibited by GM6001 and DX-2400 in both RASF and dermal fibroblasts, suggesting that the activity was derived from MT1-MMP. Dermal fibroblasts were also treated with TIMP-2 (0.5 µM) and gelatin degradation was completely blocked (Figure 4.1B). TIMP-1 at 0.5 µM partially, but not completely, inhibited degradation in both cell types. These data suggest that other TIMP-1-sensitive MMPs contribute to the gelatin degradation. Since DX-2400 completely inhibited this activity, it is most likely that it is due to MMP-2 activated by MT1-MMP. Thus collagen-induced gelatin film degradation is attributable to both direct and indirect activity of MT1-MMP.

4.2.2 DDR2 mediates collagen-induced gelatin film degradation in fibroblasts

In the previous Chapter, I showed that collagen-induced MT1-MMP expression and proMMP-2 activation are at least partially mediated by DDR2 (Section 3.2.9). Degradation of Alexa488-gelatin is inducible by collagen and dependent on both MT1-MMP and MMP-2 activity. Therefore, I next examined whether DDR2 also mediates collagen-triggered gelatin film degradation.

To analyse the role of integrin β1 and DDR2 in gelatin film degradation, expression of these receptors was knocked down by siRNA transfection. Two days post-transfection, RASF or dermal fibroblasts were seeded on top of Alexa488-gelatin-coated glass coverslips and incubated in 2% FBS DMEM for 48 h. Medium was supplemented with PureCol at 100 µg/ml as indicated. Afterwards cells were fixed in 3% PFA and stained with DAPI to visualise nuclei (RASF; Figure 4.2A) or Alexa Fluor 568-conjugated phalloidin to visualise F-actin (dermal fibroblasts; Figure 4.2B). Representative images showing similar cell numbers are shown on Figure 4.2.

Similarly to the previous experiment, fibroblasts transfected with non-targeting siRNA did not show gelatin degradation unless they were cultured with collagen present in the medium. Knockdown of DDR2 almost completely inhibited collagen-induced Alexa488-gelatin degradation in both RASF (Figure 4.2A) and dermal fibroblasts (Figure 4.2B). Knockdown of β1 integrin subunit had no effect on gelatin degradation in either cell type. Again, dermal fibroblasts showed lower levels of collagen-induced gelatin degradation in control siRNA transfected cells than corresponding RASF cells. The above results indicate that DDR2 activation by collagen results in elevated MT1-MMP activity in fibroblasts and increased substrate degradation.

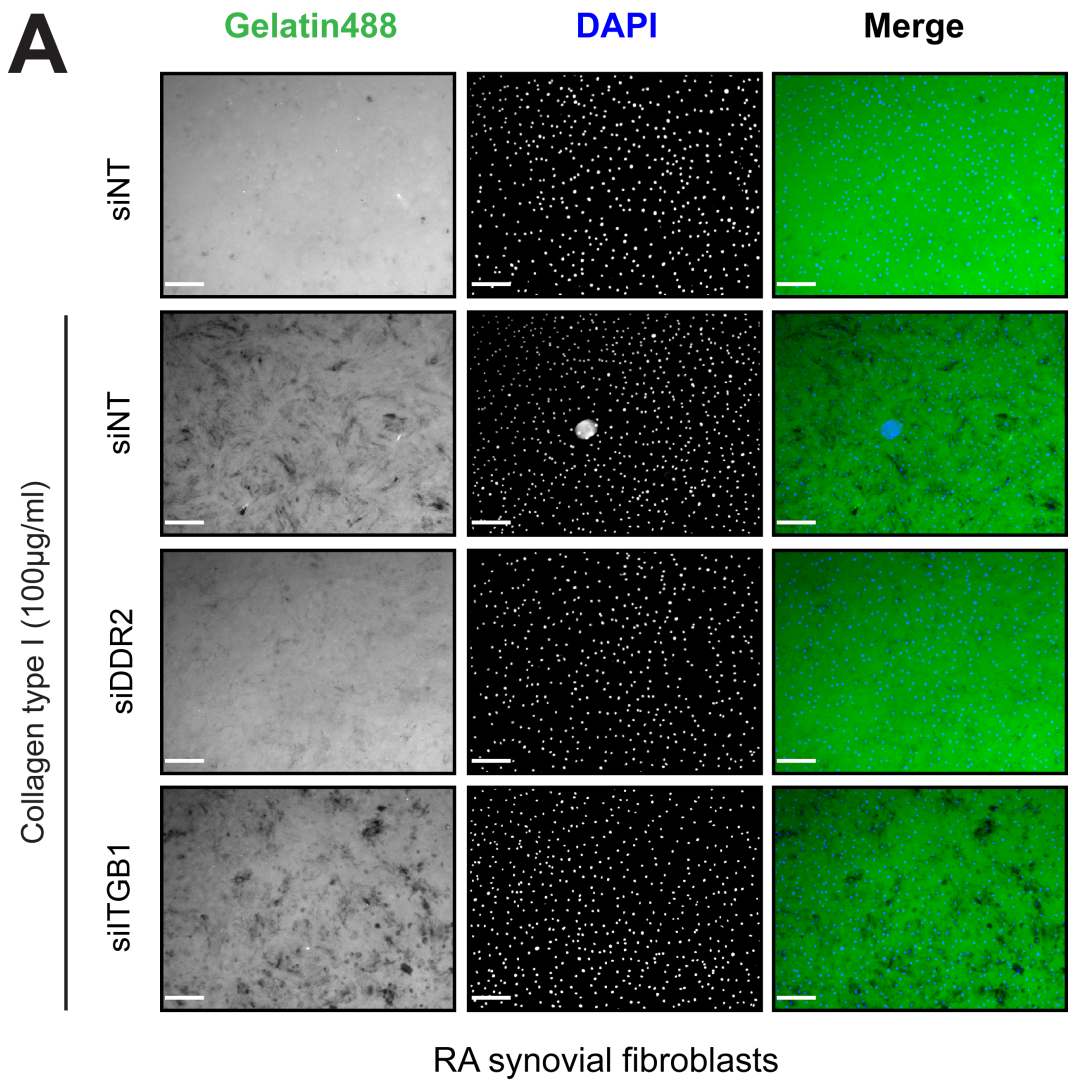
A
Gelatin488
DAPI
Merge
siNT
siNT
siDDR2
siITGB1
Collagen type I (100µg/ml)
RA synovial fibroblasts

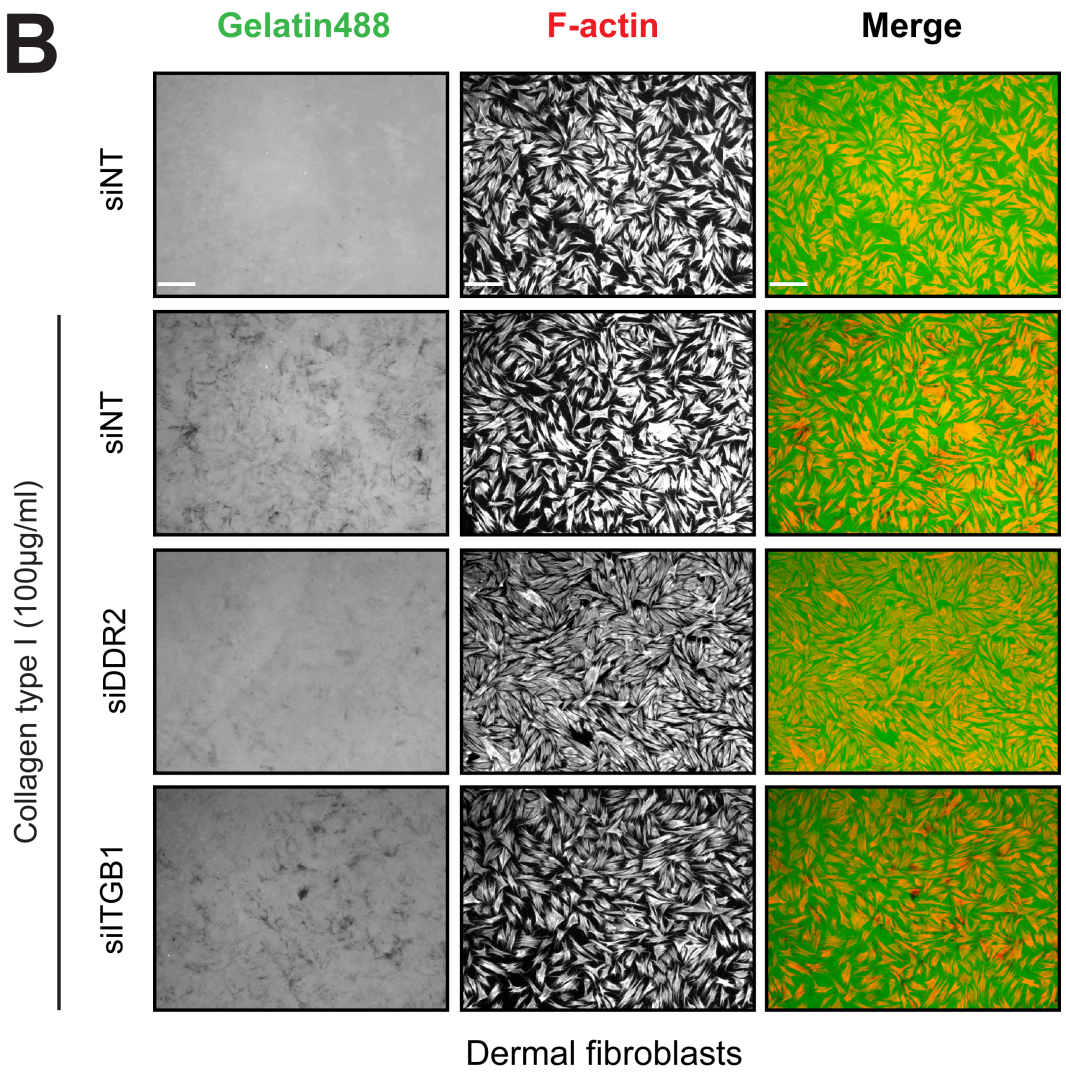

Figure 4.2: DDR2 knockdown inhibits collagen-induced gelatin film degradation. DDR2 and β1 integrin expression were knocked down by siRNA in RA synovial fibroblasts **(A)** or dermal fibroblasts **(B)**. After 2 days, cells were seeded on top of Alexa488-gelatin-coated glass coverslips and cultured in 2% FBS DMEM for further 2 days with or without PureCol in the medium (100 µg/ml). Cells were fixed with 3% PFA and stained with DAPI **(A)** or Alexa Flour 568-conjugated phalloidin **(B)**. Images were taken with a fluorescence microscope using 4 × objective lenses. Scale bar: 270 µm.

4.2.3 Collagen film degradation is inhibited by DDR2 knockdown

MT1-MMP is indispensable for the cleavage of fibrillar collagens. I have demonstrated that collagen signalling through its receptor DDR2 increases MT1-MMP activity towards proMMP-2 or gelatin. It is possible that collagen signalling may also play a role in collagen degradation. Therefore, the role of collagen receptors was further analysed in MT1-MMP-dependent collagen film degradation. I investigated whether knockdown of either integrin β1 or DDR2 had an inhibitory effect on a collagen film degradation by RASF or dermal fibroblasts.

Two days after siRNA transfection, fibroblasts were seeded on top of PureCol-coated wells. After 3 days, cells were removed by extensive trypsinization. Since trypsin does not degrade collagen, only intact collagen fibrils will remain. The collagen layer was then fixed in 3% PFA and stained with Coomassie Brilliant Blue R-250. Degradation appears as white areas against a dark background of the stained collagen. Non-targeting siRNA transfected cells were cultured in the absence or presence of GM6001 at 10 µM. Three wells were used per each treatment and representative images are shown on Figure 4.3 (RASF) and Figure 4.4 (dermal fibroblasts). Additionally, conditioned culture media from RASF were collected after 72 h and subjected to gelatin zymography (Figure 4.3C).

Although some studies show that loss of β1 integrin impairs cell attachment, all siRNA transfected cells attached equally well to the collagen matrix. No differences in attachment were observed between targeting and non-targeting siRNA transfected cells 2 hours after plating.

Substantial collagen degradation was observed in both RASF (Figure 4.3) and dermal fibroblasts (Figure 4.4) transfected with siNT. Degradation was inhibited by GM6001 in both cell types. Knockdown of DDR2 significantly reduced collagen degradation. Gelatin zymography also showed inhibition of proMMP-2 activation in siDDR2, but not in other siRNA transfected RASF (Figure 4.3C). Levels of active

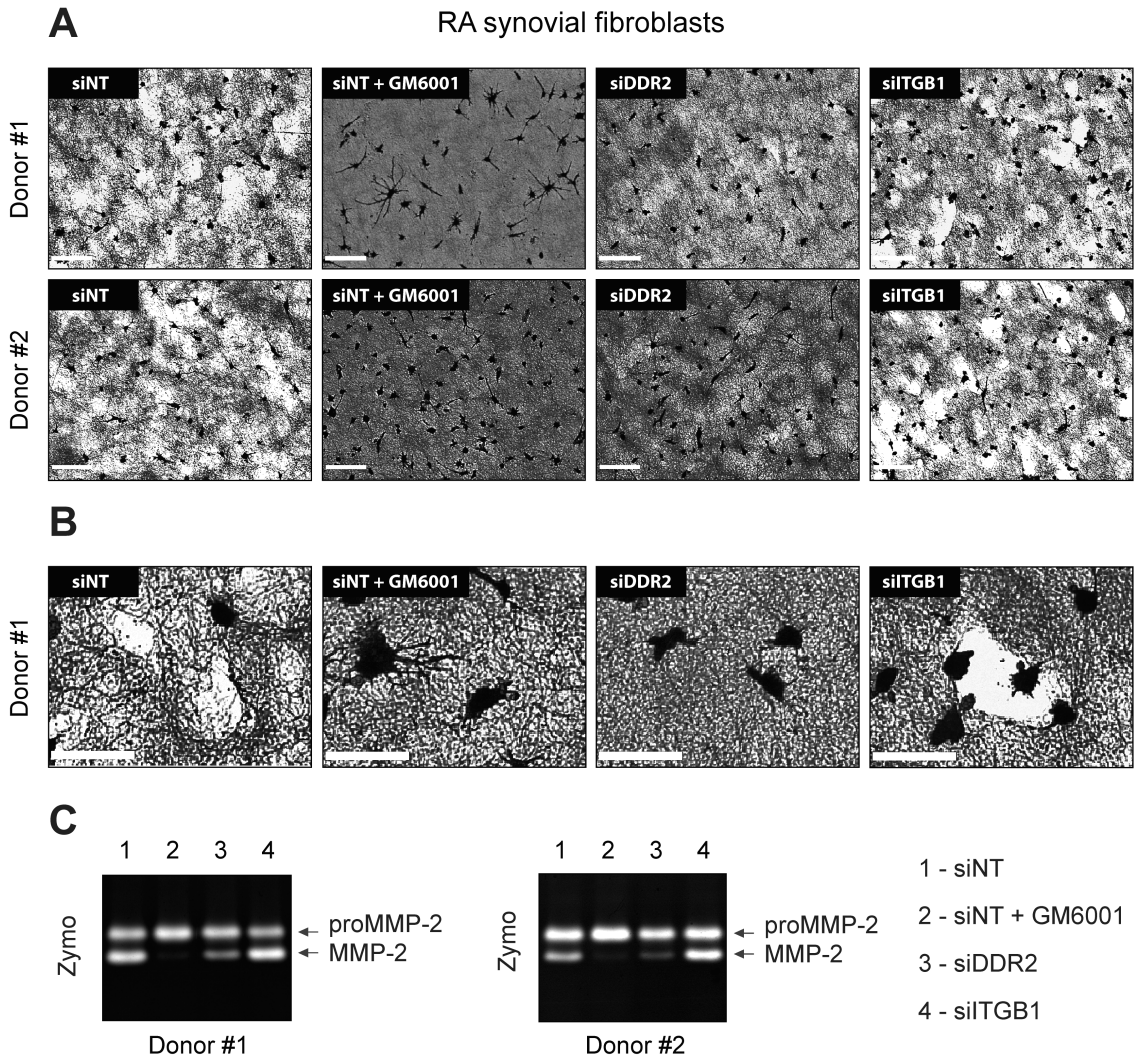

Figure 4.3: Knockdown of DDR2 inhibits collagen film degradation in RASF. DDR2 and integrin β1 expression in RASF from 2 donors was knocked down by siRNA transfection. After 2 days, cells were seeded on top of PureCol-coated 12-well plates and cultured in serum-free medium for further 3 days. GM6001 was used at 10 µM. Cells were removed by trypsinization, and the collagen layer fixed with 3% PFA and stained with Coomassie Brilliant Blue. Degradation is visible as white areas against the dark background. Three wells were used per treatment and representative images are shown. **(A)** Images were captured with a light microscope using 4 × objective lenses. Scale bar: 270 µm. **(B)** Images were taken with a light microscope using 20 × objective lens. Scale bar 55 µm. **(C)** After 3 days, culture media were analysed by gelatin zymography.

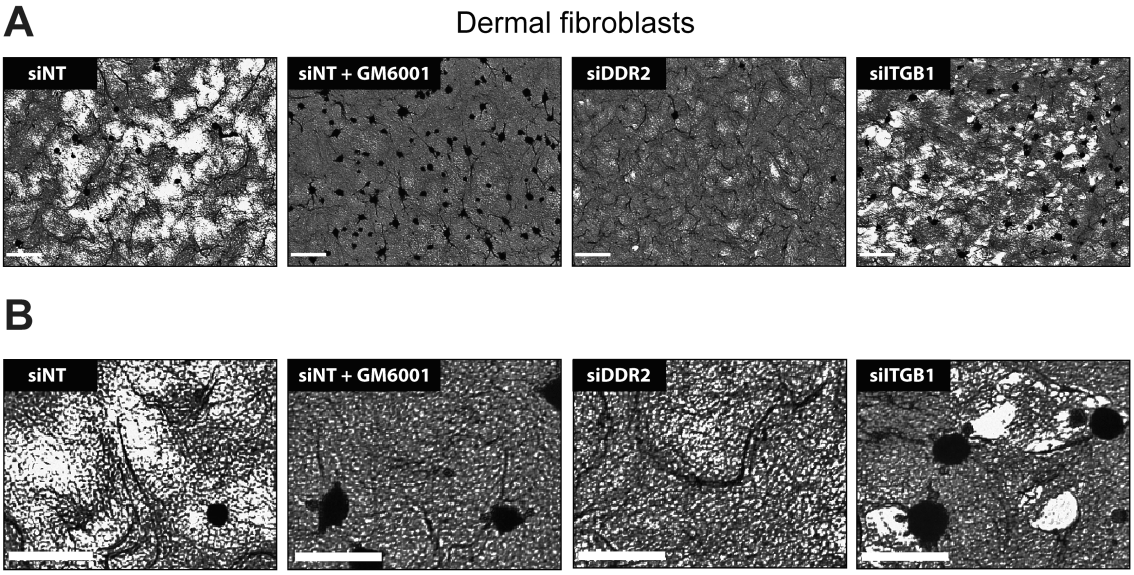

Figure 4.4: Knockdown of DDR2 inhibits collagen film degradation in dermal fibroblasts. DDR2 and integrin β1 expression in dermal fibroblasts was knocked down by siRNA transfection. After 2 days, cells were seeded on top of PureCol-coated wells (100 µl of 2.7 mg/ml) and cultured in serum-free DMEM for a further 3 days. GM6001 was supplemented at 10 µM. Cells were removed by trypsinization, the collagen layer fixed with 3% PFA and stained with Coomassie Brilliant Blue. Degradation is visible as white areas against the dark background. Three wells were used per treatment and representative images are shown. **(A)** Images were taken with a light microscope using 4 × objective lens. Scale bar: 270 µm. **(B)** Images were taken with a light microscope using 20 × objective lens. Scale bar 55 µm.

MMP-2 were lower in RASF from donor #2, and degree of collagen degradation was also lower in these cells. It can be speculated that the extent of collagen damage is relative to MT1-MMP activity and is reflected in levels of proMMP-2 activation.

Silencing of β1 integrin expression in RASF and dermal fibroblasts did not inhibit collagen degradation. Furthermore, degradation seemed to be more pronounced upon integrin knockdown. Further analysis of images captured with 20 × objective lens showed that siITGB1 cells create visibly larger and round 'holes' in the collagen layer, with well defined boundaries (Figure 4.3B and Figure 4.4B). On the contrary, control cells show a more diffuse collagen degradation. White unstained areas were almost absent in GM6001 treated and in siDDR2 cells. In conclusion,

these data indicate that collagen signalling through DDR2 is necessary for efficient MT1-MMP-dependent collagen degradation by RASF and dermal fibroblasts.

4.2.4 Collagen488 degradation assay

Both gelatin and collagen film degradation assays allowed evaluation of the ability of fibroblasts to degrade the ECM and comparison of the changes in substrate degradation in siRNA-transfected cells. In addition to the above assays, I considered quantitative methods to accurately determine changes in collagen degradation. The hydroxyproline assay is a technique frequently used to detect collagen in biological samples (Creemers et al., 1997). Hydroxyproline (4-hydroxyproline) is an amino acid commonly found in collagen and elastin. Levels of hydroxyproline detected in analysed samples correspond directly to the amount of degraded collagen (or elastin). In this technique, hydroxyproline is oxidised and reacts with p–dimethylaminobenzaldehyde resulting in formation of a colorimetric product.

I analysed serum-free culture media collected from collagen film degradation assays using the hydroxyproline assay. However, despite several attempts I was not able to detect hydroxyproline due to low detection limits and high interference from cell culture medium components. During the initial step, samples are hydrolysed in the presence of concentrated HCl overnight at 100°C. In this process medium components became charred and subsequently interfered with absorbance measurements.

Thus I decided to use fluorescently labelled collagens. A similar approach, using FITC-labelled collagen, has previously been successfully used to detect collagen degradation by HT1080 cells (Wolf et al., 2007). I conjugated type I collagen to Alexa Fluor 488 as described in Materials and Methods Section 2.10. Thick collagen layers were incubated at 37°C prior to labelling to avoid interference of the fluorescence dye with fibril formation. Cleavage of Alexa Fluor 488-labelled colla-

gen (collagen488) would result in release of fluorescent dye into the medium, which could be directly detected by fluorescence spectroscopy.

To optimise the assay, I compared labelling and degradation of CellMatrix, PureCol or a mixture (1:1 v/v) of both collagens. Initially, Alexa Fluor 488 dye was used at 20 µg/ml. Two different experimental layouts were compared: 12- or 24-well plates, filled with 500 µl or 250 µl of collagen respectively, to allow for scaling down of reaction reagents and cell numbers. Dermal fibroblasts were used in the optimisation because supplies of RA synovial fibroblasts were limited. Fibroblasts were cultured on top of the collagen488 for 5 days in serum-free and phenol red-free DMEM. GM6001 (10 µM) was added to the medium of cells cultured on top of mixed (1:1) collagens. Preliminary results are presented in Figure 4.5.

High fluorescence levels were detected in culture media collected from fibroblasts cultured on top of collagen488. Levels of detected fluorescence were on average 87% lower in GM6001-treated samples, suggesting that the increase in fluorescence

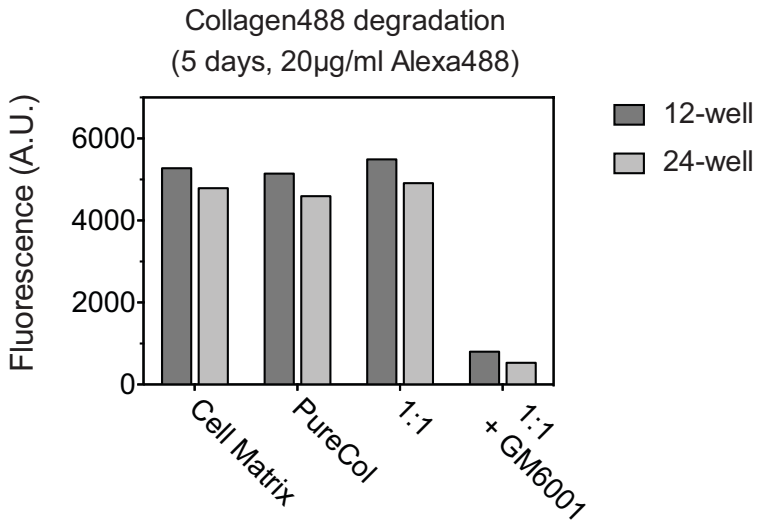

Figure 4.5: Optimisation of collagen488 degradation. Comparison of collagen488 degradation between 12-well and 24-well experimental set up. Collagen type I was labelled with 20 µg/ml Alexa Fluor 488. Equal volumes of 1:1 CellMatrix and PureCol mix (n=2) or each collagen alone (n=1) were used. Dermal fibroblasts were cultured atop of collagen488 for 5 days. GM6001 was used at 10 µM. Media were analysed by spectroscopy and fluorescence shown in arbitrary units (A.U.). Readings from sample without cells were subtracted.

was due to MMP activity. Fluorescence was slightly lower for 24-well than 12-well plates. All collagens showed comparable levels Alexa Fluor 488 release within the experimental set ups, indicating similar levels of labelling. Although the experiment was conducted with a samples number of one (see Figure 4.5), consistent results were obtained for all tested collagens.

Next, I performed a time course analysis of collagen488 degradation using CellMatrix collagen labelled with 20 µg/ml of Alexa Fluor 488 dye. Dermal fibroblasts were cultured for shorter time: 3, 4 and 5 days (Figure 4.6). In order to estimate how much fluorophore was released into the medium and what amount of the labelled collagen488 remained in the well, collagens were digested with a bacterial collagenase (100 µg/ml) and fluorescence of the cleaved collagen solution was also measured (Figure 4.6B). Fibroblasts appear to release all the available Alexa Fluor 488 dye into the medium as early as the day 3 time point. Almost no fluorescence was detected in bacterial collagenase cleaved collagen, indicating that all labelled collagen488 has been already degraded by fibroblasts. GM6001 prevented collagen488 degradation. At all time points, samples cultured in the absence of cells showed a high background from spontaneous release of the Alexa Fluor 488 dye into the medium. On average, more than 50% of fluorescence detected in fibroblast culture medium could be attributed to non-specific fluorophore release.

As almost all collagen488 has been cleaved during 3 day culture, I decided to analyse even shorter time points. To avoid high background readings due to fluorophore release, CellMatrix collagen was labelled in 24-wells with a lower concentration of Alexa Fluor 488 — 2 µg/ml rather than 20 µg/ml. Collagen488 were also extensively washed in PBS before plating fibroblasts, which were then cultured for 1 or 2 days (Figure 4.7). To further characterise a specificity of collagen488 degradation, the anti-MT1-MMP antibody DX-2400 (0.5 µM) was used in addition to GM6001 (10 µM). One sample per treatment was used, including collagen488 cultured without cells. Collagen488 samples incubated without fibroblasts were digested with bacterial collagenase to estimate the total Alexa Fluor 488 content

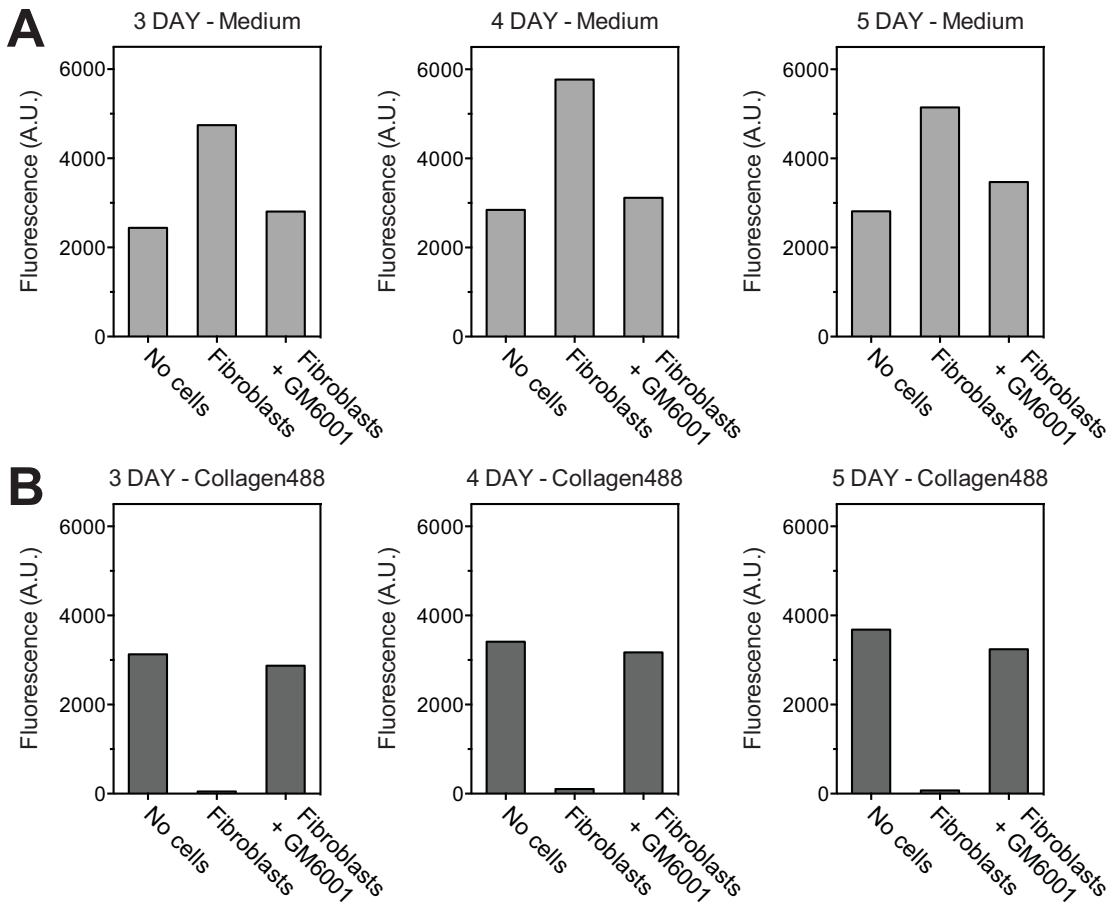

Figure 4.6: Time course analysis of collagen488 degradation. Dermal fibroblasts were cultured on collagen488 for 3, 4 or 5 days. 20 µg/ml Alexa Fluor 488 dye was used for labelling. GM6001 was added to medium at 10 µM. After culture, remaining collagen was digested with bacterial collagenase (100 µg/ml). Medium **(A)** and digested collagen **(B)** were analysed by spectroscopy and fluorescence shown in A.U. Readings from samples without cells are included in the graph. n=2.

(Figure 4.7). The volume of cleaved collagen was adjusted to match the volume of conditioned media. Additionally, media from samples without cells were analysed to detect non-specific fluorophore release. This non-specific fluorescence reading was subtracted from sample readings. Background fluorescence readings were within 27% of fluorescence released by fibroblasts at day 2.

Figure 4.7 demonstrates that lower concentrations of Alexa Fluor 488 still result in a high labelling of collagen. One day incubation showed little collagen488 degradation (Figure 4.7A), but release markedly increased at day 2 (Figure 4.7B).

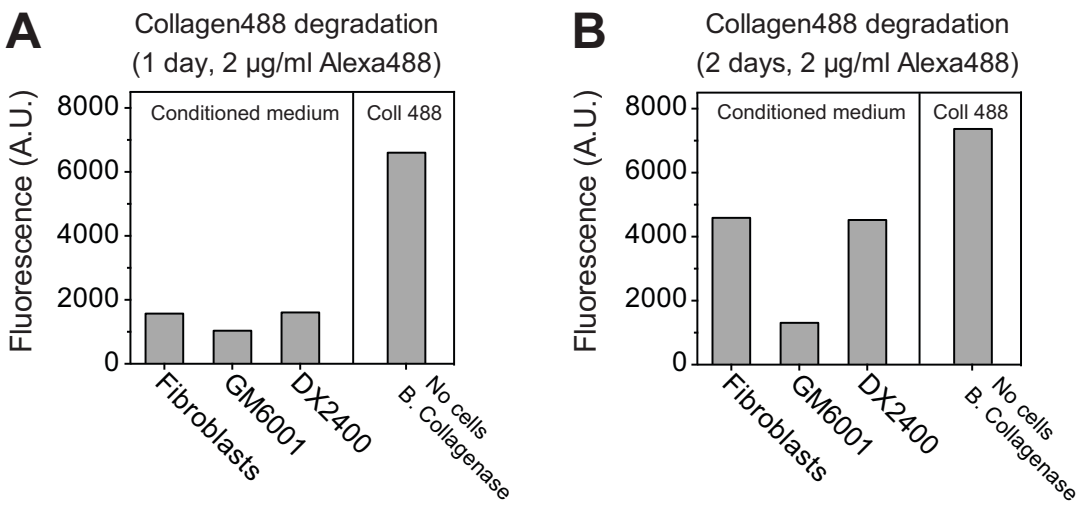

Figure 4.7: Optimisation of collagen labelling with Alexa Fluor 488. CellMatrix collagen was labelled with 2 µg/ml Alexa Fluor 488 solution in 24-well plates. Dermal fibroblasts were cultured on top of collagen488 for 2 days. GM6001 was used at 10 µM and DX-2400 MT1-MMP inhibitory antibody at 500nM. A sample cultured without cells was digested with bacterial collagenase (100 µg/ml). Medium and digested collagen were analysed by spectroscopy and fluorescence shown in A.U. n=1.

As culture medium fluorescence levels were lower than fluorescence of digested collagen488, it is likely that not all collagen488 was degraded by fibroblasts at day 2. Interestingly, although GM6001 inhibited collagen488 degradation, DX-2400 was not able to block it. Fluorescence levels of medium from DX-2400 treated fibroblasts were almost the same as that of untreated fibroblasts. Due to only a single measurement (n=1), the results were treated with caution and I decided to test collagen488 degradation using a panel of a MMP inhibitors.

In the next experiment, CellMatrix collagen was labelled with 2 µg/ml Alexa Fluor 488 dye in a 24-well plate. At the same time, a 24-well plate was coated with the same volume of CellMatrix collagen that was left unlabelled. Equal numbers of dermal fibroblasts were seeded on top of both labelled and unlabelled collagen. Fibroblasts were cultured for 2 days in the presence of the following inhibitors as indicated: GM6001 (10 µM), DX-2400 (0.5 µM), TIMP-1 and TIMP-2 at 0.5 µM. Collagen488 samples incubated without fibroblasts were digested with bacterial col-

lagenase and media were collected to analyse background fluorescence, which was within 23% of fibroblasts readings and subtracted from samples readings (Figure 4.8A). Gelatin zymography was used to analyse conditioned media from collagen488 and unlabelled collagen samples treated with inhibitors (Figure 4.8B).

The analysis of fluorescence of culture media showed that collagen488 degradation could be inhibited by GM6001, TIMP-1 and TIMP-2, but again could not be inhibited by DX-2400. Sensitivity to TIMP-1 and inability of DX-2400 to block degradation indicates that this process is MT1-MMP-independent. To confirm the effect of these inhibitors on MT1-MMP, collagen-induced proMMP-2 activation was analysed by gelatin zymography. To exclude possible effects of collagen labelling, samples obtained from unlabelled collagen were analysed for comparison. Pro-MMP-2 activation in fibroblasts was clearly inhibited by GM6001, DX-2400 and TIMP-2 but not by TIMP-1. No differences were observed between labelled and unlabelled CellMatrix collagen.

A striking observation was made when fibroblasts were cultured on top of collagen488 alone or when treated with DX-2400. On several occasions, collagen488 gels in those samples became very easy to dislocate from the well and sometimes had a dissolved, jelly-like appearance which was not observed in GM6001-treated cells. In contrast to GM6001-treated samples, increase in the volume of cell culture medium was also observed in these samples.

At this point, the assay was not further optimised, as the observed collagen488 degradation was not reflecting MT1-MMP activity. The possible implications of these results are discussed in Section 4.3.

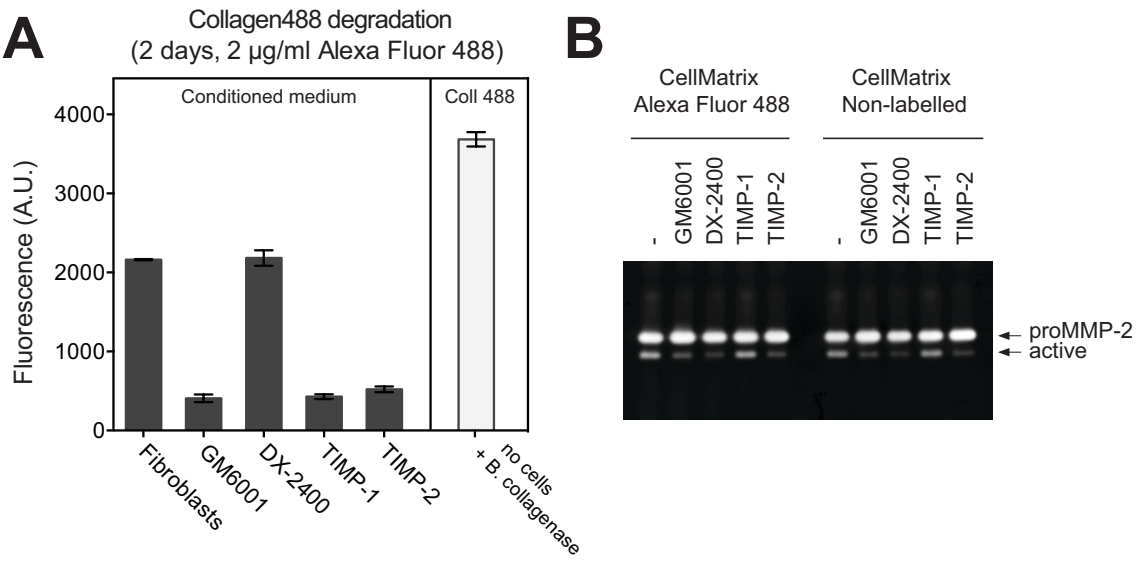

Figure 4.8: Effect of MMP inhibitors on collagen488 degradation. CellMatrix collagen was either labelled with 2 µg/ml Alexa Fluor 488 solution in 24-well plate or left unlabelled. Dermal fibroblasts were cultured on top of labelled or unlabelled collagen for 2 days. The following inhibitors were used: GM6001 (10 µM), DX-2400 (0.5 µM), TIMP-1 (0.5 µM) and TIMP-2 (0.5 µM). Collagen488 sample without cells was digested with bacterial collagenase (100 µg/ml). **(A)** Fluorescence of medium and digested collagen was measured by spectroscopy and shown in arbitrary units (A.U.). n=2. **(B)** Zymography analysis of conditioned medium from cells cultured on top of collagen488 or unlabelled collagen.

4.2.5 DDR2 knockdown partially inhibits collagen invasion in transwell invasion assay

The transwell invasion assay is commonly used to assess the invasiveness of a wide range of cells (Palmisano and Itoh, 2010). The bottom parts of transwell chambers are fitted with porous PET membranes which can be coated with a reconstituted ECM, such as Matrigel or collagen. Cells are seeded on top of the matrix and allowed to migrate to the bottom side of the membranes. Invaded cells are then stained and counted.

Because cells primarily utilise MT1-MMP to invade 3D collagen gels, I used collagen-coated transwells to analyse invasion of synovial and dermal fibroblasts. Expression of integrin β1 or DDR2 was knocked down by siRNA transfection. After two days, equal numbers of cells were seeded on top of collagen-coated transwells

and cultured for 3 days, at which point cells were fixed, stained and counted. Four transwells per treatment were used in each experiment. Statistical analysis was done using one-way ANOVA with Bonferroni Multiple Comparison Test.

Two separate experiments with RA synovial fibroblasts from different donors were performed. The numbers of invading RASF transfected with non-targeting siRNA differed between the two experiments, with average invasion numbers around 3500 and 1300 respectively. Differences could be attributed to the variability between assays or invasive potential of RASF. Figure 4.9A illustrates combined data for RASF from these two experiments. Due to differences in invasion, data are represented as a percent (%) of the average number of invading non-targeting siRNA transfected cells and analysed by ANOVA.

Invasion was strongly inhibited by GM6001, with 94% reduction (*** $p \leq 0.001$). DDR2 knockdown resulted in significant decrease in RASF invasion (* $p \leq 0.05$ siDDR2 vs. siNT and ** $p \leq 0.01$ siDDR2 vs. siITGB1). RASF transfected with DDR2-targeting siRNA invaded collagen approximately 36% less than control cells. There were no significant differences between invasion of siNT and siITGB1 samples.

For dermal fibroblasts, cell invasion numbers were much lower than for RASF. The average number of invading siNT cells was around 200 (Figure 4.9B). Similarly to RASF, invasion was inhibited by GM6001 (93% inhibition; * $p \leq 0.05$). Statistical analysis by ANOVA did not show significant differences between invasion of siNT and siDDR2 cells or between siNT and siITGB1 cells. Although not statistically significant, Figure 4.9B shows reduction of invasion of siDDR2 cells by 53%. Even though the variation in numbers of invading siITGB1 cells was substantial, the average invasion was comparable and no different to invasion of control siNT cells.

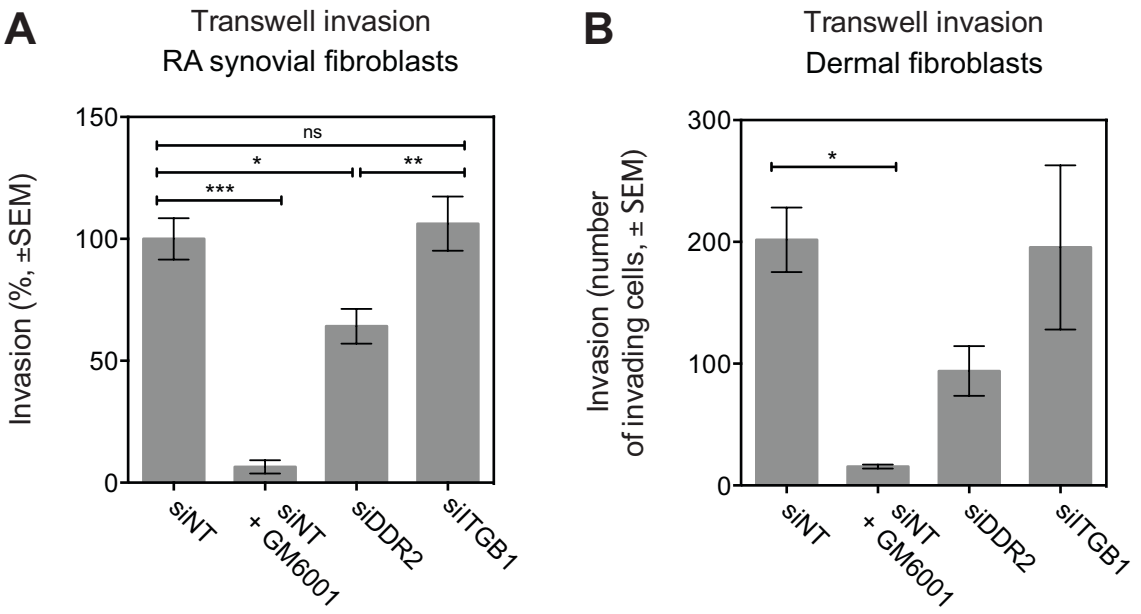

Figure 4.9: Fibroblast invasion in transwell assay is inhibited by DDR2 knockdown. Expression of collagen receptors was knocked down in fibroblasts by siRNA transfection. After 2 days cells were cultured on top of collagen-coated transwells. GM6001 was supplemented at 10 µM. After 3 days non-invading cells and collagen were removed, remaining cells fixed with 3% PFA, stained and counted. **(A) RA synovial fibroblasts**. Data from two separate experiments are combined and represented as percentage of average siNT invasion (± SEM). 1:1 mix of collagen was used. n=8; * $p \leq 0.05$, ** $p \leq 0.01$, *** $p \leq 0.001$. **(B) Dermal fibroblasts.** Data represented as number of invading cells ± SEM. CellMatrix collagen was used. n=4; * $p \leq 0.05$.

4.2.6 DDR2 is not required for 3D collagen migration in microcarrier beads invasion assay

Invasion of fibroblasts suspended within 3D collagen matrix was subsequently analysed by microcarrier beads invasion assay. First of all, I have performed a time course analysis of fibroblast invasion. The same numbers of either RASF or dermal fibroblasts were attached to microcarrier beads and suspended within CellMatrix collagen. Cells were allowed to migrate away from the beads for 72 h and images taken at 24 h intervals (Figure 4.10). At the 24 h time point, fibroblasts started to elongate within the collagen matrix and very little invasion was observed. Time course analysis showed that the majority of cells migrated away from the bead sur-

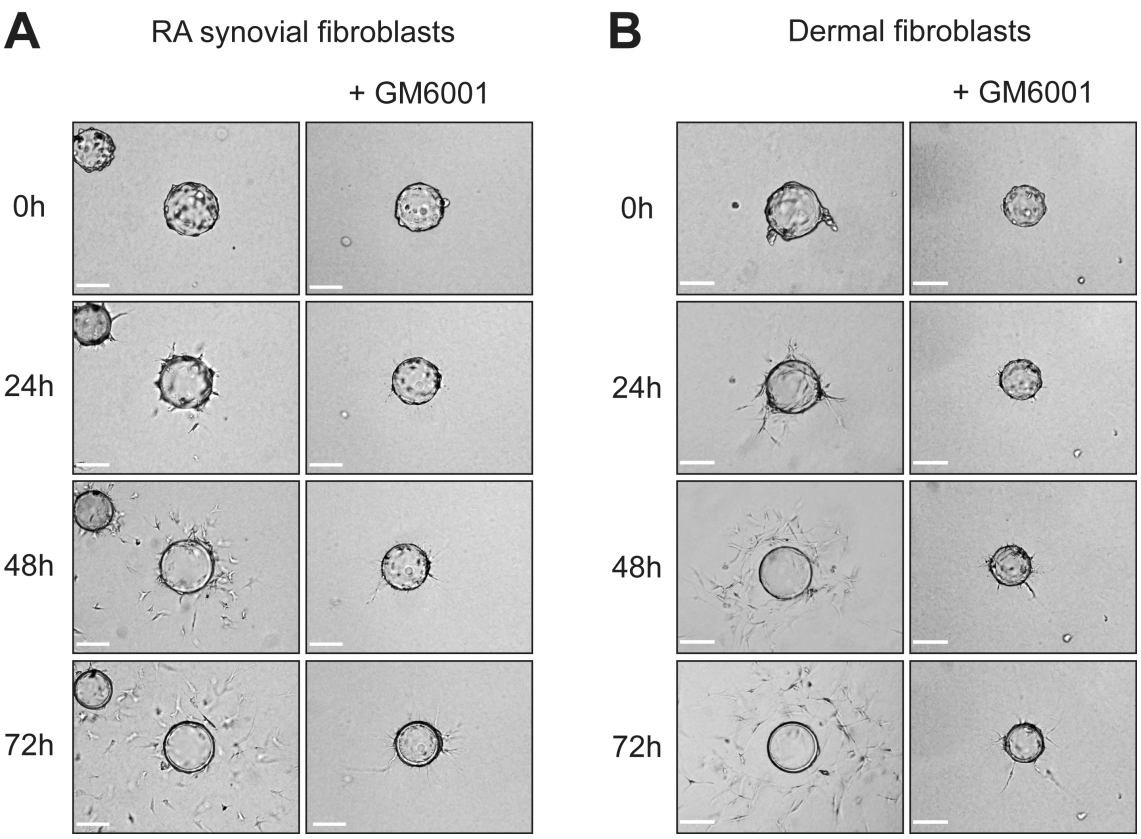

Figure 4.10: Time course analysis of fibroblast migration within 3D collagen in microcarrier beads invasion assay. (A) RASF or **(B)** dermal fibroblasts were attached to gelatin-coated microcarrier beads, embedded within CellMatrix collagen, final concentration approximately 2.2 mg/ml) and incubated at 37°C for 30 min. Afterwards, 0.5 ml of 10% FBS containing DMEM was added on top of collagen gel. GM6001 was supplemented at 10 µM. Cells were cultured for 72 h and images were captured at 24 h intervals with 10 × objective lens. Scale bar: 110 µm.

face in a radial pattern after 72 h. There were no noticeable differences in invasion between synovial and dermal fibroblasts. GM6001 (10 µM) inhibited cell migration, which indicates that invasion is MMP-dependent. Fibroblasts exhibit a spindle-like shape when migrating within collagen.

Invasion distances were compared in RASF from two different donors in which collagen receptors were knocked down by siRNA transfection. Cells were attached to beads 48 h posttransfection and allowed to invade collagen for a further 72 h. Migration distances of individual cells were measured in µm and are presented as a scatter-plot graph on Figure 4.11. Approximately 1/4 of all counted control cells

were still attached to beads (3/4 of cells invaded into collagen gel). The percentages of invading cells for each particular treatment are specified below the scatter-plots on Figure 4.11. Comparison between groups was made with ANOVA with Bonferroni Multiple Comparison Test. GM6001 significantly reduced invasion of siNT cells from both RASF donors (*** $p \leq 0.001$). Although median migration was almost identical for control cells from the two donors, for donor #2, the range of migration was twice that observed for donor #1.

Contrary to results obtained in the transwell assay, knockdown of DDR2 expression did not inhibit invasion of fibroblasts suspended within 3D collagen. The number of invading cells, as well as the median migration distance and range of invasion were almost identical in siNT and siDDR2 cells from both RASF donors. Interestingly, knockdown of β1 integrin resulted in changes in RASF invasion, however none of the observed differences were statistically significant. The percent of invading cells was lower (57%) in siITGB1 samples, and the median migration distance was also lower than in control cells. It was also observed that many cells lacking β1 integrin had a round shape, instead of the typical spindle-like appearance characteristic for invading fibroblasts, as illustrated on Figure 4.13.

From the scatter-plot analysis on Figure 4.11 it was apparent that the median migration distance was lower for siITGB1 cells, however they did not show a particularly reduced range of migration. For informative purposes non-migrating cells were removed from the scatter-plot and the resulting graph shown in Figure 4.12. The graph demonstrates that indeed less siITGB1 cells were invading collagen, but those which were able to migrate did not show any apparent defect in invasion, as evident by lack of differences in migration distance between treatments.

To further analyse the discrepancies between the transwell and microcarrier beads invasion assays, I decided to test different collagen preparations. Acid-extracted collagens such as CellMatrix are preferred in invasion assays as they form more compact, cross-linked collagen gels with smaller pores, which require proteolytic action of cells to migrate within them. Gels formed by pepsin-extracted

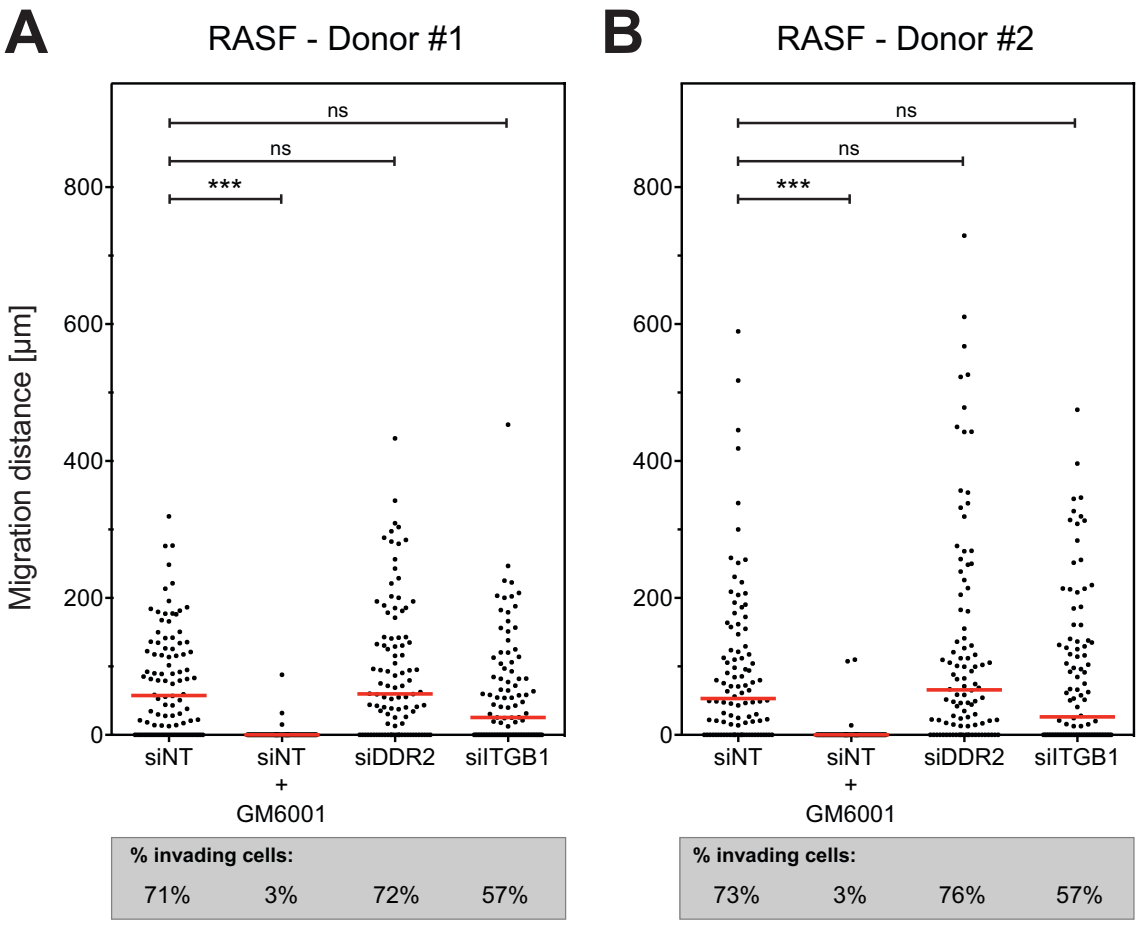

Figure 4.11: Role of collagen receptors in microcarrier beads invasion assay. Expression of DDR2 and integrin β1 was knocked down in RASF by siRNA transfection. After 2 days cells were attached to microcarrier beads and embedded within CellMatrix collagen at a final concentration of approximately 2.2mg/ml. GM6001 was added at 10 µM. Cells were cultured for a further 3 days, fixed with 3% PFA and images were taken with a light microscope using 10 × objective lens. Migration distance (µm) was measured in ImageJ software. The fraction of cells that migrated away from the bead are represented as a percent of total counted cells (% invading cells). Bar represents median migration distance; n=100; *** $p \leq 0.001$.

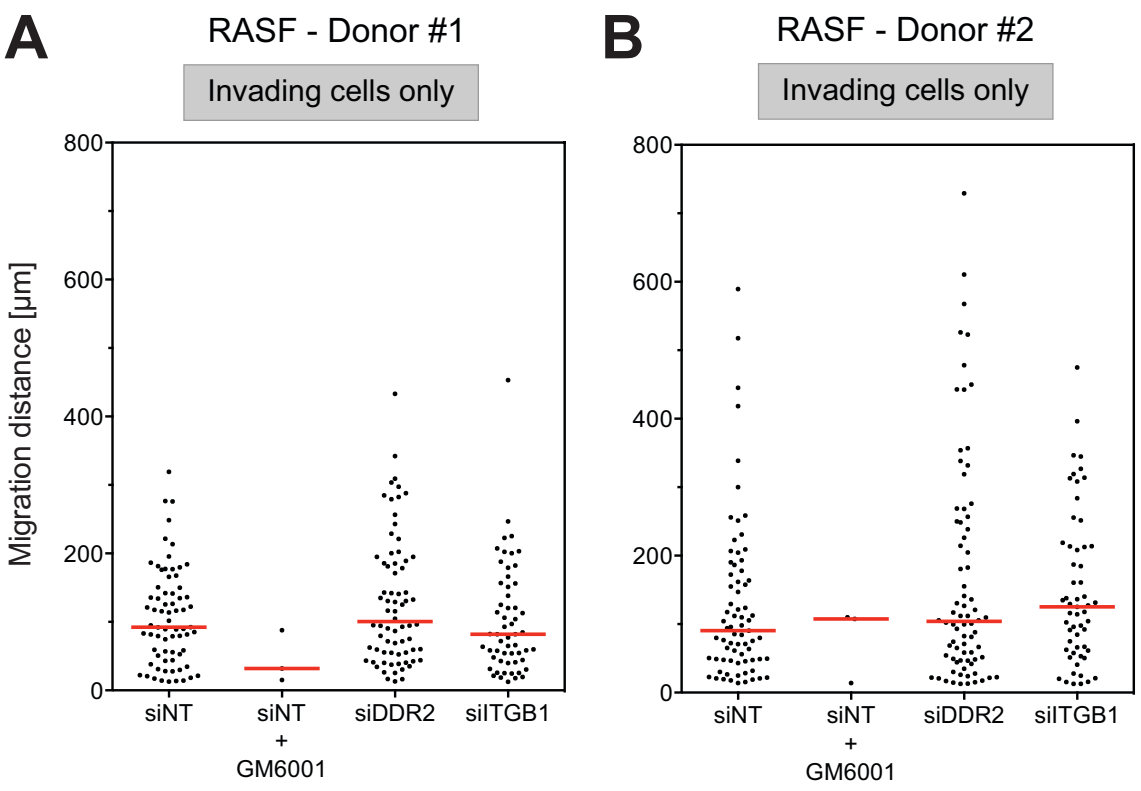

Figure 4.12: Analysis of migration distance of collagen invading cells. Graph represents migration distance of cells that showed only invasion into surrounding collagen gel. Cells that had not migrated were excluded from the graph. Bar represents median migration distance.

collagens lack telopeptides and thus form less cross-linked gels, resulting in collagen scaffolds with larger pores which cells can negotiate without proteolysis (Sabeh et al., 2009b). As observed in Chapter 3, PureCol collagen stimulates cells better than CellMatrix and induces more proMMP-2 activation. For that reason I tested either CellMatrix or several mixtures of CellMatrix and PureCol in different proportions: 2:1, 1:1 and 1:2 v/v respectively. Dermal fibroblasts were attached to microcarrier beads, embedded within these collagens and cultured for 72 h as described previously (Figure 4.14). GM6001 inhibited migration of dermal fibroblasts in all collagen preparations tested (Figure 4.14A). Median migration distance and range were also nearly identical across all samples (Figure 4.14B).

Because invasion within all collagen gels was inhibited by GM6001 and therefore MMP-dependent, all collagen preparations were suitable to analyse MMP-

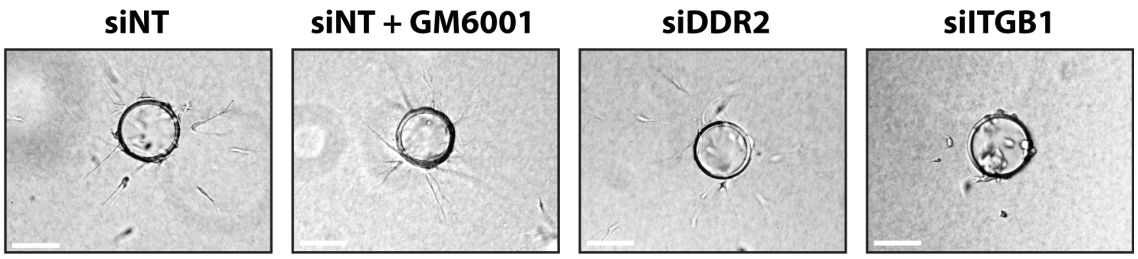

Figure 4.13: Comparison of cell shape of siRNA-transfected fibroblasts during 3D collagen invasion. During microcarrier beads invasion assay, siITGB1 transfected cells show a round cell shape instead of the characteristic spindle shape. Scale bar: 110 µm.

dependent invasion. I thus decided to compare CellMatrix with a 1:2 mixture of CellMatrix and PureCol, as it provides the highest concentration of pepsin-treated PureCol. Again, expression of collagen receptors was knocked down by siRNA transfection in RASF and dermal fibroblasts. 48 h posttransfection cells were attached to beads, the sample divided into two and embedded within either CellMatrix or mixed collagen gel (1:2) and cultured for 72 h. Cell migration distance was measured as described and results are represented in Figure 4.15.

Overall, little variation was observed between different collagen preparations with the exception of invasion of siITGB1 fibroblasts. Contrary to the results of the first microcarrier beads invasion experiment, knockdown of integrin β1 did not result in any significant inhibition of invasion in CellMatrix collagen only. However, invasion was significantly inhibited in the mixed collagen gel, with siITGB1 RASF showing significantly more inhibition versus control cells (Figure 4.15B; *** $p \leq 0.001$) than dermal fibroblasts (Figure 4.15D; * $p \leq 0.05$).

Synovial fibroblasts showed a slightly higher range of migration and median migration distance than dermal fibroblasts. Fibroblasts embedded within CellMatrix collagen also seemed to invade further than in the mixed collagen matrix. No other major differences in invasion were observed between synovial (Figure 4.15A,B) and dermal fibroblasts (Figure 4.15C,D). As in the previous experiment, knockdown of DDR2 had no significant effect on cell invasion and range in either collagen type,

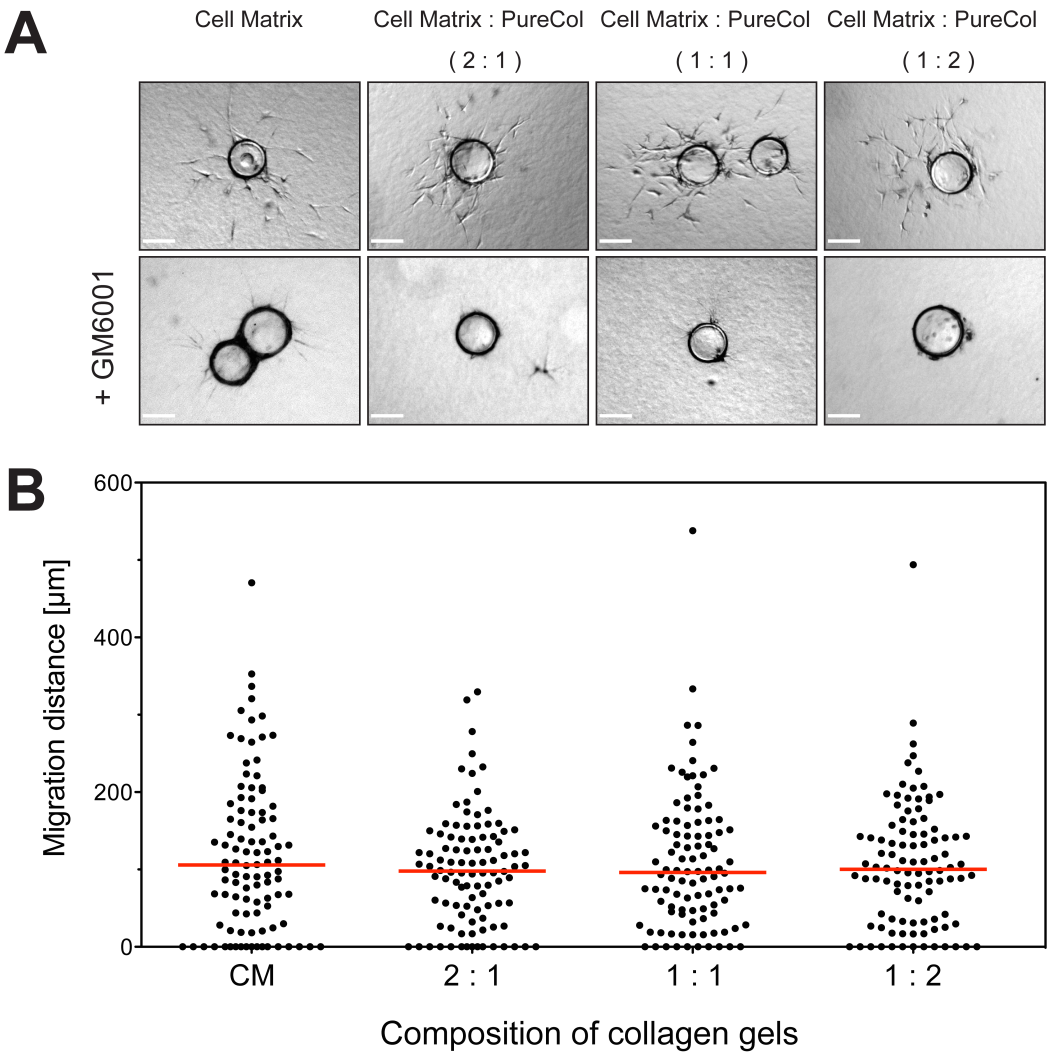

Figure 4.14: Fibroblast invasion within different preparations of 3D collagen gels during microcarrier beads assay. (A) The same number of dermal fibroblasts were attached to microcarrier beads and embedded within CellMatrix collagen or a mixture of CellMatrix and PureCol (2:1, 1:1 or 1:2 v/v) at 2.2 mg/ml final concentration. GM6001 was added at 10 µM. Cells were cultured for 3 days, fixed with 3% PFA and images taken with 10 × objective lens. Scale bar: 110 µm **(B)** Migration distance (µm) of fibroblasts were measured in ImageJ software; bar represents median migration distance; n=100. *CM* - CellMatrix collagen.

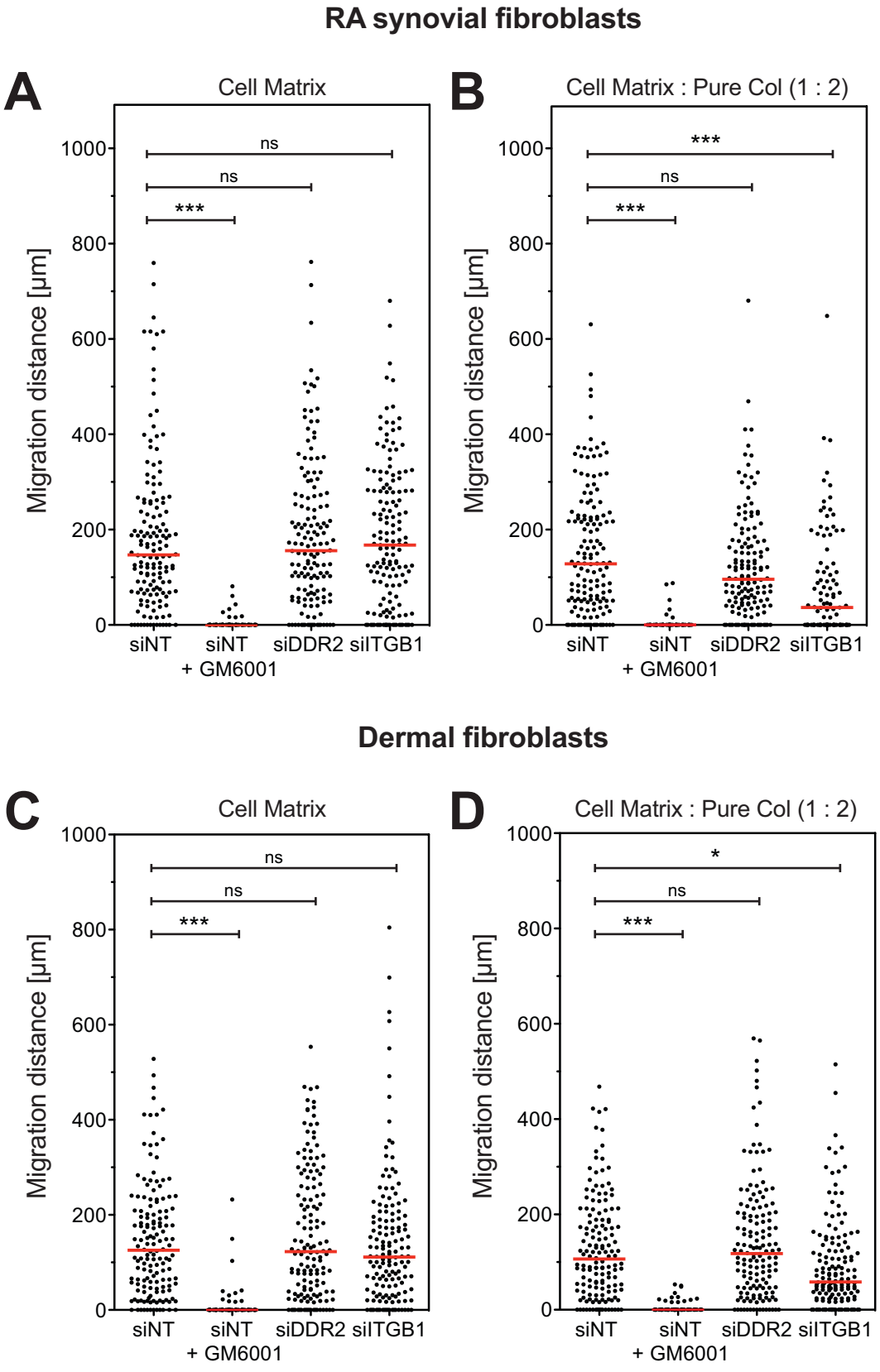
RA synovial fibroblasts
A
Cell Matrix
B
Cell Matrix : Pure Col (1 : 2)
Migration distance [µm]
1000
800
600
400
200
0
ns
ns
***
***
ns
***
siNT
siNT + GM6001
siDDR2
siITGB1
Dermal fibroblasts
C
Cell Matrix
D
Cell Matrix : Pure Col (1 : 2)
*

Figure 4.15: Effect of collagen gel composition on migration of siRNA transfected fibroblasts in microcarrier beads invasion assay. Expression of collagen receptors DDR2 and integrin β1 was knocked down by siRNA in RA synovial fibroblasts **(A,B)** or dermal fibroblasts **(C,D)**. After two days cells were attached to microcarrier beads and embedded within collagen: CellMatrix **(A,C)** or 1:2 mixture of CellMatrix and PureCol respectively **(B,D)**. Cells were cultured for a further 3 days (with or without 10 µM GM6001), fixed in 3% PFA, migration distances measured and represented in µm. Bar represents median migration distance; * $p \leq 0.05$, *** $p \leq 0.001$; Number of counted cells n=150 with exception of: **(A)** siNT+GM6001 n=58 **(B)** siNT+GM6001 n=49; siITGB1 n=101 **(C)** siNT+GM6001 n=57 **(D)** siNT+GM6001 n=53.

as observed for both RASF and dermal fibroblasts. GM6001 inhibited collagen invasion in all samples (*** $p \leq 0.001$). In conclusion, the invasive capability of RASF and dermal fibroblasts in different collagen preparations was not altered by DDR2 silencing. Knockdown of β1 integrin reduced the ability of cells to migrate within a collagen matrix, especially in matrices containing a higher ratio of pepsin-extracted collagen.

In addition to the above findings, analysis of images showed an interesting pattern of cell invasion within 3D collagen gels, as illustrated on Figure 4.16. Some of the fibroblasts were identified to follow each other, in a head-to-tail manner. The leading cell appeared to 'clear the path' for the trailing cells. Cells invaded at regular intervals, but cell-cell contacts were not readily visible in most cases.

Such multicellular invasion was reported previously for HT1080 cells and fibroblasts (Fisher et al., 2009; Gaggioli et al., 2007). The leader cells proteolytically degrade the collagen matrix and form so-called single cell invasion tunnels — SCITs — with the diameter of the cell's nuclei (Fisher et al., 2009). Those tunnels can be afterwards traversed by following cells without proteolytic cleavage of collagen. Even though MMP inhibitors block formation of SCITs, they do not block migration within already formed collagen tunnels. It is possible that fibroblasts in this study formed similar tunnels within collagen which were subsequently used by other fibroblasts. As a result, invasion of trailing cells does not require MT1-MMP.

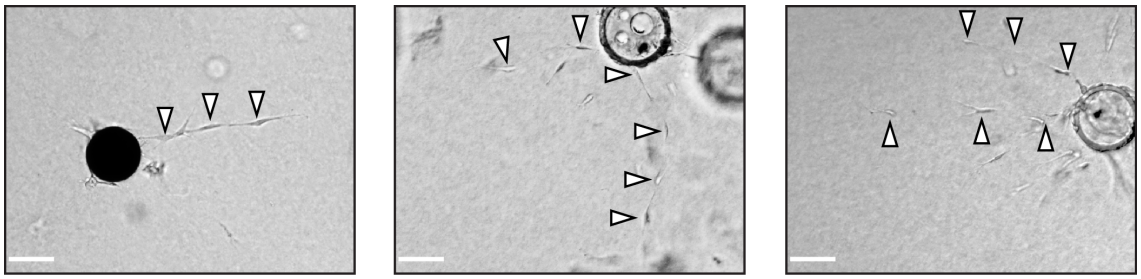

Figure 4.16: Multicellular invasion of fibroblasts within 3D collagen. During microcarrier beads invasion assay, fibroblasts showed chain-like cell invasion within the collagen matrix. Cells invaded head-to-tail, at regular intervals as indicated by arrow heads. Scale bar: 110 µm.

4.2.7 Dasatinib inhibits RASF invasion and motility

I investigated whether DDR2 inhibition by dasatinib has the same effect as DDR2 knockdown. Dasatinib is a small molecule tyrosine kinase inhibitor. It was developed to treat chronic myeloid leukaemia by inhibition of BCR-ABL kinase and was subsequently approved by the US Food and Drug Administration (FDA) for clinical use (Lombardo et al., 2004). In addition, it is a potent inhibitor of DDR1 and DDR2 kinases, but it also inhibits Src family kinases, PDGFRβ and p38 (Day et al., 2008; Lombardo et al., 2004). Dasatinib prevents collagen-induced autophosphorylation of DDR2 with a reported IC50 within the low nanomolar range (Day et al., 2008).

First, I examined the effect of dasatinib on proMMP-2 activation in RA synovial fibroblasts. Synoviocytes were transfected with non-targeting or DDR2-targeting siRNA, in triplicates. 2 days after transfection, PureCol was added to the medium at 100 µg/ml. GM6001 was used at 10 µM and dasatinib at 100 nM. After 3 days medium was collected and analysed by gelatin zymography, cell lysates were analysed by Western Blotting (Figure 4.17A). Levels of active MMP-2 on zymograms were measured by densitometry. Active MMP-2 detected in collagen-treated siNT cells was arbitrarily set to 100% and all other measurements are represented as percent of this value. Densitometry results are shown on Figure 4.17B.

As in previous experiments, DDR2 silencing resulted in significant reduction of proMMP-2 activation upon collagen stimulation. Dasatinib treatment resulted

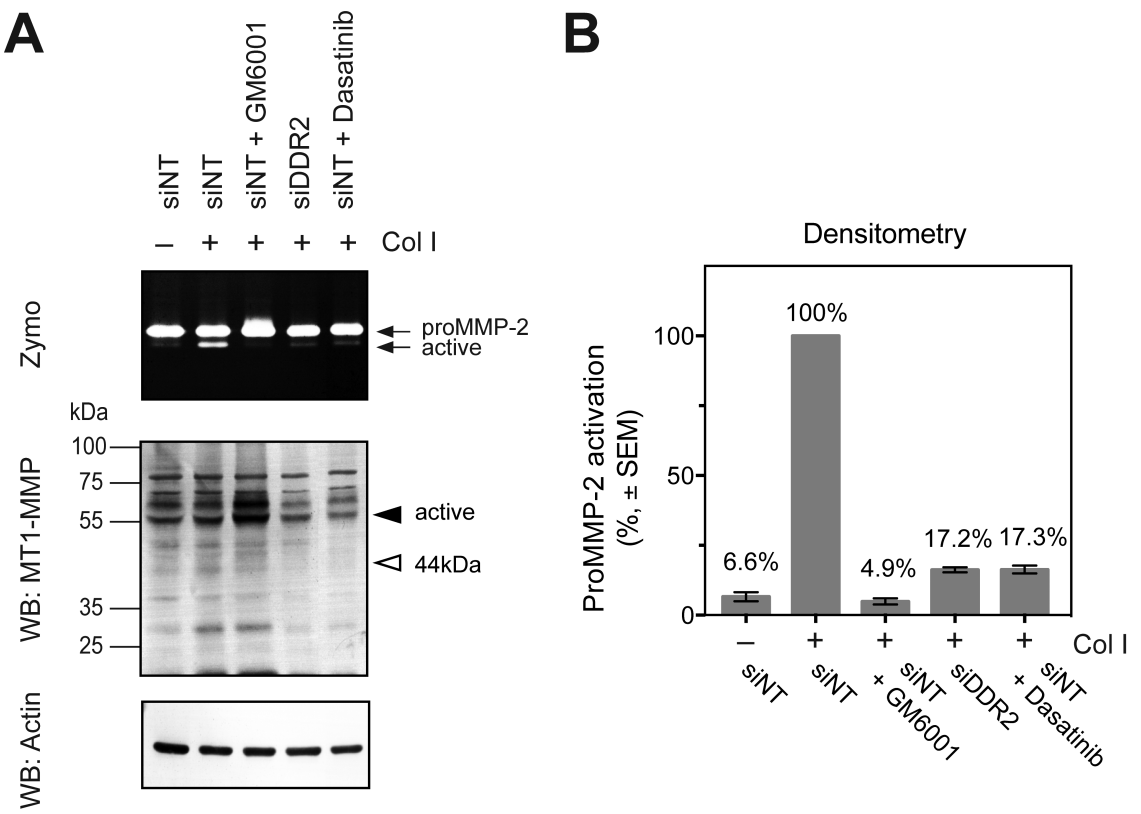

Figure 4.17: Dasatinib prevents collagen-induced proMMP-2 activation. Tyrosine kinase inhibitor dasatinib reduces proMMP-2 activation in RA synovial fibroblasts stimulated with collagen. **(A)** RA synovial fibroblasts transfected with non-targeting or DDR2-targeting siRNA were cultured in absence (–) or presence (+) of PureCol in medium (100 µg/ml) for 2 days. GM6001 (10 µM) and dasatinib (100 nM) were supplemented into the medium as indicated. Samples were done in triplicates. Medium was analysed by zymography and cell lysates by Western Blotting. **(B)** Zymograms were analysed by densitometry to asses levels of active MMP-2. Measurements are represented as percentage (%) of active MMP-2 in siNT cells stimulated with collagen (100%). Data shown as mean ± SEM. n=3.

in almost identical reduction in proMMP-2 activation (average 82.8% and 82.7% reduction for siDDR2 and dasatinib respectively). GM6001 blocked proMMP-2 activation in control cells by more than 95%, to the level observed in untreated siNT cells. DDR2 depletion as well as dasatinib treatment result in lower levels of MT1-MMP. Furthermore, no MT1-MMP processing was observed in these samples. In conclusion, dasatinib exerts a similar effect on MT1-MMP activation as DDR2 knockdown, preventing proMMP-2 activation, MT1-MMP expression and processing.

As DDR2 silencing had a discernible effect on RASF invasion into 3D collagen, I investigated the action of dasatinib on RASF transwell invasion. The same numbers of RA synovial fibroblasts were seeded on top of collagen-coated transwells and cultured for 3 days in the absence or presence of either GM6001 (10 µM) or dasatinib (100 nM). Four transwells were used per treatment. Migrating cells were counted and differences between groups were analysed by ANOVA. Results are presented in Figure 4.18.

A significant reduction of invading cells was observed for GM6001 (*** $p \leq 0.001$) and dasatinib (*** $p \leq 0.001$) treatments in comparison to control cells. Synovial fibroblast invasion into collagen matrix could be inhibited by dasatinib. To verify if the inability of dasatinib-treated cells to invade the 3D ECM results from reduced collagen cleavage by MT1-MMP, a collagen film degradation assay was performed. RASF were substituted with dermal fibroblasts, which were cultured on top of PureCol-coated wells. Serum-free medium was supplemented with GM6001 (10 µM) or dasatinib (100 nM). After 5 days cells were removed by trypsin and

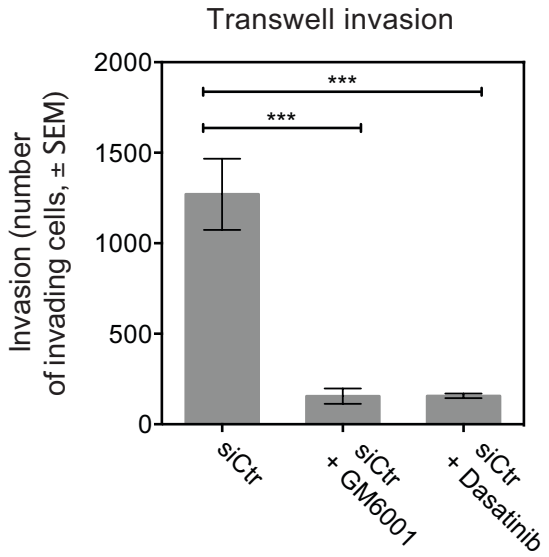

Figure 4.18: Collagen invasion is inhibited by dasatinib. RA synovial fibroblasts were cultured on top of CellMatrix-coated transwells for 3 days. GM6001 was used at 10 µM and dasatinib at 100 nM. Invading cells were stained and counted. Numbers of invading cells are shown as mean ± SEM. n=4; *** $p \leq 0.001$.

the remaining collagen was fixed and stained. Representative images are shown on Figure 4.19.

Dermal fibroblasts degraded the collagen matrix as demonstrated by the presence of visible white areas. Degradation was greatly reduced by GM6001. In general, dasatinib treatment resulted in less degraded collagen matrix but in some areas degradation was clearly visible as 'holes'. However, some of the dasatinib-treated cells were found detached and floating after the incubation period. Fibroblasts seem to degrade and simultaneously remodel the ECM, resulting in an uneven collagen layer. The majority of dasatinib-treated cells neither degraded nor remodelled collagen, which therefore resembles matrix incubated without cells (Figure 4.19).

The degradation pattern observed upon dasatinib treatment ('holes') could result from reduced mobility of fibroblasts on the substrate, which would increase focal degradation of the collagen layer because cells were unable to move. To examine this possibility, RASF motility was examined with an *in vitro* wound healing assay, that assesses the ability of fibroblasts to migrate across a cell-free gap. Silicone inserts with two chambers were used to generate a 500 µm gap between adhered RA synovial fibroblasts. Inserts were attached to the bottom of 24-well plates and 1.3×10^4 RASF seeded within each of the insert's chambers. Fibroblasts were allowed to adhere overnight in complete medium to create a confluent cell layer. The next day, medium was changed 30 min before removing inserts to complete DMEM

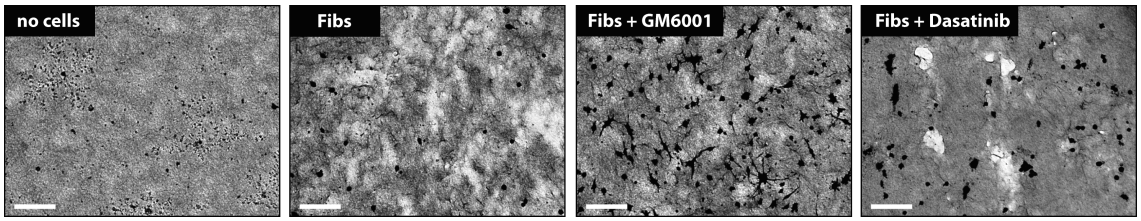

Figure 4.19: Collagen film degradation in dasatinib-treated fibroblasts. Dermal fibroblasts were cultured on top of PureCol-coated 12-well plates (100 µl of 2.7mg/ml collagen). GM6001 was supplemented into medium at 10 µM, dasatinib at 100 nM. After 5 days cells were removed by trypsin treatment, the collagen layer was fixed in 3% PFA and stained with Coomassie Brilliant Blue-250. Images were taken with a light microscope using 4 × lens. Scale bar: 270 µm.

supplemented either with dasatinib or equal volume of DMSO as a control. Two dasatinib concentrations were used — 50 nM and 100 nM. Inserts were then removed thus creating a gap between attached fibroblasts (0 h time point). Cells were incubated for a further 24 h. Images were taken at the beginning of the experiment (0 h) and after 8 and 24 hours. Images of matching areas at different time points are shown in Figure 4.20.

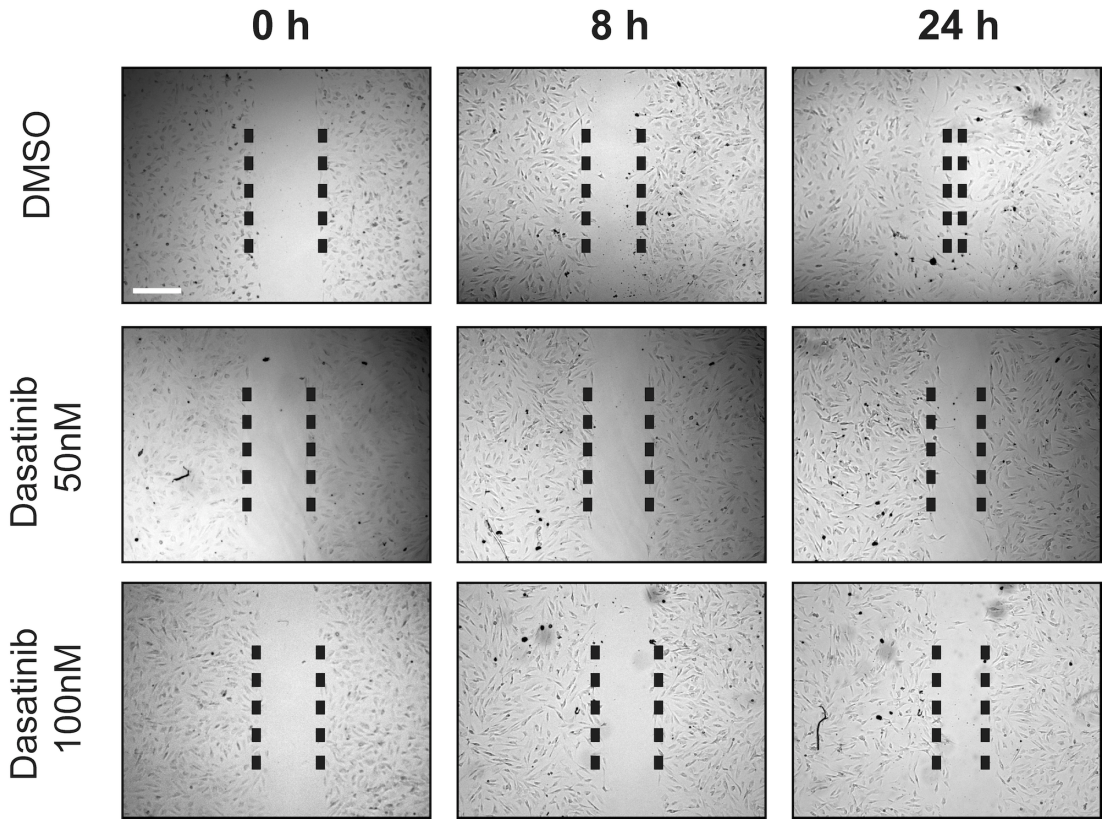

Figure 4.20: Dasatinib inhibits fibroblasts migration in a wound healing assay. Silicone inserts were used to generate a 500 µm cell free gap in order to asses fibroblast migration. RASF (1.3×10^4) were seeded within silicone inserts placed onto 24-well plates. Cells were allowed to adhere overnight to enable formation of a confluent cell layer. Medium was exchanged 30 minutes prior to insert removal and contained either DMSO (control) or dasatinib at 50 nM or 100 nM. After inserts were removed (0 h), fibroblasts were cultured for a further 24 h. Images of matching areas of the same well were captured at indicated time points with a light microscope using $4 \times$ objective lens. Vertical dotted lines show the cell migration front. Scale bar: 270 µm.

DMSO-treated fibroblasts started to migrate across the gap within 8 h and opposite migration fronts almost closed the gap after 24 h. Dasatinib reduced motility of RA synovial fibroblasts. Migration fronts of cell monolayers showed very little movement during the 24 hour incubation period. The two doses of dasatinib resulted in similar inhibition of motility. No negative effects of dasatinib treatment on cell phenotype were observed.

4.3 Discussion

In this Chapter, I have demonstrated that collagen is able to induce MT1-MMP activity, leading to extensive substrate degradation and that this signalling is mediated by DDR2. RA synovial fibroblasts are able to extensively degrade and invade collagen, and their invasiveness exceeds that of dermal fibroblasts. Silencing of DDR2 reduced gelatin degradation as well as collagen degradation and invasion. All of these processes have previously been demonstrated to be MT1-MMP-dependent (Artym et al., 2006; Miller et al., 2009; Palmisano and Itoh, 2010). Although transwell invasion was inhibited by DDR2 silencing, migration within 3D collagen is independent of DDR2. However, it is possible that at least some of the cells do not require MT1-MMP to invade collagen due to multicellular migration within preformed tunnels in collagen gels. As a consequence, those cells do not require DDR2 signalling for invasion.

In my study, the ability of fibroblasts to degrade collagen or gelatin was not compromised by knockdown of β1 integrin. In terms of invasion, transwell invasion was not inhibited by silencing of β1 integrin but these cells showed reduced migration within 3D collagen in the microcarrier beads assay. This is in agreement with a study reported by Wolf et al. (2007), where inhibition of β1 integrin activity by antibodies did not affect degradation of collagen, but reduced migration speed within a 3D collagen matrix in HT1080 cells.

Impaired invasion can be a result of reduced proteolytic activity or inability to propel the cell body within the ECM. Because loss of β1 integrin did not inhibit fibroblast capability to degrade collagen, it is likely that reduced migration within the 3D matrix was a result of disrupted adhesion to the ECM. Cells depend on integrins for attachment to substratum. Ligand binding initiates integrin aggregation and binding of adaptor proteins such as talin and vinculin which connect their cytoplasmic tails to actin filaments. In turn, contractile actomyosin complexes of actin and non-muscle myosin II generate traction force to translocate the cell body forwards. Loss of integrins results in weaker substrate adhesions and reduced ability to generate a pulling force. The round shape of siITGB1 cells within collagen confirms low substrate adhesion during migration. Similarly, cells treated with anti-integrin antibodies also adopt a round phenotype (Barbolina et al., 2007; Wolf et al., 2013, 2007).

I observed that synovial and dermal fibroblasts cultured *in vitro* require collagen as an 'activator' of MT1-MMP function. This was particularly visible in the Alexa488-gelatin assay where no gelatin degradation was detected until collagen was added into the medium. Although substantial amounts of active MT1-MMP were already present in fibroblasts, gelatin degradation was not initiated despite the fact that gelatin is easier to digest than collagen. Stimulation with collagen had a similar effect on proMMP-2 activation, as discussed in Chapter 3.

Several mechanisms are involved in regulation of MT1-MMP function, including gene transcription, intracellular trafficking, autocatalytic processing and enzyme dimerisation. As demonstrated in the previous Chapter, collagen upregulates levels of MT1-MMP mRNA in fibroblasts which could explain the increased activity, however, expression was elevated only a few-fold. Moreover, levels of active protein on the cell surface did not change significantly in the presence of collagen unless an MMP inhibitor was added to prevent MT1-MMP processing. This indicates that the observed activation of MT1-MMP function cannot be explained exclusively by an increased level of expression.

It is possible that MT1-MMP activation results from increased concentration of MT1-MMP on the cell surface. It has been reported that a considerable amount of MT1-MMP is internalised in unstimulated cells. Collagen-induced accumulation of MT1-MMP on the cell membrane could be achieved through modulation of a number of processes such as endocytosis or targeted trafficking. In fact, collagen has been shown to interfere with clathrin-mediated endocytosis of MT1-MMP, leading to increased cell membrane levels of MT1-MMP (Lafleur et al., 2006). The effect of collagen stimulation is autocatalytic processing of MT1-MMP resulting in formation of the 44 kDa species, which has been reported to reduce enzyme endocytosis (Cho et al., 2008). MT1-MMP is also targeted to and retained at focal adhesions and invadopodia, where substrate degradation occurs (Artym et al., 2006; Steffen et al., 2008; Woskowicz et al., 2013). The above mechanisms increase cell membrane levels of active MT1-MMP and could facilitate formation of a fully active MT1-MMP dimer, necessary for proMMP-2 activation and collagen cleavage (Itoh et al., 2008)

Preliminary results from the collagen488 degradation assay indicate a potential new mechanism of collagen degradation in addition to MT1-MMP. MMP inhibitors GM6001, TIMP-1 and TIMP-2 inhibited collagen488 degradation, suggesting involvement of an active MMP that is not membrane bound. This MT1-MMP-independent collagen degradation was only observed when cells were cultured in serum-free medium, suggesting that serum components would effectively inhibit the collagenase. These results are of particular interest, as mechanisms initiating MMP activation in an *in vivo* environment are not fully understood. *In vitro*, MMPs can be activated by trypsin, plasmin or other active MMPs and activated MMP-3 is considered a potent activator of MMP-1 and MMP-9. Although the identity of the active MMP was not confirmed, expression of MMPs is reportedly also induced by collagen, including collagenases MMP-1 and MMP-13 in RA synovial fibroblasts (Su et al., 2009; Zhang et al., 2006a). Based on our observations, we speculate that collagen, already shown to promote MMP-2 activation, is a likely candidate as an activator of other soluble MMP collagenases. It is of great interest to identify

the MMP responsible for this collagen degradation and to investigate whether its activity is dependent on DDR2-mediated collagen signalling.

Dasatinib is one of the few reported inhibitors of DDR1 and DDR2 and it is a potent inhibitor of DDR2 kinase. It efficiently reduced collagen-induced proMMP-2 activation, MT1-MMP expression and processing. Cells treated with dasatinib were unable to invade collagen in the transwell assay, however the effect of dasatinib on collagen degradation was unclear and some cells were still able to degrade collagen. We postulate that degradation could be at least in part attributed to reduced cell motility. Nevertheless, DDR2 knockdown and dasatinib treatment had similar effects on inhibiting MT1-MMP activity.

In conclusion, collagen is not only a protein that supports tissue structure but also a signalling molecule that induces changes in cell behaviour. My results show that collagen binding by DDR2 results in an increase in MT1-MMP activity and acquisition of an aggressive and invasive phenotype. Further investigation of the role of DDR2 in RA development would be important to understand the pathogenesis of RA.

Chapter 5

Analysis of DDR2 binding to collagen

5.1 Introduction

In the previous Chapters, I have demonstrated that the DDR2 receptor mediates collagen-induced MT1-MMP expression as well as functional activation of the enzyme already present on the cell surface. It is therefore particularly important to understand mechanisms of collagen binding by DDR2 and subsequent activation of the receptor.

My data show that synovial fibroblasts exhibit distinct levels of MT1-MMP activation depending on the source of type I collagen used. I observed that stimulation of synoviocytes with pepsin-extracted collagens resulted in higher levels of active MMP-2 than incubation with acid-extracted collagens (Section 3.2.3, Figure 3.4). During collagen extraction with pepsin, the enzyme cleaves N- and C-terminal telopeptides from collagen molecules (Sato et al., 2000). Telopeptides are short non-helical fragments where cross-links are formed and their loss affects fibril formation and stability. The discrepancy in proMMP-2 activation induced by these collagens indicates different levels of MT1-MMP activation through DDR2. Therefore, these

data suggest that DDR2 might be activated differently depending on the collagen structure.

To address this question, I sought to evaluate the effect of pepsin-extracted PureCol and acid-extracted CellMatrix collagens on DDR2 activation. Those collagens were used to analyse MT1-MMP activation in fibroblasts as well as to induce phosphorylation of DDR2 expressed in HEK293 cells. In addition, I evaluated binding of purified DDR proteins to collagen. For this purpose I created DDR-Fc constructs that consist of the extracellular domains of DDRs (including their collagen-binding site) and are covalently dimerised via cysteine in the Fc tag.

The aim of this part of the thesis is to determine whether cartilage is able to induce proMMP-2 and MT1-MMP activation in RASF, and if DDR2 is also involved in this process. Moreover, as a recent study demonstrated that RASF show greater invasion into proteoglycan-depleted cartilage (Miller et al., 2009), I planned to investigate if such cartilage induces higher activation of MMP-2 and MT1-MMP. Because proteoglycans are depleted early in RA, this might provide an important insight into how cartilage structure influences activation of MT1-MMP during disease.

5.2 Results

5.2.1 Differential activation of fibroblasts by PureCol and CellMatrix

In order to examine the effect of different collagen preparations on MT1-MMP activity, collagen films of CellMatrix collagen; a 1:1 mixture of CellMatrix and PureCol; and PureCol collagen were prepared. RASF and skin fibroblasts were seeded on top of the film and cultured in serum-free medium, with or without GM6001, for 2 days. Cell lysates were analysed by Western Blotting and media were collected and subjected to gelatin zymography.

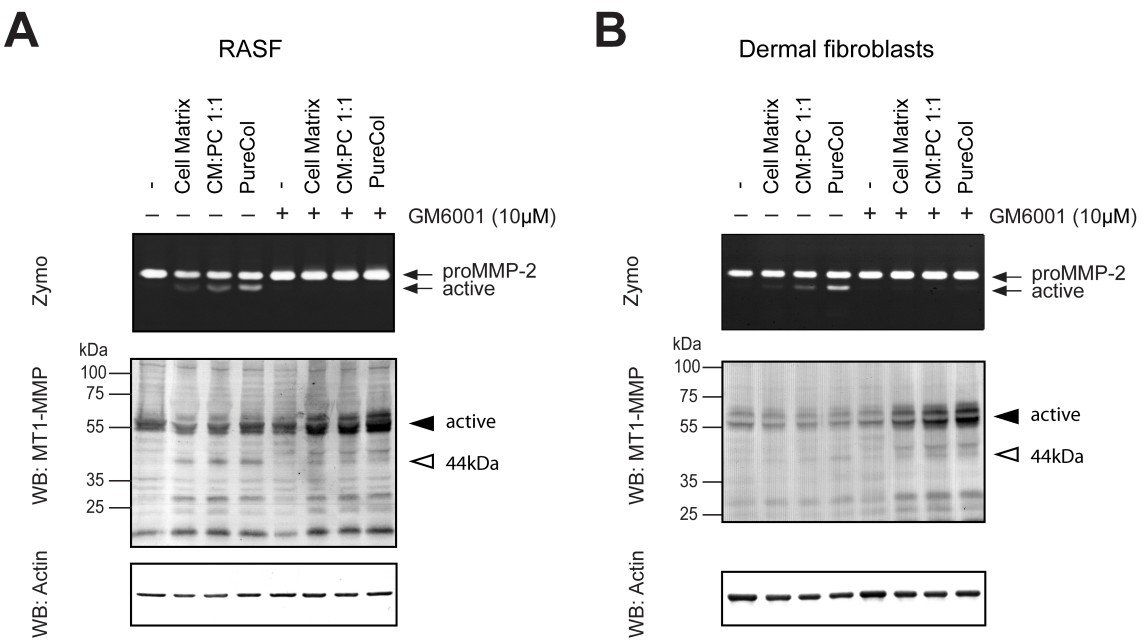

Figure 5.1: Analysis of proMMP-2 activation by CellMatrix and PureCol collagens. RASF **(A)** or dermal fibroblasts **(B)** were cultured either on plastic or on collagen-coated wells. Wells were coated with CellMatrix, PureCol or 1:1 mix of two collagens and incubated 1 h at 37°C before plating cells. All collagens were used at 2.7 mg/ml. Cells were cultured in serum-free medium in the presence (+) or absence (–) of GM6001 at 10 µM. Media were collected after 2 days and analysed by gelatin zymography and cell lysates analysed by Western Blotting. *CM* - CellMatrix, *PC* - PureCol.

Stimulation of fibroblasts with PureCol resulted in much higher levels of active MMP-2 than stimulation with CellMatrix (Figure 5.1). CellMatrix collagen triggered only limited proMMP-2 activation in both cell types. The increase in active MMP-2 appears to be dependent on PureCol concentration as a 1:1 collagen mix resulted in intermediate levels of active enzyme. In addition, PureCol (alone or mixed) induced greater MT1-MMP processing, especially in RASF (Figure 5.1A). In dermal fibroblasts, MT1-MMP processing was only visible in PureCol-treated cells (Figure 5.1B). GM6001 prevents MT1-MMP processing by inhibiting enzyme activity and therefore its addition during cell culture reflects an increase in MT1-MMP expression upon collagen stimulation. The highest MT1-MMP levels were observed in PureCol-treated cells, in the presence of GM6001. The increased MT1-

MMP expression also appeared to be dependent on PureCol concentration and the increase was minimal in CellMatrix-induced cells.

To further characterise the differences in fibroblast activation by these collagens, conditioned media from dermal fibroblasts cultured on CellMatrix and PureCol were analysed by gelatin and casein zymography. Gelatin zymography showed similar results to those reported above, with PureCol inducing higher levels of active MMP-2 than CellMatrix (Figure 5.2A). Interestingly, casein zymography showed a clear increase in a casein-degradative activity in PureCol-treated samples (Figure 5.2B). CellMatrix did not induce an increase in the casein degradation in comparison to non-treated cells. A faint band corresponding in size to active MMP-1 was detected in the conditioned medium from PureCol stimulated samples. This might indicate presence of another activated MMP in addition to MMP-2 in conditioned medium from PureCol-treated cells, confirming that indeed this collagen induces greater fibroblast activation.

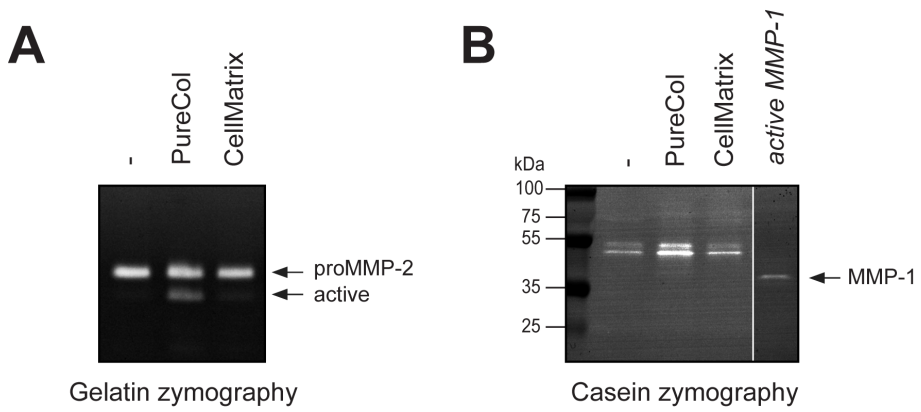

Figure 5.2: Zymography analysis of MMP activity induced by CellMatrix and PureCol collagens. Dermal fibroblasts were cultured on collagen-coated wells in serum-free medium for 2 days. Conditioned media were collected and subjected to gelatin **(A)** and casein **(B)** zymography. For casein zymography, activated recombinant MMP-1 was loaded on a gel alongside samples of conditioned media.

5.2.2 Analysis of collagen-induced DDR2 phosphorylation in HEK293 cells

PureCol induces higher proMMP-2 activation and MT1-MMP expression than CellMatrix, therefore indicating higher activation of the DDR2 receptor and downstream signalling pathways. Therefore, the effect of these two collagens on levels of DDR2 phosphorylation were investigated next. For this purpose, HEK293 cells were transiently transfected with an empty (mock) vector or a DDR2-expressing plasmid. Cells were stimulated by addition of collagen to the culture medium or by incubation on top of 2D collagen. DDR2 was reported to be activated by collagens present in the medium at concentrations as low as 10 µg/ml (Vogel et al., 1997). Here, I used 100 µg/ml of collagen as this concentration induced proMMP-2 activation in fibroblasts. Cells were incubated with collagens for 1 h and lysed afterwards.

Total cell lysates were subjected to Western Blotting and probed for DDR2, actin and phosphotyrosine (pY) to detect DDR2 phosphorylation (Figure 5.3). An analysis of pY Western blots showed that collagen induces phosphorylation of a 130 kDa protein in DDR2-expressing cells. No phosphorylation was detected in the absence of collagen or in mock transfected cells. The above data indicate that the 130 kDa protein corresponds to phosphorylated DDR2. As shown on Figure 5.3, PureCol induced higher levels of DDR2 phosphorylation than CellMatrix collagen. Furthermore, phosphorylation was also higher for cells incubated on 2D PureCol than when PureCol was present in the medium. A 1:1 mix of both collagens induced intermediate levels of phosphorylated DDR2. Interestingly, no increase in phosphorylation was observed in cells cultured on 2D CellMatrix, however addition of this collagen into the medium resulted in a slightly elevated phosphorylation.

On a Western blot, overexpressed DDR2 is detected as three differently glycosylated proteins of ~130 kDa size. The highest molecular weight form most likely corresponds to the mature and fully glycosylated DDR2, which is present on the cell surface (Blissett et al., 2009). Strikingly, incubation of DDR2-overexpressing cells

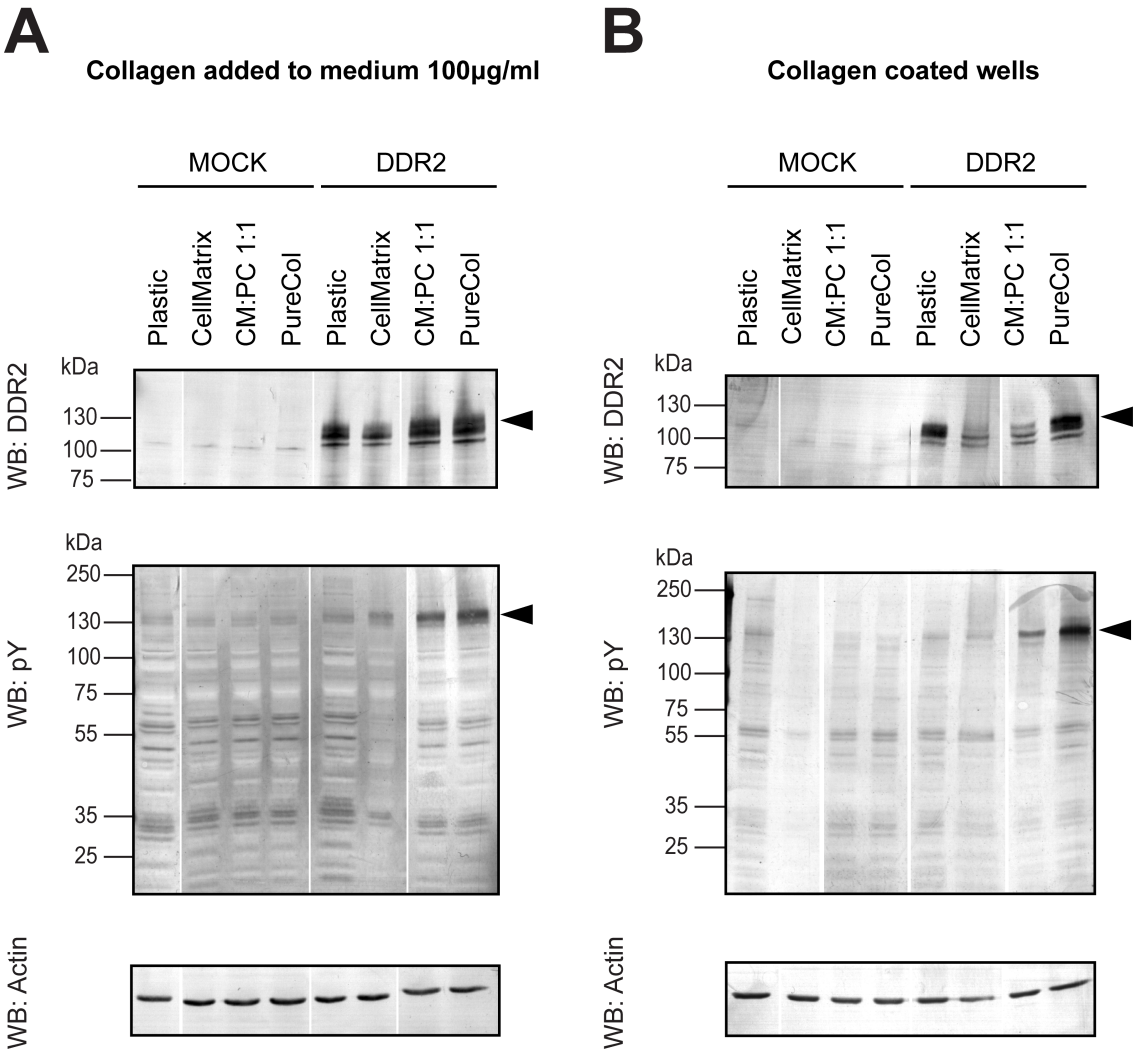

Figure 5.3: Analysis of DDR2 phosphorylation by CellMatrix and PureCol. HEK293 cells were transiently transfected with mock or DDR2 expressing vector. After 2 days, collagens were added into the medium at 100 µg/ml **(A)** or cells were cultured on collagen-coated wells **(B)**. Cells were incubated with collagens for 1 h and lysed. Cell lysates were analysed by Western Blotting using anti-DDR2, anti-phosphotyrosine (anti-pY) and anti-actin antibodies. *CM* - CellMatrix, *PC* - PureCol.

on CellMatrix resulted in an almost complete disappearance of the highest molecular weight species of DDR2 (Figure 5.3B). Levels of lower molecular weight forms of DDR2 remained unchanged. In samples where CellMatrix was added into the medium, loss of mature DDR2 was less pronounced (Figure 5.3A). No changes in DDR2 protein levels were observed in PureCol stimulated cells, however cells plated on 1:1 collagen mix show a lower amount of mature DDR2.

Collectively, these results indicate that in contrast to PureCol, stimulation of cells with CellMatrix collagen leads to loss of the cell surface DDR2 and diminished DDR2 signalling. Furthermore, DDR2 phosphorylation in the collagen-treated cells appears to correlate with levels of the cell surface DDR2.

5.2.3 Characterisation of DDR2 ectodomain shedding

Observed changes in the amount of DDR2 in the cell lysates occurred during a short incubation time and affected only mature and fully glycosylated DDR2. Therefore it is unlikely that the collagen stimulation significantly changed DDR2 expression during this time. It has been shown that collagen induces shedding of DDR1 ectodomain, resulting in accumulation of a 60 kDa fragment in the medium, however no shedding of DDR2 has been reported yet (Fu et al., 2013; Slack et al., 2006; Vogel, 2002). DDRs are closely related proteins and it is possible that DDR2 ectodomain is also cleaved in the presence of collagen, resulting in a loss of the extracellular fragment. To establish whether DDR2 shedding occurs upon collagen stimulation, I analysed the conditioned culture medium for the presence of ~60 kDa DDR2 ectodomain. HEK293 cells were transiently transfected with either mock or DDR2 expression vector. Next, cells were incubated on 2D collagen for 1 h, with or without GM6001 (10 µM) or dasatinib (100 nM) in the medium. Cell lysates were collected and subjected to Western blot analysis. Conditioned serum-free media were collected, spun down to remove the cell debris and incubated with trichloroacetic acid (TCA; 10% v/v of total volume) at 4°C for 18 h. Protein precip-

itates were resuspended in 30 µl of a 1 × sample buffer. 15 µl of a total precipitate fraction was analysed by Western Blotting to detect the shed form of DDR2. As demonstrated on Figure 5.4, I was unable to identify the shed form in any of the TCA precipitates, despite the fact that CellMatrix induced loss of mature DDR2. Moreover, the observed loss of DDR was not due to shedding by metalloproteinases as GM6001 did not block it. Dasatinib completely abrogated phosphorylation of DDR2 by collagens, but it did not prevent DDR2 loss. Analysis of pY Western blot showed an additional phosphorylated band in CellMatrix-stimulated cells in the presence of GM6001, but the identity of this protein is unknown.

Because I was not able to identify the shed form of DDR2 in the culture medium during a 1 h incubation time, I tried to detect this ectodomain at longer time points after collagen stimulation. HEK293-EBNA cells stably expressing DDR2 were used to ensure an equal expression of DDR2 in all cells. Cells were cultured on top of collagen-coated wells for the indicated times. Culture media were collected for TCA precipitation. Precipitation was carried out overnight at 4°C and precipitates were resuspended in 15 µl of 1 × sample buffer, and subjected to Western Blotting.

As illustrated on Figure 5.5, ~60 kDa ectodomain of DDR2 was detected in all TCA precipitation fractions, even in samples not stimulated with collagen. Shed form accumulated in the medium and its highest levels were observed at the 8 h final time point. Although PureCol appears to induce slightly higher shedding of DDR2, no major differences were observed between samples incubated in the presence or absence of collagen. The data indicate that DDR2 undergoes constitutive shedding under these conditions. CellMatrix did not increase shedding and no increase in the amount of shed form was observed in comparison to unstimulated samples, despite the fact that mature DDR2 was absent in cell lysates.

To identify the sheddase activity responsible for the DDR2 cleavage, cells were stimulated with collagen for 8 h in the presence of the metalloproteinase inhibitor, marimastat. Marimastat is a broad-spectrum inhibitor of metalloproteinases, including MMPs as well as members of ADAMTS and ADAM families. HEK293-

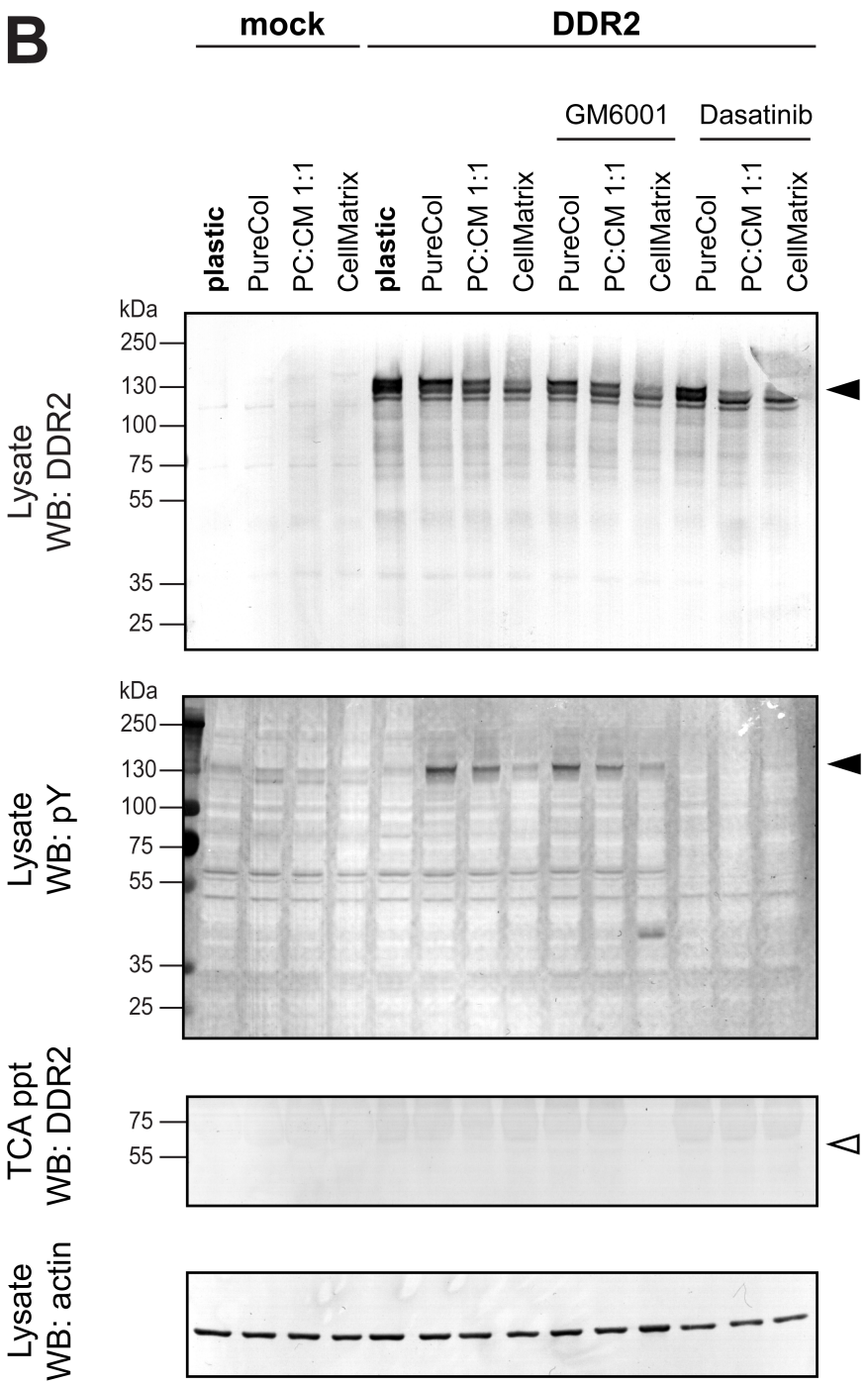

Figure 5.4: Collagen binding but not signalling induces loss of cell surface DDR2. HEK293 cells were transiently transfected with mock or DDR2 expressing vector. Cells were incubated on collagen-coated wells for 1 h. GM6001 (10 µM) or dasatinib (100 nM) were supplemented into serum-free medium as indicated. Cell lysates were analysed by Western Blotting and probed for DDR2, pY and actin. Medium was incubated overnight with TCA at 4°C to precipitate proteins. Precipitates (*ppt*) were resuspended in 30 µl of 1 × sample buffer, of which 15 µl were analysed by Western Blotting. To detect shed DDR2 in the precipitated fraction, Western blot membranes were probed using an antibody recognising ECD of DDR2. Black arrowhead indicates glycosylated DDR2, whereas open arrowhead indicates 60 kDa marker of shed form of DDR2.

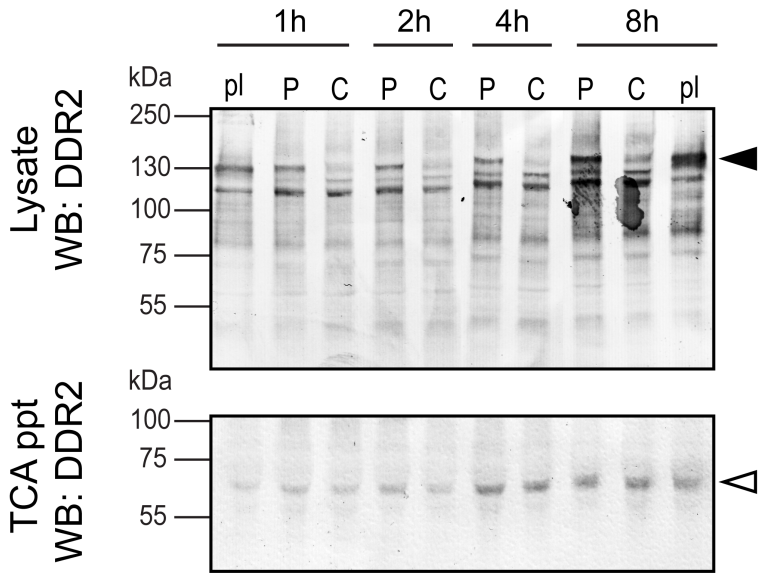

Figure 5.5: Time course analysis of DDR2 shedding. HEK293-EBNA cells stably expressing DDR2 were cultured on plastic or collagen film for the indicated time (1–8 h). Wells were coated with 2.7mg/ml PureCol or CellMatrix. Afterwards, cell lysates were analysed by Western Blotting and culture media were TCA precipitated overnight at 4°C. Protein precipitates *(ppt)* were resuspended in 15 µl of 1 × sample buffer, all of which was subjected to Western Blotting. Black arrowhead indicates glycosylated DDR2, whereas open arrowhead indicates 60 kDa shed form of DDR2. *pl* - plastic; *P* - PureCol;*C* - CellMatrix.

EBNA cells expressing DDR2 were incubated on CellMatrix or PureCol-coated wells for 8 h in the absence or presence of marimastat, dasatinib or DMSO as a control vehicle (Figure 5.6). Cell lysates were collected and subjected to Western Blotting. Serum-free media were TCA precipitated and analysed by Western Blotting for the presence of DDR2 ectodomain.

As previously shown, dasatinib did not prevent loss of DDR2 from the cell surface. It also did not prevent shedding of DDR2. Marimastat inhibited accumulation of the 60 kDa shed fragment of DDR2 in collagen-treated cells (both PureCol and CellMatrix). However, marimastat did not prevent loss of full length DDR2 in cells treated with CellMatrix.

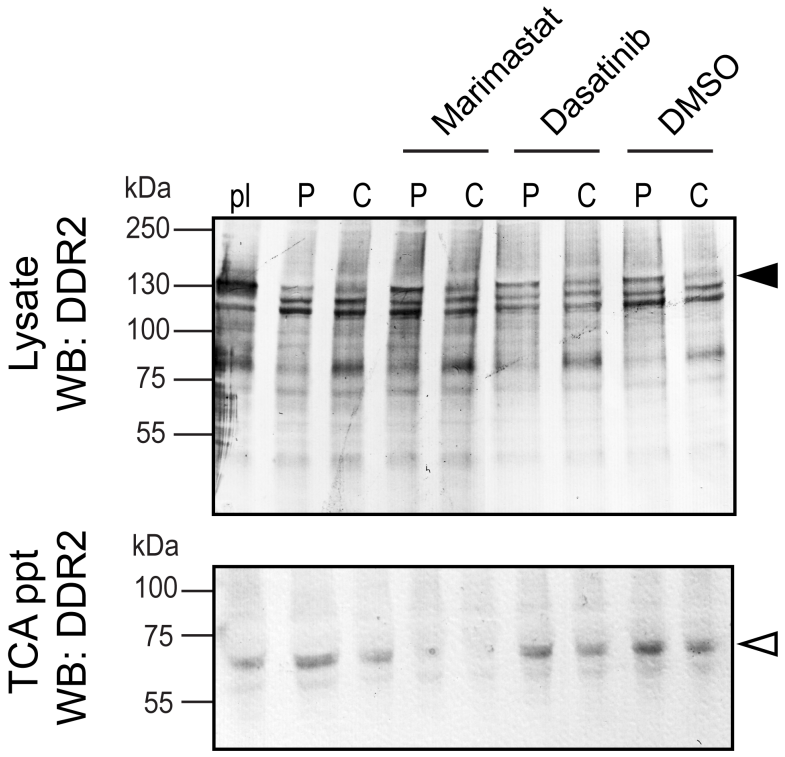

Figure 5.6: Marimastat prevents DDR2 shedding. HEK293-EBNA cells stably expressing DDR2 were cultured on collagen-coated wells for 8 h. Serum-free medium was supplemented with 20 µM marimastat or 100 nM dasatinib as indicated. DMSO was used as a solvent control. Cell lysates were analysed by Western Blotting. Media were TCA precipitated overnight at 4°C and precipitates *(ppt)* resuspended in 15 µl of 1 × sample buffer, all of which was subjected to Western Blotting. Black arrowhead indicates glycosylated DDR2, whereas open arrowhead indicates 60 kDa shed form of DDR2. *pl* - plastic; *P* - PureCol; *C* - CellMatrix.

5.2.4 Collagen induces changes in DDR2 levels in fibroblasts

I have demonstrated that in HEK293 cells overexpressing DDR2, the receptor undergoes constitutive shedding and incubation with CellMatrix also results in changes in the amount of fully glycosylated DDR2 in cell lysates. To confirm these findings in primary cells, I cultured RASF and dermal fibroblasts on 2D PureCol and CellMatrix. After 4 hours of incubation, cells were lysed and serum-free media were TCA precipitated and subjected to Western Blotting (Figure 5.7).

In agreement with results from DDR2 overexpression in HEK293 cells, CellMatrix resulted in significant loss of glycosylated DDR2 in both synovial and dermal fibroblasts. PureCol also initiated loss of DDR2, albeit less efficiently in comparison to the CellMatrix collagen. However, no shed form of DDR2 was detected in TCA precipitates of medium after 4 hour incubation or even longer incubation times (up to 48 h).

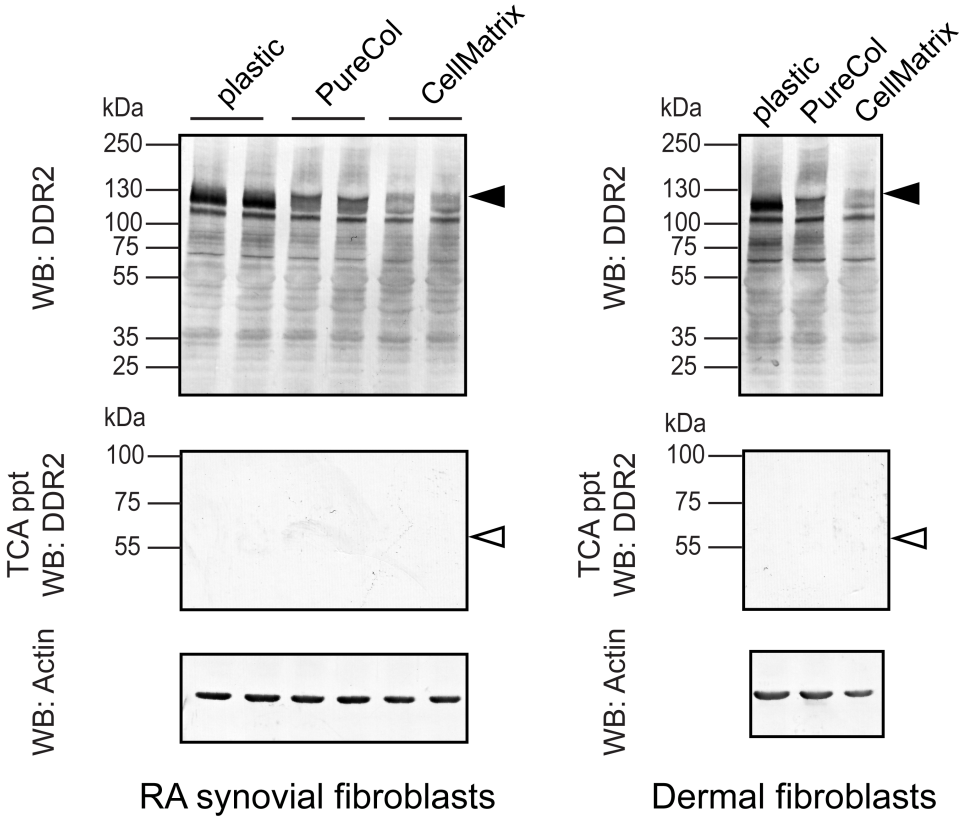

Figure 5.7: Comparison of effect of CellMatrix and PureCol on DDR2 levels in fibroblasts. RASF and dermal fibroblasts were incubated on collagen-coated wells for 4 hours. Afterwards cells lysates were analysed by Western Blotting. Culture media were TCA precipitated overnight at 4°C. Protein precipitates were resuspended in 15 µl of 1 × sample buffer and all of which was analysed by Western Blotting. Black arrowhead indicates glycosylated DDR2, whereas open arrowhead indicates 60 kDa marker of shed form of DDR2.

5.2.5 Expression and purification of recombinant DDR-Fc proteins

To determine whether the discrepancy in DDR2 activation by CellMatrix and PureCol is a result of differences in collagen recognition, I analysed binding of DDRs to these collagens. For this purpose chimeric, recombinant DDR-Fc proteins were created, consisting of ECD of DDRs tagged with rabbit IgG Fc region. In total, five constructs were made: DDR1-Fc, DDR2-Fc and non-binding DDR1-W53A-Fc, DDR1-R105A-Fc and DDR2-W52A-Fc as negative controls. DDR1 constructs were made in order to compare collagen binding properties of DDR1 and DDR2. Similar DDR constructs have previously been successfully used in several studies to determine the specificity of DDR1 and DDR2 binding to different types of collagen (Carafoli et al., 2009; Leitinger, 2003; Leitinger and Kwan, 2006; Leitinger et al., 2004; Xu et al., 2010).

Non-binding constructs have the indicated residues mutated to alanine: W^{53} and R^{105} in DDR1 and W^{52} in DDR2. These amino acids were selected based on data from the crystal structure of DDR2 discoidin domain bound to collagenous peptide published by Carafoli et al. (2009). The selected amino acids are conserved in DDR1 and DDR2 and form part of a collagen binding pocket. W^{52} in DDR2 is critical for collagen binding and its mutation to alanine abrogates binding to collagen and receptor activation (Carafoli et al., 2009). In a study by Abdulhussein et al. (2004), mutation of the corresponding W^{53} in DDR1 did not block activation of the receptor, therefore an additional DDR1-R105A-Fc construct was made, as R^{105} mutation to alanine was reported to disrupt collagen binding.

Figure 5.8 shows schematic representation of DDR-Fc protein constructs used in this study. DDR-Fc proteins comprise ECDs of DDRs, which are tagged at the C-terminus with the Fc fragment of rabbit IgG. Fc tags have been shown not to interfere with binding of DDR fusion constructs to collagen (Xu et al., 2010). ECDs were identified in the UniProt online database and include the first 416 amino acids

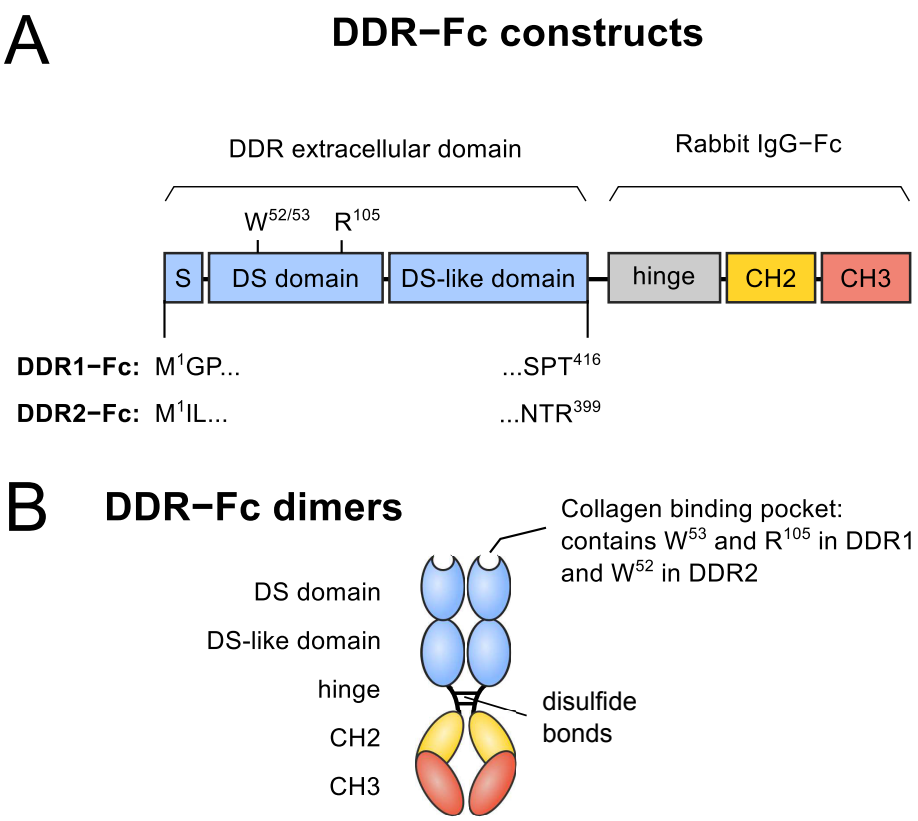

Figure 5.8: Schematic representation of DDR-Fc protein structure. (A) DDR-Fc chimera constructs are comprised of extracellular domains (ECDs) of DDRs linked at their C-terminus to the Fc region of a rabbit IgG. Between DDR ECD and Fc region there is a seven amino acid long spacer. First and last amino acids of DDR ECDs are indicated, as well as crucial W^{52} in DDR2 and W^{53} and R^{105} residues in DDR1 discoidin (DS) domains. **(B)** Upon expression in mammalian cells disulfide bonds are formed in the hinge region of Fc fragment, resulting in a formation of a soluble DDR-Fc dimer. *CH* - constant domain of heavy chain.

for DDR1 (M^1–T^{416}) and the first 398 amino acids for DDR2 (M^1–R^{399}). ECDs comprise the signal sequence, discoidin domain and discoidin-like domain. Fc fragments contain the hinge region, which act as a flexible linker, and two constant domains — CH2 and CH3 (Figure 5.8A). On the cell surface, DDRs are present as constitutive dimers (Abdulhussein et al., 2008; Noordeen et al., 2006). In recombinant DDR-Fc proteins, dimers are ensured by formation of disulfide bonds between two Fc regions (Figure 5.8B). Although the collagen binding mode of DDRs on the cell surface has not been determined yet, it had been demonstrated that DDR-Fc proteins require dimerisation to bind the collagen (Leitinger, 2003).

Figure 5.9 shows the overall strategy for a purification of DDR-Fc proteins. ECDs of DDRs were amplified by PCR from cDNA templates. Mutations were introduced by PCR as described in Materials and Methods (Section 2.12.1). First, ECDs were cloned to the pFc1 vector to introduce an Fc tag. Afterwards DDR-Fc fragments were subcloned into the pCEP4 vector to enable episomal expression in HEK293-EBNA cells. Stable HEK293-EBNA cell lines for each DDR-Fc protein were made. Proteins were expressed into serum-free medium and purified using affinity chromatography, based on a protocol described by Leitinger (2003). Purification steps are presented in Figure 5.10A. Fractions containing the majority of the protein were combined, dialysed against PBS and protein concentration was adjusted to 1 µM.

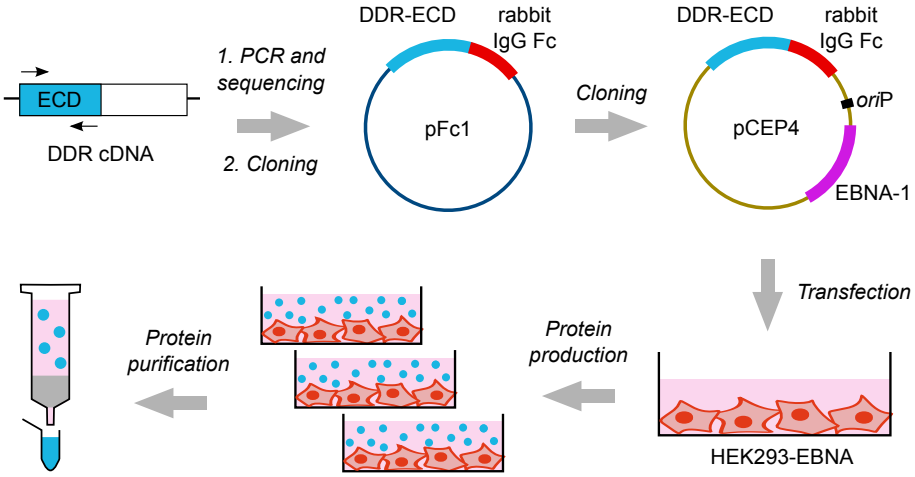

Figure 5.9: Cloning, expression and purification of DDR-Fc proteins. ECDs of DDRs were amplified by PCR, sequenced and cloned into pFc1 vector to introduce a rabbit IgG Fc tag. DDR-ECD-Fc fragments were subcloned into pCEP4 vector, to enable episomal expression of DDR-Fc from HEK293-EBNA. Stably transfected HEK293-EBNA cells secrete soluble DDR-Fc proteins into the medium. Proteins are purified from collected media using affinity chromatography (Protein A Sepharose).

The predicted molecular weight, without a signal peptide, of a DDR1-Fc dimer is 140 kDa and DDR2-Fc dimer is 137.2 kDa, as determined by an online ProtParam tool at ExPASy Bioinformatics Resource Portal. DDR-Fc proteins were purified to

homogeneity as demonstrated by a single band detected by SDS-PAGE analysis (Figure 5.10B). The reactivity of DDR-Fc constructs was confirmed by Western Blotting using anti-(rabbit IgG Fc region) antibodies (Figure 5.11A) as well as antibodies recognising ECDs of DDR1 or DDR2 (Figure 5.11B). DDR-Fc proteins were recognised by both anti-rabbit IgG and anti-DDR antibodies. The dimerisation of DDR-Fc proteins was also confirmed. Samples were resolved on a SDS-PAGE under reducing or non-reducing conditions, using a sample buffer with or without β-Me respectively, and subsequently analysed by Western Blotting. On Western blots DDR-Fc dimers run as a single band of ~200 kDa under non-reducing conditions, whereas under reducing conditions, they run as a single band of ~90 kDa.

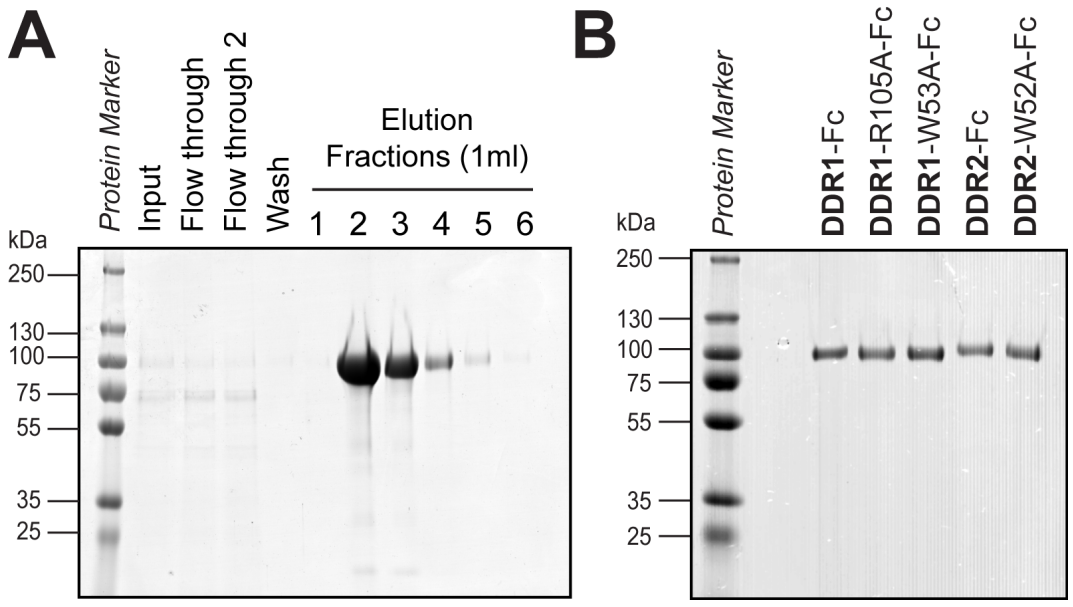

Figure 5.10: Purification of DDR-Fc proteins. **(A)** Culture medium (~200 ml) from HEK293-EBNA stably expressing DDR1-Fc was passed through a Protein A Sepharose affinity chromatography column (0.5 ml). Samples from each purification step (input media, column flow through, PBS wash and elution fractions) were mixed with an equal volume of 2 × sample buffer with β-Me and 20 µl resolved on a 7% SDS-PAGE under reducing conditions. Gels were stained with Coomassie Brilliant Blue-250 and throughly de-stained. **(B)** Purified DDR-Fc proteins were dialysed against PBS and the concentration adjusted to 1 µM. Equal volumes of purified proteins were mixed with 2 × sample buffer with β-Me and resolved on a 7% SDS-PAGE under reducing conditions (420 ng of DDR1 constructs per lane; 412 ng of DDR2 constructs per lane). Afterwards, gels were stained with Coomassie Brilliant Blue-250 and throughly de-stained.

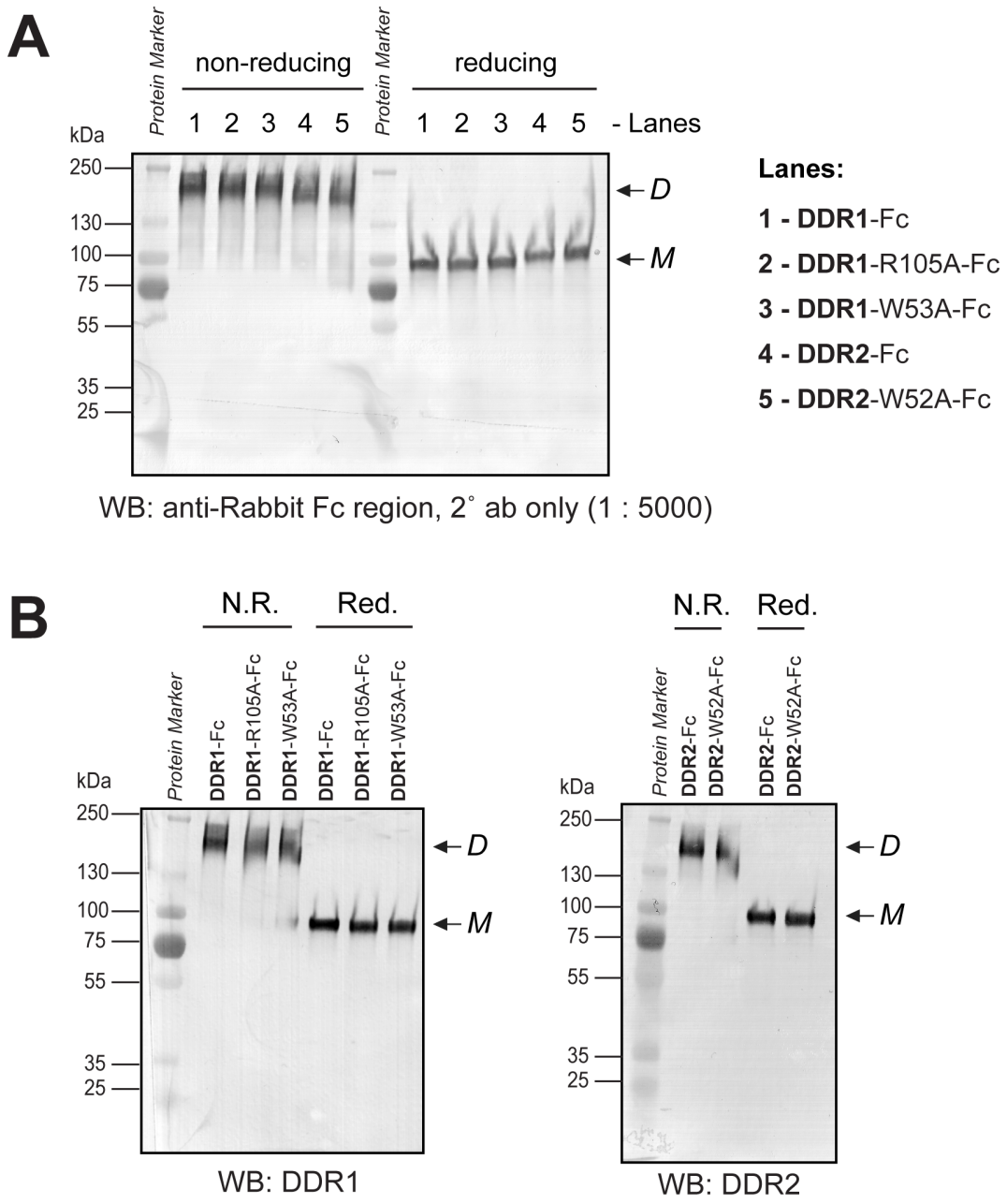

Figure 5.11: Western Blot analysis of purified DDR-Fc proteins. Purified DDR-Fc proteins were analysed by Western Blot using specific antibodies. Samples were resolved by SDS-PAGE under reducing ***(Red.)*** or non-reducing conditions ***(N.R.)***, with or without β-Me in the sample buffer respectively. Under non-reducing conditions samples run as a single ~200 kDa band of dimerised ***(D)*** protein. Under reducing conditions proteins run as a ~90 kDa monomer ***(M)***. **(A)** Membranes were probed only with secondary AP-conjugated anti-(rabbit IgG) antibody at 1:5000 dilution applied for 1 h. This antibody recognised the Fc tag present in all DDR-Fc constructs. 1.5 ng of protein per lane was applied under non-reducing conditions, and 15 ng per lane under reducing conditions. **(B)** Membranes were probed for DDR1 or DDR2 with antibodies recognising their ECDs. Single bands were observed for all samples. 10 ng of proteins were applied per lane.

5.2.6 Solid phase binding assay to detect DDR-Fc binding to immobilised collagen.

The binding of DDR-Fc proteins to the immobilised collagen was analysed by a solid phase binding assay. First, I determined an optimal blocking buffer for DDR-Fc constructs, as a similar DDR1-Fc protein was previously found to exhibit non-specific binding to BSA (Leitinger et al., 2004). Two blocking buffers were compared: 1 mg/ml BSA in PBS-T and 0.05 mg/ml κ-casein in PBS-T. To perform the assay, 96-well plates were coated with 100 µg/ml of CellMatrix overnight at 4°C. Plates were subsequently incubated with blocking buffers for 1 h at room temperature. Next, 50 µl of 250 nM DDR1-Fc or DDR2-Fc diluted in blocking buffers were added to wells and incubated for 3 hours. Binding was detected using HRP-conjugated anti-(rabbit IgG) antibodies, which recognise the Fc fragment of rabbit IgG present in all DDR constructs. A low background signal was detected in samples incubated with an anti-rabbit antibody only (no DDR-Fc protein). Figure 5.12 shows comparison of DDR1-Fc and DDR2-Fc binding to non-coated or collagen-coated wells, blocked with BSA or κ-casein.

Both DDR-Fc constructs showed a specific and strong binding to collagen. In comparison to BSA, blocking with κ-casein resulted in a lower non-specific binding to plastic. Also, a stronger signal was obtained for collagen-coated wells blocked with κ-casein. Because κ-casein produces a higher signal to background ratio, 0.05 mg/ml κ-casein in PBS-T was used as a blocking buffer throughout the study.

Next, I compared binding of DDR-Fc constructs to immobilised CellMatrix and PureCol collagens in a solid phase binding assay. Ten-fold dilutions of DDR-Fc proteins, ranging from 250 nM to 0.025 pM, were prepared in the blocking buffer. Proteins were incubated on 96-well plates, coated with a 100 µg/ml CellMatrix or PureCol. Figure 5.13 illustrates binding of all DDR-Fc constructs to these collagens or plastic.

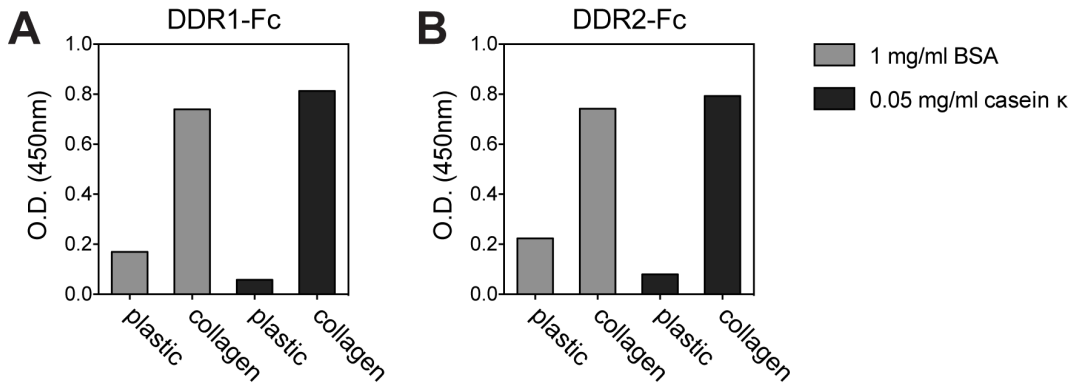

Figure 5.12: Optimisation of a solid phase binding assay for DDR-Fc binding to collagen. 96-well plates coated with 100 µg/ml of CellMatrix collagen were blocked with either 1 mg/ml BSA in PBS-T or 0.05 mg/ml κ-casein in PBS-T for 1 h at room temperature. DDR1-Fc and DDR-2 Fc were diluted in a corresponding blocking solution to 250 nM and incubated on plates for 3 h. A HRP-conjugated anti-(rabbit IgG) antibody (1:3000) was used to detect bound DDR-Fc proteins. The reaction was developed by addition of a TMB substrate and stopped by H_2SO_4. Plates were read at 450 nm. Assay was performed in duplicate.

Almost no binding to plastic was detected for any of the constructs. DDR1-Fc and DDR2-Fc showed a high affinity, dose-dependent and saturable binding to both immobilised collagens. The maximal binding was similar for all collagens. However, some differences in the binding affinity were detected. DDR1-Fc exhibited a half-maximum binding to PureCol at ~0.5 nM and to CellMatrix at ~6 nM. This indicates that DDR1-Fc has a higher affinity for PureCol than for CellMatrix collagen. In contrast to the DDR1 construct, DDR2-Fc exhibited a somewhat higher affinity for CellMatrix rather than PureCol. Half-maximal binding of DDR2-Fc to PureCol was ~2.5 nM and to CellMatrix was ~1.3 nM. DDR1-R105A-Fc, DDR1-W52A-Fc and DDR2-W53A-Fc constructs did not show binding to collagen at lower concentrations, but show some binding at 250 nM.

This assay provides invaluable information about the specificity of DDR binding, however it does not accurately represent the structure of the collagen matrix in a physiological state. In order to evaluate binding of DDRs to collagen gels, I thus modified the solid phase binding assay. A small volume, 10 µl, of 1.5 mg/ml collagen solution was placed as a drop in the centre of 96-wells and incubated at 37°C to

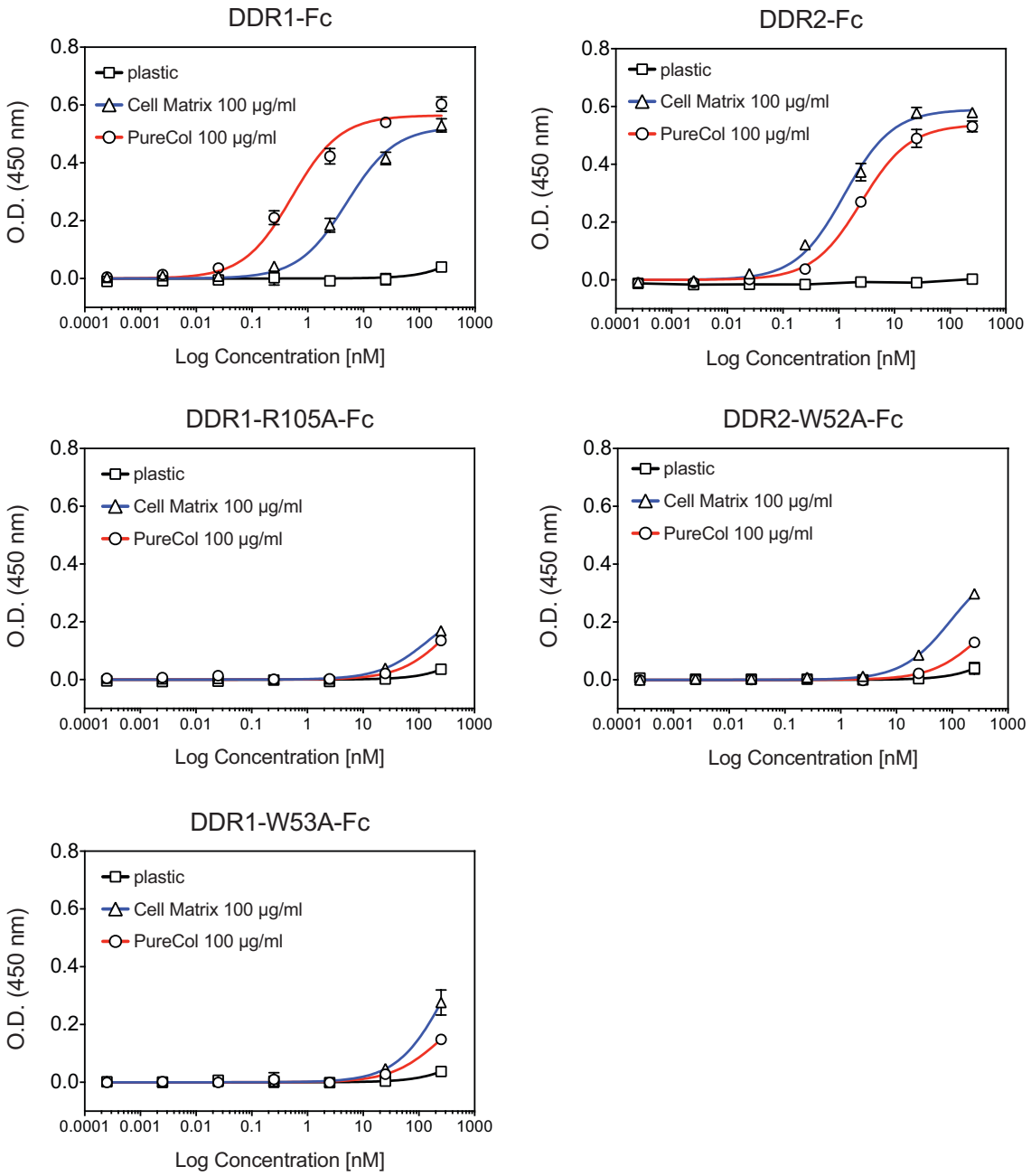

Figure 5.13: Solid phase binding assay for analysis of DDR-Fc protein binding to immobilised collagen. The binding of individual DDR-Fc constructs to immobilised PureCol and CellMatrix was analysed by a solid phase binding assay. 96-well plates were coated with collagens at 100 µg/ml. Plates were blocked with 0.05 mg/ml κ-casein in PBS-T for 1 h. Ten-fold dilutions of DDR-Fc proteins in blocking buffer were incubated on plates for 3 h. All assays were performed in triplicate. Plates were read at 450 nm and data shown as mean ± SD.

initiate fibril formation. The binding of DDR-Fc to this collagen was subsequently analysed by a solid phase binding assay, as previously described. Unfortunately, this approach resulted in a high background signal stemming from the non-specific binding of the detection antibody to the collagen matrix. I found that a 10 µl drop of collagen applied in the centre of the well resulted in less non-specific binding than an evenly coated well with the same volume of collagen (by applying 50 µl of collagen solution and removing 40 µl). Figure 5.14 demonstrates the levels of background signal generated by the non-specific antibody binding in relation to the varying CellMatrix concentrations. All HRP-conjugated antibodies available in our lab showed similar non-specific binding to high concentration collagen gels. Several measures were taken to reduce the background signal, including testing different blocking solutions (1 mg/ml BSA, 10% dry-skimmed milk, 10% goat serum, 10% FBS) or extensive washing with a high salt buffers, but with no success.

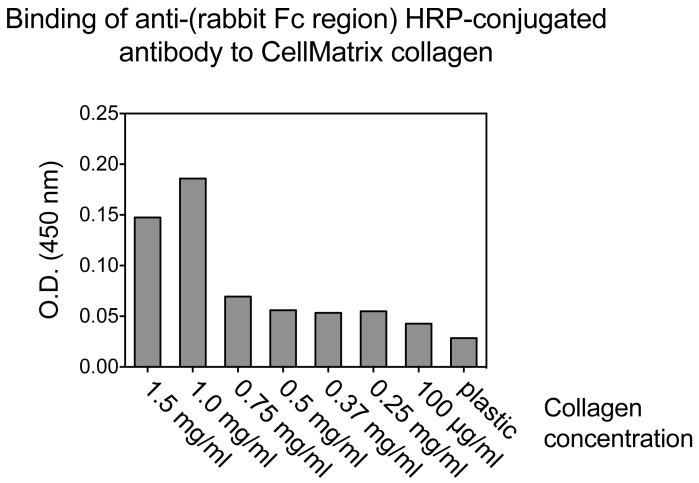

Figure 5.14: Non-specific antibody binding to fibrillar collagen. The binding of an anti-(rabbit IgG) antibody to CellMatrix collagen was analysed by a solid phase binding assay in the absence of DDR-Fc protein. This antibody is used to detect DDR-Fc proteins bound to the collagen, however it displays a non-specific binding to collagen gels. CellMatrix collagen was neutralised and diluted to the indicated concentrations in PBS-T, 10 µl of which were placed in the middle of 96-well plates and incubated at 37°C for 1 h. A sample of 100 µg/ml collagen immobilised at 4°C was also included. Afterwards plates were blocked in 0.05 mg/ml κ-casein for 1 h and incubated for 1 h with an anti-(rabbit IgG) diluted 1:3000 in a blocking buffer. Plates were developed as previously described and read at 450 nm. Assay was performed in duplicate.

The highest collagen concentration that yields a relatively low background signal is 0.75 mg/ml collagen, therefore I decided to use this concentration in a solid phase binding assay. CellMatrix collagen was first neutralised and then diluted to 0.75 mg/ml in PBS. Drops of 10 µl of collagen solution were placed in the centre of 96-well plates and incubated at 37°C for 1 h to initiate fibril formation. Afterwards, a solid phase binding assay was carried out as previously described. Ten-fold dilutions of DDR-Fc proteins, ranging from 250 nM to 0.025 pM, were prepared in a blocking buffer and incubated with collagen for 3 hours.

Results of the DDR-Fc construct binding to the fibrillar CellMatrix collagen are illustrated in Figure 5.15. A dose-dependent, specific and saturable binding was detected for DDR1-Fc and DDR2-Fc. DDR1-R105A-Fc and DDR1-W53A-Fc did not show dose-dependent binding, and detected signals showed high deviations. DDR2-W52A-Fc binding to collagen was largely absent. This confirms specific binding of DDR1-Fc and DDR2-Fc. Figure 5.15 indicates that DDR2-Fc binds more to CellMatrix gel than DDR1-Fc, as it shows higher maximal binding. Moreover, both constructs show high affinity binding, with a half-maximal binding within a subnanomolar range (~0.8 nM for DDR1-Fc, and ~0.1 nM for DDR2-Fc).

Next, I analysed binding of DDR2-Fc to CellMatrix as well as PureCol gels using the same assay. In order to further reduce the background signal, collagens were used at 0.05 mg/ml. Ten-fold dilutions of DDR-Fc proteins, ranging from 500 nM to 0.05 pM, were prepared in blocking buffer and incubated with collagen for 3 hours. Afterwards, the solid phase binding assay was carried out as previously described and results are shown in Figure 5.16. DDR2-Fc binds to both collagens, however there is much more variation in binding to PureCol. Moreover, DDR2-Fc exhibits higher maximal binding to CellMatrix than to PureCol. The half-maximal binding is nearly identical for the two collagens and is within subnanomolar range (~0.35 nM).

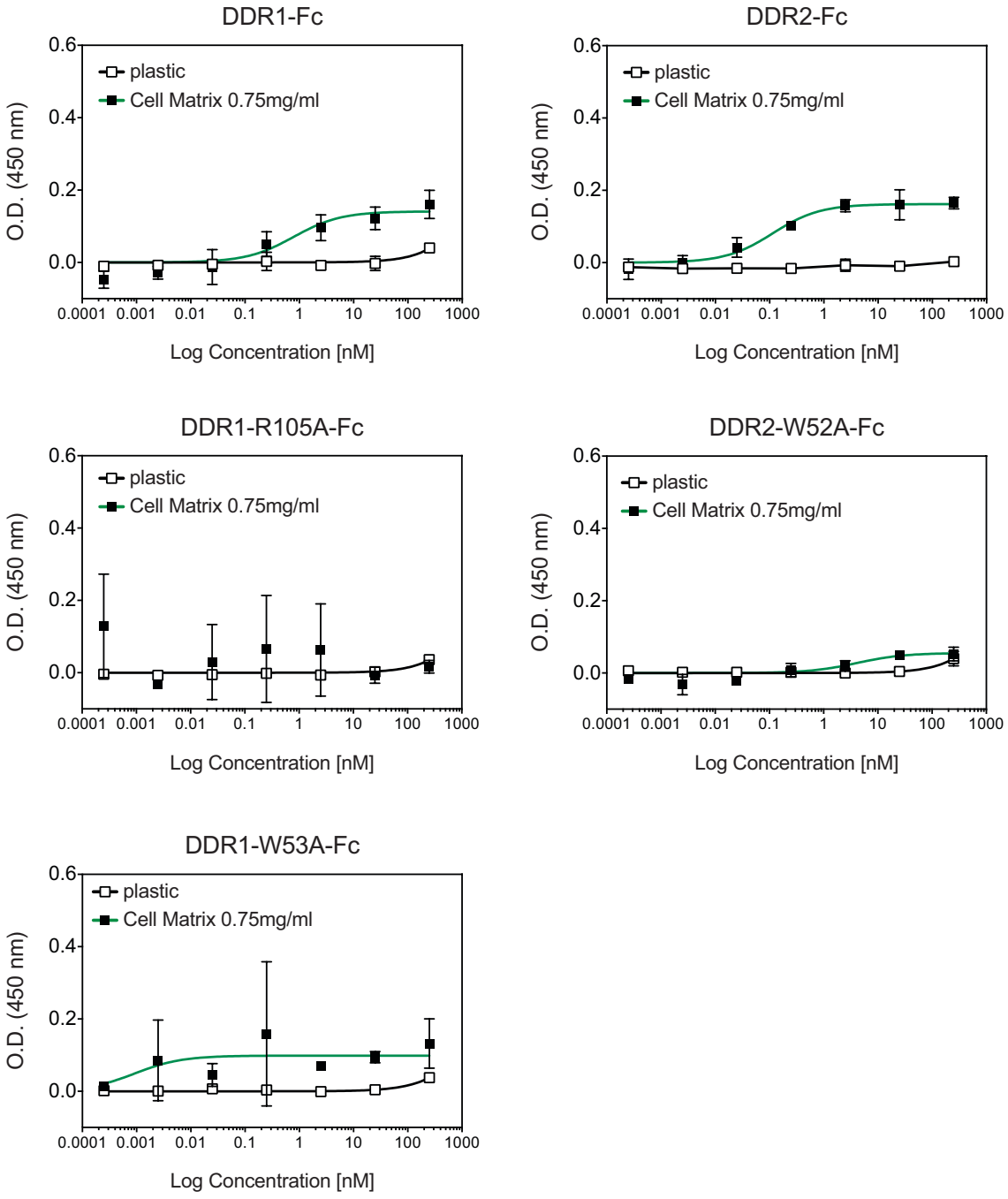

Figure 5.15: Solid phase binding assay for analysis of DDR-Fc protein binding to the CellMatrix collagen gel. Binding of individual DDR-Fc constructs to fibrillar collagen was analysed by a solid phase binding assay. CellMatrix collagen was neutralised and diluted to 0.75 mg/ml in PBS. 10 µl of collagen was placed in a centre of 96-wells and incubated at 37°C for 1 h to initiate collagen fibrillogenesis. Plates were blocked with 0.05 mg/ml κ-casein in PBS-T for 1 h. Ten-fold dilutions of DDR-Fc proteins in blocking buffer were incubated on plates for 3 h. All assays were performed in triplicate. Plates were read at 450 nm and data shown as mean ± SD.

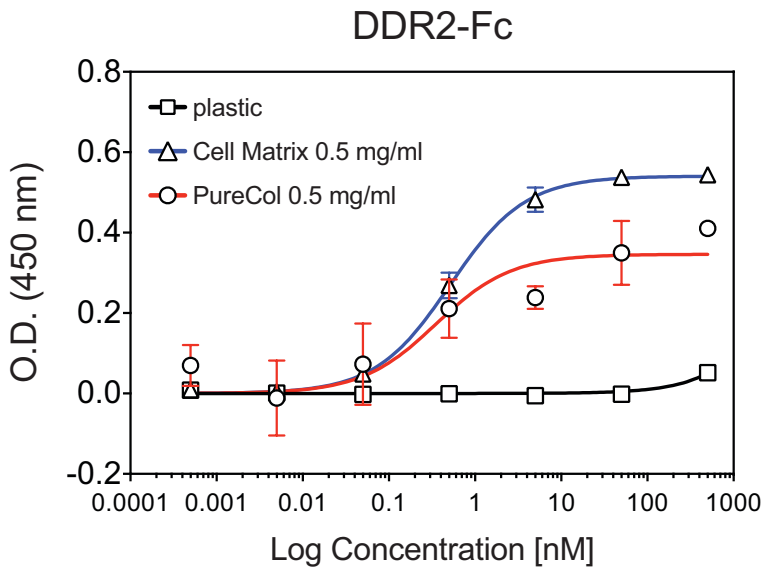

Figure 5.16: Analysis of a DDR2-Fc binding to fibrillar CellMatrix and PureCol. The binding of DDR2-Fc to fibrillar CellMatrix and PureCol was analysed by a solid phase binding assay. 10 µl of 0.5 mg/ml collagens were placed in the centre of 96-well plates and incubated at 37°C for 1 h to induce fibrillogenesis. Plates were blocked in 0.05 mg/ml of κ-casein in PBS-T and incubated with ten-fold dilutions of DDR2-Fc in a blocking buffer for 3 h. Plates were read at 450 nm. Assay was performed in triplicate. Data are represented as mean ± SD.

5.2.7 Analysis of DDR-Fc binding to collagen gel

In addition to the solid phase binding assay, the binding of DDR-Fc constructs to fibrillar collagen was confirmed by Western blot analysis. DDR-Fc proteins were incubated with CellMatrix or 1:1 mix of CellMatrix and PureCol. 10 µl of 1.5 mg/ml collagen were placed in the centre of 96-well plates and incubated for 1 h at 37°C to induce fibrillogenesis. In order to prevent non-specific binding, some collagen samples were air-dried and re-hydrated in a blocking solution before DDR-Fc proteins were applied. Plates were blocked with 0.05 mg/ml κ-casein for 1 h. DDR-Fc constructs were diluted in blocking buffer and incubated on collagen for 3 hours. Afterwards samples were washed in PBS-T for 1 h or 18 h at room temperature.

Samples were lysed in a 2 × sample buffer and analysed by Western Blotting. The results are represented in Figure 5.17. Similar results were obtained for fibrillar and re-hydrated fibrillar collagens after an overnight wash, indicating comparable

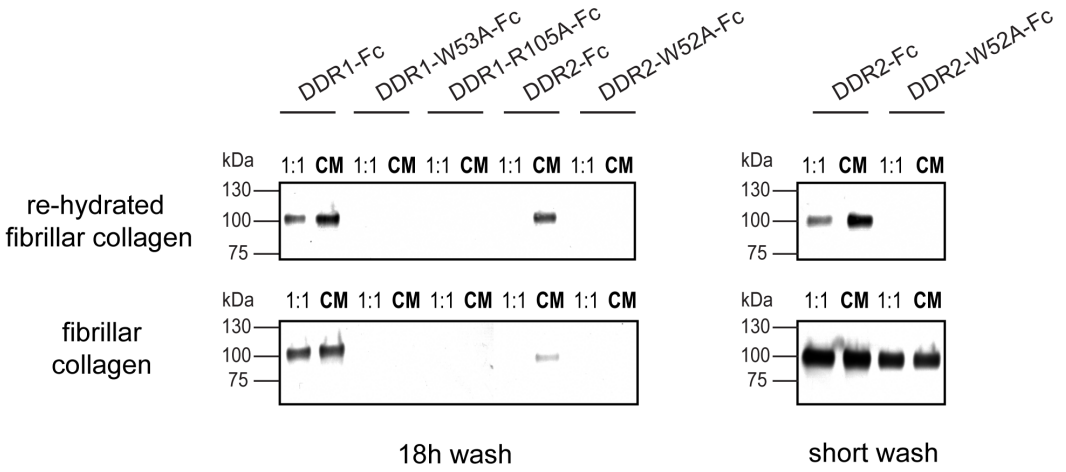

Figure 5.17: Detection of DDR-Fc binding to fibrillar collagen by Western Blotting. CellMatrix (CM) or a 1:1 mix of CellMatrix and PureCol were neutralised and diluted to 1.5 mg/ml in PBS. 10 µl of collagen solution was placed in the centre of a 96-well and incubated for 1 h at 37°C to induce fibril formation. A subset of collagen samples was air-dried for 18 h at room temperature. All samples were incubated with 0.05 mg/ml κ-casein in PBS-T as a blocking buffer for 1 h at room temperature. Air-dried collagen re-hydrated during the incubation. DDR-Fc constructs were diluted to 250 nM in blocking solution and incubated on collagen for 3 h. Afterwards samples were washed several times in PBS-T for 1 h (short wash) or for 18 h. Samples were lysed in 2 × sample buffer, boiled and subjected to Western Blotting. Membranes were probed for anti-(rabbit IgG Fc region) antibody.

binding properties of both collagen preparations. In samples that were washed in PBS-T only for 1 h, re-hydrated collagen shows more specific binding. The negative control DDR2-W52A-Fc construct did not bind to re-hydrated collagens after 1 h of washing, however a pronounced binding of this construct was detected to fibrillar collagen. In general, DDR2-Fc was found to bind more to the CellMatrix than to the mix of two collagens. In addition, no binding to mixed collagen was detected after an overnight wash. DDR1-Fc also showed higher binding to CellMatrix, however noticeable binding was detected for the collagen mix as well. No binding of DDR1-R105A-Fc, DDR1-W53A-Fc and DDR2-W52A-Fc to collagen was detected after overnight washing in PBS-T, indicating specific binding of DDR1-Fc and DDR2-Fc.

In summary, DDR2 shows higher affinity binding to CellMatrix collagen than to PureCol, although the latter induces greater DDR2 activation. Results were confirmed using solid phase binding assay using immobilised collagen as well as 3D collagen gels.

5.2.8 Role of DDR2 in cartilage-induced proMMP-2 activation

So far, I have shown that collagen stimulation, with both collagen type I and II, activates MT1-MMP and induces MMP-2 processing. In order to determine whether cartilage also induces MT1-MMP activation, RASF were attached to bovine cartilage explants and analysed for proMMP-2 activation. Bovine nasal septum cartilage was frozen and thawed three times to kill chondrocytes. Cartilage explants were then cut into $3 \times 5 \times 10\,\text{mm}$ pieces, washed with 10% FBS DMEM and placed in a 24-well plate. Approximately 1.5×10^5 RASF were seeded on top of the cartilage in 15 µl for 3–4 h to allow cells to attach to the cartilage matrix. Then cartilage was transferred to a new well using sterile forceps and serum-free DMEM was added to cover the cartilage (~700 µl). The same number of cells was seeded in an empty well as a control. An equal volume of medium was added to all wells, including those from which cartilage had been transferred, to allow any unattached cells to grow and therefore estimate how many cells remained attached to the cartilage.

Figure 5.18A shows images of bovine cartilage explants that were incubated with and without cells. RASF are clearly visible attached to the cartilage matrix. Zymography analysis of conditioned medium from RASF cultured in the presence of cartilage shows proMMP-2 activation, which is inhibited by GM6001 (Figure 5.18B). Moreover, cartilage also induces high expression of MT1-MMP, as observed in cells treated with GM6001. It can be concluded that cartilage matrix indeed activates MT1-MMP, increases it expression and promotes MMP-2 activation.

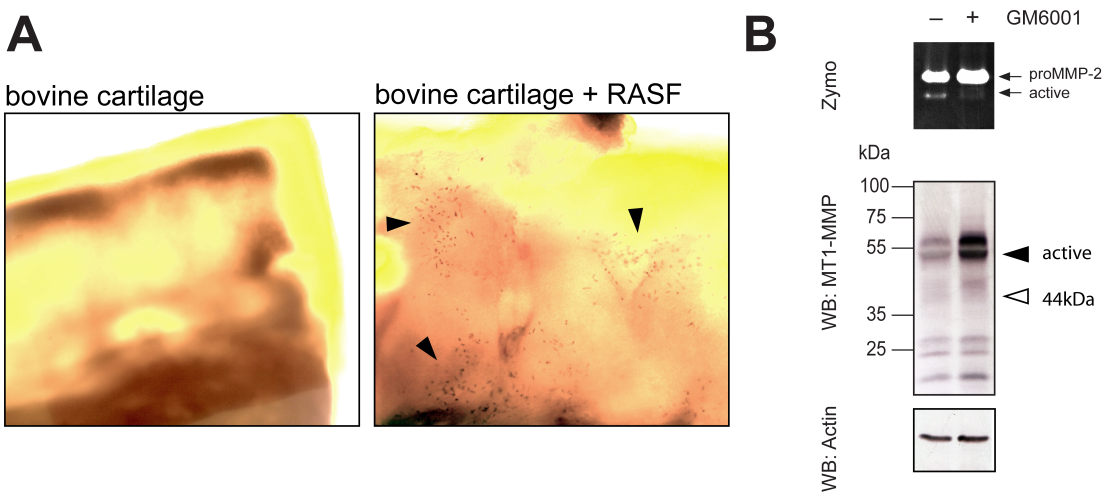

Figure 5.18: Cartilage induces activation of proMMP-2. RASF were applied on top of cartilage fragments in 15 µl of 10% FBS DMEM for 3–4 hours, cartilage transferred to new well, overlaid with serum-free medium and cultured for further 3 days. **(A)** Images of RASF attached to bovine cartilage explants. Images were taken at 4 ×. Areas where cells attached to cartilage are indicated by arrow heads. **(B)** Zymography analysis of cultured medium and Western Blots of MT1-MMP and actin of cell lysates from cells attached to cartilage. GM6001 was added at 20 µM.

Next, I investigated whether removal of proteoglycans from the tissue results in different RASF activation. As reported previously, RASF invasion into cartilage explants from which proteoglycans has been removed is greater than into intact cartilage (Miller et al., 2009). Because MT1-MMP is considered to be the collagenase that mediates RASF invasion, we thought that proteoglycan-depleted cartilage might provide greater stimuli for MT1-MMP activation. Furthermore, I examined if cartilage-dependent activation of MMP-2 is mediated by DDR2.

To remove proteoglycans, cartilage explants were incubated with trypsin at 100 µg/ml for 18 h followed by incubation with soybean trypsin inhibitor at 200 µg/ml for 24 h. Trypsin is able to remove proteoglycans from the cartilage, however it does not degrade collagen. Before plating cells, untreated and trypsin-digested cartilage pieces were washed several times with 10% FBS DMEM. RASF transfected with siDDR2 or siNT were attached to cartilage explants for 4 h as previously described. Afterwards, explants with attached cells were transferred to another culture well, overlaid with an equal volume of serum-free medium and cultured for further 4 days.

Samples were prepared in duplicate where possible, due to low cell numbers. Conditioned media were analysed by gelatin zymography and cells were lysed in 100 µl of a 2 × SDS sample buffer to analyse by Western Blotting (Figure 5.19).

Cells attached to both intact and trypsin-treated cartilage. Unexpectedly, zymography analysis revealed that cartilage explants incubated without cells showed a residual pro and active MMP-2, however pre-treatment with trypsin removed all residual MMP-2.

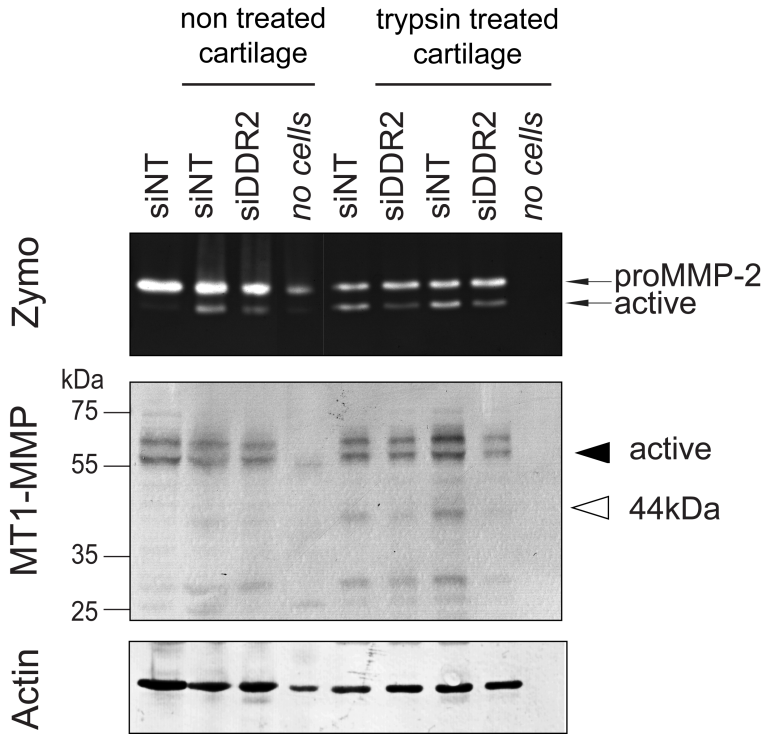

Figure 5.19: Knockdown of DDR2 expression inhibits proMMP-2 activation by cartilage. RASF were transfected with siRNA and after 24 h were attached to cartilage and incubated for further 4 days. Bovine cartilage was either untreated or pre-treated with 100 µg/ml trypsin for 18 h followed by 24 h incubation with soybean trypsin inhibitor at 200 µg/ml.

Both cartilages induced proMMP-2 activation in siRNA-transfected cells. The trypsin-treated cartilage seemed to be more efficient in inducing activation as it shows about 50% activation of proMMP-2 to active form, while 10% or less activation was observed in the non-treated cartilage. This is also evident with generation of 44 kDa MT1-MMP. Knockdown of DDR2 notably reduced levels of active MMP-2, especially in cells cultured on the cartilage treated with trypsin. The DDR2 knockdown also prevented processing of the MT1-MMP to 44 kDa species in these samples.

5.3 Discussion

Knowledge about mechanisms regulating the activation of synovial fibroblasts during invasion is vital to the understanding of RA pathogenesis. Here I present the evidence that RASF are activated not only by purified and reconstituted collagen but also by cartilage tissue. Importantly, cartilage increases MT1-MMP expression and proMMP-2 activation. In agreement with previous experiments (Section 3.2.9), the cartilage-induced increase in MT1-MMP expression and activity is mediated through the DDR2 receptor. Interestingly, proteoglycan-depleted cartilage induces greater MT1-MMP (and presumably DDR2) activation, as demonstrated by higher levels of active MMP-2 and elevated MT1-MMP processing. Although cartilage invasion was not investigated in this study, a report by Miller et al. (2009) demonstrated that RASF show deeper invasion into proteoglycan-depleted cartilage. Taken together, the above results strongly suggest that the high level of MT1-MMP expression in synovial cells at the pannus-cartilage junction in RA specimens is likely to be at least in part due to cartilage signalling. It is well recognised that MT1-MMP expression directly correlates with cell invasiveness and this study confirms that cartilage signalling contributes to the aggressive behaviour of invading cells.

My data also strongly suggest that DDR2 is a regulator of MT1-MMP function and that the cartilage matrix provides unique signals for DDR2 activation. Addi-

tionally, PureCol and CellMatrix collagens induced different levels of MT1-MMP expression as well as of DDR2 autophosphorylation. CellMatrix induced very low expression and activity of MT1-MMP, probably because it did not significantly increase DDR2 phosphorylation and signalling. As mentioned earlier, these collagens differ in structure as pepsin-extracted PureCol does not have telopeptides. Although PureCol is still able to form fibrils, lack of telopeptide regions reduces numbers of cross-links and such collagen shows lower thermal stability and lower fibril strength (Sato et al., 2000). During RA, telopeptides in collagen type II in the cartilage might be cleaved e.g. by soluble MMP-13 and possibly such tissue could induce higher DDR2 signalling. Collectively, this suggests that not only proteoglycan removal from cartilage, but also the structure of collagen might provide important cues for receptor activation and MT1-MMP expression.

The variation in cellular responses initiated by these collagens could be a consequence of differences in binding affinity to DDR2 and/or distinct ability to induce DDR2 activation. Surprisingly, the DDR2-Fc construct used here shows high affinity interaction with both collagens. DDR2-Fc displays even higher affinity for immobilised CellMatrix collagen, although this collagen induces significantly less DDR2 activation. DDRs require a native triple helical structure of collagen for activation and can be activated by monomeric collagen, but efficient proMMP-2 activation is induced only by fibrillar collagen (Ruangpanit et al., 2001). Analysis of DDR2-Fc binding to fibrillar collagen, either by a solid phase binding assay or by Western Blotting, also indicates high affinity binding to CellMatrix collagen. Despite the high affinity, CellMatrix appears to activate DDR2 receptor less than PureCol. This could result from non-productive binding of CellMatrix to collagen, which does not result in receptor phosphorylation or signalling. However, although CellMatrix induces significantly lower DDR2 phosphorylation, it exerts an unexpected effect on cell's DDR2 levels, indicating that it is able to induce a cellular response. Cells cultured on CellMatrix show noticeably reduced levels of fully glycosylated DDR2 in their cell lysates.

Loss of DDR2 from the cell surface could be a consequence of shedding of its ectodomain after collagen binding, which has been reported for DDR1. However, no increase of DDR2 shedding was observed in CellMatrix stimulated cells after up to 8 hours of incubation. The loss of DDR2 was not inhibited by any of the tested inhibitors, including marimastat which prevented accumulation of shed form in the medium, indicating the presence of some other mechanism. After ligand-induced activation, numerous signalling receptors, including RTKs, are internalised to regulate signalling. Activation of EGFR, a prototypical RTK, induces receptor internalisation into early endosomes, from which it can be recycled to the cell surface or, alternatively, shuffled to late endosome/lysosome compartments for degradation. A study by Mihai et al. (2009) demonstrated that DDR1 undergoes a rapid aggregation and endocytosis within minutes after collagen stimulation. Internalised DDR1 localises to Rab5-positive early endosomes and is reportedly recycled back to the cell surface after 60 min (Mihai et al., 2009). The same study however reports persistent reduction in cellular levels of DDR1 from 10 to up to 60 min after collagen addition, possibly resulting from receptor degradation. Further analysis is required to determine whether DDR2 also undergoes internalisation and intracellular degradation.

To my knowledge, this is the first report demonstrating shedding of the DDR2 ectodomain. It is unclear whether shedding also occurs in fibroblasts, as I was unable to detect the shed form of DDR2 in these cells. Ectodomain shedding is a mechanism that regulates the function of many transmembrane proteins and is often mediated by ADAMs. Shedding of the collagen-binding ectodomain of DDR1 prevents further activation of the receptor and has been shown to regulate cell migration and signalling latency (Yasuyuki Shitomi, Yoshifumi Itoh, manuscript submitted). Data from Dr. Itoh's lab also indicate that collagen-induced shedding of DDR1 is mediated by a member of the ADAM family. Consistent with their results, shedding was inhibited by marimastat and it is therefore likely that DDR2 is cleaved by a similar or same protease. Although collagen did not significantly

increase shedding of DDR2 over the 8 h incubation period, analysis of culture media at later time points (e.g. 24 h) is necessary to confirm collagen-induced shedding.

The reasons for diminished levels of DDR2 on the cell surface are not clear at this moment. Plausible explanations include ectodomain shedding or endocytosis followed by degradation. It is unlikely that collagen inhibits DDR2 expression, because levels of immature DDR2 remain unchanged. Ultimately, lower cell surface levels of DDR2 result in less collagen binding and signalling, as observed in CellMatrix-stimulated cells. In summary, these data provide important insights into collagen and cartilage recognition by DDR2.

Chapter 6

General discussion and future work

6.1 Discussion

MT1-MMP is a major cellular collagenase. It has been demonstrated that this enzyme plays a prominent role in many physiological and pathological processes. Its activity is rigorously regulated on many levels in order to maintain tissue homeostasis. High MT1-MMP expression has been documented in several different diseases, including RA and cancer, where it correlates with uncontrolled cellular invasion and extensive ECM degradation. However, mechanisms of MT1-MMP upregulation are not well understood. In RA, MT1-MMP is highly expressed in invading synovial cells in the pannus which are in direct contact with the cartilage. This observation, as well as the fact that MT1-MMP activity can be induced by collagen, prompted us to hypothesise that MT1-MMP expression in synovial fibroblasts is upregulated by the cartilage matrix. The aim of this thesis was to examine our hypothesis and investigate mechanisms of MT1-MMP activation in RASF during RA development.

The main finding of my thesis was identification of DDR2 as a receptor which mediates collagen-induced MT1-MMP activation in fibroblasts. I demonstrated, for the first time, that MT1-MMP activity and expression in fibroblasts are increased

through DDR2-mediated collagen signalling. Although it is still not known if DDR2 is the sole receptor responsible for mediating collagen-induced MT1-MMP activation, DDR2 knockdown clearly decreased MT1-MMP-dependent collagen degradation and invasion. I have also demonstrated that MT1-MMP activity is also induced by the cartilage tissue, and that this signalling is mediated by DDR2 as well. These findings strongly suggest that the high level of MT1-MMP detected at the pannus-cartilage junction could be due to DDR2-mediated induction of MT1-MMP by the cartilage tissue in RASF.

Little is known about signalling pathways initiated by DDR2. A Src kinase had been shown to associate with DDR2 upon collagen binding and to mediate downstream signalling (Ikeda et al., 2002; Yang et al., 2005). In agreement with these studies, I have found that a Src inhibitor decreased collagen-induced MT1-MMP activation. A recent study provided compelling evidence that the collagen-induced DDR2 signalling in breast cancer cells activates Src and ERK2, which in turn stabilise the transcription factor SNAIL1, resulting in MT1-MMP expression (Zhang et al., 2013). Furthermore, another study showed that overexpression of SNAIL1 induces MT1-MMP and MT2-MMP upregulation in breast cancer cells and promotes cell invasion (Ota et al., 2009). SNAIL1 is a transcription factor mainly implicated in epithelial-to-mesenchymal transition, but a recent report indicates that it has a prominent function in mesenchymal cells as well (Peinado et al., 2007). Mouse embryonic fibroblasts deficient in SNAIL1 have a phenotype similar to MT1-MMP null fibroblasts: they are unable to degrade collagen, are less invasive and show lower MT1-MMP levels in response to collagen (Rowe et al., 2009). It would be interesting to investigate whether DDR2 also mediates MT1-MMP expression through the SNAIL1 transcription factor in synovial fibroblasts.

The current study also shows that fibrillar collagens and cartilage act as activators of MT1-MMP expression and function in synovial and dermal fibroblasts. They not only induced a prolonged transcriptional activation of the *MT1-MMP* gene, but also promoted a functional activation of MT1-MMP already expressed on the cell

surface. This was particularly visible in proMMP-2 activation and gelatin degradation assays, where no MT1-MMP activity was detected unless the collagen was introduced. The precise nature of this non-transcriptional activation is not clear at the moment. It is possible that it involves regulation of the MT1-MMP endocytosis and targeted trafficking to the substrate degradation sites. As a result, local concentration of the enzyme on the plasma membrane increases, promoting formation of the functional MT1-MMP dimer. ConA or collagen stimulation were demonstrated to inhibit MT1-MMP endocytosis (Lafleur et al., 2006; Remacle et al., 2003), and MT1-MMP localisation to invadopodia and collagen attachment sites were also reported (Artym et al., 2006; Bravo-Cordero et al., 2007). Further research is required to determine the mechanism of functional activation of MT1-MMP by collagen.

Although integrins are major collagen receptors there is no consensus about their role in regulating MT1-MMP functions. My data indicate that collagen-binding integrins do not play any role in collagen-induced MT1-MMP activation. My results corroborate the findings published by Sakai et al. (2011) who demonstrated that β1 integrin knockdown does not influence proMMP-2 activation in malignant mesothelioma cells. Since all collagen-binding integrins contain the β1 subunit, we concluded that collagen-binding integrins do not play a direct role in fibroblast activation by collagen.

Although it has been reported that inflammatory cytokines including IL-1 and TNF-α upregulate MT1-MMP in RASF, my data indicate that TNF-α and IL-1β do not influence MT1-MMP expression or activity in cultured fibroblasts. These data are supported by the fact that the promotor region of MT1-MMP lacks AP-1 binding sites (Lohi et al., 2000). It is therefore unlikely that these cytokines are responsible for MT1-MMP activation *in vivo*. Because TNF-α and IL-1β do not appear to regulate MT1-MMP function, this may at least partially explain the failure of anti-inflammatory drugs to effectively prevent cartilage damage in RA (Choy et al., 2013).

I have also found that collagen induced expression and activation of MMP collagenases other than MT1-MMP, as observed during the collagen488 degradation assay. This finding, while preliminary, suggests a broader role of collagen signalling in RA progression. Although the function of DDR2 in the process described above has not been investigated in this study, it has been already reported that collagen upregulates expression of MMP-1 and MMP-13 in synovial fibroblasts through DDR2 (Su et al., 2009; Wang et al., 2002; Zhang et al., 2006a). Because little is known about activation of these MMPs *in vivo*, it is tempting to speculate that they are also activated by collagen-induced DDR2 activation.

6.1.1 DDR2 as a receptor of damaged ECM

The identification of DDR2 as an activator of MT1-MMP raises the following question: what are the mechanisms regulating DDR2 activation? DDR2 is constitutively expressed in mesenchymal cells and its ligand, collagen, is the most abundant protein in the human body. Despite this, expression of MT1-MMP in healthy tissues is usually low. We hypothesise that DDR2 is a receptor that recognises 'damaged' collagen. Recognition of collagen within injured, but not in the normal tissues, would therefore initiate the MMP-dependent ECM remodelling, which appears to be hijacked in RA. In agreement with our hypothesis, we found that proteoglycan-depleted cartilage induces greater proMMP-2 activation (Section 5.2.8) and synovial cell invasion (Miller et al., 2009) than intact cartilage. These data are further supported by studies showing that initial damage to the tissue is a prerequisite for an uncontrolled matrix degradation during disease. A study by Korb-Pap et al. (2012) demonstrated that in the inflammatory model of arthritis, loss of proteoglycans in the cartilage precedes pannus attachment and promotes its invasion. In the OA model, overexpression of DDR2 in chondrocytes does not initiate the degradation of the cartilage unless an initial damage to the pericellular matrix had occurred (Xu et al., 2011).

If this is the case, what would be the 'damaged' collagen? DDRs are not activated by denatured collagen, whereas monomeric collagen, although shown to activate the DDR2 receptor, is unstable *in vivo* and does not support proMMP-2 activation (Leikina et al., 2002; Ruangpanit et al., 2001). Therefore these forms of collagen would be unlikely to activate DDR2 in tissues. Under physiological conditions, collagens spontaneously assemble into fibrils. Until now, however, it has not been investigated whether collagen fibrils activate DDR2. In the present study I have shown that DDR2 binds to and is activated by fibrillar collagen. Moreover, MMP-2 activation is also induced by the cartilage tissue, confirming that DDR2 recognises tissue-derived collagen as well.

Strikingly, I have observed differences in the ability of different form of collagens, namely CellMatrix and PureCol collagens, to induce MT1-MMP activation. Initially we thought that the structure of collagen fibrils might influence DDR activation. Based on data from collagen fibre diffraction, Orgel and co-workers proposed a model of molecular collagen type I assembly (Orgel et al., 2006). This model provides valuable insight into the supramolecular collagen structure and possible protein-collagen interactions (Sweeney et al., 2008). DDR2 binding sites in collagen monomer can be mapped onto the 3D structure of collagen fibrils derived from the Orgel model to assess the accessibility of these sites for receptor binding.

Figure 6.1 illustrates the proposed model and molecular packing of collagen type I. The basic units of the collagen fibril are microfibrils. Microfibrils consist of a repeated arrangement of five collagen monomers, which form a rope-like, supertwisted structure. Neighbouring microfibrils interdigitate to form a larger collagen fibril. The molecular packing reveals that the C-terminal telopeptides face the fibril exterior and N-terminal telopeptides are hidden within the fibril (Orgel et al., 2006).

Mapping of MMP cleavage site and binding sites for DDR and integrin showed that they are confined to a specific region within the collagen fibril, in close proximity to the C-telopeptide. Although these sites are scattered on a monomer, due to twisting and staggered arrangement of collagen molecules within microfibril they

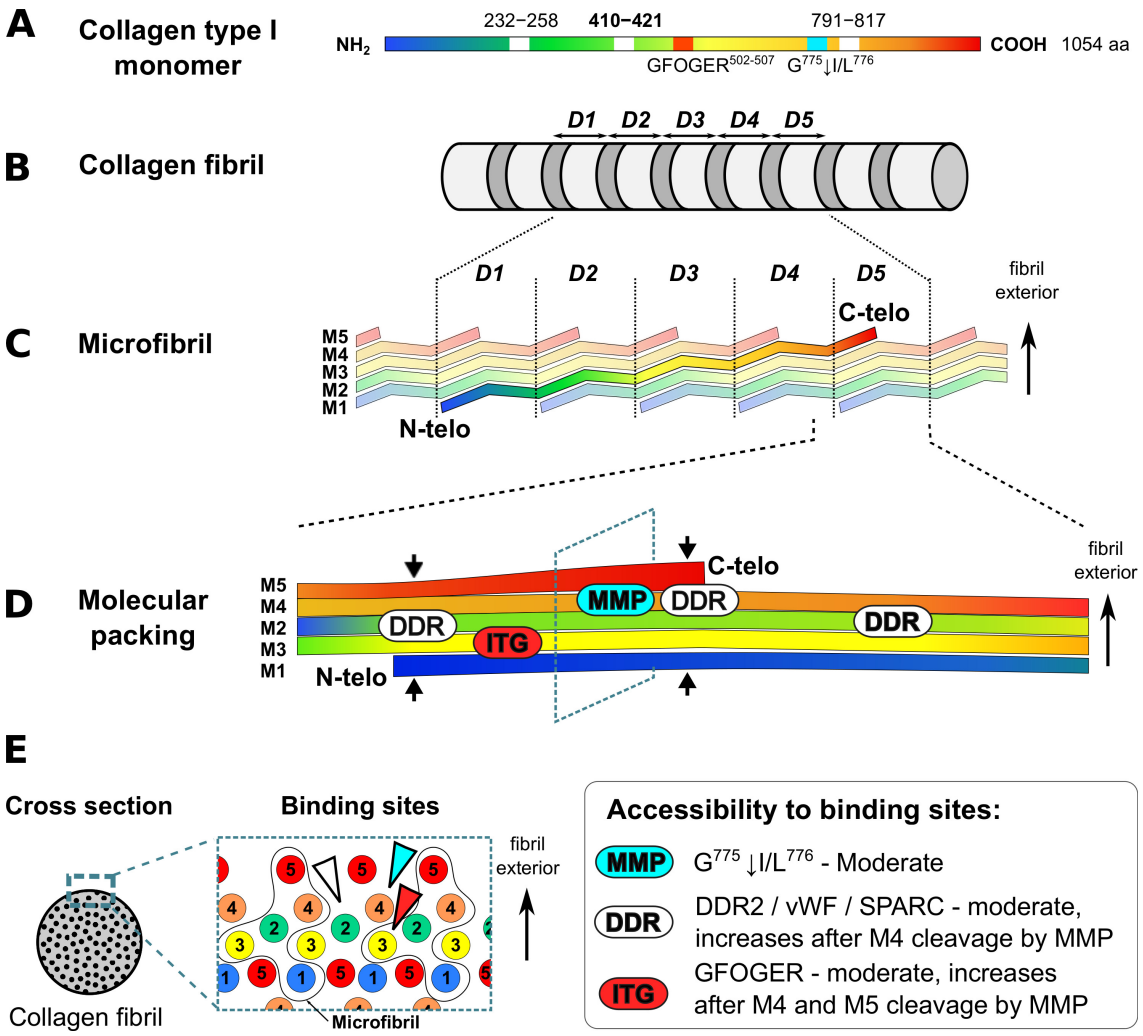

Figure 6.1: Molecular organisation of type I collagen fibril. **(A)** Schematic representation of a collagen type I monomer, which has been rainbow-coloured — from blue at the N-terminus to red at the C-terminus. Colour coded binding sites for DDR (white) and integrin (red) as well as the MMP cleavage site (red) have been indicated. **(B)** Collagen fibrils show a banding pattern with a *D*-periodicity. Each collagen molecule spans five *D* periods ***(D1-D5)***. **(C)** 2D representation of collagen microfibril. Five collagen monomers ***(M1-M5)*** constitute the microfibril and individual microfibrils interdigitate and super-twist, so that the C-terminal telopeptides ***(C-telo)*** face the fibril surface (exterior) and the N-terminal telopeptides ***(N-telo)*** are buried within the fibril **(D)** Molecular packing within D period of microfibril. Binding sites for MMPs, DDR2 and integrin ***(ITG)*** within the microfibril are indicated. Cross-linking sites within telopeptides are indicated by arrows. **(E)** Cross section view of the indicated D5 period shows molecular packing within the microfibril and orientation of collagen molecules. Location of the MMP, DDR2 and integrin binding sites within the cross section are indicated by colour-coded arrowheads. Access to these binding sites is predicted to be partially restricted by the neighbouring M4 collagen molecule and C-telopeptide. Figure adapted from Orgel et al. (2011b) and Nagase and Visse (2011).

are clustered within the overlap region. It has been proposed that access to the MMP cleavage site is partially restricted due to the neighbouring collagen monomer and the C-telopeptide. Cleavage of either of these elements would fully expose the MMP cleavage site and allow collagenolysis (Perumal et al., 2008). Indeed, telopeptide cleavage by MMP-3 appears to promote collagen degradation (Wu et al., 1991). Access to the DDR2 binding site also seems to be partially restricted and, similar to MMP site, accessibility is predicted to increase after C-telopeptide cleavage and/or MMP-mediated cleavage of the collagen monomer (Orgel et al., 2011a). Since CellMatrix collagen is an acid-extracted collagen and contains intact telopeptide regions, we thought that this collagen would not be able to support DDR2 binding due to steric hindrance, which would explain the lower MT1-MMP activation by CellMatrix. Surprisingly, DDR2 binds to CellMatrix with even greater affinity than to PureCol. However, DDR2 bound to this collagen appears to be quickly downregulated and no DDR2 phosphorylation or MT1-MMP activation were observed. The reason for this is not known at this moment, however, it might provide an interesting regulatory mechanism for DDR2 activation.

Another possibility for the increased receptor activation by damaged ECM is lack of proteoglycans within cartilage, which would expose collagen fibrils. It is a plausible mechanism in the context of RA, where proteoglycans in the cartilage are degraded at early stages of the disease by aggrecanases, including ADAMTS-4 and ADAMTS-5. ADAMTS-4 has been shown to degrade other small leucine-rich proteoglycans that bind to the collagen fibril surface, in close proximity to the DDR2 binding site as well (Kashiwagi et al., 2004). These proteoglycans include decorin, biglycan and fibromodulin and they have been shown to regulate stability and diameter of the forming collagen fibrils. More importantly, the DDR2 binding site within collagen is also recognised by vWF (Von Willebrand factor) and SPARC (secreted protein acidic and rich in cysteine) (Giudici et al., 2008). Binding of these proteins to the collagen would mask DDR2 binding sites and prevent recognition by the receptor. In fact, a similar mechanism has been proposed for MMP-1 as

addition of decorin to collagen prevents its cleavage by MMP-1 *in vitro* (Li et al., 2013). Moreover, treatment of collagen type II with anti-biglycan antibodies causes decomposition of collagen into smaller fibrils, potentially revealing binding epitopes (Antipova and Orgel, 2012). Therefore, degradation of proteoglycans could result in either perturbance of the fibril structure or unmasking of recognition sites within the microfibril, leading to DDR2 binding and activation.

Based on these data, we would like to propose a mechanism of collagen-induced MT1-MMP activation, illustrated on Figure 6.2. In healthy tissues, DDR2 may exhibit a high affinity binding to fibrillar collagens in their physiological state, but this binding would result in effective receptor downregulation, either by receptor shedding or intracellular degradation. As a result no signal would be propagated, and MT1-MMP expression would not be upregulated. Alternatively, collagen is not recognised e.g. due to the masking of binding sites by SPARC or proteoglycans. During injury or disease, cartilage becomes damaged and DDR2 is activated by the tissue. Cartilage damage can either occur by proteolytic removal or mechanistic translocation of C-terminal telopeptides, cleavage of the collagen molecules by MMP collagenases or degradation of proteoglycans. DDR2 activation results in signal transduction through Src and, possibly, ERK2 and SNAIL1. As a result, MT1-MMP expression and activity increases, leading to acquisition of the invasive phenotype by the cell. In addition, the upregulated DDR2 expression seen in RA synovium would contribute to increased receptor signalling (Su et al., 2009; Wang et al., 2002).

Based on the data I showed in this study, it is tempting to speculate that similar DDR2 signalling pathways could contribute to malignant conditions also characterised by high MT1-MMP expression, such as cancers and liver fibrosis (Ohtani et al., 1996; Sato et al., 1994; Takahara et al., 1997). Interestingly, chronic liver injury is often characterised by fibrosis, an extensive production of collagen type I-rich matrix by hepatic stellate cells. These cells also show high DDR2 expression and activation of proMMP-2 in response to collagen (Olaso et al., 2001). Several cancers, such as pancreatic ductal adenocarcinoma, are also associated with abnor-

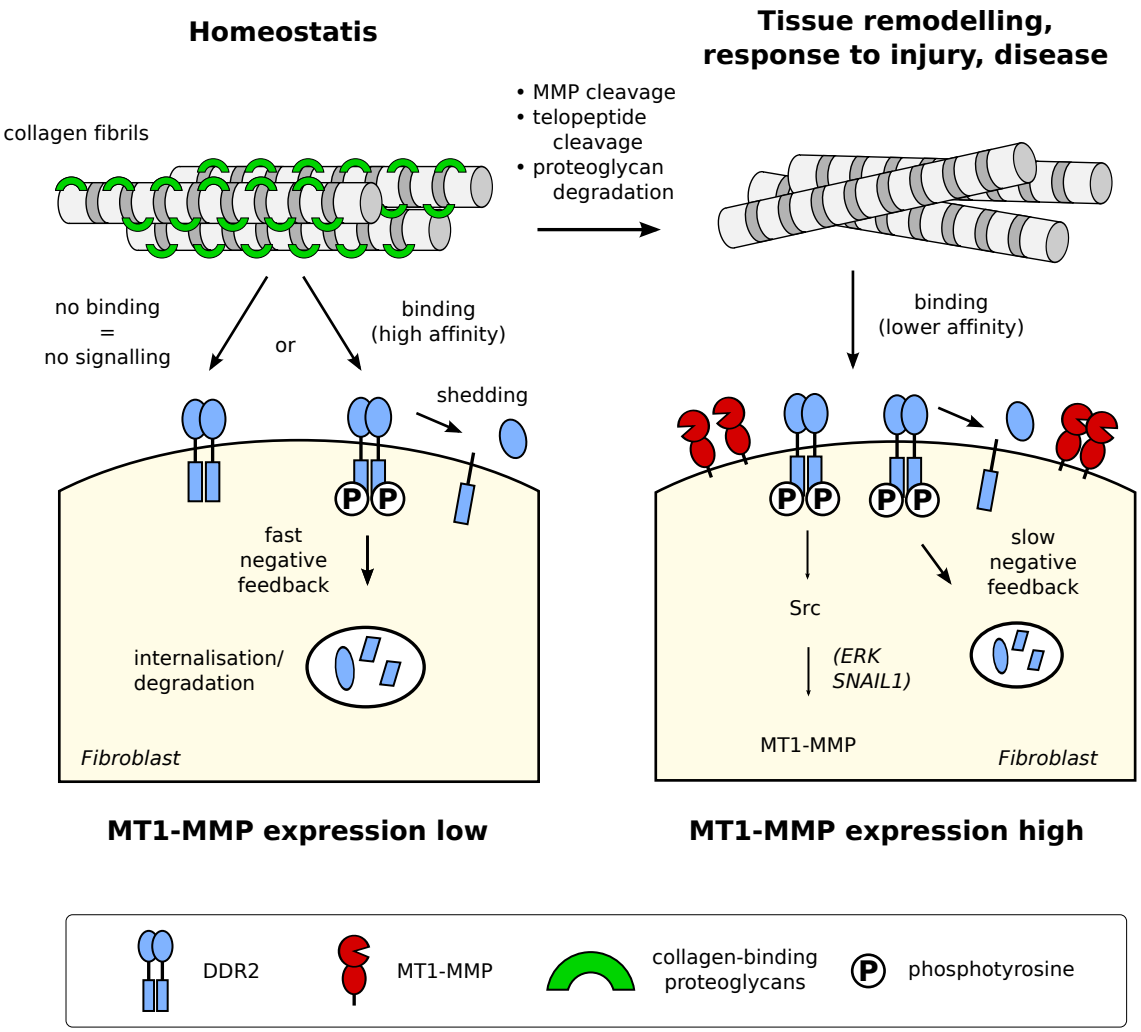

Figure 6.2: Proposed mechanism of DDR2 activation. During homeostasis DDR2 does not induce collagen-signalling, either because collagen fibrils are not recognised by the receptor (masked epitopes) or alternatively binding to the collagen fibril induces downregulation of the receptor through shedding or intracellular degradation. Unmasking of epitopes and/or change of fibril structure due to MMP cleavage, removal of telopeptides or degradation of collagen-bound proteoglycans results in persistent activation of DDR2. In turn, initiation of downstream signalling results in MT1-MMP expression and activation.

mal expression of collagen-rich ECM — a process called the desmoplastic reaction. It has been shown that increased collagen expression at the sites of tumour invasion co-localise with MT1-MMP expression (Bisson et al., 2003; Gilles et al., 1996; Shields et al., 2012). Taken all together, I therefore propose that identification of a novel DDR pathway of collagen-induced MT1-MMP expression would shed a new light into pathogenesis of various disorders including RA, cancer and chronic liver injury.

6.2 Future work

I have shown that collagen-induced DDR2 activation results in an increase in MT1-MMP expression and functions. However, further research is required to fully understand the mechanisms of DDR2 activation and collagen recognition during health and disease. Most importantly, it is essential to determine how DDR2 is activated by structurally different fibrillar collagens. For this purpose, acid-extracted collagen gels could be treated with proteases, for example: MMPs (such as recombinant MMP-1 or MMP-3) or neutrophil elastase. MMPs and neutrophil elastase remove telopeptides, and MMP-1 is also able to cleave collagen. Subsequently, the ability of proteinase-treated collagens to induce proMMP-2 activation in fibroblasts as well as binding to and activation of DDR2 receptor would be analysed and compared with untreated collagen. Similarly, cartilage would be treated with proteases as described above, followed by analysis of DDR2 binding (using DDR-Fc constructs) and phosphorylation (using cells overexpressing DDR2) as well as proMMP-2 activation in fibroblasts. These results would provide an additional insight into collagen signalling during injury or under pathological conditions.

At present, the fate of DDR2 after collagen binding is not known. My data indicate that DDR2 is constitutively shed and also appears to be degraded upon collagen binding. To prove whether shedding is indeed enhanced by collagen treatment, longer stimulation of cells with collagen should be performed and culture

media analysed for the presence of DDR2 ectodomain. Intracellular degradation is a common mechanism of downregulation of many different RTKs, including EGFR. At the moment, it is not known whether DDR2 is internalised upon collagen binding, but a recent report indicates that phosphorylated DDR2 is ubiquitinated and degraded (Yu et al., 2014). Confocal microscopy could be employed to analyse DDR2 internalisation and cellular localisation upon collagen stimulation. At the same time, blocking of endocytosis pathways and lysosomal degradation would provide necessary data to establish whether DDR2 is degraded intracellularly.

6.3 Therapeutic implications

At present, treatments for RA do not target joint tissue degradation despite this being a hallmark of the disease. Therefore, there is still an unmet need for drugs that prevent joint damage, especially loss of the cartilage. There is considerable evidence that blocking MT1-MMP function alone prevents invasion of RA synovial fibroblasts into the cartilage (Miller et al. 2009; Rutkauskaite et al. 2005; Sabeh et al. 2010; Yoshifumi Itoh, unpublished results). However, there are currently no MT1-MMP inhibitors that could be used to prevent the cartilage degradation in RA. Although an MT1-MMP inhibitory antibody, DX-2400, has been shown to be effective in preclinical cancer models, its safety and efficacy still need to be confirmed in human clinical trials. In this context DDR2, which mediates MT1-MMP expression and functional activation, could be considered as a potential therapeutic target for RA treatment.

Here, I reported that dasatinib, a potent DDR2 inhibitor, prevented DDR2 autophosphorylation and subsequent MT1-MMP activation in response to collagen. Moreover, invasive behaviour and motility of synovial fibroblasts were significantly attenuated by dasatinib treatment. Dasatinib, and closely related imatinib and nilotinib, are small molecule tyrosine kinase inhibitors targeting the oncogenic BCR-ABL kinase and are approved drugs for chronic myeloid leukaemia. All of them

have been reported to inhibit DDR phosphorylation (Day et al., 2008), but they have much broader specificity and also inhibit the Src family of kinases (including Src, Lck and Yes kinases), proto-oncogene c-Kit, beta-type platelet-derived growth factor receptor and p38 (Lombardo et al., 2004).

In support of application of a tyrosine kinase inhibitor for RA treatment, imatinib showed efficacy in treatment and prevention of murine collagen-induced arthritis (Paniagua et al., 2006). Reported case studies showed that imatinib administration resulted in a considerable clinical improvement in three RA patients (Eklund and Joensuu, 2003; Miyachi et al., 2003). Preliminary data in Dr. Itoh's lab showed that administration of dasatinib effectively halted progression of collagen-induced arthritis in mice. Although the detailed mechanisms of action of these inhibitors are not completely understood and they likely inhibit other tyrosine kinases, it is possible that inhibition of DDR2-mediated MT1-MMP activation could have a therapeutic effect. The development of a potent and selective inhibitor for DDR2 would be required for an effective treatment. Recent discoveries of an DDR1 inhibitory antibody as well as selective small molecule inhibitors for DDR1 indicate that development of targeted DDR2 inhibitors may be feasible (Carafoli et al., 2012; Kim et al., 2013). It is possible that such a kinase inhibitor may be developed as a future disease-modifying drug for RA.

6.4 Conclusion

RA is a debilitating disease, which often leads to physical disability due to joint damage. Cartilage degradation by the pannus tissue is irreversible and can progress even in the absence of joint inflammation. In recent years, MT1-MMP had been demonstrated to be a key collagenase in RA pathogenesis. In this thesis, I confirmed the central role of MT1-MMP in synovial cell invasion. In addition, I identified DDR2 as an upstream activator of MT1-MMP activity, which mediates cartilage collagen-driven synovial cell invasion in the RA joint. We propose that DDR2 is

a receptor that detects damaged ECM e.g. during disease or injury, and becomes activated when it recognises abnormal collagen. We also believe that collagen signalling through DDR2 may apply to other diseases characterised by disregulated collagen synthesis and MT1-MMP activity, such as tissue fibrosis and cancer. Overall, this work has expanded understanding of mechanisms governing MT1-MMP function in disease and could help in the development of new therapeutics to block MT1-MMP-dependent cell invasion in the future.

Bibliography

Aarvak, T., Natvig, J. B. (2001) "Cell-cell interactions in synovitis: antigen presenting cells and T cell interaction in rheumatoid arthritis". *Arthritis Res* **3**:13–7.

Abdulhussein, R., Koo, D. H. H., Vogel, W. F. (2008) "Identification of disulfide-linked dimers of the receptor tyrosine kinase DDR1". *J Biol Chem* **283**:12026–33.

Abdulhussein, R., McFadden, C., Fuentes-Prior, P., Vogel, W. F. (2004) "Exploring the collagen-binding site of the DDR1 tyrosine kinase receptor". *J Biol Chem* **279**:31462–70.

Adley, B. P., Gleason, K. J., Yang, X. J., Stack, M. S. (2009) "Expression of membrane type 1 matrix metalloproteinase (MMP-14) in epithelial ovarian cancer: high level expression in clear cell carcinoma". *Gynecol Oncol* **112**:319–24.

Afzal, S., Lalani, E. N., Poulsom, R., Stubbs, A., Rowlinson, G., Sato, H., Seiki, M., Stamp, G. W. (1998) "MT1-MMP and MMP-2 mRNA expression in human ovarian tumors: possible implications for the role of desmoplastic fibroblasts". *Hum Pathol* **29**:155–65.

Aletaha, D., Funovits, J., Smolen, J. S. (2011) "Physical disability in rheumatoid arthritis is associated with cartilage damage rather than bone destruction". *Ann Rheum Dis* **70**:733–9.

Aletaha, D., Neogi, T., Silman, A. J., Funovits, J., Felson, D. T., Bingham, C. O., Birnbaum, N. S., Burmester, G. R., Bykerk, V. P., Cohen, M. D., Combe, B., Costenbader, K. H., Dougados, M., Emery, P., Ferraccioli, G., Hazes, J. M. W., Hobbs, K., Huizinga, T. W. J., Kavanaugh, A., Kay, J., Kvien, T. K., Laing, T., Mease, P., Ménard, H. A., Moreland, L. W., Naden, R. L., Pincus, T., Smolen, J. S., Stanislawska-Biernat, E., Symmons, D., Tak, P. P., Upchurch, K. S., Vencovsky, J., Wolfe, F., Hawker, G. (2010) "2010 rheumatoid arthritis classification criteria: an American College of Rheumatology/European League Against Rheumatism collaborative initiative". *Ann Rheum Dis* **69**:1580–8.

Ali, B. R., Xu, H., Akawi, N. A., John, A., Karuvantevida, N. S., Langer, R., Al-Gazali, L., Leitinger, B. (2010) "Trafficking defects and loss of ligand binding are the underlying causes of all reported DDR2 missense mutations found in SMED-SL patients". *Hum Mol Genet* **19**:2239–50.

Allard, S. A., Bayliss, M. T., Maini, R. N. (1990) "The synovium-cartilage junction of the normal human knee. Implications for joint destruction and repair". *Arthritis Rheum* **33**:1170–9.

Allard, S. A., Muirden, K. D., Maini, R. N. (1991) "Correlation of histopathological features of pannus with patterns of damage in different joints in rheumatoid arthritis". *Ann Rheum Dis* **50**:278–83.

Alves, F., Saupe, S., Ledwon, M., Schaub, F., Hiddemann, W., Vogel, W. F. (2001) "Identification of two novel, kinase-deficient variants of discoidin domain receptor 1: differential expression in human colon cancer cell lines". *FASEB J* **15**:1321–3.

Andereya, S., Streich, N., Schmidt-Rohlfing, B., Mumme, T., Müller-Rath, R., Schneider, U. (2006) "Comparison of modern marker proteins in serum and synovial fluid in patients with advanced osteoarthrosis and rheumatoid arthritis". *Rheumatol Int* **26**:432–8.

Anilkumar, N., Uekita, T., Couchman, J. R., Nagase, H., Seiki, M., Itoh, Y. (2005) "Palmitoylation at Cys574 is essential for MT1-MMP to promote cell migration". *FASEB J* **19**:1326–8.

Annabi, B., Lachambre, M., Bousquet-Gagnon, N., Pagé, M., Gingras, D., Béliveau, R. (2001) "Localization of membrane-type 1 matrix metalloproteinase in caveolae membrane domains". *Biochem J* **353**:547–53.

Antipova, O., Orgel, J. P. R. O. (2012) "Non-enzymatic decomposition of collagen fibers by a biglycan antibody and a plausible mechanism for rheumatoid arthritis". *PLoS ONE* **7**:e32241.

Artym, V. V., Zhang, Y., Seillier-Moiseiwitsch, F., Yamada, K. M., Mueller, S. C. (2006) "Dynamic interactions of cortactin and membrane type 1 matrix metalloproteinase at invadopodia: defining the stages of invadopodia formation and function". *Cancer Res* **66**:3034–43.

Azzam, H. S., Thompson, E. W. (1992) "Collagen-induced activation of the M(r) 72,000 type IV collagenase in normal and malignant human fibroblastoid cells". *Cancer Res* **52**:4540–4.

Bair, E. L., Chen, M. L., Mcdaniel, K., Sekiguchi, K., Cress, A. E., Nagle, R. B., Bowden, G. T. (2005) "Membrane type 1 matrix metalloprotease cleaves laminin-10 and promotes prostate cancer cell migration". *Neoplasia* **7**:380–9.

Barbolina, M. V., Adley, B. P., Ariztia, E. V., Liu, Y., Stack, M. S. (2007) "Microenvironmental regulation of membrane type 1 matrix metalloproteinase activity in ovarian carcinoma cells via collagen-induced EGR1 expression". *J Biol Chem* **282**:4924–31.

Barczyk, M., Carracedo, S., Gullberg, D. (2010) "Integrins". *Cell Tissue Res* **339**:269–80.

Bargal, R., Cormier-Daire, V., Ben-Neriah, Z., Merrer, M. L., Sosna, J., Melki, J., Zangen, D. H., Smithson, S. F., Borochowitz, Z., Belostotsky, R., Raas-Rothschild, A. (2009) "Mutations in DDR2 gene cause SMED with short limbs and abnormal calcifications". *Am J Hum Genet* **84**:80–4.

Basile, J. R., Holmbeck, K., Bugge, T. H., Gutkind, J. S. (2007) "MT1-MMP controls tumor-induced angiogenesis through the release of semaphorin 4D". *J Biol Chem* **282**:6899–905.

Belkin, A. M., Akimov, S. S., Zaritskaya, L. S., Ratnikov, B. I., Deryugina, E. I., Strongin, A. Y. (2001) "Matrix-dependent proteolysis of surface transglutaminase by membrane-type metalloproteinase regulates cancer cell adhesion and locomotion". *J Biol Chem* **276**:18415–22.

Berrier, A. L., Yamada, K. M. (2007) "Cell-matrix adhesion". *J Cell Physiol* **213**:565–73.

Billinghurst, R. C., Dahlberg, L., Ionescu, M., Reiner, A., Bourne, R., Rorabeck, C., Mitchell, P., Hambor, J., Diekmann, O., Tschesche, H., Chen, J., Wart, H. V., Poole, A. R. (1997) "Enhanced cleavage of type II collagen by collagenases in osteoarthritic articular cartilage". *J Clin Invest* **99**:1534–45.

Bini, A., Wu, D., Schnuer, J., Kudryk, B. J. (1999) "Characterization of stromelysin 1 (MMP-3), matrilysin (MMP-7), and membrane type 1 matrix metalloproteinase (MT1-MMP) derived fibrin(ogen) fragments D-dimer and D-like monomer: NH2-terminal

sequences of late-stage digest fragments". *Biochemistry* **38**:13928–36.

Bisson, C., Blacher, S., Polette, M., Blanc, J.-F., Kebers, F., Desreux, J., Tetu, B., Rosenbaum, J., Foidart, J.-M., Birembaut, P., Noel, A. (2003) "Restricted expression of membrane type 1-matrix metalloproteinase by myofibroblasts adjacent to human breast cancer cells". *Int J Cancer* **105**:7–13.

Blissett, A. R., Garbellini, D., Calomeni, E. P., Mihai, C., Elton, T. S., Agarwal, G. (2009) "Regulation of collagen fibrillogenesis by cell-surface expression of kinase dead DDR2". *J Mol Biol* **385**:902–11.

Bombardier, C., Barbieri, M., Parthan, A., Zack, D. J., Walker, V., Macarios, D., Smolen, J. S. (2012) "The relationship between joint damage and functional disability in rheumatoid arthritis: a systematic review". *Ann Rheum Dis* **71**:836–44.

Bravo-Cordero, J. J., Marrero-Diaz, R., Megías, D., Genís, L., García-Grande, A., García, M. A., Arroyo, A. G., Montoya, M. C. (2007) "MT1-MMP proinvasive activity is regulated by a novel Rab8-dependent exocytic pathway". *EMBO J* **26**:1499–510.

Brew, K., Nagase, H. (2010) "The tissue inhibitors of metalloproteinases (TIMPs): an ancient family with structural and functional diversity". *Biochim Biophys Acta* **1803**:55–71.

Brinckerhoff, C. E., Matrisian, L. M. (2002) "Matrix metalloproteinases: a tail of a frog that became a prince". *Nat Rev Mol Cell Biol* **3**:207–214.

Bromley, M., Bertfield, H., Evanson, J. M., Woolley, D. E. (1985) "Bidirectional erosion of cartilage in the rheumatoid knee joint". *Ann Rheum Dis* **44**:676–81.

Burmester, G. R. (2012) "RA in 2011: Advances in diagnosis, treatment and definition of remission". *Nat Rev Rheumatol* **8**:65–6.

Bury, A. F. (1981) "Analysis of protein and peptide mixtures: Evaluation of three sodium dodecyl sulphate-polyacrylamide gel electrophoresis buffer systems". *Journal of Chromatography A* **213**:491–500.

Carafoli, F., Bihan, D., Stathopoulos, S., Konitsiotis, A. D., Kvansakul, M., Farndale, R. W., Leitinger, B., Hohenester, E. (2009) "Crystallographic insight into collagen recognition by discoidin domain receptor 2". *Structure* **17**:1573–81.

Carafoli, F., Mayer, M. C., Shiraishi, K., Pecheva, M. A., Chan, L. Y., Nan, R., Leitinger, B., Hohenester, E. (2012) "Structure of the discoidin domain receptor 1 extracellular region bound to an inhibitory Fab fragment reveals features important for signaling". *Structure* **20**:688–97.

Cardillo, M. R., Silverio, F. D., Gentile, V. (2006) "Quantitative immunohistochemical and in situ hybridization analysis of metalloproteinases in prostate cancer". *Anticancer Res* **26**:973–82.

Ceponis, A., Hietanen, J., Tamulaitiene, M., Partsch, G., Pätiälä, H., Konttinen, Y. T. (1999) "A comparative quantitative morphometric study of cell apoptosis in synovial membranes in psoriatic, reactive and rheumatoid arthritis". *Rheumatology (Oxford)* **38**:431–40.

Ceponis, A., Konttinen, Y. T., Imai, S., Tamulaitiene, M., Li, T. F., Xu, J. W., Hietanen, J., Santavirta, S., Fassbender, H. G. (1998) "Synovial lining, endothelial and inflammatory mononuclear cell proliferation in synovial membranes in psoriatic and reactive arthritis: a comparative quantitative morphometric study". *Br J Rheumatol* **37**:170–8.

Cha, H. J., Okada, A., Kim, K. W., Sato, H., Seiki, M. (2000) "Identification of cis-acting promoter elements that support expression of membrane-type 1 matrix metalloproteinase (MT1-MMP) in v-src transformed Madin-Darby canine kidney cells". *Clin Exp Metastasis* **18**:675–81.

Chen, W. T., Chen, J. M., Parsons, S. J., Parsons, J. T. (1985) "Local degradation of fibronectin at sites of expression of the transforming gene product pp60src". *Nature* **316**:156–8.

Cho, J.-A., Osenkowski, P., Zhao, H., Kim, S., Toth, M., Cole, K., Aboukameel, A., Saliganan, A., Schuger, L., Bonfil, R. D., Fridman, R. (2008) "The inactive 44-kDa processed form of membrane type 1 matrix metalloproteinase (MT1-MMP) enhances proteolytic activity via regulation of endocytosis of active MT1-MMP". *J Biol Chem* **283**:17391–405.

Choy, E. (2012) "Understanding the dynamics: pathways involved in the pathogenesis of rheumatoid arthritis". *Rheumatology (Oxford)* **51 Suppl 5**:v3–11.

Choy, E. H., Kavanaugh, A. F., Jones, S. A. (2013) "The problem of choice: current biologic agents and future prospects in RA". *Nat Rev Rheumatol* **9**:154–63.

Chun, T.-H., Hotary, K. B., Sabeh, F., Saltiel, A. R., Allen, E. D., Weiss, S. J. (2006) "A pericellular collagenase directs the 3-dimensional development of white adipose tissue". *Cell* **125**:577–91.

Chun, T.-H., Sabeh, F., Ota, I., Murphy, H., McDonagh, K. T., Holmbeck, K., Birkedal-Hansen, H., Allen, E. D., Weiss, S. J. (2004) "MT1-MMP-dependent neovessel formation within the confines of the three-dimensional extracellular matrix". *J Cell Biol* **167**:757–67.

Covington, M. D., Burghardt, R. C., Parrish, A. R. (2006) "Ischemia-induced cleavage of cadherins in NRK cells requires MT1-MMP (MMP-14)". *Am J Physiol Renal Physiol* **290**:F43–51.

Creemers, L. B., Jansen, D. C., van Veen-Reurings, A., van den Bos, T., Everts, V. (1997) "Microassay for the assessment of low levels of hydroxyproline". *BioTechniques* **22**:656–8.

Danks, L., Sabokbar, A., Gundle, R., Athanasou, N. A. (2002) "Synovial macrophage-osteoclast differentiation in inflammatory arthritis". *Ann Rheum Dis* **61**:916–21.

Davidson, R. K., Waters, J. G., Kevorkian, L., Darrah, C., Cooper, A., Donell, S. T., Clark, I. M. (2006) "Expression profiling of metalloproteinases and their inhibitors in synovium and cartilage". *Arthritis Res Ther* **8**:R124.

Day, E., Waters, B., Spiegel, K., Alnadaf, T., Manley, P. W., Buchdunger, E., Walker, C., Jarai, G. (2008) "Inhibition of collagen-induced discoidin domain receptor 1 and 2 activation by imatinib, nilotinib and dasatinib". *Eur J Pharmacol* **599**:44–53.

Delaissé, J.-M., Andersen, T. L., Engsig, M. T., Henriksen, K., Troen, T., Blavier, L. (2003) "Matrix metalloproteinases (MMP) and cathepsin K contribute differently to osteoclastic activities". *Microsc Res Tech* **61**:504–13.

Deryugina, E. I., Ratnikov, B. I., Postnova, T. I., Rozanov, D. V., Strongin, A. Y. (2002) "Processing of integrin alpha(v) subunit by membrane type 1 matrix metalloproteinase stimulates migration of breast carcinoma cells on vitronectin and enhances tyrosine phosphorylation of focal adhesion kinase". *J Biol Chem* **277**:9749–56.

Devy, L., Huang, L., Naa, L., Yanamandra, N., Pieters, H., Frans, N., Chang, E., Tao, Q., Vanhove, M., Lejeune, A., van Gool, R., Sexton, D. J., Kuang, G., Rank, D., Hogan, S., Pazmany, C., Ma, Y. L., Schoonbroodt, S., Nixon, A. E., Ladner, R. C., Hoet, R., Henderikx, P., Tenhoor, C., Rabbani, S. A., Valentino, M. L., Wood, C. R., Dransfield, D. T. (2009) "Selective inhibition of matrix metalloproteinase-14 blocks tumor growth, invasion, and angiogenesis". *Cancer Res* **69**:1517–26.

Dodge, G. R., Pidoux, I., Poole, A. R. (1991) "The degradation of type II collagen in rheumatoid arthritis: an immunoelectron microscopic study". *Matrix* **11**:330–8.

Dodge, G. R., Poole, A. R. (1989) "Immunohistochemical detection and immunochemical analysis of type II collagen degradation in human normal, rheumatoid, and osteoarthritic articular cartilages and in explants of bovine articular cartilage cultured with interleukin 1". *J Clin Invest* **83**:647–61.

d'Ortho, M. P., Will, H., Atkinson, S., Butler, G., Messent, A., Gavrilovic, J., Smith, B., Timpl, R., Zardi, L., Murphy, G. (1997) "Membrane-type matrix metalloproteinases 1 and 2 exhibit broad-spectrum proteolytic capacities comparable to many matrix metalloproteinases". *Eur J Biochem* **250**:751–757.

du Montcel, S. T., Michou, L., Petit-Teixeira, E., Osorio, J., Lemaire, I., Lasbleiz, S., Pierlot, C., Quillet, P., Bardin, T., Prum, B., Cornelis, F., Clerget-Darpoux, F. (2005) "New classification of HLA-DRB1 alleles supports the shared epitope hypothesis of rheumatoid arthritis susceptibility". *Arthritis Rheum* **52**:1063–8.

Durigova, M., Nagase, H., Mort, J. S., Roughley, P. J. (2010) "MMPs are less efficient than ADAMTS5 in cleaving aggrecan core protein". *Matrix Biol* **30**:145–53.

Egeblad, M., Werb, Z. (2002) "New functions for the matrix metalloproteinases in cancer progression". *Nat Rev Cancer* **2**:161–74.

Eisenach, P. A., de Sampaio, P. C., Murphy, G., Roghi, C. (2012) "Membrane type 1 matrix metalloproteinase (MT1-MMP) ubiquitination at Lys581 increases cellular invasion through type I collagen". *J Biol Chem* **287**:11533–45.

Eklund, K. K., Joensuu, H. (2003) "Treatment of rheumatoid arthritis with imatinib mesylate: clinical improvement in three refractory cases". *Ann Med* **35**:362–7.

Ellerbroek, S. M., Fishman, D. A., Kearns, A. S., Bafetti, L. M., Stack, M. S. (1999) "Ovarian carcinoma regulation of matrix metalloproteinase-2 and membrane type 1 matrix metalloproteinase through beta1 integrin". *Cancer Res* **59**:1635–41.

Ellerbroek, S. M., Wu, Y. I., Overall, C. M., Stack, M. S. (2001) "Functional interplay between type I collagen and cell surface matrix metalloproteinase activity". *J Biol Chem* **276**:24833–42.

Elliott, M. J., Maini, R. N., Feldmann, M., Long-Fox, A., Charles, P., Bijl, H., Woody, J. N. (1994) "Repeated therapy with monoclonal antibody to tumour necrosis factor alpha (cA2) in patients with rheumatoid arthritis". *Lancet* **344**:1125–7.

Endo, K., Takino, T., Miyamori, H., Kinsen, H., Yoshizaki, T., Furukawa, M., Sato, H. (2003) "Cleavage of syndecan-1 by membrane type matrix metalloproteinase-1 stimulates cell migration". *J Biol Chem* **278**:40764–70.

Engler, A. J., Sen, S., Sweeney, H. L., Discher, D. E. (2006) "Matrix elasticity directs stem cell lineage specification". *Cell* **126**:677–89.

Evans, B. R., Mosig, R. A., Lobl, M., Martignetti, C. R., Camacho, C., Grum-Tokars, V., Glucksman, M. J., Martignetti, J. A. (2012) "Mutation of Membrane Type-1 Metalloproteinase, MT1-MMP, Causes the Multicentric Osteolysis and Arthritis Disease Winchester Syndrome". *Am J Hum Genet* **91**:572–6.

Farndale, R. W., Lisman, T., Bihan, D., Hamaia, S., Smerling, C. S., Pugh, N., Konitsiotis, A., Leitinger, B., de Groot, P. G., Jarvis, G. E., Raynal, N. (2008) "Cell-collagen interactions: the use of peptide Toolkits to investigate collagen-receptor interactions". *Biochem Soc Trans* **36**:241–50.

Feldmann, M., Brennan, F. M., Maini, R. N. (1996) "Role of cytokines in rheumatoid arthritis". *Annu Rev Immunol* **14**:397–440.

Feldmann, M., Maini, S. R. N. (2008) "Role of cytokines in rheumatoid arthritis: an education in pathophysiology and therapeutics". *Immunol Rev* **223**:7–19.

Ferri, N., Carragher, N. O., Raines, E. W. (2004) "Role of discoidin domain receptors 1 and 2 in human smooth muscle cell-mediated collagen remodeling: potential implications in

atherosclerosis and lymphangioleiomyomatosis". *Am J Pathol* **164**:1575–85.

Filippov, S., Koenig, G. C., Chun, T.-H., Hotary, K. B., Ota, I., Bugge, T. H., Roberts, J. D., Fay, W. P., Birkedal-Hansen, H., Holmbeck, K., Sabeh, F., Allen, E. D., Weiss, S. J. (2005) "MT1-matrix metalloproteinase directs arterial wall invasion and neointima formation by vascular smooth muscle cells". *J Exp Med* **202**:663–71.

Fingleton, B. (2008) "MMPs as therapeutic targets–still a viable option?". *Semin Cell Dev Biol* **19**:61–8.

Firestein, G. S. (2003) "Evolving concepts of rheumatoid arthritis". *Nature* **423**:356–61.

Firestein, G. S., Echeverri, F., Yeo, M., Zvaifler, N. J., Green, D. R. (1997) "Somatic mutations in the p53 tumor suppressor gene in rheumatoid arthritis synovium". *Proc Natl Acad Sci USA* **94**:10895–900.

Fisher, K. E., Sacharidou, A., Stratman, A. N., Mayo, A. M., Fisher, S. B., Mahan, R. D., Davis, M. J., Davis, G. E. (2009) "MT1-MMP- and Cdc42-dependent signaling co-regulate cell invasion and tunnel formation in 3D collagen matrices". *J Cell Sci* **122**:4558–69.

Fosang, A. J., Rogerson, F. M., East, C. J., Stanton, H. (2008) "ADAMTS-5: the story so far". *Eur Cell Mater* **15**:11–26.

Franco, C., Hou, G., Ahmad, P. J., Fu, E. Y. K., Koh, L., Vogel, W. F., Bendeck, M. P. (2008) "Discoidin domain receptor 1 (ddr1) deletion decreases atherosclerosis by accelerating matrix accumulation and reducing inflammation in low-density lipoprotein receptor-deficient mice". *Circ Res* **102**:1202–11.

Fraser, A., Fearon, U., Billinghurst, R. C., Ionescu, M., Reece, R., Barwick, T., Emery, P., Poole, A. R., Veale, D. J. (2003) "Turnover of type II collagen and aggrecan in cartilage matrix at the onset of inflammatory arthritis in humans: relationship to mediators of systemic and local inflammation". *Arthritis Rheum* **48**:3085–95.

Frittoli, E., Palamidessi, A., Disanza, A., Scita, G. (2011) "Secretory and endo/exocytic trafficking in invadopodia formation: the MT1-MMP paradigm". *Eur J Cell Biol* **90**:108–14.

Fu, H.-L., Sohail, A., Valiathan, R. R., Wasinski, B. D., Kumarasiri, M., Mahasenan, K. V., Bernardo, M. M., Tokmina-Roszyk, D., Fields, G. B., Mobashery, S., Fridman, R. (2013) "Shedding of discoidin domain receptor 1 by membrane-type matrix metalloproteinases". *J Biol Chem* **288**:12114–29.

Gabriel, S. E., Michaud, K. (2009) "Epidemiological studies in incidence, prevalence, mortality, and comorbidity of the rheumatic diseases". *Arthritis Res Ther* **11**:229.

Gaggioli, C., Hooper, S., Hidalgo-Carcedo, C., Grosse, R., Marshall, J. F., Harrington, K., Sahai, E. (2007) "Fibroblast-led collective invasion of carcinoma cells with differing roles for RhoGTPases in leading and following cells". *Nat Cell Biol* **9**:1392–400.

Gálvez, B. G., Matías-Román, S., Yáñez-Mó, M., Sánchez-Madrid, F., Arroyo, A. G. (2002) "ECM regulates MT1-MMP localization with beta1 or alphavbeta3 integrins at distinct cell compartments modulating its internalization and activity on human endothelial cells". *J Cell Biol* **159**:509–21.

Gálvez, B. G., Matías-Román, S., Yáñez-Mó, M., Vicente-Manzanares, M., Sánchez-Madrid, F., Arroyo, A. G. (2004) "Caveolae are a novel pathway for membrane-type 1 matrix metalloproteinase traffic in human endothelial cells". *Mol Biol Cell* **15**:678–87.

Garnero, P., Gineyts, E., Christgau, S., Finck, B., Delmas, P. D. (2002) "Association of baseline levels of urinary glucosyl-galactosyl-pyridinoline and type II collagen C-telopeptide with progression of joint destruction in patients with early rheumatoid arthritis". *Arthritis Rheum* **46**:21–30.

Gilles, C., Polette, M., Piette, J., Munaut, C., Thompson, E. W., Birembaut, P., Foidart, J. M. (1996) "High level of MT-MMP expression is associated with invasiveness of cervical cancer cells". *Int J Cancer* **65**:209–13.

Giudici, C., Raynal, N., Wiedemann, H., Cabral, W. A., Marini, J. C., Timpl, R., Bächinger, H. P., Farndale, R. W., Sasaki, T., Tenni, R. (2008) "Mapping of SPARC/BM-40/osteonectin-binding sites on fibrillar collagens". *J Biol Chem* **283**:19551–60.

Glasson, S. S., Askew, R., Sheppard, B., Carito, B., Blanchet, T., Ma, H.-L., Flannery, C. R., Peluso, D., Kanki, K., Yang, Z., Majumdar, M. K., Morris, E. A. (2005) "Deletion of active ADAMTS5 prevents cartilage degradation in a murine model of osteoarthritis". *Nature* **434**:644–8.

Goldbach-Mansky, R., Lee, J. M., Hoxworth, J. M., Smith, D., Duray, P., Schumacher, R. H., Yarboro, C. H., Klippel, J., Kleiner, D., El-Gabalawy, H. S. (2000) "Active synovial matrix metalloproteinase-2 is associated with radiographic erosions in patients with early synovitis". *Arthritis Res* **2**:145–53.

Goldring, M. B., Marcu, K. B. (2009) "Cartilage homeostasis in health and rheumatic diseases". *Arthritis Res Ther* **11**:224.

Goldring, M. R. (2012) "Cartilage and chondrocytes". In: Firestein, G. S., Budd, R. C., Gabriel, S. E., McInnes, I. B., O'Dell, J. R. (Eds.), Kelley's Textbook of Rheumatology, 9th Edition. Saunders, pp. 33 – 60.

Goldring, S. R. (2003) "Pathogenesis of bone and cartilage destruction in rheumatoid arthritis". *Rheumatology (Oxford)* **42 Suppl 2**:ii11–6.

Goldring, S. R., Goldring, M. R. (2012) "Biology of the Normal Joint". In: Firestein, G. S., Budd, R. C., Gabriel, S. E., McInnes, I. B., O'Dell, J. R. (Eds.), Kelley's Textbook of Rheumatology, 9th Edition. Saunders, pp. 1 – 20.

Golubkov, V. S., Chekanov, A. V., Cieplak, P., Aleshin, A. E., Chernov, A. V., Zhu, W., Radichev, I. A., Zhang, D., Dong, P. D., Strongin, A. Y. (2010) "The Wnt/planar cell polarity (PCP) protein tyrosine kinase-7 (PTK7) is a highly efficient proteolytic target of membrane type-1 matrix metalloproteinase (MT1-MMP): implications in cancer and embryogenesis". *J Biol Chem* **285**:35740–9.

Gomis-Rüth, F. X. (2003) "Structural aspects of the metzincin clan of metalloendopeptidases". *Mol Biotechnol* **24**:157–202.

Gravallese, E. M., Harada, Y., Wang, J. T., Gorn, A. H., Thornhill, T. S., Goldring, S. R. (1998) "Identification of cell types responsible for bone resorption in rheumatoid arthritis and juvenile rheumatoid arthritis". *Am J Pathol* **152**:943–51.

Gravallese, E. M., Manning, C., Tsay, A., Naito, A., Pan, C., Amento, E., Goldring, S. R. (2000) "Synovial tissue in rheumatoid arthritis is a source of osteoclast differentiation factor". *Arthritis Rheum* **43**:250–8.

Gregersen, P. K., Silver, J., Winchester, R. J. (1987) "The shared epitope hypothesis. An approach to understanding the molecular genetics of susceptibility to rheumatoid arthritis". *Arthritis Rheum* **30**:1205–13.

Guo, C., Piacentini, L. (2003) "Type I collagen-induced MMP-2 activation coincides with up-regulation of membrane type 1-matrix metalloproteinase and TIMP-2 in cardiac fibroblasts". *J Biol Chem* **278**:46699–708.

Haas, T. L., Davis, S. J., Madri, J. A. (1998) "Three-dimensional type I collagen lattices induce coordinate expression of matrix metalloproteinases MT1-MMP and MMP-2 in microvascular endothelial cells". *J Biol Chem* **273**:3604–10.

Haas, T. L., Stitelman, D., Davis, S. J., Apte, S. S., Madri, J. A. (1999) "Egr-1 mediates extracellular matrix-driven transcription of membrane type 1 matrix metalloproteinase

in endothelium". *J Biol Chem* **274**:22679–85.

Han, Y. P., Tuan, T. L., Wu, H., Hughes, M., Garner, W. L. (2001) "TNF-alpha stimulates activation of pro-MMP2 in human skin through NF-(kappa)B mediated induction of MT1-MMP". *J Cell Sci* **114**:131–139.

Harburger, D. S., Calderwood, D. A. (2009) "Integrin signalling at a glance". *J Cell Sci* **122**:159–63.

Heinegård, D. (2009) "Proteoglycans and more–from molecules to biology". *Int J Exp Pathol* **90**:575–86.

Hernandez-Barrantes, S., Toth, M., Bernardo, M. M., Yurkova, M., Gervasi, D. C., Raz, Y., Sang, Q. A., Fridman, R. (2000) "Binding of active (57 kDa) membrane type 1-matrix metalloproteinase (MT1-MMP) to tissue inhibitor of metalloproteinase (TIMP)-2 regulates MT1-MMP processing and pro-MMP-2 activation". *J Biol Chem* **275**:12080–9.

Hikita, A., Yana, I., Wakeyama, H., Nakamura, M., Kadono, Y., Oshima, Y., Nakamura, K., Seiki, M., Tanaka, S. (2006) "Negative regulation of osteoclastogenesis by ectodomain shedding of receptor activator of NF-kappaB ligand". *J Biol Chem* **281**:36846–55.

Hitchon, C., Wong, K., Ma, G., Reed, J., Lyttle, D., El-Gabalawy, H. (2002) "Hypoxia-induced production of stromal cell-derived factor 1 (CXCL12) and vascular endothelial growth factor by synovial fibroblasts". *Arthritis Rheum* **46**:2587–97.

Hitchon, C. A., El-Gabalawy, H. S. (2003) "The histopathology of early synovitis". *Clin Exp Rheumatol* **21**:S28–36.

Hitchon, C. A., El-Gabalawy, H. S. (2011) "The synovium in rheumatoid arthritis". *Open Rheumatol J* **5**:107–14.

Holmbeck, K., Bianco, P., Caterina, J., Yamada, S., Kromer, M., Kuznetsov, S. A., Mankani, M., Robey, P. G., Poole, A. R., Pidoux, I., Ward, J. M., Birkedal-Hansen, H. (1999) "MT1-MMP-deficient mice develop dwarfism, osteopenia, arthritis, and connective tissue disease due to inadequate collagen turnover". *Cell* **99**:81–92.

Holmbeck, K., Bianco, P., Pidoux, I., Inoue, S., Billinghurst, R. C., Wu, W., Chrysovergis, K., Yamada, S., Birkedal-Hansen, H., Poole, A. R. (2005) "The metalloproteinase MT1-MMP is required for normal development and maintenance of osteocyte processes in bone". *J Cell Sci* **118**:147–56.

Holmbeck, K., Bianco, P., Yamada, S., Birkedal-Hansen, H. (2004) "MT1-MMP: a tethered collagenase". *J Cell Physiol* **200**:11–9.

Hotary, K., Allen, E., Punturieri, A., Yana, I., Weiss, S. J. (2000) "Regulation of cell invasion and morphogenesis in a three-dimensional type I collagen matrix by membrane-type matrix metalloproteinases 1, 2, and 3". *J Cell Biol* **149**:1309–23.

Hotary, K., Li, X.-Y., Allen, E., Stevens, S. L., Weiss, S. J. (2006) "A cancer cell metalloprotease triad regulates the basement membrane transmigration program". *Genes Dev* **20**:2673–86.

Hotary, K. B., Allen, E. D., Brooks, P. C., Datta, N. S., Long, M. W., Weiss, S. J. (2003) "Membrane type I matrix metalloproteinase usurps tumor growth control imposed by the three-dimensional extracellular matrix". *Cell* **114**:33–45.

Hotary, K. B., Yana, I., Sabeh, F., Li, X.-Y., Holmbeck, K., Birkedal-Hansen, H., Allen, E. D., Hiraoka, N., Weiss, S. J. (2002) "Matrix metalloproteinases (MMPs) regulate fibrin-invasive activity via MT1-MMP-dependent and -independent processes". *J Exp Med* **195**:295–308.

Hou, G., Vogel, W., Bendeck, M. P. (2001) "The discoidin domain receptor tyrosine kinase DDR1 in arterial wound repair". *J Clin Invest* **107**:727–35.

Humphreys, J. H., Verstappen, S. M. M., Hyrich, K. L., Chipping, J. R., Marshall, T., Symmons, D. P. M. (2013) "The incidence of rheumatoid arthritis in the UK: comparisons using the 2010 ACR/EULAR classification criteria and the 1987 ACR classification criteria. Results from the Norfolk Arthritis Register". *Ann Rheum Dis* **72**:1315–20.

Humphries, J. D., Byron, A., Humphries, M. J. (2006) "Integrin ligands at a glance". *J Cell Sci* **119**:3901–3.

Hynes, R. O. (2002) "Integrins: bidirectional, allosteric signaling machines". *Cell* **110**:673–87.

Ikeda, K., Wang, L.-H., Torres, R., Zhao, H., Olaso, E., Eng, F. J., Labrador, P., Klein, R., Lovett, D., Yancopoulos, G. D., Friedman, S. L., Lin, H. C. (2002) "Discoidin domain receptor 2 interacts with Src and Shc following its activation by type I collagen". *J Biol Chem* **277**:19206–12.

Imboden, J. B. (2009) "The immunopathogenesis of rheumatoid arthritis". *Annual review of pathology* **4**:417–34.

Itoh, Y. (2006) "MT1-MMP: a key regulator of cell migration in tissue". *IUBMB Life* **58**:589–96.

Itoh, Y., Ito, N., Nagase, H., Evans, R. D., Bird, S. A., Seiki, M. (2006) "Cell surface collagenolysis requires homodimerization of the membrane-bound collagenase MT1-MMP". *Mol Biol Cell* **17**:5390–9.

Itoh, Y., Ito, N., Nagase, H., Seiki, M. (2008) "The second dimer interface of MT1-MMP, the transmembrane domain, is essential for ProMMP-2 activation on the cell surface". *J Biol Chem* **283**:13053–13062.

Itoh, Y., Palmisano, R., Anilkumar, N., Nagase, H., Miyawaki, A., Seiki, M. (2011) "Dimerization of MT1-MMP during cellular invasion detected by fluorescence resonance energy transfer". *Biochem J* **440**:319–26.

Itoh, Y., Seiki, M. (2006) "MT1-MMP: a potent modifier of pericellular microenvironment". *J Cell Physiol* **206**:1–8.

Itoh, Y., Takamura, A., Ito, N., Maru, Y., Sato, H., Suenaga, N., Aoki, T., Seiki, M. (2001) "Homophilic complex formation of MT1-MMP facilitates proMMP-2 activation on the cell surface and promotes tumor cell invasion". *EMBO J* **20**:4782–4793.

Jabaiah, A., Daugherty, P. S. (2011) "Directed evolution of protease beacons that enable sensitive detection of endogenous MT1-MMP activity in tumor cell lines". *Chem Biol* **18**:392–401.

Jain, A., Miller, M.-C., Troeberg, L., Itoh, Y., Brennan, F., Nanchahal, J. (2009) "Invasive potential of human rheumatoid tenosynovial cells is in part MT1-MMP dependent". *J Hand Surg Am* **34**:1282–90.

Jay, G. D., Britt, D. E., Cha, C. J. (2000) "Lubricin is a product of megakaryocyte stimulating factor gene expression by human synovial fibroblasts". *J Rheumatol* **27**:594–600.

Jiang, A., Lehti, K., Wang, X., Weiss, S. J., Keski-Oja, J., Pei, D. (2001) "Regulation of membrane-type matrix metalloproteinase 1 activity by dynamin-mediated endocytosis". *Proc Natl Acad Sci USA* **98**:13693–8.

Jiang, W. G., Davies, G., Martin, T. A., Parr, C., Watkins, G., Mason, M. D., Mansel, R. E. (2006) "Expression of membrane type-1 matrix metalloproteinase, MT1-MMP in human breast cancer and its impact on invasiveness of breast cancer cells". *International Journal of Molecular Medicine* **17**:583–90.

Jin, G., Zhang, F., Chan, K. M., Wong, H. L. X., Liu, B., Cheah, K. S. E., Liu, X., Mauch, C., Liu, D., Zhou, Z. (2011) "MT1-MMP cleaves Dll1 to negatively regulate Notch signalling to maintain normal B-cell development". *EMBO J* **30**:2281–93.

Johnson, J. D., Edman, J. C., Rutter, W. J. (1993) "A receptor tyrosine kinase found in breast carcinoma cells has an extracellular discoidin I-like domain". *Proc Natl Acad Sci USA* **90**:5677–81.

Kajita, M., Itoh, Y., Chiba, T., Mori, H., Okada, A., Kinoh, H., Seiki, M. (2001) "Membrane-type 1 matrix metalloproteinase cleaves CD44 and promotes cell migration". *J Cell Biol* **153**:893–904.

Kamat, A. A., Fletcher, M., Gruman, L. M., Mueller, P., Lopez, A., Landen, C. N., Han, L., Gershenson, D. M., Sood, A. K. (2006) "The clinical relevance of stromal matrix metalloproteinase expression in ovarian cancer". *Clin Cancer Res* **12**:1707–14.

Kanazawa, A., Oshima, T., Yoshihara, K., Tamura, S., Yamada, T., Inagaki, D., Sato, T., Yamamoto, N., Shiozawa, M., Morinaga, S., Akaike, M., Kunisaki, C., Tanaka, K., Masuda, M., Imada, T. (2010) "Relation of MT1-MMP gene expression to outcomes in colorectal cancer". *J Surg Oncol* **102**:571–5.

Kano, K., de Evsikova, C. M., Young, J., Wnek, C., Maddatu, T. P., Nishina, P. M., Naggert, J. K. (2008) "A novel dwarfism with gonadal dysfunction due to loss-of-function allele of the collagen receptor gene, Ddr2, in the mouse". *Mol Endocrinol* **22**:1866–80.

Karmakar, S., Kay, J., Gravallese, E. M. (2010) "Bone damage in rheumatoid arthritis: mechanistic insights and approaches to prevention". *Rheum Dis Clin North Am* **36**:385–404.

Karsdal, M. A., Larsen, L., Engsig, M. T., Lou, H., Ferreras, M., Lochter, A., Delaissé, J.-M., Foged, N. T. (2002) "Matrix metalloproteinase-dependent activation of latent transforming growth factor-beta controls the conversion of osteoblasts into osteocytes by blocking osteoblast apoptosis". *J Biol Chem* **277**:44061–7.

Karsdal, M. A., Madsen, S. H., Christiansen, C., Henriksen, K., Fosang, A. J., Sondergaard, B. C. (2008) "Cartilage degradation is fully reversible in the presence of aggrecanase but not matrix metalloproteinase activity". *Arthritis Res Ther* **10**:R63.

Karsdal, M. A., Woodworth, T., Henriksen, K., Maksymowych, W. P., Genant, H., Vergnaud, P., Christiansen, C., Schubert, T., Qvist, P., Schett, G., Platt, A., Bay-Jensen, A.-C. (2011) "Biochemical markers of ongoing joint damage in rheumatoid arthritis–current and future applications, limitations and opportunities". *Arthritis Res Ther* **13**:215.

Kashiwagi, M., Enghild, J. J., Gendron, C., Hughes, C., Caterson, B., Itoh, Y., Nagase, H. (2004) "Altered Proteolytic Activities of ADAMTS-4 Expressed by C-terminal Processing". *J Biol Chem* **279**:10109–10119.

Kashiwagi, M., Tortorella, M., Nagase, H., Brew, K. (2001) "TIMP-3 is a potent inhibitor of aggrecanase 1 (ADAM-TS4) and aggrecanase 2 (ADAM-TS5)". *J Biol Chem* **276**:12501–4.

Kazes, I., Elalamy, I., Sraer, J. D., Hatmi, M., Nguyen, G. (2000) "Platelet release of trimolecular complex components MT1-MMP/TIMP2/MMP2: involvement in MMP2 activation and platelet aggregation". *Blood* **96**:3064–9.

Kim, H.-G., Tan, L., Weisberg, E. L., Liu, F., Canning, P., Choi, H. G., Ezell, S. A., Wu, H., Zhao, Z., Wang, J., Mandinova, A., Griffin, J. D., Bullock, A. N., Liu, Q., Lee, S. W., Gray, N. S. (2013) "Discovery of a Potent and Selective DDR1 Receptor Tyrosine Kinase Inhibitor". *ACS Chem Biol* **8**:2145–50.

Knäuper, V., Bailey, L., Worley, J. R., Soloway, P., Patterson, M. L., Murphy, G. (2002) "Cellular activation of proMMP-13 by MT1-MMP depends on the C-terminal domain of MMP-13". *FEBS Lett* **532**:127–30.

Knight, C. G., Morton, L. F., Onley, D. J., Peachey, A. R., Messent, A. J., Smethurst, P. A., Tuckwell, D. S., Farndale, R. W., Barnes, M. J. (1998) "Identification in collagen

type I of an integrin alpha2 beta1-binding site containing an essential GER sequence". *J Biol Chem* **273**:33287–94.

Knight, C. G., Morton, L. F., Peachey, A. R., Tuckwell, D. S., Farndale, R. W., Barnes, M. J. (2000) "The collagen-binding A-domains of integrins alpha(1)beta(1) and alpha(2)beta(1) recognize the same specific amino acid sequence, GFOGER, in native (triple-helical) collagens". *J Biol Chem* **275**:35–40.

Kobayashi, I., Ziff, M. (1975) "Electron microscopic studies of the cartilage-pannus junction in rheumatoid arthritis". *Arthritis Rheum* **18**:475–83.

Koenig, G. C., Rowe, R. G., Day, S. M., Sabeh, F., Atkinson, J. J., Cooke, K. R., Weiss, S. J. (2012) "MT1-MMP-dependent remodeling of cardiac extracellular matrix structure and function following myocardial infarction". *Am J Pathol* **180**:1863–78.

Komano, Y., Nanki, T., Hayashida, K., Taniguchi, K., Miyasaka, N. (2006) "Identification of a human peripheral blood monocyte subset that differentiates into osteoclasts". *Arthritis Res Ther* **8**:R152.

Konitsiotis, A., Raynal, N., Bihan, D., Hohenester, E., Farndale, R. W., Leitinger, B. (2008) "Characterization of high affinity binding motifs for the discoidin domain receptor DDR2 in collagen". *J Biol Chem* **283**:6861–8.

Konttinen, Y. T., Ainola, M., Valleala, H., Ma, J., Ida, H., Mandelin, J., Kinne, R. W., Santavirta, S., Sorsa, T., López-Otín, C., Takagi, M. (1999a) "Analysis of 16 different matrix metalloproteinases (MMP-1 to MMP-20) in the synovial membrane: different profiles in trauma and rheumatoid arthritis". *Ann Rheum Dis* **58**:691–7.

Konttinen, Y. T., Ceponis, A., Takagi, M., Ainola, M., Sorsa, T., Sutinen, M., Salo, T., Ma, J., Santavirta, S., Seiki, M. (1998) "New collagenolytic enzymes/cascade identified at the pannus-hard tissue junction in rheumatoid arthritis: destruction from above". *Matrix Biol* **17**:585–601.

Konttinen, Y. T., Salo, T., Hanemaaijer, R., Valleala, H., Sorsa, T., Sutinen, M., Ceponis, A., Xu, J. W., Santavirta, S., Teronen, O., López-Otín, C. (1999b) "Collagenase-3 (MMP-13) and its activators in rheumatoid arthritis: localization in the pannus-hard tissue junction and inhibition by alendronate". *Matrix Biol* **18**:401–12.

Korb-Pap, A., Stratis, A., Mühlenberg, K., Niederreiter, B., Hayer, S., Echtermeyer, F., Stange, R., Zwerina, J., Pap, T., Pavenstädt, H., Schett, G., Smolen, J. S., Redlich, K. (2012) "Early structural changes in cartilage and bone are required for the attachment and invasion of inflamed synovial tissue during destructive inflammatory arthritis". *Ann Rheum Dis* **71**:1004–11.

Koshikawa, N., Giannelli, G., Cirulli, V., Miyazaki, K., Quaranta, V. (2000) "Role of cell surface metalloprotease MT1-MMP in epithelial cell migration over laminin-5". *J Cell Biol* **148**:615–624.

Koshikawa, N., Schenk, S., Moeckel, G., Sharabi, A., Miyazaki, K., Gardner, H., Zent, R., Quaranta, V. (2004) "Proteolytic processing of laminin-5 by MT1-MMP in tissues and its effects on epithelial cell morphology". *FASEB J* **18**:364–6.

Kotake, S., Nanke, Y., Mogi, M., Kawamoto, M., Furuya, T., Yago, T., Kobashigawa, T., Togari, A., Kamatani, N. (2005) "IFN-gamma-producing human T cells directly induce osteoclastogenesis from human monocytes via the expression of RANKL". *Eur J Immunol* **35**:3353–63.

Kotani, M., Hirata, K., Ogawa, S., Habiro, K., Ishida, Y., Tanuma, S., Horai, R., Iwakura, Y., Kishimoto, H., Abe, R. (2006) "CD28-dependent differentiation into the effector/memory phenotype is essential for induction of arthritis in interleukin-1 receptor antagonist-deficient mice". *Arthritis Rheum* **54**:473–81.

Kridel, S. J., Sawai, H., Ratnikov, B. I., Chen, E. I., Li, W., Godzik, A., Strongin, A. Y., Smith, J. W. (2002) "A unique substrate binding mode discriminates membrane type-1 matrix metalloproteinase from other matrix metalloproteinases". *J Biol Chem* **277**:23788–93.

Kvien, T. K. (2004) "Epidemiology and burden of illness of rheumatoid arthritis". *Pharmacoeconomics* **22**:1–12.

Labrador, J. P., Azcoitia, V., Tuckermann, J., Lin, C., Olaso, E., Mañes, S., Brückner, K., Goergen, J. L., Lemke, G., Yancopoulos, G., Angel, P., Martínez, C., Klein, R. (2001) "The collagen receptor DDR2 regulates proliferation and its elimination leads to dwarfism". *EMBO Rep* **2**:446–52.

Lafleur, M. A., Mercuri, F. A., Ruangpanit, N., Seiki, M., Sato, H., Thompson, E. W. (2006) "Type I collagen abrogates the clathrin-mediated internalization of membrane type 1 matrix metalloproteinase (MT1-MMP) via the MT1-MMP hemopexin domain". *J Biol Chem* **281**:6826–40.

Lafyatis, R., Remmers, E. F., Roberts, A. B., Yocum, D. E., Sporn, M. B., Wilder, R. L. (1989) "Anchorage-independent growth of synoviocytes from arthritic and normal joints. Stimulation by exogenous platelet-derived growth factor and inhibition by transforming growth factor-beta and retinoids". *J Clin Invest* **83**:1267–76.

Lark, M. W., Bayne, E. K., Flanagan, J., Harper, C. F., Hoerrner, L. A., Hutchinson, N. I., Singer, I. I., Donatelli, S. A., Weidner, J. R., Williams, H. R., Mumford, R. A., Lohmander, L. S. (1997) "Aggrecan degradation in human cartilage. Evidence for both matrix metalloproteinase and aggrecanase activity in normal, osteoarthritic, and rheumatoid joints". *J Clin Invest* **100**:93–106.

Lee, A. Y., Akers, K. T., Collier, M., Li, L., Eisen, A. Z., Seltzer, J. L. (1997) "Intracellular activation of gelatinase A (72-kDa type IV collagenase) by normal fibroblasts". *Proc Natl Acad Sci USA* **94**:4424–9.

Lee, D. M., Weinblatt, M. E. (2001) "Rheumatoid arthritis". *Lancet* **358**:903–11.

Lehti, K., Lohi, J., Juntunen, M. M., Pei, D., Keski-Oja, J. (2002) "Oligomerization through hemopexin and cytoplasmic domains regulates the activity and turnover of membrane-type 1 matrix metalloproteinase". *J Biol Chem* **277**:8440–8.

Lehti, K., Lohi, J., Valtanen, H., Keski-Oja, J. (1998) "Proteolytic processing of membrane-type-1 matrix metalloproteinase is associated with gelatinase A activation at the cell surface". *Biochem J* **334 (Pt 2)**:345–53.

Leikina, E., Mertts, M. V., Kuznetsova, N., Leikin, S. (2002) "Type I collagen is thermally unstable at body temperature". *Proc Natl Acad Sci USA* **99**:1314–8.

Leitinger, B. (2003) "Molecular analysis of collagen binding by the human discoidin domain receptors, DDR1 and DDR2. Identification of collagen binding sites in DDR2". *J Biol Chem* **278**:16761–9.

Leitinger, B. (2011) "Transmembrane Collagen Receptors". *Annu Rev Cell Dev Biol* **27**:265–90.

Leitinger, B., Hohenester, E. (2007) "Mammalian collagen receptors". *Matrix Biol* **26**:146–55.

Leitinger, B., Kwan, A. P. L. (2006) "The discoidin domain receptor DDR2 is a receptor for type X collagen". *Matrix Biol* **25**:355–64.

Leitinger, B., Steplewski, A., Fertala, A. (2004) "The D2 period of collagen II contains a specific binding site for the human discoidin domain receptor, DDR2". *J Mol Biol* **344**:993–1003.

Li, X.-Y., Ota, I., Yana, I., Sabeh, F., Weiss, S. J. (2008) "Molecular dissection of the structural machinery underlying the tissue-invasive activity of membrane type-1 matrix

metalloproteinase". *Mol Biol Cell* **19**:3221–33.

Li, Y., Aoki, T., Mori, Y., Ahmad, M., Miyamori, H., Takino, T., Sato, H. (2004) "Cleavage of lumican by membrane-type matrix metalloproteinase-1 abrogates this proteoglycan-mediated suppression of tumor cell colony formation in soft agar". *Cancer Res* **64**:7058–7064.

Li, Y., Xia, W., Liu, Y., Remmer, H. A., Voorhees, J., Fisher, G. J. (2013) "Solar ultraviolet irradiation induces decorin degradation in human skin likely via neutrophil elastase". *PLoS ONE* **8**:e72563.

Little, C. B., Meeker, C. T., Golub, S. B., Lawlor, K. E., Farmer, P. J., Smith, S. M., Fosang, A. J. (2007) "Blocking aggrecanase cleavage in the aggrecan interglobular domain abrogates cartilage erosion and promotes cartilage repair". *J Clin Invest* **117**:1627–36.

Livak, K. J., Schmittgen, T. D. (2001) "Analysis of relative gene expression data using real-time quantitative PCR and the 2(-Delta Delta C(T)) Method". *Methods* **25**:402–8.

Lohi, J., Keski-Oja, J. (1995) "Calcium ionophores decrease pericellular gelatinolytic activity via inhibition of 92-kDa gelatinase expression and decrease of 72-kDa gelatinase activation". *J Biol Chem* **270**:17602–9.

Lohi, J., Lehti, K., Valtanen, H., Parks, W. C., Keski-Oja, J. (2000) "Structural analysis and promoter characterization of the human membrane-type matrix metalloproteinase-1 (MT1-MMP) gene". *Gene* **242**:75–86.

Lohi, J., Lehti, K., Westermarck, J., Kähäri, V. M., Keski-Oja, J. (1996) "Regulation of membrane-type matrix metalloproteinase-1 expression by growth factors and phorbol 12-myristate 13-acetate". *Eur J Biochem* **239**:239–47.

Lombardo, L. J., Lee, F. Y., Chen, P., Norris, D., Barrish, J. C., Behnia, K., Castaneda, S., Cornelius, L. A. M., Das, J., Doweyko, A. M., Fairchild, C., Hunt, J. T., Inigo, I., Johnston, K., Kamath, A., Kan, D., Klei, H., Marathe, P., Pang, S., Peterson, R., Pitt, S., Schieven, G. L., Schmidt, R. J., Tokarski, J., Wen, M.-L., Wityak, J., Borzilleri, R. M. (2004) "Discovery of N-(2-chloro-6-methyl- phenyl)-2-(6-(4-(2-hydroxyethyl)-piperazin-1-yl)-2-methylpyrimidin-4- ylamino)thiazole-5-carboxamide (BMS-354825), a dual Src/Abl kinase inhibitor with potent antitumor activity in preclinical assays". *J Med Chem* **47**:6658–61.

Lowin, T., Straub, R. H. (2011) "Integrins and their ligands in rheumatoid arthritis". *Arthritis Res Ther* **13**:244.

Lu, C., Li, X.-Y., Hu, Y., Rowe, R. G., Weiss, S. J. (2010) "MT1-MMP controls human mesenchymal stem cell trafficking and differentiation". *Blood* **115**:221–9.

Lukas, C., van der Heijde, D., Fatenajad, S., Landewé, R. (2010) "Repair of erosions occurs almost exclusively in damaged joints without swelling". *Ann Rheum Dis* **69**:851–5.

Lundy, S. K., Sarkar, S., Tesmer, L. A., Fox, D. A. (2007) "Cells of the synovium in rheumatoid arthritis. T lymphocytes". *Arthritis Res Ther* **9**:202.

Luo, B.-H., Carman, C. V., Springer, T. A. (2007) "Structural basis of integrin regulation and signaling". *Annu Rev Immunol* **25**:619–47.

Määttä, M., Soini, Y., Liakka, A., Autio-Harmainen, H. (2000) "Differential expression of matrix metalloproteinase (MMP)-2, MMP-9, and membrane type 1-MMP in hepatocellular and pancreatic adenocarcinoma: implications for tumor progression and clinical prognosis". *Clin Cancer Res* **6**:2726–34.

MacGregor, A. J., Snieder, H., Rigby, A. S., Koskenvuo, M., Kaprio, J., Aho, K., Silman, A. J. (2000) "Characterizing the quantitative genetic contribution to rheumatoid arthritis using data from twins". *Arthritis Rheum* **43**:30–7.

Machold, K. P., Stamm, T. A., Nell, V. P. K., Pflugbeil, S., Aletaha, D., Steiner, G., Uffmann, M., Smolen, J. S. (2007) "Very recent onset rheumatoid arthritis: clinical

and serological patient characteristics associated with radiographic progression over the first years of disease". *Rheumatology (Oxford)* **46**:342–9.

Madsen, D. H., Engelholm, L. H., Ingvarsen, S., Hillig, T., Wagenaar-Miller, R. A., Kjøller, L., Gårdsvoll, H., Høyer-Hansen, G., Holmbeck, K., Bugge, T. H., Behrendt, N. (2007) "Extracellular collagenases and the endocytic receptor, urokinase plasminogen activator receptor-associated protein/Endo180, cooperate in fibroblast-mediated collagen degradation". *J Biol Chem* **282**:27037–45.

Marco, E. D., Cutuli, N., Guerra, L., Cancedda, R., Luca, M. D. (1993) "Molecular cloning of trkE, a novel trk-related putative tyrosine kinase receptor isolated from normal human keratinocytes and widely expressed by normal human tissues". *J Biol Chem* **268**:24290–5.

Martignetti, J. A., Aqeel, A. A., Sewairi, W. A., Boumah, C. E., Kambouris, M., Mayouf, S. A., Sheth, K. V., Eid, W. A., Dowling, O., Harris, J., Glucksman, M. J., Bahabri, S., Meyer, B. F., Desnick, R. J. (2001) "Mutation of the matrix metalloproteinase 2 gene (MMP2) causes a multicentric osteolysis and arthritis syndrome". *Nat Genet* **28**:261–5.

Martin, K. H., Hayes, K. E., Walk, E. L., Ammer, A. G., Markwell, S. M., Weed, S. A. (2012) "Quantitative measurement of invadopodia-mediated extracellular matrix proteolysis in single and multicellular contexts". *J Vis Exp*:e4119.

Mauri, C., Ehrenstein, M. R. (2007) "Cells of the synovium in rheumatoid arthritis. B cells". *Arthritis Res Ther* **9**:205.

McInnes, I. B., Schett, G. (2011) "The pathogenesis of rheumatoid arthritis". *N Engl J Med* **365**:2205–19.

McQuibban, G. A., Butler, G. S., Gong, J. H., Bendall, L., Power, C., Clark-Lewis, I., Overall, C. M. (2001) "Matrix metalloproteinase activity inactivates the CXC chemokine stromal cell-derived factor-1". *J Biol Chem* **276**:43503–8.

McQuibban, G. A., Gong, J.-H., Wong, J. P., Wallace, J. L., Clark-Lewis, I., Overall, C. M. (2002) "Matrix metalloproteinase processing of monocyte chemoattractant proteins generates CC chemokine receptor antagonists with anti-inflammatory properties in vivo". *Blood* **100**:1160–7.

Medici, D., Nawshad, A. (2010) "Type I collagen promotes epithelial-mesenchymal transition through ILK-dependent activation of NF-kappaB and LEF-1". *Matrix Biol* **29**:161–5.

Migita, K., Eguchi, K., Kawabe, Y., Ichinose, Y., Tsukada, T., Aoyagi, T., Nakamura, H., Nagataki, S. (1996) "TNF-alpha-mediated expression of membrane-type matrix metalloproteinase in rheumatoid synovial fibroblasts". *Immunology* **89**:553–7.

Mihai, C., Chotani, M., Elton, T. S., Agarwal, G. (2009) "Mapping of DDR1 distribution and oligomerization on the cell surface by FRET microscopy". *J Mol Biol* **385**:432–45.

Miller, M.-C., Manning, H. B., Jain, A., Troeberg, L., Dudhia, J., Essex, D., Sandison, A., Seiki, M., Nanchahal, J., Nagase, H., Itoh, Y. (2009) "Membrane type 1 matrix metalloproteinase is a crucial promoter of synovial invasion in human rheumatoid arthritis". *Arthritis Rheum* **60**:686–97.

Mitra, S. K., Hanson, D. A., Schlaepfer, D. D. (2005) "Focal adhesion kinase: in command and control of cell motility". *Nat Rev Mol Cell Biol* **6**:56–68.

Mitsui, H., Tsuchiya, N., Okinaga, S., Matsuta, K., Yoshimura, K., Nishimura, A. (2001) "Expression of membrane-type matrix metalloproteinases in synovial tissue from patients with rheumatoid arthritis or osteoarthritis". *Modern Rheumatology* **11**:34–39.

Miyachi, K., Ihara, A., Hankins, R. W., Murai, R., Maehiro, S., Miyashita, H. (2003) "Efficacy of imatinib mesylate (STI571) treatment for a patient with rheumatoid arthritis developing chronic myelogenous leukemia". *Clin Rheumatol* **22**:329–32.

Mori, H., Tomari, T., Koshikawa, N., Kajita, M., Itoh, Y., Sato, H., Tojo, H., Yana, I., Seiki, M. (2002) "CD44 directs membrane-type 1 matrix metalloproteinase to lamellipodia by associating with its hemopexin-like domain". *EMBO J* **21**:3949–3959.

Mu, D., Cambier, S., Fjellbirkeland, L., Baron, J. L., Munger, J. S., Kawakatsu, H., Sheppard, D., Broaddus, V. C., Nishimura, S. L. (2002) "The integrin alpha(v)beta8 mediates epithelial homeostasis through MT1-MMP-dependent activation of TGF-beta1". *J Cell Biol* **157**:493–507.

Müller-Ladner, U., Kriegsmann, J., Franklin, B. N., Matsumoto, S., Geiler, T., Gay, R. E., Gay, S. (1996) "Synovial fibroblasts of patients with rheumatoid arthritis attach to and invade normal human cartilage when engrafted into SCID mice". *Am J Pathol* **149**:1607–15.

Murphy, D. A., Courtneidge, S. A. (2011) "The 'ins' and 'outs' of podosomes and invadopodia: characteristics, formation and function". *Nat Rev Mol Cell Biol* **12**:413–26.

Murphy, G. (2011) "Tissue inhibitors of metalloproteinases". *Genome Biol* **12**:233.

Murphy, G., Nagase, H. (2008) "Reappraising metalloproteinases in rheumatoid arthritis and osteoarthritis: destruction or repair?". *Nature clinical practice Rheumatology* **4**:128–35.

Murphy, G., Nagase, H. (2011) "Localizing matrix metalloproteinase activities in the pericellular environment". *FEBS J* **278**:2–15.

Myllyharju, J., Kivirikko, K. I. (2004) "Collagens, modifying enzymes and their mutations in humans, flies and worms". *Trends Genet* **20**:33–43.

Nagano, M., Hoshino, D., Koshikawa, N., Akizawa, T., Seiki, M. (2012) "Turnover of focal adhesions and cancer cell migration". *International Journal of Cell Biology* **2012**:310616.

Nagase, H., Kashiwagi, M. (2003) "Aggrecanases and cartilage matrix degradation". *Arthritis Res Ther* **5**:94–103.

Nagase, H., Visse, R. (2011) "Triple Helicase Activity and the Structural Basis of Collagenolysis". In: Parks, W. C., Mecham, R. P. (Eds.), Extracellular Matrix Degradation. Vol. 2. Springer Berlin Heidelberg, pp. 95–122.

Nagase, H., Visse, R., Murphy, G. (2006) "Structure and function of matrix metalloproteinases and TIMPs". *Cardiovasc Res* **69**:562–73.

Nakada, M., Yamada, A., Takino, T., Miyamori, H., Takahashi, T., Yamashita, J., Sato, H. (2001) "Suppression of membrane-type 1 matrix metalloproteinase (MMP)-mediated MMP-2 activation and tumor invasion by testican 3 and its splicing variant gene product, N-Tes". *Cancer Res* **61**:8896–902.

Nakamura, H., Suenaga, N., Taniwaki, K., Matsuki, H., Yonezawa, K., Fujii, M., Okada, Y., Seiki, M. (2004) "Constitutive and induced CD44 shedding by ADAM-like proteases and membrane-type 1 matrix metalloproteinase". *Cancer Res* **64**:876–82.

Ng, C. T., Biniecka, M., Kennedy, A., McCormick, J., Fitzgerald, O., Bresnihan, B., Buggy, D., Taylor, C. T., O'Sullivan, J., Fearon, U., Veale, D. J. (2010) "Synovial tissue hypoxia and inflammation in vivo". *Ann Rheum Dis* **69**:1389–95.

Nguyen, M., Arkell, J., Jackson, C. J. (2000) "Three-dimensional collagen matrices induce delayed but sustained activation of gelatinase A in human endothelial cells via MT1-MMP". *Int J Biochem Cell Biol* **32**:621–31.

Nishimura, K., Sugiyama, D., Kogata, Y., Tsuji, G., Nakazawa, T., Kawano, S., Saigo, K., Morinobu, A., Koshiba, M., Kuntz, K. M., Kamae, I., Kumagai, S. (2007) "Meta-analysis: diagnostic accuracy of anti-cyclic citrullinated peptide antibody and rheumatoid factor for rheumatoid arthritis". *Ann Intern Med* **146**:797–808.

Noordeen, N. A., Carafoli, F., Hohenester, E., Horton, M. A., Leitinger, B. (2006) "A transmembrane leucine zipper is required for activation of the dimeric receptor tyrosine kinase DDR1". *J Biol Chem* **281**:22744–51.

Nuttall, R. K., Sampieri, C. L., Pennington, C. J., Gill, S. E., Schultz, G. A., Edwards, D. R. (2004) "Expression analysis of the entire MMP and TIMP gene families during mouse tissue development". *FEBS Lett* **563**:129–34.

Nyalendo, C., Beaulieu, E., Sartelet, H., Michaud, M., Fontaine, N., Gingras, D., Béliveau, R. (2008) "Impaired tyrosine phosphorylation of membrane type 1-matrix metalloproteinase reduces tumor cell proliferation in three-dimensional matrices and abrogates tumor growth in mice". *Carcinogenesis* **29**:1655–64.

Nyalendo, C., Michaud, M., Beaulieu, E., Roghi, C., Murphy, G., Gingras, D., Béliveau, R. (2007) "Src-dependent phosphorylation of membrane type I matrix metalloproteinase on cytoplasmic tyrosine 573: role in endothelial and tumor cell migration". *J Biol Chem* **282**:15690–9.

Oh, J., Takahashi, R., Kondo, S., Mizoguchi, A., Adachi, E., Sasahara, R. M., Nishimura, S., Imamura, Y., Kitayama, H., Alexander, D. B., Ide, C., Horan, T. P., Arakawa, T., Yoshida, H., Nishikawa, S., Itoh, Y., Seiki, M., Itohara, S., Takahashi, C., Noda, M. (2001) "The membrane-anchored MMP inhibitor RECK is a key regulator of extracellular matrix integrity and angiogenesis". *Cell* **107**:789–800.

Ohkubo, S., Miyadera, K., Sugimoto, Y., Matsuo, K., Wierzba, K., Yamada, Y. (1999) "Identification of substrate sequences for membrane type-1 matrix metalloproteinase using bacteriophage peptide display library". *Biochem Biophys Res Commun* **266**:308–13.

Ohtake, Y., Tojo, H., Seiki, M. (2006) "Multifunctional roles of MT1-MMP in myofiber formation and morphostatic maintenance of skeletal muscle". *J Cell Sci* **119**:3822–32.

Ohtani, H., Motohashi, H., Sato, H., Seiki, M., Nagura, H. (1996) "Dual over-expression pattern of membrane-type metalloproteinase-1 in cancer and stromal cells in human gastrointestinal carcinoma revealed by in situ hybridization and immunoelectron microscopy". *Int J Cancer* **68**:565–70.

Ohuchi, E., Imai, K., Fujii, Y., Sato, H., Seiki, M., Okada, Y. (1997) "Membrane type 1 matrix metalloproteinase digests interstitial collagens and other extracellular matrix macromolecules". *J Biol Chem* **272**:2446–2451.

Okada, A., Bellocq, J. P., Rouyer, N., Chenard, M. P., Rio, M. C., Chambon, P., Basset, P. (1995) "Membrane-type matrix metalloproteinase (MT-MMP) gene is expressed in stromal cells of human colon, breast, and head and neck carcinomas". *Proc Natl Acad Sci USA* **92**:2730–4.

Okada, A., Tomasetto, C., Lutz, Y., Bellocq, J. P., Rio, M. C., Basset, P. (1997) "Expression of matrix metalloproteinases during rat skin wound healing: evidence that membrane type-1 matrix metalloproteinase is a stromal activator of pro-gelatinase A". *J Cell Biol* **137**:67–77.

Olaso, E., Ikeda, K., Eng, F. J., Xu, L., Wang, L. H., Lin, H. C., Friedman, S. L. (2001) "DDR2 receptor promotes MMP-2-mediated proliferation and invasion by hepatic stellate cells". *J Clin Invest* **108**:1369–78.

Olaso, E., Lin, H.-C., Wang, L.-H., Friedman, S. L. (2011) "Impaired dermal wound healing in discoidin domain receptor 2-deficient mice associated with defective extracellular matrix remodeling". *Fibrogenesis & Tissue Repair* **4**:5.

Orgel, J. P. R. O., Antipova, O., Sagi, I., Bitler, A., Qiu, D., Wang, R., Xu, Y., Antonio, J. D. S. (2011a) "Collagen fibril surface displays a constellation of sites capable of promoting fibril assembly, stability, and hemostasis". *Connect Tissue Res* **52**:18–24.

Orgel, J. P. R. O., Antonio, J. D. S., Antipova, O. (2011b) "Molecular and structural mapping of collagen fibril interactions". *Connect Tissue Res* **52**:2–17.

Orgel, J. P. R. O., Irving, T. C., Miller, A., Wess, T. J. (2006) "Microfibrillar structure of type I collagen in situ". *Proc Natl Acad Sci USA* **103**:9001–5.

Ota, I., Li, X.-Y., Hu, Y., Weiss, S. J. (2009) "Induction of a MT1-MMP and MT2-MMP-dependent basement membrane transmigration program in cancer cells by Snail1". *Proc Natl Acad Sci USA* **106**:20318–23.

Overall, C. M., Sodek, J. (1990) "Concanavalin A produces a matrix-degradative phenotype in human fibroblasts. Induction and endogenous activation of collagenase, 72-kDa gelatinase, and Pump-1 is accompanied by the suppression of the tissue inhibitor of matrix metalloproteinases". *J Biol Chem* **265**:21141–51.

Padyukov, L., Silva, C., Stolt, P., Alfredsson, L., Klareskog, L. (2004) "A gene-environment interaction between smoking and shared epitope genes in HLA-DR provides a high risk of seropositive rheumatoid arthritis". *Arthritis Rheum* **50**:3085–92.

Page-McCaw, A., Ewald, A. J., Werb, Z. (2007) "Matrix metalloproteinases and the regulation of tissue remodelling". *Nat Rev Mol Cell Biol* **8**:221–33.

Pakozdi, A., Amin, M. A., Haas, C. S., Martinez, R. J., Haines, G. K., Santos, L. L., Morand, E. F., David, J. R., Koch, A. E. (2006) "Macrophage migration inhibitory factor: a mediator of matrix metalloproteinase-2 production in rheumatoid arthritis". *Arthritis Res Ther* **8**:R132.

Palmisano, R., Itoh, Y. (2010) "Analysis of MMP-dependent cell migration and invasion". *Methods Mol Biol* **622**:379–92.

Paniagua, R. T., Sharpe, O., Ho, P. P., Chan, S. M., Chang, A., Higgins, J. P., Tomooka, B. H., Thomas, F. M., Song, J. J., Goodman, S. B., Lee, D. M., Genovese, M. C., Utz, P. J., Steinman, L., Robinson, W. H. (2006) "Selective tyrosine kinase inhibition by imatinib mesylate for the treatment of autoimmune arthritis". *J Clin Invest* **116**:2633–42.

Pap, T., Franz, J. K., Hummel, K. M., Jeisy, E., Gay, R., Gay, S. (2000a) "Activation of synovial fibroblasts in rheumatoid arthritis: lack of Expression of the tumour suppressor PTEN at sites of invasive growth and destruction". *Arthritis Res* **2**:59–64.

Pap, T., Shigeyama, Y., Kuchen, S., Fernihough, J. K., Simmen, B., Gay, R. E., Billingham, M., Gay, S. (2000b) "Differential expression pattern of membrane-type matrix metalloproteinases in rheumatoid arthritis". *Arthritis Rheum* **43**:1226–1232.

Pei, D. (1999) "Identification and characterization of the fifth membrane-type matrix metalloproteinase MT5-MMP". *J Biol Chem* **274**:8925–32.

Peinado, H., Olmeda, D., Cano, A. (2007) "Snail, Zeb and bHLH factors in tumour progression: an alliance against the epithelial phenotype?". *Nat Rev Cancer* **7**:415–28.

Perentes, J. Y., Kirkpatrick, N. D., Nagano, S., Smith, E. Y., Shaver, C. M., Sgroi, D., Garkavtsev, I., Munn, L. L., Jain, R. K., Boucher, Y. (2011) "Cancer cell-associated MT1-MMP promotes blood vessel invasion and distant metastasis in triple-negative mammary tumors". *Cancer Res* **71**:4527–38.

Perumal, S., Antipova, O., Orgel, J. P. R. O. (2008) "Collagen fibril architecture, domain organization, and triple-helical conformation govern its proteolysis". *Proc Natl Acad Sci USA* **105**:2824–9.

Petrella, B. L., Lohi, J., Brinckerhoff, C. E. (2005) "Identification of membrane type-1 matrix metalloproteinase as a target of hypoxia-inducible factor-2 alpha in von Hippel-Lindau renal cell carcinoma". *Oncogene* **24**:1043–52.

Petrow, P. K., Wernicke, D., Westhoff, C. S., Hummel, K. M., Bräuer, R., Kriegsmann, J., Gromnica-Ihle, E., Gay, R. E., Gay, S. (2002) "Characterisation of the cell type-

specificity of collagenase 3 mRNA expression in comparison with membrane type 1 matrix metalloproteinase and gelatinase A in the synovial membrane in rheumatoid arthritis". *Ann Rheum Dis* **61**:391–7.

Playford, M. P., Butler, R. J., Wang, X. C., Katso, R. M., Cooke, I. E., Ganesan, T. S. (1996) "The genomic structure of discoidin receptor tyrosine kinase". *Genome Res* **6**:620–7.

Poincloux, R., Lizárraga, F., Chavrier, P. (2009) "Matrix invasion by tumour cells: a focus on MT1-MMP trafficking to invadopodia". *J Cell Sci* **122**:3015–24.

Polette, M., Gilles, C., Marchand, V., Seiki, M., Tournier, J. M., Birembaut, P. (1997) "Induction of membrane-type matrix metalloproteinase 1 (MT1-MMP) expression in human fibroblasts by breast adenocarcinoma cells". *Clin Exp Metastasis* **15**:157–63.

Polette, M., Nawrocki, B., Gilles, C., Sato, H., Seiki, M., Tournier, J. M., Birembaut, P. (1996) "MT-MMP expression and localisation in human lung and breast cancers". *Virchows Arch* **428**:29–35.

Popova, S. N., Lundgren-Akerlund, E., Wiig, H., Gullberg, D. (2007) "Physiology and pathology of collagen receptors". *Acta Physiol (Oxf)* **190**:179–87.

Porter, S., Clark, I. M., Kevorkian, L., Edwards, D. R. (2005) "The ADAMTS metalloproteinases". *Biochem J* **386**:15–27.

Pratta, M. A., Yao, W., Decicco, C., Tortorella, M. D., Liu, R.-Q., Copeland, R. A., Magolda, R., Newton, R. C., Trzaskos, J. M., Arner, E. C. (2003) "Aggrecan protects cartilage collagen from proteolytic cleavage". *J Biol Chem* **278**:45539–45.

Prince, F. H. M., Bykerk, V. P., Shadick, N. A., Lu, B., Cui, J., Frits, M., Iannaccone, C. K., Weinblatt, M. E., Solomon, D. H. (2012) "Sustained rheumatoid arthritis remission is uncommon in clinical practice". *Arthritis Res Ther* **14**:R68.

Ratnikov, B. I., Rozanov, D. V., Postnova, T. I., Baciu, P. G., Zhang, H., DiScipio, R. G., Chestukhina, G. G., Smith, J. W., Deryugina, E. I., Strongin, A. Y. (2002) "An alternative processing of integrin alpha(v) subunit in tumor cells by membrane type-1 matrix metalloproteinase". *J Biol Chem* **277**:7377–85.

Raychaudhuri, S., Sandor, C., Stahl, E. A., Freudenberg, J., Lee, H.-S., Jia, X., Alfredsson, L., Padyukov, L., Klareskog, L., Worthington, J., Siminovitch, K. A., Bae, S.-C., Plenge, R. M., Gregersen, P. K., Bakker, P. I. W. D. (2012) "Five amino acids in three HLA proteins explain most of the association between MHC and seropositive rheumatoid arthritis". *Nat Genet* **44**:291–296.

Raynal, N., Hamaia, S. W., Siljander, P. R.-M., Maddox, B., Peachey, A. R., Fernandez, R., Foley, L. J., Slatter, D. A., Jarvis, G. E., Farndale, R. W. (2006) "Use of synthetic peptides to locate novel integrin alpha2beta1-binding motifs in human collagen III". *J Biol Chem* **281**:3821–31.

Remacle, A., Murphy, G., Roghi, C. (2003) "Membrane type I-matrix metalloproteinase (MT1-MMP) is internalised by two different pathways and is recycled to the cell surface". *J Cell Sci* **116**:3905–16.

Remacle, A. G., Chekanov, A. V., Golubkov, V. S., Savinov, A. Y., Rozanov, D. V., Strongin, A. Y. (2006) "O-glycosylation regulates autolysis of cellular membrane type-1 matrix metalloproteinase (MT1-MMP)". *J Biol Chem* **281**:16897–905.

Remacle, A. G., Golubkov, V. S., Shiryaev, S. A., Dahl, R., Stebbins, J. L., Chernov, A. V., Cheltsov, A. V., Pellecchia, M., Strongin, A. Y. (2012) "Novel MT1-MMP small-molecule inhibitors based on insights into hemopexin domain function in tumor growth". *Cancer Res* **72**:2339–49.

Remacle, A. G., Rozanov, D. V., Baciu, P. C., Chekanov, A. V., Golubkov, V. S., Strongin, A. Y. (2005) "The transmembrane domain is essential for the microtubular trafficking

of membrane type-1 matrix metalloproteinase (MT1-MMP)". *J Cell Sci* **118**:4975–84.

Rengel, Y., Ospelt, C., Gay, S. (2007) "Proteinases in the joint: clinical relevance of proteinases in joint destruction". *Arthritis Res Ther* **9**:221.

Ricard-Blum, S. (2011) "The collagen family". *Cold Spring Harb Perspect Biol* **3**:a004978.

Ridley, A. J. (2011) "Life at the leading edge". *Cell* **145**:1012–22.

Riggins, K. S., Mernaugh, G., Su, Y., Quaranta, V., Koshikawa, N., Seiki, M., Pozzi, A., Zent, R. (2010) "MT1-MMP-mediated basement membrane remodeling modulates renal development". *Exp Cell Res* **316**:2993–3005.

Rinaldi, N., Schwarz-Eywill, M., Weis, D., Leppelmann-Jansen, P., Lukoschek, M., Keilholz, U., Barth, T. F. (1997) "Increased expression of integrins on fibroblast-like synoviocytes from rheumatoid arthritis in vitro correlates with enhanced binding to extracellular matrix proteins". *Ann Rheum Dis* **56**:45–51.

Rowe, R. G., Keena, D., Sabeh, F., Willis, A. L., Weiss, S. J. (2011) "Pulmonary Fibroblasts Mobilize the Membrane-Tethered Matrix Metalloprotease, MT1-MMP, to Destructively Remodel and Invade Interstitial Type I Collagen Barriers". *Am J Physiol Lung Cell Mol Physiol* **301**:L683–92.

Rowe, R. G., Li, X.-Y., Hu, Y., Saunders, T. L., Virtanen, I., de Herreros, A. G., Becker, K.-F., Ingvarsen, S., Engelholm, L. H., Bommer, G. T., Fearon, E. R., Weiss, S. J. (2009) "Mesenchymal cells reactivate Snail1 expression to drive three-dimensional invasion programs". *J Cell Biol* **184**:399–408.

Rozanov, D. V., Hahn-Dantona, E., Strickland, D. K., Strongin, A. Y. (2004) "The low density lipoprotein receptor-related protein LRP is regulated by membrane type-1 matrix metalloproteinase (MT1-MMP) proteolysis in malignant cells". *J Biol Chem* **279**:4260–8.

Ruangpanit, N., Chan, D., Holmbeck, K., Birkedal-Hansen, H., Polarek, J., Yang, C., Bateman, J. F., Thompson, E. W. (2001) "Gelatinase A (MMP-2) activation by skin fibroblasts: dependence on MT1-MMP expression and fibrillar collagen form". *Matrix Biol* **20**:193–203.

Ruangpanit, N., Price, J. T., Holmbeck, K., Birkedal-Hansen, H., Guenzler, V., Huang, X., Chan, D., Bateman, J. F., Thompson, E. W. (2002) "MT1-MMP-dependent and -independent regulation of gelatinase A activation in long-term, ascorbate-treated fibroblast cultures: regulation by fibrillar collagen". *Exp Cell Res* **272**:109–18.

Rutkauskaite, E., Volkmer, D., Shigeyama, Y., Schedel, J., Pap, G., Müller-Ladner, U., Meinecke, I., Alexander, D., Gay, R. E., Drynda, S., Neumann, W., Michel, B. A., Aicher, W. K., Gay, S., Pap, T. (2005) "Retroviral gene transfer of an antisense construct against membrane type 1 matrix metalloproteinase reduces the invasiveness of rheumatoid arthritis synovial fibroblasts". *Arthritis Rheum* **52**:2010–4.

Ruyssen-Witrand, A., Constantin, A., Cambon-Thomsen, A., Thomsen, M. (2012) "New insights into the genetics of immune responses in rheumatoid arthritis". *Tissue Antigens* **80**:105–18.

Sabeh, F., Fox, D., Weiss, S. J. (2010) "Membrane-type I matrix metalloproteinase-dependent regulation of rheumatoid arthritis synoviocyte function". *J Immunol* **184**:6396–406.

Sabeh, F., Li, X.-Y., Saunders, T. L., Rowe, R. G., Weiss, S. J. (2009a) "Secreted versus membrane-anchored collagenases: relative roles in fibroblast-dependent collagenolysis and invasion". *J Biol Chem* **284**:23001–11.

Sabeh, F., Ota, I., Holmbeck, K., Birkedal-Hansen, H., Soloway, P., Balbin, M., Lopez-Otin, C., Shapiro, S., Inada, M., Krane, S., Allen, E., Chung, D., Weiss, S. J. (2004) "Tumor cell traffic through the extracellular matrix is controlled by the membrane-

anchored collagenase MT1-MMP". *J Cell Biol* **167**:769–81.

Sabeh, F., Shimizu-Hirota, R., Weiss, S. J. (2009b) "Protease-dependent versus -independent cancer cell invasion programs: three-dimensional amoeboid movement revisited". *J Cell Biol* **185**:11–9.

Sakai, K., Nakamura, T., Suzuki, Y., Imizu, T., Matsumoto, K. (2011) "3-D collagen-dependent cell surface expression of MT1-MMP and MMP-2 activation regardless of integrin B1 function and matrix stiffness". *Biochem Biophys Res Commun* **412**:98–103.

Sambrook, J., Russell, D. W. (2001) "Plasmids and Their Usefulness in Molecular Cloning". In: Sambrook, J., Russell, D. W. (Eds.), Molecular Cloning: A Laboratory Manual, 3rd Edition. Cold Spring Harbor Laboratory Press, p. Protocol 1.32.

Sarkissian, M., Lafyatis, R. (1999) "Integrin engagement regulates proliferation and collagenase expression of rheumatoid synovial fibroblasts". *J Immunol* **162**:1772–9.

Sato, H., Kinoshita, T., Takino, T., Nakayama, K., Seiki, M. (1996) "Activation of a recombinant membrane type 1-matrix metalloproteinase (MT1-MMP) by furin and its interaction with tissue inhibitor of metalloproteinases (TIMP)-2". *FEBS Lett* **393**:101–4.

Sato, H., Takino, T., Okada, Y., Cao, J., Shinagawa, A., Yamamoto, E., Seiki, M. (1994) "A matrix metalloproteinase expressed on the surface of invasive tumour cells". *Nature* **370**:61–65.

Sato, K., Ebihara, T., Adachi, E., Kawashima, S., Hattori, S., Irie, S. (2000) "Possible involvement of aminotelopeptide in self-assembly and thermal stability of collagen I as revealed by its removal with proteases". *J Biol Chem* **275**:25870–5.

Schett, G. (2007) "Cells of the synovium in rheumatoid arthritis. Osteoclasts". *Arthritis Res Ther* **9**:203.

Schett, G. (2012) "Biology, Physiology, and Morphology of Bone". In: Firestein, G. S., Budd, R. C., Gabriel, S. E., McInnes, I. B., O'Dell, J. R. (Eds.), Kelley's Textbook of Rheumatology, 9th Edition. Saunders, pp. 61 – 66.

Schett, G., Gravallese, E. (2012) "Bone erosion in rheumatoid arthritis: mechanisms, diagnosis and treatment". *Nat Rev Rheumatol* **8**:656–64.

Scott, D. L. (2012) "Biologics-based therapy for the treatment of rheumatoid arthritis". *Clin Pharmacol Ther* **91**:30–43.

Seemayer, C. A., Kuchen, S., Kuenzler, P., Rihosková, V., Rethage, J., Aicher, W. K., Michel, B. A., Gay, R. E., Kyburz, D., Neidhart, M., Gay, S. (2003) "Cartilage destruction mediated by synovial fibroblasts does not depend on proliferation in rheumatoid arthritis". *Am J Pathol* **162**:1549–57.

Seiki, M. (1999) "Membrane-type matrix metalloproteinases". *APMIS* **107**:137–143.

Seiki, M. (2003) "Membrane-type 1 matrix metalloproteinase: a key enzyme for tumor invasion". *Cancer Lett* **194**:1–11.

Selvais, C., D'Auria, L., Tyteca, D., Perrot, G., Lemoine, P., Troeberg, L., Dedieu, S., Noël, A., Nagase, H., Henriet, P., Courtoy, P. J., Marbaix, E., Emonard, H. (2011) "Cell cholesterol modulates metalloproteinase-dependent shedding of low-density lipoprotein receptor-related protein-1 (LRP-1) and clearance function". *FASEB J* **25**:2770–81.

Shields, M. A., Krantz, S. B., Bentrem, D. J., Dangi-Garimella, S., Munshi, H. G. (2012) "Interplay between B1-integrin and Rho signaling regulates the differential scattering and motility of pancreatic cancer cells by snail and slug". *J Biol Chem* **287**:6218–29.

Shiozawa, S., Shiozawa, K., Fujita, T. (1983) "Morphologic observations in the early phase of the cartilage-pannus junction. Light and electron microscopic studies of active cellular pannus". *Arthritis Rheum* **26**:472–8.

Shoulders, M. D., Raines, R. T. (2009) "Collagen structure and stability". *Annu Rev Biochem* **78**:929–58.

Shrivastava, A., Radziejewski, C., Campbell, E., Kovac, L., McGlynn, M., Ryan, T. E., Davis, S., Goldfarb, M. P., Glass, D. J., Lemke, G., Yancopoulos, G. D. (1997) "An orphan receptor tyrosine kinase family whose members serve as nonintegrin collagen receptors". *Mol Cell* **1**:25–34.

Shuo, T., Koshikawa, N., Hoshino, D., Minegishi, T., Ao-Kondo, H., Oyama, M., Sekiya, S., Iwamoto, S., Tanaka, K., Seiki, M. (2012) "Detection of the heterogeneous O-glycosylation profile of MT1-MMP expressed in cancer cells by a simple MALDI-MS method". *PLoS ONE* **7**:e43751.

Silman, A. J., Newman, J., MacGregor, A. J. (1996) "Cigarette smoking increases the risk of rheumatoid arthritis. Results from a nationwide study of disease-discordant twins". *Arthritis Rheum* **39**:732–5.

Slack, B. E., Siniaia, M. S., Blusztajn, J. K. (2006) "Collagen type I selectively activates ectodomain shedding of the discoidin domain receptor 1: involvement of Src tyrosine kinase". *J Cell Biochem* **98**:672–84.

Smith, M. D. (2011) "The normal synovium". *Open Rheumatol J* **5**:100–6.

Smolen, J. S., Steiner, G. (2003) "Therapeutic strategies for rheumatoid arthritis". *Nat Rev Drug Discov* **2**:473–88.

Smolian, H., Aurer, A., Sittinger, M., Zacher, J., Bernimoulin, J. P., Burmester, G. R., Kolkenbrock, H. (2001) "Secretion of gelatinases and activation of gelatinase A (MMP-2) by human rheumatoid synovial fibroblasts". *Biol Chem* **382**:1491–9.

Song, R.-H., Tortorella, M. D., Malfait, A.-M., Alston, J. T., Yang, Z., Arner, E. C., Griggs, D. W. (2007) "Aggrecan degradation in human articular cartilage explants is mediated by both ADAMTS-4 and ADAMTS-5". *Arthritis Rheum* **56**:575–85.

Song, S., Shackel, N. A., Wang, X. M., Ajami, K., McCaughan, G. W., Gorrell, M. D. (2011) "Discoidin domain receptor 1: isoform expression and potential functions in cirrhotic human liver". *Am J Pathol* **178**:1134–44.

Soto, H., Hevezi, P., Roth, R. B., Pahuja, A., Alleva, D., Acosta, H. M., Martinez, C., Ortega, A., Lopez, A., Araiza-Casillas, R., Zlotnik, A. (2008) "Gene array analysis comparison between rat collagen-induced arthritis and human rheumatoid arthritis". *Scand J Immunol* **68**:43–57.

Sroka, I. C., Nagle, R. B., Bowden, G. T. (2007) "Membrane-type 1 matrix metalloproteinase is regulated by sp1 through the differential activation of AKT, JNK, and ERK pathways in human prostate tumor cells". *Neoplasia* **9**:406–17.

Stanton, H., Gavrilovic, J., Atkinson, S. J., d'Ortho, M. P., Yamada, K. M., Zardi, L., Murphy, G. (1998) "The activation of ProMMP-2 (gelatinase A) by HT1080 fibrosarcoma cells is promoted by culture on a fibronectin substrate and is concomitant with an increase in processing of MT1-MMP (MMP-14) to a 45 kDa form". *J Cell Sci* **111 (Pt 18)**:2789–98.

Stanton, H., Melrose, J., Little, C. B., Fosang, A. J. (2011) "Proteoglycan degradation by the ADAMTS family of proteinases". *Biochim Biophys Acta* **1812**:1616–29.

Stanton, H., Rogerson, F. M., East, C. J., Golub, S. B., Lawlor, K. E., Meeker, C. T., Little, C. B., Last, K., Farmer, P. J., Campbell, I. K., Fourie, A. M., Fosang, A. J. (2005) "ADAMTS5 is the major aggrecanase in mouse cartilage in vivo and in vitro". *Nature* **434**:648–52.

Steffen, A., Dez, G. L., Poincloux, R., Recchi, C., Nassoy, P., Rottner, K., Galli, T., Chavrier, P. (2008) "MT1-MMP-dependent invasion is regulated by TI-VAMP/VAMP7". *Curr Biol* **18**:926–31.

Stephens, L. E., Sutherland, A. E., Klimanskaya, I. V., Andrieux, A., Meneses, J., Pedersen, R. A., Damsky, C. H. (1995) "Deletion of beta 1 integrins in mice results in inner cell mass failure and peri-implantation lethality". *Genes Dev* **9**:1883–95.

Stöcker, W., Grams, F., Baumann, U., Reinemer, P., Gomis-Rüth, F. X., Mckay, D. B., Bode, W. (1995) "The metzincins–topological and sequential relations between the astacins, adamalysins, serralysins, and matrixins (collagenases) define a superfamily of zinc-peptidases". *Protein Sci* **4**:823–40.

Strongin, A. Y., Collier, I., Bannikov, G., Marmer, B. L., Grant, G. A., Goldberg, G. I. (1995) "Mechanism of cell surface activation of 72-kDa type IV collagenase. Isolation of the activated form of the membrane metalloprotease". *J Biol Chem* **270**:5331–8.

Su, J., Yu, J., Ren, T., Zhang, W., Zhang, Y., Liu, X., Sun, T., Lu, H., Miyazawa, K., Yao, L. (2009) "Discoidin domain receptor 2 is associated with the increased expression of matrix metalloproteinase-13 in synovial fibroblasts of rheumatoid arthritis". *Mol Cell Biochem* **330**:141–52.

Sweeney, S. M., Orgel, J. P., Fertala, A., McAuliffe, J. D., Turner, K. R., Lullo, G. A. D., Chen, S., Antipova, O., Perumal, S., Ala-Kokko, L., Forlino, A., Cabral, W. A., Barnes, A. M., Marini, J. C., Antonio, J. D. S. (2008) "Candidate cell and matrix interaction domains on the collagen fibril, the predominant protein of vertebrates". *J Biol Chem* **283**:21187–97.

Szabova, L., Chrysovergis, K., Yamada, S. S., Holmbeck, K. (2008) "MT1-MMP is required for efficient tumor dissemination in experimental metastatic disease". *Oncogene* **27**:3274–81.

Takahara, T., Furui, K., Yata, Y., Jin, B., Zhang, L. P., Nambu, S., Sato, H., Seiki, M., Watanabe, A. (1997) "Dual expression of matrix metalloproteinase-2 and membrane-type 1-matrix metalloproteinase in fibrotic human livers". *Hepatology* **26**:1521–9.

Takahashi, M., Tsunoda, T., Seiki, M., Nakamura, Y., Furukawa, Y. (2002) "Identification of membrane-type matrix metalloproteinase-1 as a target of the beta-catenin/Tcf4 complex in human colorectal cancers". *Oncogene* **21**:5861–7.

Takino, T., Miyamori, H., Kawaguchi, N., Uekita, T., Seiki, M., Sato, H. (2003) "Tetraspanin CD63 promotes targeting and lysosomal proteolysis of membrane-type 1 matrix metalloproteinase". *Biochem Biophys Res Commun* **304**:160–6.

Takino, T., Miyamori, H., Watanabe, Y., Yoshioka, K., Seiki, M., Sato, H. (2004) "Membrane type 1 matrix metalloproteinase regulates collagen-dependent mitogen-activated protein/extracellular signal-related kinase activation and cell migration". *Cancer Res* **64**:1044–9.

Takino, T., Sato, H., Shinagawa, A., Seiki, M. (1995) "Identification of the second membrane-type matrix metalloproteinase (MT-MMP-2) gene from a human placenta cDNA library. MT-MMPs form a unique membrane-type subclass in the MMP family". *J Biol Chem* **270**:23013–20.

Tam, E. M., Moore, T. R., Butler, G. S., Overall, C. M. (2004) "Characterization of the distinct collagen binding, helicase and cleavage mechanisms of matrix metalloproteinase 2 and 14 (gelatinase A and MT1-MMP): the differential roles of the MMP hemopexin c domains and the MMP-2 fibronectin type II modules in collagen triple helicase activities". *J Biol Chem* **279**:43336–44.

Taniwaki, K., Fukamachi, H., Komori, K., Ohtake, Y., Nonaka, T., Sakamoto, T., Shiomi, T., Okada, Y., Itoh, T., Itohara, S., Seiki, M., Yana, I. (2007) "Stroma-derived matrix metalloproteinase (MMP)-2 promotes membrane type 1-MMP-dependent tumor growth in mice". *Cancer Res* **67**:4311–9.

Tchetverikov, I., Ronday, H. K., El, B. V., Kiers, G. H., Verzijl, N., TeKoppele, J. M., Huizinga, T. W. J., DeGroot, J., Hanemaaijer, R. (2004) "MMP profile in paired serum and synovial fluid samples of patients with rheumatoid arthritis". *Ann Rheum Dis* **63**:881–3.

Thathiah, A., Carson, D. D. (2004) "MT1-MMP mediates MUC1 shedding independent of TACE/ADAM17". *Biochem J* **382**:363–73.

Théret, N., Lehti, K., Musso, O., Clément, B. (1999) "MMP2 activation by collagen I and concanavalin A in cultured human hepatic stellate cells". *Hepatology* **30**:462–8.

Tochowicz, A., Goettig, P., Evans, R., Visse, R., Shitomi, Y., Palmisano, R., Ito, N., Richter, K., Maskos, K., Franke, D., Svergun, D., Nagase, H., Bode, W., Itoh, Y. (2011) "The dimer interface of the membrane type 1 matrix metalloproteinase hemopexin domain: crystal structure and biological functions". *J Biol Chem* **286**:7587–600.

Tohyama, C. T., Yamakawa, M., Murasawa, A., Nakazono, K., Ishikawa, H. (2006) "Local cell proliferation in rheumatoid synovial tissue: analysis by cyclin expression". *Clin Rheumatol* **25**:801–6.

Tomasek, J. J., Halliday, N. L., Updike, D. L., Ahern-Moore, J. S., Vu, T. K., Liu, R. W., Howard, E. W. (1997) "Gelatinase A activation is regulated by the organization of the polymerized actin cytoskeleton". *J Biol Chem* **272**:7482–7.

Tortorella, M. D., Arner, E. C., Hills, R., Easton, A., Korte-Sarfaty, J., Fok, K., Wittwer, A. J., Liu, R.-Q., Malfait, A.-M. (2004) "Alpha2-macroglobulin is a novel substrate for ADAMTS-4 and ADAMTS-5 and represents an endogenous inhibitor of these enzymes". *J Biol Chem* **279**:17554–61.

Toth, M., Hernandez-Barrantes, S., Osenkowski, P., Bernardo, M. M., Gervasi, D. C., Shimura, Y., Meroueh, O., Kotra, L. P., Gálvez, B. G., Arroyo, A. G., Mobashery, S., Fridman, R. (2002) "Complex pattern of membrane type 1 matrix metalloproteinase shedding. Regulation by autocatalytic cells surface inactivation of active enzyme". *J Biol Chem* **277**:26340–50.

Troeberg, L., Nagase, H. (2004) "Zymography of metalloproteinases". *Curr Protoc Protein Sci* **Chapter 21**:Unit 21.15.

Troeberg, L., Nagase, H. (2012) "Proteases involved in cartilage matrix degradation in osteoarthritis". *Biochim Biophys Acta* **1824**:133–45.

Tunyogi-Csapo, M., Kis-Toth, K., Radacs, M., Farkas, B., Jacobs, J. J., Finnegan, A., Mikecz, K., Glant, T. T. (2008) "Cytokine-controlled RANKL and osteoprotegerin expression by human and mouse synovial fibroblasts: fibroblast-mediated pathologic bone resorption". *Arthritis Rheum* **58**:2397–408.

Uekita, T., Itoh, Y., Yana, I., Ohno, H., Seiki, M. (2001) "Cytoplasmic tail-dependent internalization of membrane-type 1 matrix metalloproteinase is important for its invasion-promoting activity". *J Cell Biol* **155**:1345–1356.

Valiathan, R. R., Marco, M., Leitinger, B., Kleer, C. G., Fridman, R. (2012) "Discoidin domain receptor tyrosine kinases: new players in cancer progression". *Cancer Metastasis Rev* **31**:295–321.

van Lent, P. L. E. M., Span, P. N., Sloetjes, A. W., Radstake, T. R. D. J., van Lieshout, A. W. T., Heuvel, J. J. T. M., Sweep, C. G. J., van den Berg, W. B. (2005) "Expression and localisation of the new metalloproteinase inhibitor RECK (reversion inducing cysteine-rich protein with Kazal motifs) in inflamed synovial membranes of patients with rheumatoid arthritis". *Ann Rheum Dis* **64**:368–74.

van Meurs, J. B., van Lent, P. L., Holthuysen, A. E., Singer, I. I., Bayne, E. K., van den Berg, W. B. (1999) "Kinetics of aggrecanase- and metalloproteinase-induced neoepitopes in various stages of cartilage destruction in murine arthritis". *Arthritis Rheum*

42:1128–39.

Verstappen, S. M. M., Poole, A. R., Ionescu, M., King, L. E., Abrahamowicz, M., Hofman, D. M., Bijlsma, J. W. J., Lafeber, F. P. J. G., group (SRU), U. R. A. C. S. (2006) "Radiographic joint damage in rheumatoid arthritis is associated with differences in cartilage turnover and can be predicted by serum biomarkers: an evaluation from 1 to 4 years after diagnosis". *Arthritis Res Ther* **8**:R31.

Vogel, W. (1999) "Discoidin domain receptors: structural relations and functional implications". *FASEB J* **13 Suppl**:S77–82.

Vogel, W., Brakebusch, C., Fässler, R., Alves, F., Ruggiero, F., Pawson, T. (2000) "Discoidin domain receptor 1 is activated independently of beta(1) integrin". *J Biol Chem* **275**:5779–84.

Vogel, W., Gish, G. D., Alves, F., Pawson, T. (1997) "The discoidin domain receptor tyrosine kinases are activated by collagen". *Mol Cell* **1**:13–23.

Vogel, W. F. (2002) "Ligand-induced shedding of discoidin domain receptor 1". *FEBS Lett* **514**:175–80.

Vogel, W. F., Abdulhussein, R., Ford, C. E. (2006) "Sensing extracellular matrix: an update on discoidin domain receptor function". *Cell Signal* **18**:1108–16.

Vogel, W. F., Aszódi, A., Alves, F., Pawson, T. (2001) "Discoidin domain receptor 1 tyrosine kinase has an essential role in mammary gland development". *Mol Cell Biol* **21**:2906–17.

Wang, J., Lü, H., Liu, X., Deng, Y., Sun, T., Li, F., Ji, S., Nie, X., Yao, L. (2002) "Functional analysis of discoidin domain receptor 2 in synovial fibroblasts in rheumatoid arthritis". *J Autoimmun* **19**:161–8.

Wang, P., Nie, J., Pei, D. (2004a) "The hemopexin domain of membrane-type matrix metalloproteinase-1 (MT1-MMP) Is not required for its activation of proMMP2 on cell surface but is essential for MT1-MMP-mediated invasion in three-dimensional type I collagen". *J Biol Chem* **279**:51148–55.

Wang, X., Liang, J., Koike, T., Sun, H., Ichikawa, T., Kitajima, S., Morimoto, M., Shikama, H., Watanabe, T., Sasaguri, Y., Fan, J. (2004b) "Overexpression of human matrix metalloproteinase-12 enhances the development of inflammatory arthritis in transgenic rabbits". *Am J Pathol* **165**:1375–83.

Wang, X., Ma, D., Keski-Oja, J., Pei, D. (2004c) "Co-recycling of MT1-MMP and MT3-MMP through the trans-Golgi network. Identification of DKV582 as a recycling signal". *J Biol Chem* **279**:9331–6.

Wang, Y., McNiven, M. A. (2012) "Invasive matrix degradation at focal adhesions occurs via protease recruitment by a FAK-p130Cas complex". *J Cell Biol* **196**:375–85.

Wart, H. E. V., Birkedal-Hansen, H. (1990) "The cysteine switch: a principle of regulation of metalloproteinase activity with potential applicability to the entire matrix metalloproteinase gene family". *Proc Natl Acad Sci USA* **87**:5578–82.

Wilkins, J. A., Li, A., Ni, H., Stupack, D. G., Shen, C. (1996) "Control of beta1 integrin function. Localization of stimulatory epitopes". *J Biol Chem* **271**:3046–51.

Williams, K. C., Coppolino, M. G. (2011) "Phosphorylation of Membrane Type 1-Matrix Metalloproteinase (MT1-MMP) and Its Vesicle-associated Membrane Protein 7 (VAMP7)-dependent Trafficking Facilitate Cell Invasion and Migration". *J Biol Chem* **286**:43405–16.

Wolf, K., Lindert, M. T., Krause, M., Alexander, S., Riet, J. T., Willis, A. L., Hoffman, R. M., Figdor, C. G., Weiss, S. J., Friedl, P. (2013) "Physical limits of cell migration: control by ECM space and nuclear deformation and tuning by proteolysis and traction force". *J Cell Biol* **201**:1069–84.

Wolf, K., Wu, Y. I., Liu, Y., Geiger, J., Tam, E., Overall, C., Stack, M. S., Friedl, P. (2007) "Multi-step pericellular proteolysis controls the transition from individual to collective cancer cell invasion". *Nat Cell Biol* **9**:893–904.

Woskowicz, A. M., Weaver, S. A., Shitomi, Y., Ito, N., Itoh, Y. (2013) "MT-LOOP-dependent localization of membrane type I matrix metalloproteinase (MT1-MMP) to the cell adhesion complexes promotes cancer cell invasion". *J Biol Chem* **288**:35126–37.

Wu, J. J., Lark, M. W., Chun, L. E., Eyre, D. R. (1991) "Sites of stromelysin cleavage in collagen types II, IX, X, and XI of cartilage". *J Biol Chem* **266**:5625–8.

Wu, Y. I., Munshi, H. G., Sen, R., Snipas, S. J., Salvesen, G. S., Fridman, R., Stack, M. S. (2004) "Glycosylation broadens the substrate profile of membrane type 1 matrix metalloproteinase". *J Biol Chem* **279**:8278–89.

Xu, H., Raynal, N., Stathopoulos, S., Myllyharju, J., Farndale, R. W., Leitinger, B. (2010) "Collagen binding specificity of the discoidin domain receptors: Binding sites on collagens II and III and molecular determinants for collagen IV recognition by DDR1". *Matrix Biol* **30**:16–26.

Xu, L., Peng, H., Wu, D., Hu, K., Goldring, M. B., Olsen, B. R., Li, Y. (2005) "Activation of the discoidin domain receptor 2 induces expression of matrix metalloproteinase 13 associated with osteoarthritis in mice". *J Biol Chem* **280**:548–55.

Xu, L., Polur, I., Servais, J. M., Hsieh, S., Lee, P. L., Goldring, M. B., Li, Y. (2011) "Intact pericellular matrix of articular cartilage is required for unactivated discoidin domain receptor 2 in the mouse model". *Am J Pathol* **179**:1338–46.

Xu, Y., Gurusiddappa, S., Rich, R. L., Owens, R. T., Keene, D. R., Mayne, R., Höök, A., Höök, M. (2000) "Multiple binding sites in collagen type I for the integrins alpha1beta1 and alpha2beta1". *J Biol Chem* **275**:38981–9.

Yamanaka, H., Makino, K., Takizawa, M., Nakamura, H., Fujimoto, N., Moriya, H., Nemori, R., Sato, H., Seiki, M., Okada, Y. (2000) "Expression and tissue localization of membrane-types 1, 2, and 3 matrix metalloproteinases in rheumatoid synovium". *Lab Invest* **80**:677–87.

Yamanishi, Y., Boyle, D. L., Clark, M., Maki, R. A., Tortorella, M. D., Arner, E. C., Firestein, G. S. (2002) "Expression and regulation of aggrecanase in arthritis: the role of TGF-beta". *J Immunol* **168**:1405–12.

Yamanishi, Y., Boyle, D. L., Green, D. R., Keystone, E. C., Connor, A., Zollman, S., Firestein, G. S. (2005) "p53 tumor suppressor gene mutations in fibroblast-like synoviocytes from erosion synovium and non-erosion synovium in rheumatoid arthritis". *Arthritis Res Ther* **7**:R12–8.

Yan, C., Boyd, D. D. (2007) "Regulation of matrix metalloproteinase gene expression". *J. Cell. Physiol.* **211**:19–26.

Yana, I., Sagara, H., Takaki, S., Takatsu, K., Nakamura, K., Nakao, K., Katsuki, M., ichiro Taniguchi, S., Aoki, T., Sato, H., Weiss, S. J., Seiki, M. (2007) "Crosstalk between neovessels and mural cells directs the site-specific expression of MT1-MMP to endothelial tip cells". *J Cell Sci* **120**:1607–14.

Yana, I., Weiss, S. J. (2000) "Regulation of membrane type-1 matrix metalloproteinase activation by proprotein convertases". *Mol Biol Cell* **11**:2387–401.

Yang, K., Kim, J. H., Kim, H. J., Park, I.-S., Kim, I. Y., Yang, B.-S. (2005) "Tyrosine 740 phosphorylation of discoidin domain receptor 2 by Src stimulates intramolecular autophosphorylation and Shc signaling complex formation". *J Biol Chem* **280**:39058–66.

Yoshihara, Y., Nakamura, H., Obata, K., Yamada, H., Hayakawa, T., Fujikawa, K., Okada, Y. (2000) "Matrix metalloproteinases and tissue inhibitors of metalloproteinases in

synovial fluids from patients with rheumatoid arthritis or osteoarthritis". *Ann Rheum Dis* **59**:455–61.

Yu, J., Zhao, H., Zhang, Y., Liu, Y.-C., Yao, L., Li, X., Su, J. (2014) "Ubiquitin ligase Cbl-b acts as a negative regulator in discoidin domain receptor 2 signaling via modulation of its stability". *FEBS Lett*:–.

Yun, S., Dardik, A., Haga, M., Yamashita, A., Yamaguchi, S., Koh, Y., Madri, J. A., Sumpio, B. E. (2002) "Transcription factor Sp1 phosphorylation induced by shear stress inhibits membrane type 1-matrix metalloproteinase expression in endothelium". *J Biol Chem* **277**:34808–14.

Zhang, H., Qi, M., Li, S., Qi, T., Mei, H., Huang, K., Zheng, L., Tong, Q. (2012) "microRNA-9 targets matrix metalloproteinase 14 to inhibit invasion, metastasis, and angiogenesis of neuroblastoma cells". *Mol Cancer Ther* **11**:1454–66.

Zhang, K., Corsa, C. A., Ponik, S. M., Prior, J. L., Piwnica-Worms, D., Eliceiri, K. W., Keely, P. J., Longmore, G. D. (2013) "The collagen receptor discoidin domain receptor 2 stabilizes SNAIL1 to facilitate breast cancer metastasis". *Nat Cell Biol* **15**:677–87.

Zhang, W., Ding, T., Zhang, J., Su, J., Li, F., Liu, X., Ma, W., Yao, L. (2006a) "Expression of discoidin domain receptor 2 (DDR2) extracellular domain in pichia pastoris and functional analysis in synovial fibroblasts and NIT3T3 cells". *Mol Cell Biochem* **290**:43–53.

Zhang, W., Matrisian, L. M., Holmbeck, K., Vick, C. C., Rosenthal, E. L. (2006b) "Fibroblast-derived MT1-MMP promotes tumor progression in vitro and in vivo". *BMC Cancer* **6**:52.

Zhang, W.-M., Kapyla, J., Puranen, J. S., Knight, C. G., Tiger, C.-F., Pentikainen, O. T., Johnson, M. S., Farndale, R. W., Heino, J., Gullberg, D. (2003) "alpha 11beta 1 integrin recognizes the GFOGER sequence in interstitial collagens". *J Biol Chem* **278**:7270–7.

Zhou, Z., Apte, S. S., Soininen, R., Cao, R., Baaklini, G. Y., Rauser, R. W., Wang, J., Cao, Y., Tryggvason, K. (2000) "Impaired endochondral ossification and angiogenesis in mice deficient in membrane-type matrix metalloproteinase I". *Proc Natl Acad Sci U S A* **97**:4052–4057.

Zigrino, P., Ayachi, O., Schild, A., Kaltenberg, J., Zamek, J., Nischt, R., Koch, M., Mauch, C. (2012) "Loss of epidermal MMP-14 expression interferes with angiogenesis but not with re-epithelialization". *Eur J Cell Biol* **91**:748–56.

Zigrino, P., Drescher, C., Mauch, C. (2001) "Collagen-induced proMMP-2 activation by MT1-MMP in human dermal fibroblasts and the possible role of alpha2beta1 integrins". *Eur J Cell Biol* **80**:68–77.